

Northumbria Research Link

Citation: Toomey, Jasmine A. (2020) In vitro co-targeting of PARP-1 and HDAC-1 in prostate cells of varying maspin status. Doctoral thesis, Northumbria University.

This version was downloaded from Northumbria Research Link:
<http://nrl.northumbria.ac.uk/id/eprint/44836/>

Northumbria University has developed Northumbria Research Link (NRL) to enable users to access the University's research output. Copyright © and moral rights for items on NRL are retained by the individual author(s) and/or other copyright owners. Single copies of full items can be reproduced, displayed or performed, and given to third parties in any format or medium for personal research or study, educational, or not-for-profit purposes without prior permission or charge, provided the authors, title and full bibliographic details are given, as well as a hyperlink and/or URL to the original metadata page. The content must not be changed in any way. Full items must not be sold commercially in any format or medium without formal permission of the copyright holder. The full policy is available online: <http://nrl.northumbria.ac.uk/policies.html>



**Northumbria
University**
NEWCASTLE



UniversityLibrary

***In vitro* co-targeting of PARP-1 and
HDAC-1 in prostate cells of varying
maspin status**

Jasmine A Toomey

PhD

2020

***In vitro* co-targeting of PARP-1 and
HDAC-1 in prostate cells of varying
maspin status**

Jasmine A Toomey

A thesis submitted in partial fulfilment of
the requirements of the University of
Northumbria at Newcastle for the award of
Doctor of Philosophy

Research undertaken in the faculty of
Health and Life sciences

April 2020

Abstract

Prostate cancer is the most common form of cancer in males. In the UK, 1 in 8 males will develop prostate cancer in their lifetime, making research into this condition important. Current research is focused on the identification and development of new therapeutic targets and the repurposing of existing drugs for cancer therapy; to specifically exploit aggressive tumours associated with poor prognosis.

Constitutive activation of the inflammatory transcription factor Nuclear factor kappa-light-chain-enhancer of activated B cells (NF- κ B) and reduced expression of the tumour suppressor maspin have both been implicated in prostate cancer progression. Poly (ADP-ribose) polymerase-1 (PARP-1), a DNA strand break repair protein, is a known transcriptional co-regulator of NF- κ B. Continuous activation of PARP-1 is implicated in increased inflammatory signalling, cellular dysfunction and consequently tumour progression. Previous studies have shown that inhibition of NF- κ B using PARP inhibitors can sensitise tumour cells to chemotherapeutic agents. Histone deacetylases (HDAC) play a role in the modification and regulation of gene expression and HDAC-1 is highly expressed and activated in metastatic prostate cancer. It is also involved in the repair of DNA double strand breaks by Homologous recombination (HR). Maspin is an endogenous inhibitor of HDAC-1 and studies have shown that HDAC-1 inhibitors limit activation of NF- κ B, stimulate re-expression of maspin and induce a “*BRCAness* phenotype”. To this end, combined inhibition of PARP-1 and HDAC-1 to target NF- κ B and HDAC-1 may serve as a novel therapy in tumours which are deficient in maspin.

The interactive effects between NF- κ B, PARP-1 and maspin on the cellular behaviours of prostate cancer cells proficient (PC3) or depleted (DU145) for maspin were investigated in the presence or absence of specific inhibitors of PARP-1 (Rucaparib) and HDAC-1 (Trichostatin A), alone and in combination. A normal prostate cell line (PNT1A) proficient for maspin was also used. Mouse embryonic fibroblasts (MEF) proficient and deficient for NF- κ B subunits were utilised to compare maspin expression levels and investigate sensitivity to treatments. siRNA was also used

in mechanistic studies to explore the roles of maspin and PARP-1 in cell survival following treatment with Rucaparib and TSA, alone and in combination.

Rucaparib as a single agent significantly reduced survival in DU145 prostate cancer cells depleted in maspin, compared to PNT1A and PC3 prostate cells proficient for maspin. DU145 cells expressed reduced levels of PARP-1 protein and increased levels of IKK α . MEF cells deficient for IKK α expressed maspin and were less sensitive to Rucaparib than MEF cells expressing IKK α . Maspin silencing by siRNA in cells proficient for maspin reduced PARP-1 expression levels and enhanced cell sensitivity to Rucaparib. PARP-1 silencing by siRNA in DU145 and PC3 cells expressing differential levels of maspin did not significantly affect sensitivity to Rucaparib. These data indicate that increased sensitivity to Rucaparib is likely independent to reduced PARP-1 protein levels but may be in part due to increased levels of IKK α and consequently maspin. IKK α may therefore serve as a potential target for cancer therapy and maspin expression may represent a novel predictive biomarker for PARP inhibitor sensitivity in prostate cancers.

Combination of TSA with Rucaparib reduced prostate cancer survival, supporting tumour specific sensitivity to co-treatment. At GI₅₀ concentrations there was no significant difference in cell sensitivity, following co-treatment, between DU145 and PC3 cells, suggesting that sensitivity to co-treatment is independent of IKK α and maspin expression status. Despite a lack of variance in cell survival between DU145 and PC3 cells in the presence of co-treatments at GI₅₀, there was a significant increase in DNA single and double strand break in DU145 cells, compared to PNT1A and PC3 cells. RAD51 expression was reduced in both DU145 and PC3 cells exposed to co-treatment, indicating dysfunctional DNA DSB repair by HR in both of these cell lines. The increased DNA damage response to co-treatment at GI₅₀ in DU145 cells could therefore be attributable to a known *BRCA* mutation or increased “PARP trapping” at DNA breaks. HDAC inhibitors are known to induce a “*BRCA*ness” phenotype and sensitise cells to DNA repair inhibitors by reducing the capacity to repair DSBs *via* HR. Loss of HR capacity requires a reliance on the NHEJ pathway for DNA repair and this pathway is upregulated by PARP. Acetylation of PARP-1 in the presence of TSA may lead to the promotion of DNA repair by NHEJ. However, in the presence of Rucaparib, NHEJ is blocked *via* “PARP trapping” at the site of DNA breaks,

resulting in synthetic lethality. Combination of PARP and HDAC inhibitors represent a promising therapeutic strategy for prostate cancer irrespective of *BRCA* status.

Table of contents

Abstract	II
Table of contents	V
List of Figures	XIII
List of Tables.....	XVIII
Acknowledgments.....	I
Author’s Declaration	1
Chapter One Introduction.....	1
1.1 Cancer	1
1.1.1. Carcinogenesis.....	2
1.2 Prostate cancer	3
1.2.1 Incidence and aetiology	3
1.2.2 Diagnosis	4
1.2.3 Treatment.....	6
1.3 DNA damage and repair	7
1.3.1 Single strand BER	8
1.3.2 Double strand break repair	9
1.4 Poly ADP-ribose polymerase-1 (PARP-1)	12
1.4.1 PARP discovery	12
1.4.2 Structure of PARP-1	13
1.4.3 PARP-1 and DNA repair	15
1.4.4 PARP-1 as a mediator of tumour promoting inflammation	17
1.4.5 PARP-1 activity.....	18

1.4.6	PARP-1 activity and expression.....	18
1.4.7	PARP-1 Inhibitor development.....	19
1.5	Nuclear factor kappa B (NF- κ B).....	23
1.5.1	The NF- κ B superfamily and associated proteins.....	23
1.5.2	NF- κ B activation pathways.....	24
1.5.3	DNA damage-induced NF- κ B activation as a driver of cancer.....	26
1.6	Maspin.....	30
1.6.1	Structure and function.....	30
1.6.2	Maspin regulation.....	32
1.6.3	The role of Maspin in normal biology.....	33
1.6.4	Maspin in cancer.....	36
1.7	Histone deacetylase.....	41
1.7.1	HDAC-1 structure and function.....	41
1.7.2	HDAC-1 in cancer initiation.....	42
1.7.3	HDAC inhibitors for cancer therapy.....	43
1.8	Combined PARP and HDAC inhibition as a potential cancer therapy.....	45
1.9	Rationale and hypothesis.....	45
1.10	Aims.....	48
Chapter Two Materials and methods.....		50
2.1	Materials and reagents.....	50
2.1.1	PARP Inhibitor AG014699.....	54
2.1.2	Histone deacetylase inhibitor Trichostatin A.....	54
2.2	General methods.....	55
2.2.1	Mammalian cell culture.....	55

2.2.2	Assessment of cell and nuclear morphology	59
2.2.3	Proliferation and cytotoxicity assays	59
2.2.4	Protein expression analysis	63
2.2.5	Immunofluorescence	67
2.2.6	Quantifying single DNA breaks	69
2.2.7	Quantifying DNA double strand breaks	70
2.2.8	Scratch assay	71
2.2.9	xCELLigence real-time cell analyser (RTCA).....	72
2.2.10	Transient small interfering ribonucleic acid (siRNA) transfection.....	73
2.2.11	Statistical Analysis.....	76
Chapter Three	<i>In vitro</i> studies to characterise a panel of immortalised cell lines.....	77
3.1	Introduction.....	77
3.1.1	Cell lines.....	77
3.1.2	Cell line authentication.....	77
3.1.3	Mycoplasma	78
3.1.4	Cell proliferation	79
3.1.5	Cell morphology.....	80
3.1.6	Protein expression and localisation	80
3.2	Chapter aims	80
3.3	Results.....	81
3.3.1	Authentication of cell lines by DNA STR analysis.....	81
3.3.2	Mycoplasma screening	82
3.3.3	Proliferation rates of cell lines.....	86
3.3.4	Cell morphology.....	89

3.3.5	Protein expression and subcellular localisation.....	91
3.4	Discussion.....	103
3.4.1	Cell line authentication and mycoplasma screening	103
3.4.2	Cell proliferation rates and morphology	104
3.4.3	Protein expression and localisation	106
3.5	Summary	113
3.6	Future work.....	113
Chapter Four	Investigating the effects of PARP-1 and HDAC-1 inhibitors on cell growth and survival in cell lines with varied maspin expression.....	115
4.1	Introduction.....	115
4.1.1	Choice of inhibitors.....	115
4.1.2	Sensitivity to inhibitors and selection of methodology.....	117
4.1.3	Assessment of cell morphology in the presence and absence of Rucaparib and TSA.....	117
4.1.4	Protein expression levels in the presence of Rucaparib and TSA.....	118
4.2	Chapter aims	118
4.3	Results.....	119
4.3.1	The effects of Rucaparib on prostate cell growth and survival and selection of methodology for future experiments.....	119
4.3.2	The effects of Rucaparib on prostate cell morphology.	124
4.3.3	The effects of Rucaparib on prostate cell nuclear morphology.....	125
4.3.4	The effects of Trichostatin A on prostate cell growth and survival and selection of methodology.....	130
4.3.5	Trichostatin A affects prostate cell morphology in a dose dependent manner.....	134

4.3.6	Trichostatin A affects prostate cell nuclear morphology in a dose dependent manner.....	137
4.3.7	Evaluation of the combined effects of Rucaparib and Trichostatin A on prostate cell survival by SRB assay.....	141
4.3.8	Trichostatin A enhances the effects of Rucaparib on cellular and nuclear morphology in prostate cell lines.	144
4.3.9	The effects of Rucaparib and TSA, alone and in combination on whole protein expression.....	149
4.3.10	NFkB affects Rucaparib sensitivity in MEF cells.....	153
4.3.11	NF-kB p65 enhances TSA resistance in MEF cells.....	154
4.4	Discussion.....	156
4.4.1	The effects of Rucaparib on prostate and MEF cell survival	156
4.4.2	Rucaparib has increased effect on cell morphology and death in maspin depleted prostate cancer cells.	159
4.4.3	The effects of TSA on cell survival in prostate and MEF cells.....	160
4.4.4	TSA- cell morphology and death	162
4.4.5	Pharmacological inhibition of HDAC by TSA sensitises prostate cancer cells to the PARP-1 inhibitor Rucaparib.	163
4.4.6	Western blot analysis of Maspin, NF-kB and PARP-1 expression in prostate cell lines treated with Rucaparib, TSA as single agents and in combination.	165
4.5	Summary.....	168
4.6	Future work.....	168
Chapter Five Investigating the effects of PARP-1 and HDAC-1 inhibitors on cell migration in prostate cells with varied maspin expression.		170
5.1	Introduction.....	170

5.1.1	Cell migration.....	170
5.1.2	Assessment of cell migration in the presence and absence of Rucaparib and TSA.....	170
5.2	Chapter aims	171
5.3	Results.....	171
5.3.1	Real-time effects of Rucaparib and TSA treatment, alone and in combination, on prostate cell migration.....	171
5.3.2	The effects of Rucaparib and TSA treatment, alone and in combination, on prostate cell migration by scratch assay.....	174
5.3.3	The effects of maspin knockdown with siRNA on PC3 cell migration.	178
5.4	Discussion.....	179
5.5	Summary.....	184
5.6	Future work.....	185
Chapter Six	Investigating the effects of PARP-1 and HDAC-1 inhibitors on DNA damage in prostate cell lines of varied maspin expression.....	186
6.1	Introduction.....	186
6.2	Chapter aims	189
6.3	Results.....	190
6.3.1	DNA single strand break formation in prostate cells treated with Rucaparib and TSA, alone and in combination.....	190
6.3.2	DNA double strand break formation in prostate cells treated with Rucaparib and TSA, alone and in combination.....	194
6.3.3	Western blot analysis of RAD51 protein expression as a marker of Homologous recombination in prostate cancer cells exposed to Rucaparib and TSA, alone and in combination.....	199

6.4	Discussion.....	200
6.4.1	The effects of Rucaparib and TSA on DNA SSB formation	200
6.4.2	The effects of Rucaparib and TSA on DSB formation.....	202
6.4.3	The effects of Rucaparib and TSA on the expression of RAD51	203
6.5	Summary.....	206
6.6	Future work.....	207
Chapter Seven Investigating the effects of Maspin and PARP-1 siRNA on prostate cell sensitivity to Rucaparib and TSA.....		
7.1	Introduction.....	209
7.1.1	Cell transfection	209
7.2	Chapter aims	211
7.3	Results.....	212
7.3.1	Knockdown of maspin with siRNA in PNT1A and PC3 cells.....	212
7.3.2	The effects of maspin on PNT1A cell sensitivity to Rucaparib and TSA.....	214
7.3.3	The effects of Maspin knockdown on PARP-1 protein expression following exposure to Rucaparib and TSA, alone and in combination.	217
7.3.4	Knockdown of PARP-1 with siRNA in DU145 and PC3 cells.....	218
7.4	Discussion.....	224
7.4.1	The effects of maspin silencing on prostate cell sensitivity to Rucaparib and TSA.....	224
7.4.2	The effects of maspin knockdown on PARP-1 protein expression in PC3 cells exposed to Rucaparib and TSA.....	228
7.4.3	The effects of PARP-1 silencing on prostate cell sensitivity to Rucaparib and TSA.....	230
7.5	Summary.....	233

7.6	Future work.....	234
Chapter Eight	Summary and future directions.....	235
8.1	The stand-alone effects of the PARP inhibitor Rucaparib in prostate cells of varying maspin expression	242
8.2	Sensitivity assay selection and the hormetic response.....	250
8.3	The stand-alone effects of the HDAC inhibitor TSA in prostate cells of varying maspin expression.....	251
8.4	The combined effects of the PARP inhibitor Rucaparib and the HDAC inhibitor TSA in prostate cells of varying maspin expression.....	256
8.5	General conclusions.....	261
8.6	Future work.....	263
Appendix	265
Appendix One	265
	DU145 and PC3 cell allele reports.....	265
Appendix Two.....		267
	Maspin transfection reduces MCF-7 cell sensitivity to Rucaparib	267
Appendix Three.....		268
	Named publication	268
References	269

List of Figures

Figure 1.1: Model of base excision repair (BER).	9
Figure 1.2: The principle DNA double strand break repair pathways.	11
Figure 1.3: Schematic representation to show the process of PARylation in response to DNA damage induced PARP-1 activation.....	13
Figure 1.4: Schematic representation of the PARP-1 protein and its three domains.	14
Figure 1.5: The two sides to PARP-1 activation.	18
Figure 1.6: Schematic representation of synthetic lethality.	22
Figure 1.7: NF- κ B subunits which comprise the NF- κ B family.	24
Figure 1.8: Schematic representation of the canonical and non-canonical NF- κ B signalling pathways.....	25
Figure 1.9: X-ray crystal structure of maspin.	31
Figure 1.10: STRING network visualisation of PARP-1, HDAC-1, SERPINB5/Maspin and NF- κ B protein-protein interactions.....	47
Figure 1.11: Potential interplay between PARP-1, NF κ B, IKKa, HDAC-1 and maspin molecules and the hypothetical effects of PARP and HDAC inhibitors on the expression and regulation of these molecules.	48
Figure 2.1: Chemical structure of the potent PARP inhibitor Rucaparib.....	54
Figure 2.2: The chemical structure of HDAC inhibitor Trichostatin A.	55
Figure 2.3: Chamber layout of a haemocytometer.....	57
Figure 2.4: WST-1 is metabolised to a soluble formazan product which is indicative of cell viability.....	60
Figure 2.5: Resazurin is reduced to a resorufin product by metabolically active cells.....	63
Figure 2.6: Set up of the blotting cassette for protein transfer (Bio-Rad mini-PROTEAN® tetra cell system).....	66
Figure 2.7: Comet visual classification (0-4) following staining with DAPI.	69
Figure 2.8: siRNA gene silencing mechanism.	74

Figure 3.1: Mycoplasma testing of (A) Prostate and (B) Mouse embryonic fibroblast (MEF) cell lines by PCR using the Venor®GeM <i>OneStep</i> detection kit.	83
Figure 3.2: DAPI staining of cells contaminated with mycoplasma.....	84
Figure 3.3: DAPI staining of prostate cells to confirm the absence of Mycoplasma contamination.	85
Figure 3.4: Representative growth curves to show cell proliferation of prostate cells.	87
Figure 3.5: PNT1A, DU145 and PC3 cells proliferate exponentially at a density of 2.5x10 ⁴ /ml.	88
Figure 3.6: Cell morphology of (A) PNT1A, (B) DU145 and (C) PC3 prostate cells in culture.	90
Figure 3.7: Cell morphology of MEF cells (A) p65 ^{+/+} , (B) p65 ^{-/-} and (C) IKKa ^{-/-} in culture.	91
Figure 3.8: Representative Western blots of whole PNT1A, DU145 and PC3 prostate cell protein extracts.	93
Figure 3.9: Semi-quantitative expression of proteins in prostate cell lines.	95
Figure 3.10: Protein quantification and Immunofluorescence staining of PNT1A cells.	97
Figure 3.11: Protein quantification and Immunofluorescence staining of DU145 cells.....	99
Figure 3.12: Protein quantification and Immunofluorescence staining of PC3 cells.....	101
Figure 3.13: Western Blots of whole MEF cell protein extracts.....	103
Figure 3.14 Schematic to summarise the expression of proteins in DU145 and PC3 cells.	113
Figure 4.1 Proposed working model of TSA and Rucaparib co-treatment.....	116
Figure 4.2: Comparison of growth inhibition by Rucaparib using WST-1, SRB, Resazurin and counting in Prostate cell lines.....	121
Figure 4.3: Effect of 10µM Rucaparib on survival and growth of prostate cells, as measured by WST-1, SRB, Counting and Resazurin assays.....	123
Figure 4.4: The assessment of cell morphology in response to Rucaparib by brightfield microscopy.	125
Figure 4.5: The assessment of nuclear morphology in response to Rucaparib using DAPI staining and fluorescence microscopy.	127
Figure 4.6: Quantification of changes to nuclear morphology following a 72-hour exposure period to Rucaparib.	129

Figure 4.7: Comparison of growth inhibition by Trichostatin A using WST-1, SRB and counting methods in Prostate cell lines.	131
Figure 4.8: Comparison of percentage growth and survival inhibition using WST-1, SRB and Counting in prostate cells treated with 60nM Trichostatin A.	133
Figure 4.9: The assessment of cell morphology in response to Trichostatin A by brightfield microscopy.	136
Figure 4.10: The assessment of changes to nuclear morphology in response to Trichostatin A using DAPI staining and fluorescence microscopy.....	138
Figure 4.11: Quantification of changes to nuclear morphology following a 72 hour exposure period to Trichostatin A.	140
Figure 4.12: Combined treatment of Rucaparib and Trichostatin A enhances growth inhibition in prostate cell lines.	143
Figure 4.13: The assessment of cell morphology in response to Rucaparib and Trichostatin A, alone and in combination, by brightfield microscopy.....	145
Figure 4.14: The assessment of nuclear morphology changes in response to Rucaparib and Trichostatin A in combination using DAPI staining and fluorescence microscopy.	146
Figure 4.15: Quantification of changes to nuclear morphology following a 72 hour exposure period to Rucaparib and Trichostatin A, alone and in combination.....	148
Figure 4.16: PNT1A protein expression following exposure to treatments.....	150
Figure 4.17: DU145 protein expression following exposure to treatments.	151
Figure 4.18: PC3 protein expression following exposure to treatments.	152
Figure 4.19: Cytotoxicity to Rucaparib in Mouse embryonic fibroblast cell lines by SRB assay.	153
Figure 4.20: Cytotoxicity to Trichostatin A in Mouse embryonic fibroblast cell lines by SRB assay.	155
Figure 5.1: Real-time analysis of prostate cell migration in response to Rucaparib and TSA, alone and in combination, using the xCELLigence system.	173
Figure 5.2: Assessment of PNT1A cell migration by scratch wound healing assay in the absence or the presence of Rucaparib and TSA, alone and in combination.	175

Figure 5.3: Assessment of DU145 cell migration by scratch wound healing assay in the absence or the presence of Rucaparib and TSA, alone and in combination.	176
Figure 5.4: Assessment of PC3 cell migration by scratch wound healing assay in the absence or the presence of Rucaparib and TSA, alone and in combination.	177
Figure 5.5: Comparison of prostate cell migration in response to Rucaparib and Trichostatin A treatment, alone and in combination.	178
Figure 5.6: The effects of maspin siRNA on PC3 cell migration.	179
Figure 6.1: Detection of single strand DNA breaks in PNT1A cells exposed to Rucaparib and TSA, alone and in combination.	191
Figure 6.2: Detection of single strand DNA breaks in DU145 cells exposed to Rucaparib and TSA, alone and in combination.	192
Figure 6.3: Detection of single strand DNA breaks in PC3 cells exposed to Rucaparib and TSA, alone and in combination.	193
Figure 6.4: Comparison of single strand DNA breaks in prostate cells exposed to Rucaparib and TSA co-treatment.	194
Figure 6.5: Detection of double strand DNA breaks by γ H2AX immunofluorescence assay in PNT1A cells exposed to Rucaparib and TSA, alone and in combination.	195
Figure 6.6: Detection of double strand DNA breaks by γ H2AX immunofluorescence assay in DU145 cells exposed to Rucaparib and TSA, alone and in combination.	196
Figure 6.7: Detection of double strand DNA breaks by γ H2AX immunofluorescence assay in PC3 cells exposed to Rucaparib and TSA, alone and in combination.	197
Figure 6.8: Mean fold-change in γ H2AX foci: control following continuous exposure to Rucaparib and TSA, alone and in combination, for 72 hours.	198
Figure 6.9: RAD51 protein expression following exposure to Rucaparib, TSA and co-treatment.	200
Figure 7.1: Time course of siRNA knockdown of Maspin in PNT1A cells.	213
Figure 7.2: Time course of siRNA knockdown of Maspin in PC3 cells.	214
Figure 7.3: siRNA knockdown of maspin enhances PNT1A cell sensitivity to Rucaparib.	215
Figure 7.4: siRNA knockdown of maspin enhances PNT1A sensitivity to TSA.	216

Figure 7.5: siRNA knockdown of maspin enhances PNT1A sensitivity to Rucaparib and TSA co-treatment.....	216
Figure 7.6: The effect of maspin on the protein expression of PARP-1 in PC3 cells exposed to Rucaparib and TSA, alone and in combination.....	218
Figure 7.7: Time course of siRNA knockdown of PARP in DU145 and PC3 cells.	219
Figure 7.8: The effects of PARP-1 knockdown on DU145 cell sensitivity to Rucaparib.....	220
Figure 7.9: The effects of PARP-1 knockdown on DU145 cell sensitivity to TSA.	220
Figure 7.10: siRNA knockdown of PARP-1 enhances DU145 cell sensitivity to Rucaparib and TSA co-treatment.	221
Figure 7.11: The effects of PARP-1 knockdown on PC3 cell sensitivity to Rucaparib.	222
Figure 7.12: The effects of PARP-1 knockdown on PC3 sensitivity to TSA.	222
Figure 7.13: siRNA knockdown of PARP-1 enhances PC3 sensitivity to Rucaparib and TSA co-treatment.....	223
Figure 7.14: DU145 and PC3 cell survival following PARP-1 gene silencing and exposure to Rucaparib and TSA co-treatment. Basal PARP-1 status does not effect sensitivity to co-treatment.	224
Figure 8.1: Hypothetical model for the stand-alone effects of Rucaparib and the many facets of PARP-1 action.....	240
Figure 8.2: Hypothetical model for the combined effects of Rucaparib and TSA in the context of PARP trapping.....	241

List of Tables

Table 1.1: Hallmarks of Cancer.	1
Table 1.2: Tumour, node and metastasis (TNM) staging of Prostate cancer.	5
Table 1.3: NF- κ B signalling in various tumour types.	28
Table 1.4: Maspin expression in prostate cancer	37
Table 1.5: Maspin expression in other cancers.	38
Table 1.6: Expression of HDAC-1 in human cancers.	43
Table 2.1: Buffers and solutions	50
Table 2.2: Cell summary and culture conditions.	52
Table 2.3: Primary antibodies used for western blotting and Immunofluorescence.	52
Table 2.4: Secondary antibodies used for western blotting and Immunofluorescence.	53
Table 2.5: Preparation of diluted BSA standards.	64
Table 2.6: Human Maspin and PARP-1 siRNA target sequences	75
Table 3.1: PNT1A cell allelic data.	82
Table 3.2: DU145 cell allelic data.	82
Table 3.3: PC3 cell allelic data.	82
Table 3.4: Optimum cell densities and doubling times.	88
Table 4.1: Comparison of Rucaparib GI ₅₀ concentrations between different growth and survival assays in prostate cell lines.	120
Table 4.2: Comparing cytotoxicity to Trichostatin A in prostate cell lines by proliferation assays.	134
Table 4.3: GI ₅₀ concentrations of Rucaparib and Trichostatin A identified by SRB assay in prostate cell lines of varying maspin expression.	141
Table 4.4: MEF GI ₅₀ values following exposure to Rucaparib for 72 hours.	154
Table 4.5: MEF GI ₅₀ values following exposure to TSA for 72 hours.	155
Table 4.6: The effects of Rucaparib on the expression levels of maspin, PARP-1, NF- κ B p65 and IKK α proteins in DU145 and PC3 cells.	165

Table 4.7: The effects of TSA on the expression levels of maspin, PARP-1, NF-kB p65 and IKKa proteins in DU145 and PC3 cells	165
--	-----

Acknowledgments

First of all, I'd like to thank my principal supervisor Dr Stephany Veuger for her time, effort, support and guidance, particularly in the final stages of my project; your positivity and encouragement enabled me to believe in myself and push to the finish line. I would also like to thank my secondary supervisor Dr Hannah Walden and my former secondary supervisor Dr Rosemary Bass for their advice and support in the lab and during the writing up period.

To my fellow students, Laura, Louise, Megan, Libby, Kate, Jen, Calum and Jon – I am grateful that our paths crossed and that I managed to come out of the PhD with a great set of friends. Laura, you were the voice of reason during my darkest times. Thanks for being a shoulder to cry on and joining me on endless coffee and cake trips when I needed to “eat my feelings”.

This thesis would not be complete in its entirety without the love, support and encouragement from my family and friends. Mam, thank you for supplying the study snacks and endless cups of tea during the writing up period. You have always been behind me 100% and encouraged me to never give up, I love you very much. A special thank you must also go to my husband Jacob; you have held me together though the duration of this project and I am grateful to you for getting me through the most challenging time in my life.

Finally, I would like to dedicate this thesis to my late Aunt Irene. Your encouragement to enjoy learning in my earlier years is the reason I have come so far today. You have supported me both emotionally and financially throughout my education and I hope that I have made you proud.

Author's Declaration

I declare that the work contained in this thesis is all my own work. It has not been submitted in the past or is to be submitted at any other academic institution for any other award. The work fully acknowledges the opinions, ideas and contributions from the work of others.

Ethical clearance for the research presented in this thesis has been approved by the Northumbria University Departmental Representative (Reference: BMS33UNNJMSV2015)

Name: Jasmine A Toomey

Signature:

Date: May 2020

Chapter One Introduction

1.1 Cancer

Cancer is the most common cause of mortality in the UK after cardiovascular disease (Global Burden of Disease Cancer, 2015) and it will affect one in two at some point in life (Torjesen, 2015). The development of cancer is a multistep process characterised by genetic changes that drive abnormal and uncontrolled cell division. Without treatment these abnormal cells invade and destroy surrounding tissues around the body *via* a process known as metastasis. There are over 200 different types of cancer which are classified according to the tissue and cell type from which they arise. Cancers derived from epithelial cells are known as carcinomas and account for 90% of all cancers. Other cell types which give rise to cancer formation are those of the blood and lymphatic system (Leukaemia's and Lymphoma's), connective tissue (sarcoma) and central nervous system (Cancer Research UK).

Ten biological capabilities that enable cancer development have been identified (Table 1.1) and have the potential for exploitation. Drug development is currently focused on targeting these hallmarks (Hanahan and Weinberg, 2011).

Table 1.1: Hallmarks of Cancer.

Cancer hallmarks and targeting agents which exploit such hallmarks have been developed or are in clinical trials (Hanahan and Weinberg, 2011).

Cancer Hallmark	Targeting agent
Evade growth suppressors	Cyclin-dependant kinase inhibitors
Avoid immune destruction	Immune activating anti-CTLA4 mAb
Enabling replicative immortality	Telomerase inhibitors
Tumour promoting inflammation	Selective anti-inflammatory drugs
Activating invasion and metastasis	Inhibitors of HGF/c-Met
Inducing angiogenesis	Inhibitors of VEGF signalling
Genome instability and mutation	PARP inhibitors
Resisting cell death	Pro-apoptotic BH3 mimetics

Deregulating cellular energetics	Aerobic glycolysis inhibitors
Sustaining proliferative signalling	EGFR inhibitors

1.1.1. Carcinogenesis

The transformation of cells into invasive cancerous cells is a process known as carcinogenesis. It is a multistep process, characterised by a series of genetic and epigenetic alterations which drive tumour development. Carcinogenesis comprises three distinct stages: tumour initiation, tumour promotion and cancer progression (Pitot, 1993).

The formation of a tumour is initiated in response to irreversible genetic mutation to cellular DNA, which causes cells to break free from the normal constraints of regulated growth. Genetic mutations may be spontaneous, or due to reactive oxygen species (ROS) and harmful carcinogens which modify the molecular structure of DNA; prompting permanent genetic change during DNA synthesis. For example, 8-Oxoguanine (8-oxoG) is a product of oxidative DNA damage which induces replication errors and hinders transcription. Pairing of 8-oxoG with adenine results in a DNA base mismatch and failure to repair such DNA lesion *via* break excision repair leads to further DNA damage and genetic mutation (Allgayer et al., 2013). Damage to the epigenome which regulates gene expression, or damage to chromosomes may lead to the initiation of carcinogenesis (Franco et al., 2008).

As mutated cells expand and proliferate, tumour formation and further genetic change is promoted (Kufe et al., 2003). Alterations to genes which control the cell cycle, such as tumour suppressors and proto-oncogenes prompt uncontrolled cell growth and proliferation. These alterations are generally somatic; however, germ-line mutations of these genes may predispose an individual to heritable cancer.

Tumour suppressor genes (TSG) such as *p53*, for example, are inactivated forms of cellular genes. They control inappropriate cell growth and differentiation by initiating cell death. When TSG become mutated or deactivated they are no longer able to regulate cell growth in a controlled manner, and so cell proliferation is enhanced (Chial, 2008). Mutations in *p53* have been reported

in almost every type of cancer; ranging between 10% in haematopoietic malignancies and up to 100% in high grade carcinomas of the ovaries (Rivlin et al., 2011).

Proto-oncogenes are genes which encode growth factors, nuclear transcription factors and inhibitors of apoptosis. Conversion of a proto-oncogene into an oncogene generally occurs due to a "gain of function" mutation. Oncogene over-expression leads to increased cell proliferation and survival, as growth factors and inhibitors of apoptosis become up-regulated (Croce, 2008).

A loss of function in TSG's and a gain of function in proto-oncogenes drives cells into malignancy; the final phase of carcinogenesis whereby phenotypical change occurs. Cells begin to acquire more aggressive characteristics, such as the ability to move beyond the primary tumour location *via* the bloodstream or lymphatic system by a process known as metastasis (Kufe et al., 2003). Successful metastasis allows tumour cells to metastasise to secondary sites within the body. Metastatic tumours are accountable for ~90% of cancer-related mortalities (Spano et al., 2012).

1.2 Prostate cancer

1.2.1 Incidence and aetiology

Prostate cancer (PC) is the most common cancer in men in the UK. Over 47,000 new cases are diagnosed every year and it is estimated that will 1 in 8 males will be affected by the disease at some point in their lifetime (Prostate cancer UK). Diagnosis of PC has increased over the last 10 years, which is likely due to wide-spread implementation of the prostate specific antigen (PSA) test, increased disease awareness and consequently increased incidence (Cancer Research UK).

Whilst the exact aetiology of PC remains unclear, incidence is significantly correlated with increasing age, family history and ethnicity (Daniyal et al., 2014). According to Cancer Research UK, more than half of diagnosed cases between years 2012 and 2014 were in males aged 70 and over. Diagnosis is rare in males under the age of 50. Unlike other types of cancer, genetic markers that predispose PC have not yet been identified, despite a strong link between family history and disease development. Males with a first degree relative diagnosed with PC are 2-3 times more likely to be diagnosed than a male with no family history (Kommu et al., 2004). Black males are

twice as likely to be diagnosed with PC compared to white males of the same age in the UK (Lloyd et al., 2015).

1.2.2 Diagnosis

Early stage PC is asymptomatic. As the disease progresses symptoms begin to arise. These symptoms include bladder obstruction, dysuria, impotence, and in the later stages unexplained weight loss and bone pain in the lower back, hips and pelvis (Prostate cancer UK).

When a patient presents with symptoms indicative of PC, serum PSA is measured and a digital rectum examination (DRE) is performed. PSA is a protein produced by the prostate gland that is elevated in the presence of PC. In 1994 PSA was approved as a diagnostic marker for early stage PC, and since the widespread implementation of PSA testing the incidence of PC metastasis and mortality has decreased (Lewis and Hornberger, 2016). Routine PSA testing as a diagnostic tool for PC has led to over-diagnosis as the test is specific to the prostate but not to PC. Other factors such as prostate enlargement, prostatitis and increasing age contribute to elevated PSA levels. When PSA levels are raised, a digital rectal examination (DRE) is performed to check if the surface of the prostate gland has changed. A hard and bumpy surface is indicative of PC; however, the cancer is not always detectable as changes to the gland are generally not apparent in the early stages. PSA and DRE results are used to assess the risk of having PC, but the presence of PC is confirmed only after a transrectal ultrasonography (TRUS) guided biopsy (Prostate cancer UK).

1.2.2.1 Gleason grading and pathological staging

Upon PC diagnosis, the cancer is graded and staged to establish prognosis and to ensure appropriate treatment.

The Gleason grading system was devised in the 1960's by Dr Donald Gleason and it is the gold standard for grading PC to confirm tumour aggressiveness. The system is based on the histological examination of PC cells obtained from a biopsy, to determine how different they are in appearance from normal prostate cells (Humphrey, 2004). The morphological appearance of the cells is given a grade from 1-5, with scores 1-2 considered normal, and 3-5 cancerous. Multiple patient samples are taken, and an overall Gleason score is calculated by adding the most common sample grade

with the highest sample grade. Scores can range from 2-10 with increasing score correlating to disease progression and poor prognosis. PC is defined by an overall Gleason score between 6 and 10 (Prostate cancer UK).

The tumour, node and metastasis (TNM) staging system represented in Table 1.2 is used alongside the Gleason grading system throughout the UK. The system assesses how far a cancer has spread by identifying the size and localisation of the primary tumour (T), the extent of spread to lymph nodes (N) and/or metastasis (M) to distant sites. Once tumour grade and stage has been confirmed, patients are stratified into 3 pathologic categories; localised disease, locally advanced disease and advanced metastatic disease.

Table 1.2: Tumour, node and metastasis (TNM) staging of Prostate cancer.

The TNM staging system is used to describe the extent of spread of cancer.

TNM stage	Description
T1	The cancer cannot be seen on a scan or felt during prostate examination. It is identifiable microscopically
T2	The cancer can be identified on scans but is confined to the prostate gland
T2a	The cancer is only in half of one side of the prostate gland
T2b	The cancer is in more than half of one side of the prostate gland
T2c	The cancer is present in both sides of the prostate gland but is confined
T3a	The cancer extends beyond the outer layer of the prostate but has not spread to the seminal vesicles
T3b	The cancer has spread to the seminal vesicles
T4	The cancer has spread to nearby organs
NX	Lymph nodes cannot be assessed
N0	Nearby lymph nodes are free from cancer cells
N1	Cancer cells are present in lymph nodes near to the prostate
MX	Cancer spread was not investigated
M0	The cancer has not spread to other parts of the body
M1	The cancer has spread to other parts of the body

1.2.3 Treatment

PC treatment options are dependent on the pathological stage of the cancer upon diagnosis.

Localised PC tumours are confined to the prostate and are classified into low and high-risk localised tumours dependent on their risk of disease progression at diagnosis. Low risk PC patients, with a PSA value lower than 10ng/ml, do not receive treatment but are placed under active surveillance; whereby the PC is monitored over time for any change indicative of disease progression. A cohort study conducted in 1298 monitored males with low risk PC's for 60 months with frequent PSA tests and biopsies. At 60 months only 5 males had progressed to metastatic PC and 2 mortalities were reported (Tosoian et al., 2015). Other studies have also emphasised the effectiveness of active surveillance as an intervention for risk reclassification (Klotz et al., 2009, Welty et al., 2015). Around 30% of patients under surveillance will eventually be reclassified to high risk PC and offered treatment (Klotz and Emberton, 2014).

When the disease has progressed but is still confined to the prostate, surgical removal of the entire prostate (radical prostatectomy) and/or radiotherapy is considered. Radiotherapy directly destroys DNA within the cancerous cells by targeting them with ionising radiation (IR). When the DNA is damaged beyond repair, the cancer cells stop proliferating and die. Patients can receive radiotherapy in either of two forms: external beam or internal irradiation (brachytherapy). External beam therapy utilises high-energy rays which directly target the tumour. Brachytherapy delivers radiation directly to the site of the tumour sealed in seeds or pellets. They are implanted in the body using a needle or catheter (Begg et al., 2011, Cancer Research UK). Some patients may be selected for neo-adjuvant endocrine therapy with radical prostatectomy and/or external beam radiation if they are at increased risk of disease progression (Kent and Hussain, 2003). Five year survival for patients with locally advanced PC is 93% (Cancer Research UK), however many of these patients will still go on to develop metastatic PC.

Metastatic PC is not curable, but its progression can be controlled with endocrine therapies such as Bicalutamide and Flutamide which inhibit androgen-stimulated tumour growth. They stop testosterone and dihydrotestosterone from reaching the androgen receptor, preventing the activation of androgen regulated genes (Wirth et al., 2007, Osguthorpe and Hagler, 2011). Other

anti-androgen drugs include Cyproterone acetate, a luteinizing hormone-releasing hormone (LHRH) antagonist that reduces LH production in the pituitary gland; subsequently suppressing testosterone secretion (Hou, 2009, Reissmann et al., 2000). Response to these treatments is generally short lived and the cancerous cells eventually escape from a state of androgen dependence to androgen independence (castrate-resistant PC). It is at this stage when further treatment options are limited, and risk of mortality is increased. Chemotherapeutic agents Docetaxel and Cabazitaxel are employed as a last line therapy to slow tumour progression and provide symptomatic relief. Many side effects accompany these agents as they lack tumour specificity and damage all dividing cells. Healthy cells are highly proliferative in tissues where a demand for new cells is high, for example, bone marrow, hair and the lining of the digestive system. Damage to these healthy dividing cells induces side effects such as myelosuppression, hair loss and nausea (Cancer Research UK).

Resistance and side effects to standard treatments at advanced stages of PC highlight a need for novel therapies. In the late 1980's, complex signalling networks that regulate cellular activities such as growth and survival were discovered. Many of these signalling networks were found to be altered in cancer cells and scientists have since attempted to overcome these alterations through the development of specific targeting therapies; otherwise known as "magic bullets" (Chabner and Roberts, 2005). Research into the molecular mechanisms that drive the progression of PC is required as a means to improve treatment and disease survival.

1.3 DNA damage and repair

DNA encodes genetic information in each living cell and its integrity and stability is essential to life (Clancy, 2008). When DNA becomes damaged it is important that it is repaired efficiently to maintain normal cellular functioning and genomic stability. Defective DNA repair can lead to genetic mutation and ultimately cancer (Hoeijmakers, 2001). The ways in which DNA becomes damaged is large since it is continuously exposed to a multitude of endogenous and exogenous genotoxic insults. Endogenous damage can result from products of normal cellular metabolism, for example, hydrolysis, alkylation or oxidation by production of intracellular reactive oxygen species (ROS) (Torgovnick and Schumacher, 2015). Exogenous DNA damaging agents include

ultraviolet (UV) light, ionizing radiation (IR) and genotoxic chemicals such as those present in cigarette smoke and chemotherapeutic agents (Hoeijmakers, 2001).

Cells possess a number of distinct and highly conserved DNA damage response (DDR) pathways which coordinate the repair of damaged DNA (Curtin, 2012). The main repair pathways are Base or nucleotide excision repair (BER/NER), Non-homologous end joining (NHEJ) and Homologous recombination (HR). Poly ADP-ribose polymerase-1 (PARP-1), an enzyme associated with DNA damage and repair, has been investigated in the studies presented in this thesis. The enzyme plays a role in single strand break (SSB) BER and double strand break (DSB) HR and NHEJ repair (Swindall et al., 2013).

1.3.1 Single strand BER

BER is the primary DNA repair pathway for single strand breaks (SSB). Its main function is to protect cells against mutations induced by endogenous DNA damaging agents. The pathway is initiated by specific DNA glycosylase enzymes, such as 8-Oxoguanine-DNA glycosylase 1 (OGG1), which recognise and excise damaged DNA bases by directly binding and hydrolysing the N-glycosylic bond to generate an abasic (AP) site. Several DNA repair proteins, including PARP-1, bind to the site of excision and recruit AP-endonuclease repair enzymes (Curtin, 2012). AP-endonuclease hydrolyses the AP site, enabling repair of the DNA break by one of two sub-pathways; short-patch BER or long-patch BER.

Short-patch BER is the predominant mode of BER. AP-endonuclease generates a 3' terminus at the site of DNA damage which allows DNA polymerase β to replace the missing nucleotide using the complementary strand as a template. DNA ligase completes repair in partnership with PARP-1 and XRCC1 which acts as a scaffold protein. Long patch BER is more complex. Up to 13 nucleotides are replaced by DNA polymerase $\beta/\delta/\epsilon$ and proliferating cell nuclear antigen (PCNA). Flap endonuclease 1 (FEN1) excises the DNA flap-like structure and DNA ligase reseals the DNA strand (Krokan and Bjørås, 2013, Curtin, 2012).

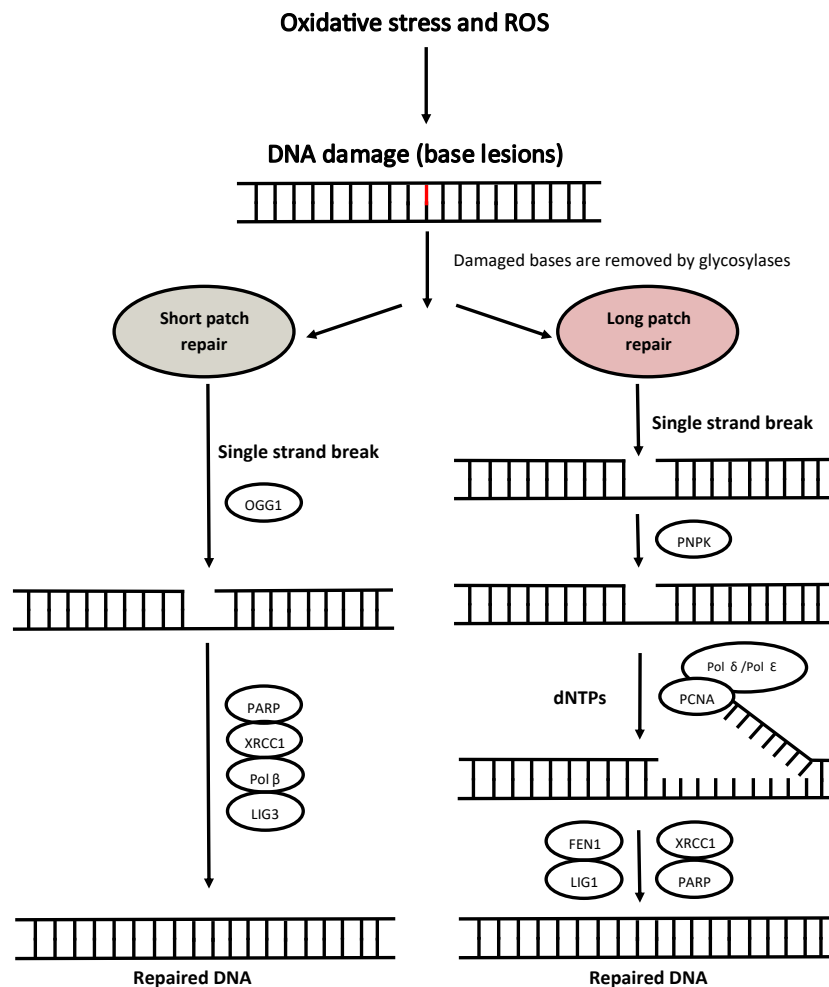


Figure 1.1: Model of base excision repair (BER).

BER is comprised of two pathways: short and long patch DNA break repair. The first steps in BER are break recognition, base removal and incision. The nick in the DNA is repaired by short patch BER (the predominant pathway) or long patch BER. The BER repair pathway in which a break is repaired is dependent on the state of the 5' and 3' ends. Ligation completes the repair process (adapted from Curtin, 2012).

1.3.2 Double strand break repair

The most dangerous form of DNA lesion is a DSB. If left unrepaired DSBs pose a major threat to genomic integrity, and may lead to genetic mutation, carcinogenesis and ultimately cell death (Hoeijmakers, 2001). They arise from IR, ROS, chemotherapeutic agents and during replication of a SSB or other type of DNA lesion. IR directly affects the structure of DNA and induces a DSB by directly colliding with it and breaking the phosphodiester backbone. It is also indirectly involved in DNA damage by splitting water molecules near DNA which generates ROS. ROS induces further damage by reacting with nearby DNA to generate abasic sites, SSBs and sugar moiety modifications which may spontaneously convert into DSBs. Together, these structural

changes to DNA result in cell cycle arrest and consequently cell death (Borrego-Soto et al., 2015, Cannan and Pederson, 2016).

To overcome the threats posed by DSBs, cells detect and repair the damaged DNA through highly conserved DSB repair pathways. The two main DSB repair pathways are NHEJ and HR (Figure 1.2). The origin and stage in the cell cycle when the DSB occurs determines which pathway is initiated to complete repair (Jackson, 2002).

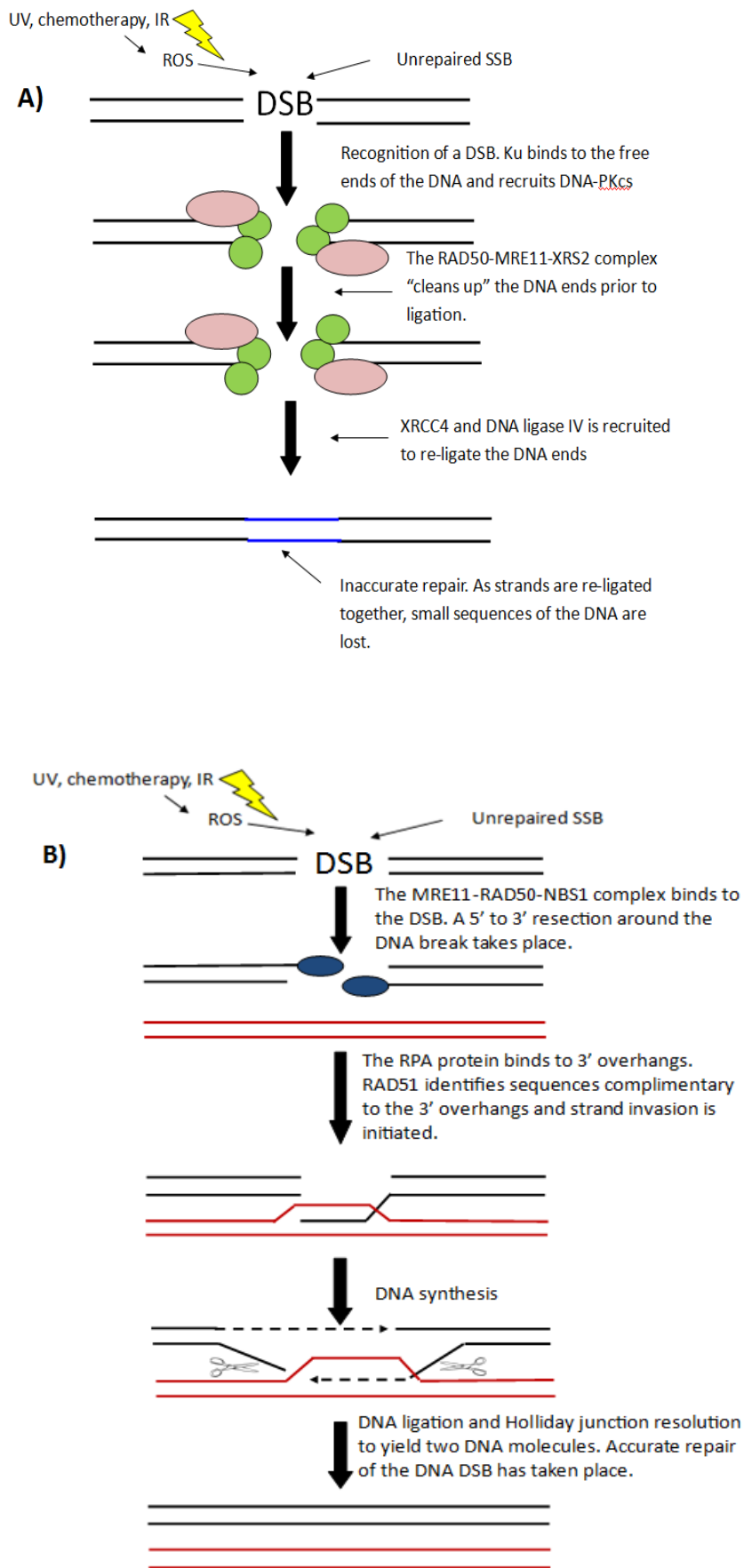


Figure 1.2: The principle DNA double strand break repair pathways.
 (A) Non-homologous end-joining and (B) Homologous recombination.

1.3.2.1 Non-homologous end joining (NHEJ)

NHEJ occurs primarily in G₀/G₁ phase of the cell cycle and is the main pathway in which DSBs are repaired (Mao et al., 2008). The pathway mediates direct rejoining of the damaged DNA in the absence of a homologous template. The initial step of the pathway is recognition and binding of the Ku heterodimer (Ku70 + Ku80) to the DSB, which leads to the recruitment and activation of DNA-dependent protein kinase, catalytic subunit (DNA-PKcs) (Davis and Chen, 2013). Ku and DNA-PKcs form an active complex to bring together the ends of the DSB in readiness for processing and re-ligation. Various proteins, such as the MRE11-RAD50-NBS1 (MRN) complex, facilitate end processing of the DNA strands which are then synthesised by DNA polymerase. DNA ligase 4 and its associated protein XRCC4 complete repair (Christmann et al., 2003).

1.3.2.2 Homologous recombination (HR)

HR is an error free template-dependent repair pathway that occurs primarily in S and G₂ phase of the cell cycle. It is the favoured mechanism for the repair of DSBs which arise due to replication fork stalling or collapse (Helleday et al., 2007). The pathway is initiated by the MRN complex which recognises and binds to a DSB, leading to the stimulation and activation of ATM; a protein kinase that phosphorylates downstream effector targets such as p53, H2AX and BRCA1. The damaged DNA is resected by the MRN complex to expose single-stranded overhangs of DNA at the 3' ends on either side of the DSB. Replication protein A (RPA) then binds to the exposed single-stranded DNA ends and unwinds the DNA secondary structure, to enable RAD51 binding and formation of a helical nucleoprotein filament. RAD51 recognises and invades a homologous sequence of intact DNA on the sister chromatid and uses it as a template to repair the broken DNA ends by DNA synthesis (Hoeijmakers, 2001, Kowalczykowski, 2015).

1.4 Poly ADP-ribose polymerase-1 (PARP-1)

1.4.1 PARP discovery

The first PARP enzyme was discovered in the 1960's when Chambon et al. (1963) discovered enhanced synthesis of an acid insoluble material when adding nicotinamide mononucleotide (NMN) to chicken liver nuclear extracts incubated with $\alpha^{32}\text{P}$ -ATP. The acid insoluble product

was later identified as a polymer of adenosine diphosphoribose (ADP-ribose), a molecule created from ATP and NMN with NAD⁺ (Nicotinamide adenine dinucleotide) as the immediate substrate (Chambon et al., 1966). Nishizuka et al. (1967) evidenced that NAD⁺ contained an ADP-ribose moiety which was integrated into the ADP-ribose polymer with the concomitant release of nicotinamide. The enzyme responsible for such reaction was initially named ADP-ribose transferase (ADPRT) but is now known as poly (ADP-ribose) polymerase-1 (PARP-1).

Since the discovery of PARP-1, many other genes containing the PARP signature have been identified and there are now 18 members of the PARP super-family (Héberlé et al., 2015, Citarelli et al., 2010). PARP's are nuclear enzymes that catalyse the transfer of ADP-ribose onto glutamic acid residues of themselves and histone proteins *via* the hydrolysis of NAD⁺ (Figure 1.3). Subsequently, Poly (ADP-ribose) (PAR) chains are formed; a process known as PARylation (Smith, 2001, de Murcia and de Murcia, 1994). PARP-1 is the most abundant isoform of the PARP super-family and will be the main focus of this thesis.

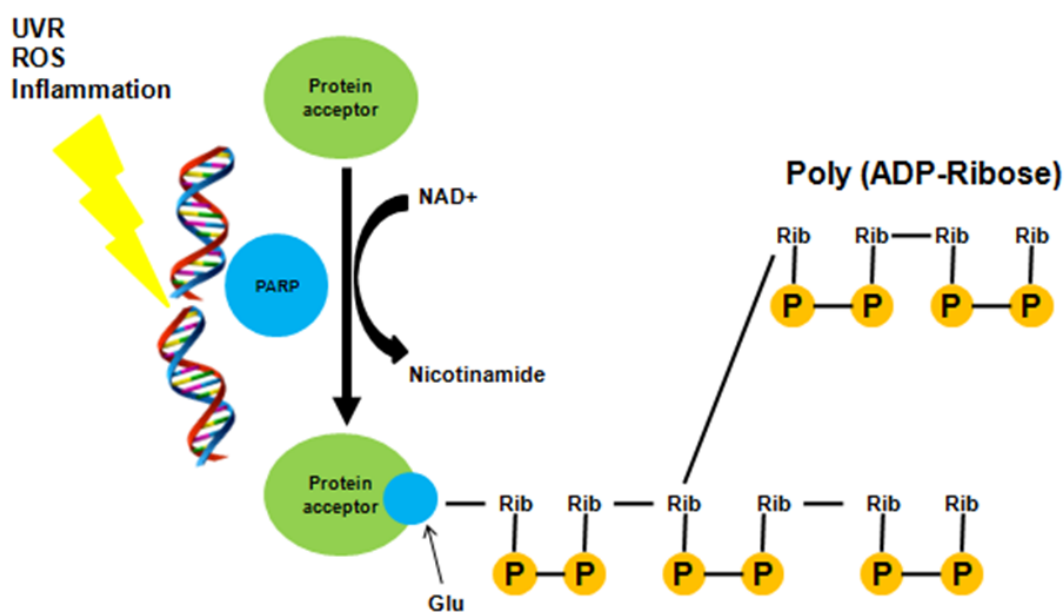


Figure 1.3: Schematic representation to show the process of PARylation in response to DNA damage induced PARP-1 activation.

1.4.2 Structure of PARP-1

The *PARP-1* gene is located on chromosome 1q41-42 and encodes the 1014 amino acid, 116KDa, PARP-1 protein. It is a nuclear enzyme that plays a role in many cellular processes including

transcriptional regulation, recombination, chromatin structure formation, gene expression, DNA repair and cellular dysfunction (Gibson and Kraus, 2012). The PARP-1 protein, shown in Figure 1.4, is comprised of three functional domains: an N-terminal DNA binding domain (DBD) , a central auto modification domain (AD) and a highly conserved C-terminal catalytic domain (CAT) (Kim et al., 2005).

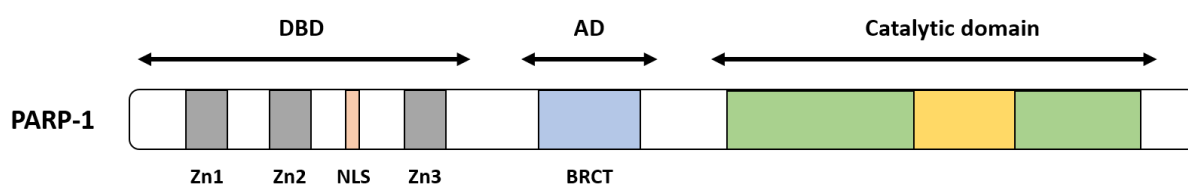


Figure 1.4: Schematic representation of the PARP-1 protein and its three domains.

The PARP signature sequence is located within the catalytic domain and comprises the sequence most conserved among PARPs (yellow box). Zn= zinc fingers, NLS= nuclear localisation zone, BRCT= BRCA1 carboxyl terminal.

The N-terminal DBD of the PARP-1 protein contains two zinc fingers (Zn1 and Zn2) which act as nick sensors to allow PARP-1 to recognise and bind to DNA breaks. The two zinc fingers play different roles in the recognition of DNA breaks. Zn1 recognises both DNA single and double strand breaks, however Zn2 detects only single strand breaks (de Murcia et al., 1994). A third zinc finger (Zn3) has more recently been identified and has been shown to play a role in the coordination of DNA-dependent enzyme activation (Langelier et al., 2011, Langelier et al., 2008). A nuclear localisation signal (NLS) that targets PARP-1 to the nucleus is also present within the N-terminal DBD.

The AD domain of PARP-1 is located in the centre of the PARP-1 enzyme. It comprises 15 highly conserved amino acid residues which allow the enzyme to poly (ADP-ribosyl)ate itself. The domain also comprises a BRCA1 C-terminal phosphopeptide-binding motif which is found in a number of proteins involved in the DNA damage response (Luo and Kraus, 2012a).

The CAT domain is the most conserved region of the PARP-1 protein. It contains the “PARP signature” sequence that is required for PAR synthesis (de Murcia et al., 1994).

1.4.3 PARP-1 and DNA repair

PARP-1 is a well-recognised DNA strand break-activated enzyme. It is best known for its role in the recognition and repair of DNA single strand breaks (SSB's) *via* the BER pathway, although it also plays a role in repair of double strand breaks (DSB's) by Homologous recombination (HR) and Non-homologous end joining (NHEJ) (Swindall et al., 2013, Veuger et al., 2004).

1.4.3.1 PARP-1 in single strand break repair

PARP-1 is catalytically activated following recognition and binding to a DNA SSB. Once active, PARP-1 transfers ADP-ribose units from nicotinamide adenine dinucleotide (NAD⁺) to itself and other substrates to produce poly ADP-ribose (PAR). This "PARylation" process creates a negatively charged target at the site of the SSB which attracts other DNA damage repair proteins to the breakage site to form the BER multi-protein complex. This complex is comprised of the scaffold protein XRCC1 (x-ray repair cross-complementing 1), DNA ligase III and DNA polymerase pol β (Javle and Curtin, 2011), as described in 1.3.1. Following PARylation, PARP-1 is released from the site of the DNA break to enable repair.

DNA damaging agents have been used to investigate the role of PARP-1 in BER. Potent activators of PARP-1 include DNA damaging agents that induce DNA lesions repaired by the BER pathway, such as monofunctional alkylating agents and ionising radiation (IR). UV irradiation on the other hand is not a potent activator of PARP-1 and predominantly causes lesions that are repaired by the NER pathway (de Murcia and de Murcia, 1994). Further studies by De Murcia et al. (1997) showed that PARP-1^{-/-} mice were more sensitive to IR and oxidative damage, and cells from these mice were increasingly sensitive to the alkylating agent N-methyl-N-nitrosourea (MNU). A more recent study by Fisher et al. (2007) assessed the importance of PARP-1 in SSB repair. PARP-1^{-/-} and wild-type DT40 chicken cells were exposed to the DNA damaging agent H₂O₂ and levels of DNA strand breaks were measured. H₂O₂ was found to induce similar levels of DNA damage in both cell types, however PARP^{-/-} cells took longer to repair DNA strand breaks following removal of the DNA damaging agent. To confirm whether the delay in strand break repair rate was due to defects in SSB repair, the experiments were repeated in Ku70^{-/-} and XRCC3^{-/-} DT40 cells which lack functional DNA DSB repair. PARP-1^{-/-} cells were still the only cells which took longer to

repair DNA strand breaks and it was therefore concluded that such observation was indeed due to defective SSB repair.

1.4.3.2 PARP-1 in double strand break repair

For decades the focus has been on the role of PARP-1 in SSB repair, however in more recent years PARP-1 has emerged as a key player in DSB repair by HR and NHEJ (De Vos et al., 2012). DSB's are cytotoxic lesions that drive genetic instability and activate cell death if unrepaired (Pfeiffer et al., 2000). Studies have revealed that PARP-1 becomes activated upon recognition and binding to a DSB (Benjamin and Gill, 1980). Its exact roles in DSB repair are still under investigation.

The interaction of PARP-1 with DSB repair proteins such as ATM, MRE11 and NBS1 highlight a role for PARP-1 in the HR repair pathway (Haince et al., 2008). PARP-1 binds to stalled replication forks arising from unrepaired SSBs and becomes activated. Once activated, PARP-1 interacts with MRE11 to “jumpstart” the stalled fork and to enable HR repair of the DNA (Bryant et al., 2009). A Biochemical study uncovered an interaction between PARP-1 and DNA-PK; a protein associated with the NHEJ DSB repair pathway (Ruscetti et al., 1998), as previously described in 1.3.2.1. PARP-1 was shown to stimulate and ADP-ribosylate DNA-PK in the presence of NAD⁺; enabling phosphorylation of PARP-1 by DNA-PK. Chemical inhibition of PARP blocked DNA-PK stimulation; suggesting that such enzymes may function together in response to DNA damage. Veuger et al. (2004) further supported the role of PARP in NHEJ DSB repair. Inhibition of PARP-1 and DNA-PK was shown to inhibit DSB repair following IR exposure, and inactive PARP-1 suppressed DNA-PK activity and vice versa. Other studies have proposed that PARP-1 is involved in an alternative NHEJ pathway which operates when the classical NHEJ pathway is genetically or chemically compromised. Wang et al. (2006) revealed that PARP-1 competes with Ku for binding to a DNA DSB and with the help of DNA ligase III is able to repair the damage.

While specific mechanisms have not yet been identified, these studies suggest that PARP is a key player in DSB repair. Cells deficient in proteins involved in both the HR or NHEJ DNA repair

pathways have shown sensitivity to PARP inhibitors and exploitation of PARP-1 as a therapeutic target in disease is a current area of investigation (Yi et al., 2019).

1.4.4 PARP-1 as a mediator of tumour promoting inflammation

Despite its anti-mutagenic role in DNA repair, PARP-1 activation is also implicated in inflammatory signalling and disease. Continuous activation of PARP-1 in response to ROS-mediated DNA damage and chronic inflammation promotes stress signalling, leading to increased inflammatory signalling, cellular dysfunction and DNA damage (Swindall et al., 2013).

One of the first mediators of inflammation identified as a target for PARP-1 was NF- κ B; a well-known inflammatory transcription factor (described in section 1.5). Briefly, hyperactivated PARP-1 upregulates NF- κ B in response to DNA damage, leading to inflammation and upregulation of pro-inflammatory cytokines such as tumour necrosis factor α and interleukin 6 (Wang et al., 2017). PARP-1 deficient cells have been found to be defective in NF- κ B dependent transcription activation, but not in its nuclear translocation, in response to TNF- α (Oliver et al., 1999). The group also discovered that macrophages from PARP^{+/+} mice exposed to lipopolysaccharide treatment presented rapid NF- κ B activation, but macrophages from PARP-1^{-/-} mice did not. The findings demonstrated a functional association between PARP-1 and NF- κ B; leading to the synthesis of inflammatory mediators.

Despite its role as a co-factor for NF- κ B, PARP-1 has also been implicated in the switch of cell death pathways from highly regulated apoptosis, to inflammatory necrosis in response to high levels of DNA damage and ROS (Swindall et al., 2013), as depicted in Figure 1.5.

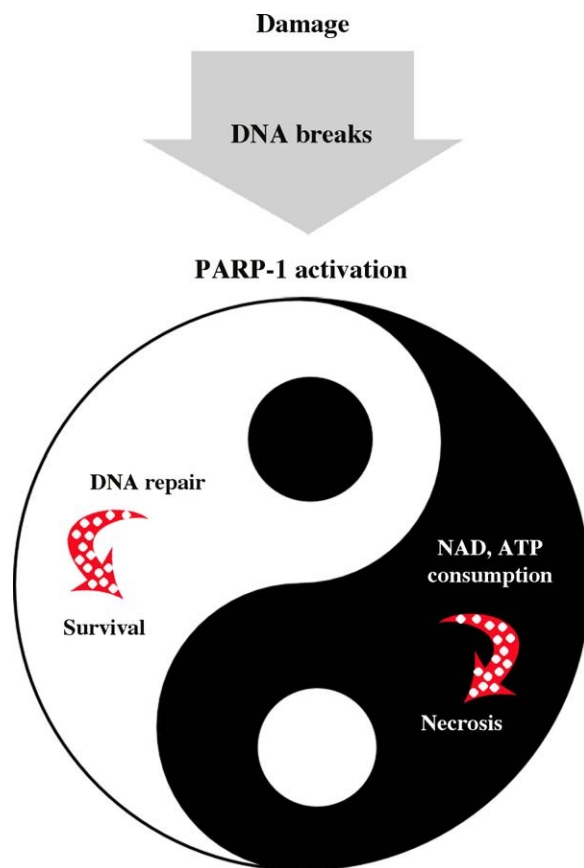


Figure 1.5: The two sides to PARP-1 activation.

PARP-1 acts as a pro-survival factor (white segment) to maintain cell survival and genomic stability. Prolonged activation of PARP-1 promotes tumorigenesis due to over production of NAD and ATP consumption which drives genetic instability and cell necrosis (black segment) (Giansanti et al., 2010).

1.4.5 PARP-1 activity

PARP-1 activation is largely driven by DNA damage (as discussed in section 1.4.3) and it is therefore not surprising that PARP-1 enzyme activity is upregulated in cancer. Increased PARP-1 activity and formation of PAR has been reported in several tumour types including hepatocellular, breast, melanoma and prostate; highlighting the potential of PARP-1 activity as a biomarker to determine which patients will be benefit from PARP inhibitor therapy (Nomura et al., 2000, Schiewer and Knudsen, 2014).

1.4.6 PARP-1 activity and expression

PARP-1 protein is overexpressed in a number of different tumour types compared to non-malignant tissues (reviewed in Wang et al. (2017)). Ossovskaya et al. (2010) assessed PARP-1 expression in over 8000 primary malignant and normal human tissues. PARP-1 expression was low in majority of normal specimens but was significantly increased in several malignancies including those derived from the breast, ovaries, uterus, skin and lung. Other studies have also

demonstrated overexpression of PARP-1 in prostate, colorectal and glioblastoma (Schiewer et al., 2012, Dziaman et al., 2014, Murnyak et al., 2017).

1.4.7 PARP-1 Inhibitor development

The first PARP inhibitor, 3-aminobezamide (3-AB), was identified almost forty years ago during a pivotal study where a defect in the BER pathway was identified in the presence of 3-AB, resulting in defective DNA repair and increased cytotoxicity to DNA methylating agents in leukaemia cells. It was these findings that demonstrated the potential of 3-AB as a therapeutic strategy for the treatment of leukaemia and other cancers (Durkacz et al., 1980). Since then, many more potent and more specific small molecule inhibitors of PARP-1 have been developed and in 2003 the first PARP-1 inhibitor (PARPi), AG014699/Rucaparib entered clinical trials (Plummer et al., 2008). There are now four PARP inhibitors (Rucaparib, Olaparib, Niraparib and Talazoparib) licensed for therapeutic use by the FDA and a number of others are in clinical development (reviewed in Yi et al. (2019)).

1.4.7.1 Rucaparib development

The studies carried out for submission of this thesis utilised the PARP inhibitor Rucaparib (AG014699). As previously mentioned, Rucaparib was the first PARP inhibitor to enter anti-cancer clinical trials and its development from bench to bedside will be described in further detail below.

Rucaparib was developed by the laboratories of Roger Griffin and Bernard Golding at Newcastle University in collaboration with Cancer Research UK and Agouron Pharmaceuticals (part of Pfizer GRB). In the early 1990s, the group aimed to make and test novel PARP inhibitors, which included the quinazolinones and the benzimidazole carboxamides, for use as both chemo- and radio-sensitizers. The compounds were tested in a range of cell culture models including human cancer cells. Despite poor aqueous solubility in all compounds tested, the benzimidazole carboxamides were most potent (Curtin et al., 2004, Smith et al., 2005). The amine substitution of 2-aryl ring at the para position of the core structure enhanced compound potency and PARP-1 inhibitory activity, however issues with aqueous solubility remained (White et al., 2004). To overcome this issue, the groups at Agouron and Newcastle developed tricyclic lactam indoles

which lead to the discovery of the lead PARP-1 inhibitor AG014361 (Reviewed in Curtin and Szabo (2013)). Further development led to the identification of AG014447 and it was the phosphate salt of this compound, AG014699 (Rucaparib), that was selected for clinical trial due to its improved aqueous solubility and high potency as a PARP-1 inhibitor in combination with temozolomide in xenograft models (Thomas et al., 2007, Plummer et al., 2008). In October 2019 Rucaparib, known commercially as Rubraca®, was approved for use on the NHS in female patients with relapsed ovarian, fallopian tube and peritoneal cancers (NICE, 2019). The therapeutic potential of PARP inhibitors is discussed in further detail below.

1.4.7.2 PARP inhibitors for cancer therapy

PARP inhibitors have shown potential in clinical medicine as potentiators of chemotherapy and radiotherapy; and as stand-alone agents which selectively kill cells with defective DNA repair (Drew and Plummer, 2009). They may be the first deliberate examples of cancer therapy targeted at a specific gene product.

1.4.7.2.1 PARP inhibitors in combination therapy

PARP inhibitors have been utilised in combination with chemo- or radiotherapy to inhibit the repair of genotoxic lesions caused by these DNA damaging therapies. Combined therapy aims to overcome single therapy resistance and improve therapeutic response.

Various studies have demonstrated the effectiveness of PARP inhibitors in combination with the alkylating agent temozolomide, a known activator of PARP-1 and inducer of SSBs in tumour cell and xenograft models (Delaney et al., 2000, Curtin et al., 2004, Calabrese et al., 2004). As previously mentioned, the first human trial using a clinical PARPi established a tolerable dose when combined with temozolomide in advanced melanoma patients (Plummer et al., 2008). The group also reported improved response rate in metastatic melanoma patients exposed to Rucaparib and temozolomide in combination, compared with temozolomide alone (Plummer et al., 2013). PARPis have also been shown to enhance the cytotoxicity of topoisomerase 1 poisons, inducers of DNA strand breaks, such as topotecan, camptothecin and irinotecan in *in vitro* and *in vivo* models. Studies have demonstrated the efficacy of the PARPi AG14361 in sensitising leukaemia cells to camptothecin by increasing the persistence of DNA strand breaks (Smith et al., 2005). *In*

vivo mouse studies demonstrated enhancement of topotecan-induced tumour growth delay following Rucaparib induced PARP-1 inhibition in neuroblastoma (Daniel et al., 2009). PARP inhibitors also enhance radiotherapy cytotoxicity in tumours (reviewed in Zaremba and Curtin (2007)). The work of Veuger et al. (2003) showed inhibition of IR-induced DNA DSB repair in mouse embryonic fibroblasts exposed to the novel PARPi AG14361; highlighting the potential of PARP inhibitors as tumour radiosensitizers. More recent studies have supported these findings, demonstrating radio-sensitization by PARP inhibition in colon, glioma and ovarian cancers (Calabrese et al., 2004, Dungey et al., 2008, Bi et al., 2018). These results support a role for combining radiotherapy and PARP inhibitors for cancer therapy in patients who fail to respond to traditional treatments. Clinical trials are currently underway (www.clinicaltrials.gov).

1.4.7.2.2 *PARP inhibitors as a monotherapy*

In 2005, two pivotal studies reported the efficacy of PARP inhibitors as stand-alone therapies in *BRCA1* and *BRCA2* defective tumours (Bryant et al., 2005, Farmer et al., 2005). Bryant et al. (2005) implanted *BRCA2* deficient and complemented cells into nude mice and monitored tumour growth following a five-day exposure to the PARP inhibitors NU1025 and AG14361, precursors to Rucaparib. Three out of the five mice subject to *BRCA2* deficient tumours were sensitive to PARP inhibition, with one mouse presenting complete remission. Farmer et al. (2005) also reported increased sensitivity of *BRCA1* and 2 deficient cell lines to the PARP inhibitors KU0058684 and KU0058948. These studies demonstrated the effectiveness of PARP inhibitors as single agents in the selective killing of tumour cells deficient in *BRCA*. They concluded that increased sensitivity to PARP inhibition in these cell lines was due to synthetic lethality; when loss of two genes is lethal and results in cell death. In this case, synthetic lethality following PARP inhibition occurred due to the accumulation of DNA SSBs resulting in un-repaired stalled replication forks and consequently DSBs. *BRCA* deficient cells are unable to repair these breaks due to defective HR and therefore are subject to death (Figure 1.6). PARP inhibitors as monotherapies are now approved for use in the clinic in patients with *BRCA* defective breast and ovarian tumours (Deeks, 2015, Moore et al., 2018, McCann and Hurvitz, 2018, Jiang et al., 2019). Evidence also supports a role for PARP inhibitors in sporadic cancers harbouring defects in other

components of the HR DNA repair pathway. These defects induce a BRCA-like phenotype and this concept is known as “BRCAness” (Reviewed in Lim and Ngeow (2016)).

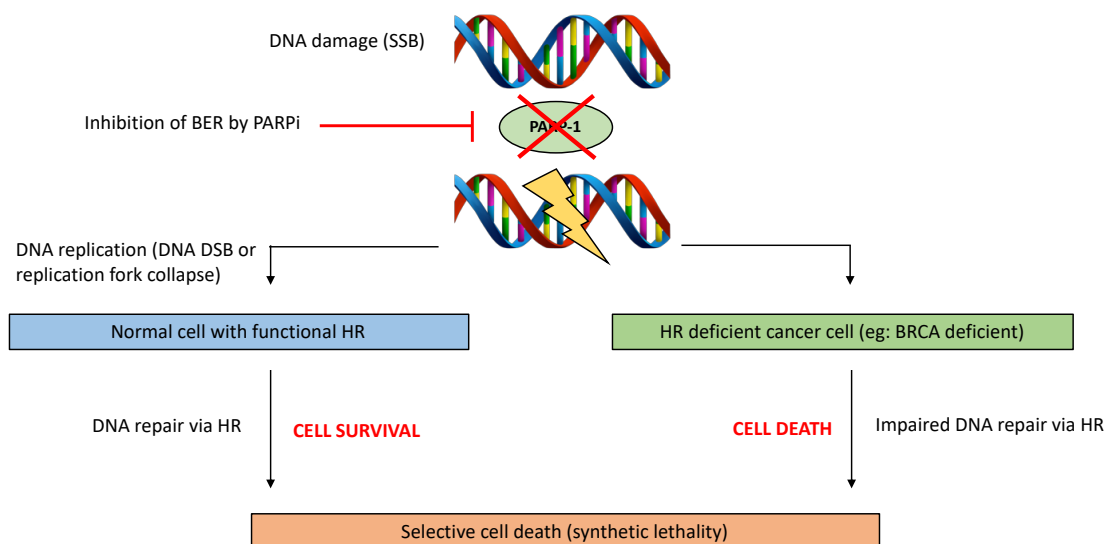


Figure 1.6: Schematic representation of synthetic lethality.

DNA damage induces SSBs which are repaired by BER. Inhibition of BER by PARP inhibition results in SSB persistence. Unrepaired SSBs lead to DSB formation which are normally repaired by HR. In the absence of BRCA, DNA cannot be repaired, or are repaired by error prone NHEJ, leading to genomic instability and cell death. Figure adapted from (Banerjee et al., 2010).

1.4.7.3 PARP inhibition in prostate cancer

Advanced prostate tumours often harbour mutations in DDR genes such as *BRCA1*, *BRCA2*, *ATM* and *RAD51*. Tumours with mutations in these genes are at increased risk of metastatic progression and poor prognosis, which makes them suitable candidates for PARPi therapy (Pritchard et al., 2016). A phase 2 clinical trial (TOPORP-A, Trial of PARP inhibition in Prostate cancer) reported a high response to the PARP inhibitor Olaparib in metastatic, castration-resistant prostate cancer patients with defective DNA-repair genes. Next generation sequencing of DNA obtained from patient biopsies identified homozygous deletions and/or deleterious mutations in DNA repair genes and 88% of tumours harbouring these defects were sensitive to Olaparib treatment (Mateo et al., 2015). These results have now received therapy designation by the FDA for treatment of *BRCA1/2* or *ATM*-mutation metastatic PC. Trials assessing potential “BRCAness” in PCs are ongoing to identify other potential biomarkers that may predict tumour response to PARPi (Ramakrishnan Geethakumari et al., 2017).

1.5 Nuclear factor kappa B (NF- κ B)

Transcription factors such as Nuclear factor kappa B (NF- κ B) regulate and respond to changes in the environment by influencing gene expression (Hayden and Ghosh, 2012). As part of a molecular signalling cascade, NF- κ B proteins are able to induce and repress the expression of genes which are involved in the regulation of important biological processes such as immune response, apoptosis, inflammation, cell stress and proliferation (Oeckinghaus and Ghosh, 2009). Dysregulation of NF- κ B activity has been implicated in the pathology of diseases such as cancer, as mentioned in section 1.4.4 and below in section 1.5.3, and recently the NF- κ B signalling pathway has shown potential for exploitation in cancer therapy (Reviewed in Pires et al. (2018).

1.5.1 The NF- κ B superfamily and associated proteins.

NF- κ B is an entire family of transcription factors which each share a N-terminal Rel homology domain (RHD) comprised of approximately 300 amino acids (Figure 1.7). The RHD is responsible for DNA binding, dimerization and nuclear translocation following interaction with inhibitors of NF- κ B (I κ B) proteins (Xiao and Fu, 2011).

There are five genes which encode the family of NF- κ B transcription factors: *NFKB1*, *NFKB2*, *RELA*, *RELB* and *c-REL*. The protein products of these genes are p50, p52, p65/RelA, RelB and c-Rel, respectively (Pires et al., 2018). RelA, RelB and c-Rel proteins contain transactivation domains (TAD) which are responsible for the transcriptional activity of these proteins at target gene promoters. The p50 and p52 proteins do not contain TADs and mediate their transcriptional activity via heterodimerisation or interaction with transcriptional regulators (Hayden and Ghosh, 2008).

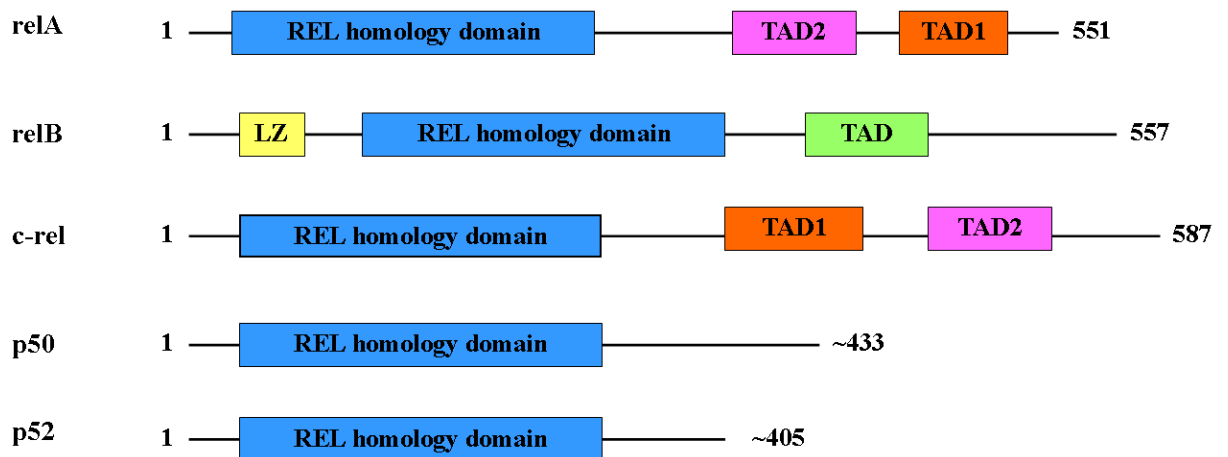


Figure 1.7: NF-κB subunits which comprise the NF-κB family.

Each subunit has a DNA binding and dimerization domain known as the REL homology domain. RelA, RelB and c-Rel also comprise other dimers which determine context-specific gene regulation by NF-κB (Perkins, 2012). LZ: leucine zipper. TAD: Transactivation domain.

1.5.2 NF-κB activation pathways.

There are two fundamental NF-κB activation pathways (Figure 1.8), referred to as the canonical (classical) and non-canonical (alternative) pathways. In both pathways, NF-κB activation within the cell is tightly controlled by an IκB kinase (IKK) complex which is comprised of: IKKα, IKKβ and NEMO (Gilmore, 2006).

1.5.2.1 Canonical activation of NF-κB

The canonical NF-κB pathway is activated in response to inflammatory stimuli in the cellular environment such as tumour necrosis factor receptor (TNFR), IL-1 receptor (IL-1R), growth factors or exposure to bacterial products such as lipopolysaccharides (LPS). These receptors activate the IκB kinase (IKK) complex, which phosphorylates and degrades IκB. NF-κB proteins are then free to translocate to the nucleus where they bind to promoter elements and activate expression of various genes (Sun and Ley, 2008, Oeckinghaus and Ghosh, 2009, Huang and Hung, 2013). For example, NF-κB induces the expression of various pro-inflammatory genes, including those encoding TNF-α or IL-1; inflammatory cytokines that are implicated in the inflammatory response to infections and disease (Tak and Firestein, 2001). The canonical pathway can also be activated by genotoxic stimuli, as discussed in section 1.5.3.

1.5.2.2 Non canonical activation of NF- κ B

The non-canonical signalling pathway for activation of NF- κ B is primarily for the activation of RelB complexes during B and T cell organ development. As such the pathway proceeds through an IKK complex excluding NEMO and becomes activated only by a small selection of specific stimuli such as: B-cell activating factor (BAFF), Lymphotoxin β (LT β), CD40 ligand and receptor activator of NF- κ B ligand (RANKL). Receptor binding leads to the synthesis of NF- κ B-inducing kinase (NIK); which causes the formation of p52 from p100 after IKK α complex activation. IKK α activation sequentially leads to phosphorylation of two serine residues adjacent to the p100 complex domain, which in turn liberates the RelB complex; allowing translocation into the nucleus and NF- κ B activated gene expression (Xiao and Fu, 2011).

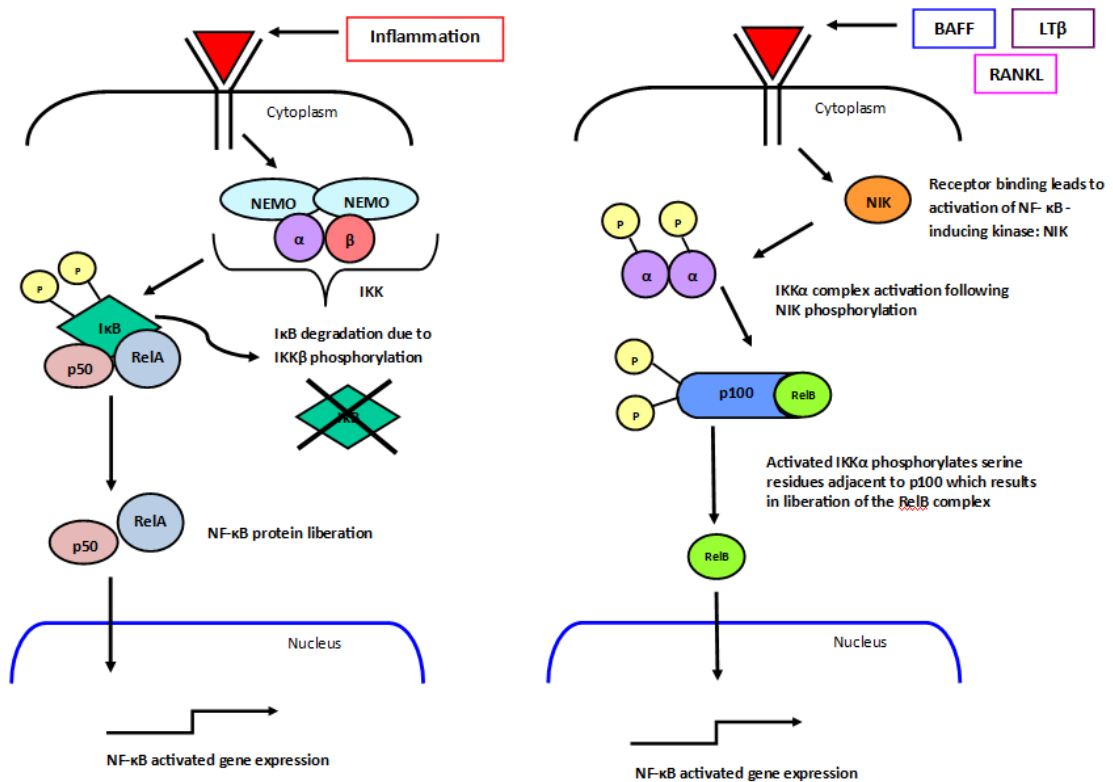


Figure 1.8: Schematic representation of the canonical and non-canonical NF- κ B signalling pathways. The canonical pathway (left) is activated by stimuli such as TNF- α and IL-1, leading to phosphorylation and degradation of I κ B. The p50-p50 heterodimer is release enabling translocation into the nucleus. The pathway may also be activated in response to genotoxic stress. The non-canonical pathway (right) results in NIK phosphorylation and activation of IKK α which phosphorylates p100. Phosphorylation of p100 liberates RelB, allowing translocation into the nucleus and activated expression. Figure adapted from Gilmore (2006).

1.5.3 DNA damage-induced NF- κ B activation as a driver of cancer.

A critical connection between NF- κ B, inflammation and cancer has been established in various human cancers including those derived from the breast, prostate, lymphoma, ovaries and lungs (Karin, 2009, Chen et al., 2011, Jin et al., 2014b, Wang et al., 2015a). NF- κ B signalling in tumour progression is complex, but may be in part due to mutational activation of upstream components in the IKK-NF- κ B signalling pathways; or exposure to pro-inflammatory stimuli in the tumour micro-environment (Karin et al., 2002). In normal cells NF- κ B activation supports the immune defence system by targeting unstable cells and eliminating them *via* the release of cytokines. In cancers, enhanced NF- κ B signalling exerts a pro-tumorigenic effect by excessive cytokine release and growth factor production (Hoesel and Schmid, 2013). The immune response caused by prolonged inflammation promotes DNA damage, leading to oncogenic mutation, cell migration and tumour initiation (Xiao and Fu, 2011).

DNA damage-induced NF- κ B activation has been widely documented and is thought to coordinate cell survival, alongside DNA repair, by upregulating anti-apoptotic genes; an enabling characteristic of cancer development (Coussens and Werb, 2002). NF- κ B activation in response to DNA damage drives carcinogenesis by enhancing cellular stress, recruiting inflammatory factors and accumulating further DNA damage; leading to malignant progression, resistance to chemotherapy and IR. To this end, chemical inhibition of NF- κ B is an attractive therapeutic target (Janssens and Tschopp, 2006). Interactions between PARP-1 and NF- κ B have been well documented. Hassa et al. (2001) showed that PARP-1 directly interacts with NF- κ B to synergistically activate transcriptional factors independent of enzymatic activity and DNA-binding activity. DNA repair inhibitors such as PARP inhibitors can limit NF- κ B activation and sensitive tumour cells to chemotherapy and IR. For example, breast cancer cell models expressing varied levels of activated NF- κ B were exposed to the PARP-1 inhibitor AG14361 following exposure to lethal doses of IR; a known inducer of NF- κ B activity. AG14361 was shown to inhibit NF- κ B binding to DNA following IR, highlighting a role for PARP-1 in the activation of NF- κ B (Veuger et al., 2009). More recent studies from the same group demonstrated that radiosensitisation by PARP-1 inhibition is exclusively due to NF- κ B inhibition, and not due to the

inhibition of DNA repair. Using the PARP inhibitor AG014699 (Rucaparib) and siRNA targeting PARP-1, they showed a significant increase in apoptosis and a reduction in cell survival following exposure to IR in mouse embryonic fibroblasts (MEF) proficient in NF- κ B p65, but not MEFs deficient in NF- κ B p65 (Hunter et al., 2012). The group proposed that IR activates PARP-1 leading to the formation of negatively charged PAR polymer and activation of NF- κ B. PAR attracts p65 binding, resulting in protection against apoptosis and radio-resistance. In the presence of Rucaparib, PARP is unable to form PAR and hence there is a reduction in DNA binding and transcriptional activation of NF- κ B following IR, with radio-sensitization and increased apoptosis. Other studies have also supported the efficacy of PARP inhibitors as inhibitors of tumour proliferation and invasion by attenuating NF- κ B signalling (Martin-Oliva et al., 2004, Wang et al., 2013).

1.5.3.1 NF- κ B activation in prostate cancer

NF- κ B signalling has been implicated in prostate cancer progression and poor prognosis. Constitutive activation and nuclear expression of NF- κ B and IKK α has been observed in aggressive AR deficient prostate cancer cell lines and patient samples, but not in AR proficient cells; suggesting that activation of NF- κ B may contribute to the malignant properties of AR deficient tumour cells (Lindholm et al., 2000). Other studies have also demonstrated that NF- κ B activation maintains androgen independent growth of prostate tumours cells (Jin et al., 2008a). The group also investigated the role of NF- κ B signalling in PC initiation and progression using a NF- κ B-activated prostate cancer mouse model. They reported activation of NF- κ B following deletion of one I κ B α allele did not induce tumorigenesis, but continuous NF- κ B activation enhanced earlier onset of PC in a Hi-Myc PC mouse model. To further explore the mechanism by which NF- κ B signalling contributes to tumour progression, an NF- κ B gene expression signature was generated from a non-malignant NF- κ B-activated androgen-depleted mouse prostate. The signature successfully distinguished between different subsets of PC and predicted clinical outcome (Jin et al., 2014b). Nuclear accumulation of IKK α is also associated with AR independent PC development and studies have found that it is necessary for metastasis in transgenic adenocarcinoma of the mouse prostate (TRAMP) mice. The exact mechanisms are

unknown but nuclear IKK α has been shown to induce a metastatic phenotype by repressing transcription of the tumour suppressor maspin (Luo et al., 2007).

Other studies have correlated constitutive activation of the NF-kB p65 subunit and its binding to DNA with increased Gleason grade and prostate tumour aggressiveness and metastasis. Metastatic PC-3M cells transfected with mutated IKB α to block NF-kB activity were injected into the prostate gland of nude mice. Mice exposed to control PC-3M cells produced fast growing, aggressive tumours, whereas PC-3M cells with IKB α mutation produced slow growing tumours with limited metastatic potential. These data show the significance of NF-kB activity as a driver of tumour progression and metastasis (Huang et al., 2001). Immunohistochemical analysis of prostate samples revealed increased nuclear staining for NF-kB p65 in high grade adenocarcinoma samples compared to benign tumour tissues (Shukla et al., 2004). A further indication for the role of NF-kB signalling in PC proliferation and progression is the inhibitory effect of the NF-kB inhibiting drug Aspirin on prostate cancer cell proliferation, migration and invasion (Lloyd et al., 2003, Bilani et al., 2017).

Together these findings support pro-inflammatory signalling and constitutive activation of NF-kB as drivers of tumour progression and malignancy in PC; making inhibition of NF-kB signalling an attractive therapeutic target.

1.5.3.2 *NF-kB in other cancers*

Aberrant NF-kB signalling has also been implicated in other cancers and examples are presented below in Table 1.3.

Table 1.3: NF-kB signalling in various tumour types.

Cancer sample	Key study findings	Reference
Breast cancer		
Breast cancer cell lines	Hormone-independent breast cancer cells presented high constitutive NF-kB activation, and this was associated with proliferation. Inhibition of NF-kB activation by repression of Ikb α super-repressor reduced proliferation.	(Yamaguchi et al., 2009)

Breast cancer cell lines and tumour specimens	NF-kB p65 was constitutively active in ER- cell lines and tumour samples. All of these tumours were poorly differentiated with metastasis and poor prognosis.	(Nakshatri et al., 1997)
Breast cancer specimens	NF-kB p65 was activated predominantly in ER- breast cancers. NF-kB disabled cell death pathways and permitted cell proliferation; contributing to tumour progression.	(Biswas et al., 2004)
Lung cancer		
Lung specimens	I κ B α phosphorylation and NF-kB p65 nuclear staining was significantly increased in non-small cell lung cancer cells compared to normal epithelial cells. I κ B α expression and nuclear p65 correlated with poor survival rates.	(Jin et al., 2008b)
Non-small cell lung cancer meta-analysis on published articles	Higher NF-kB expression was associated with short survival and was closely associated with tumour stage, metastasis and survival. They concluded that NF-kB expression may be an unfavourable prognostic marker.	(Gu et al., 2018)
Lung cancer specimens	NF-kB expression was higher in de-differentiated lung cancer specimen compared to normal specimens. Expression correlated with reduced apoptosis indicating unfavourable prognosis for overall survival.	(Zhang et al., 2006)
Haematological cancer		
Acute lymphoblastic leukaemia (ALL)	Constitutive NF-kB activation is a common characteristic in ALL and is plays a role in leukaemia cell survival.	(Kordes et al., 2000)
Acute myeloid leukaemia (AML)	Pharmacological inhibition of NF-kB in primary AML blasts induced apoptosis. This was not the Normal hematopoietic stem cells were not affected by such inhibition suggesting that inhibition of the NF-kB pathway as a potential therapeutic approach for AML.	(Frelin et al., 2005)
Ovarian cancer		
Ovarian cancer specimens	NF-kB p65 expression was increased in epithelial ovarian tumours compared to normal ovarian tissue and expression was correlated to poor histological differentiation and late clinical stage.	(Guo et al., 2008)
Ovarian cancer specimens	NF-kB p65 and RelB were co-expressed with IKK α in newly diagnosed advanced ovarian cancers. NF-kB p50 expression was associated with poorer prognosis. They proposed that the p50 gene is a direct target for the p65 gene and becomes upregulated to attenuate the cascade. p50 homodimer accumulation in the cytoplasm fails to down-regulate NF-kB target pro-survival factors in the ovarian cells.	(Annunziata et al., 2010)

Skin cancer		
Melanoma and melanocyte cells	NF-kB is constitutively active in melanoma cells compared to normal melanocytes and is further increased under oxidative stress.	(Meyskens et al., 1999)
Tissue biopsies	NF-kB p65 proteins are overexpressed in the nuclei of dysplastic nevi and melanoma cells compared to normal nevi and melanocytes. IKB α expression is decreased in melanomas relative to normal skin.	(McNulty et al., 2004)

1.6 Maspin

Maspin is a 42kDa protein encoded by the class II tumour suppressor gene *SERPINB5*. It was first identified as a tumour suppressor in 1994 by subtractive hybridisation to identify candidate tumour suppressor genes in human breast carcinoma cells (Zou et al., 1994). Class II tumour suppressor genes function in the negative regulation of cell growth. These genes are not altered at the DNA level, but changes to their regulation, and consequently expression, effect their phenotype (Sager, 1997).

1.6.1 Structure and function

Maspin belongs to the serine protease inhibitor (serpin) superfamily. The distinctive structural characteristics of serpin members are 3 β -pleated sheets (A-C), 8-9 α -helices (A-H) and a reactive centre loop (RCL) which enables optimal configuration for protease binding and inhibition (Law et al., 2006). Figure 1.9 illustrates the crystal structure of maspin. It is a unique member of the serpin family and is characterised as a non-inhibitory serpin due to its short, hydrophobic RCL which makes it incapable of protease inhibition.

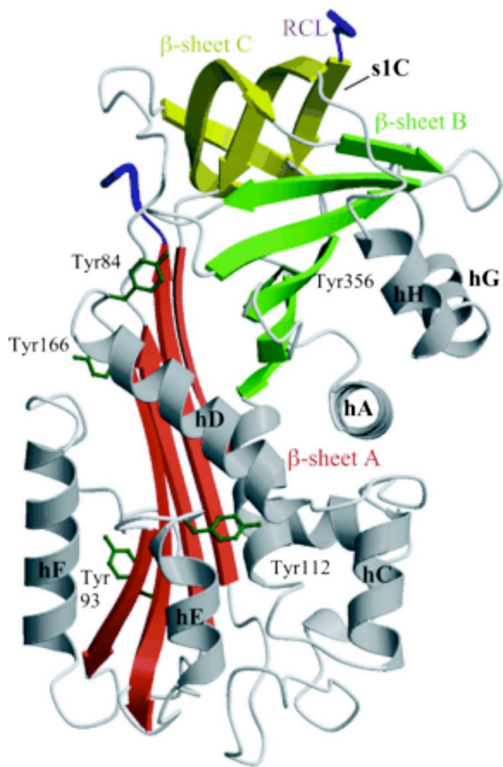


Figure 1.9: X-ray crystal structure of maspin.

Maspin is comprised of 3 β -pleated sheets, α -helices and a short RCL. Figure from (Law et al., 2005)

Despite its non-inhibitory activity, the RCL of maspin has been shown to be required for many of maspin's functional abilities such as its effects on cell adhesion, invasion and apoptosis (Sheng et al., 1996, Ngamkitidechakul et al., 2003, Khanaree et al., 2013). Other studies have refuted the role of the RCL of maspin as an inhibitor of cell migration and invasion (Cella et al., 2006, Ravenhill et al., 2010). Such contentions in the literature highlight a need to conduct further research to ascertain the effect of the RCL on cell behaviours.

Another unique aspect of the maspin protein structure is its G α -helix (G-helix) which is capable of an "open and closed" conformational change which results in a rearrangement of charged residues within the molecule (Law et al., 2005). A fully functioning G-helix is essential for maspin functioning and effects of cell migration and adhesion. Mutations in the G-helix have been found to attenuate the inhibition of cell migration and adhesion by maspin in breast and prostate tumour cells; highlighting a requirement for a functional G-helix to enable the tumour suppressive action of maspin (Ravenhill et al., 2010). More recent reports have also confirmed a role for the G-helix

of maspin on the migration and adhesion of endothelial cells and potential application as anti-angiogenic therapy (Zha et al., 2015).

1.6.2 Maspin regulation

Maspin expression in epithelial cells is regulated by various transcription factors within the maspin promoter such as Ets and Ap1. The Ets site is able to activate transcription alone whereas the Ap1 site requires assistance from Ets to achieve activation and subsequent expression of maspin. Reduced Ets and Ap1 site function has been reported in primary breast and prostate tumour cells expressing reduced levels of maspin. Function was abolished in invasive breast and prostate tumour cells (Zhang et al., 1997a, Zhang et al., 1997b). To this end, loss of maspin expression during tumour progression may be in part due to the absence of transactivation through Ets and Ap1 binding sites within the maspin promoter region.

The tumour suppressor gene *p53* has also been implicated in the regulation of maspin. Maspin expression was increased in maspin deficient breast and prostate cancer cells following adenoviral mediated expression of wild type *p53*. DNA-damaging agents and cytotoxic drugs induced the expression of maspin in cells containing wild type *p53* (Zou et al., 2000). An inverse correlation between mutant *p53* and maspin expression has been identified in other cancers including gastric, colon and ovarian (Zhang and Zhang, 2002, Song et al., 2002, Lee et al., 2008, Alvarez Secord et al., 2011).

Maspin expression can be epigenetically regulated and changes in expression are associated with DNA methylation, histone deacetylation and chromatic accessibility (Khalkhali-Ellis, 2006). Aberrant epigenetic regulation has been associated with maspin gene silencing; an oncogenic process in various cancers including those of the breast, prostate, thyroid and colon (Zou et al., 1994, Boltze et al., 2003, Bettstetter et al., 2005, Wu et al., 2010). Both methylation and histone deacetylation are reversible biological modifications and treatment of maspin deficient cancer cells with demethylating agents and histone deacetylase (HDAC) inhibitors has been shown to induce the re-expression of maspin; making them attractive therapeutic targets (Domann et al., 2000, Murakami et al., 2004, Abbas and Gupta, 2008). Interestingly, maspin specifically interacts and endogenously inhibits histone deacetylase 1 (HDAC-1) and therefore the inhibitory

maspin/HDAC-1 interaction may be the molecular basis for the tumour suppressor effects of maspin (Kaplun et al., 2012).

1.6.3 The role of Maspin in normal biology.

To fully elucidate the roles of Maspin in cancer progression it is important to understand its biological function in normal organ development.

1.6.3.1 Mammary gland

Maspin was originally identified in human mammary epithelial cells and has since been found to play an important role in mammary gland development. Transgenic mice were shown to overexpress maspin in the mammary gland under the control of the whey acidic protein (WAP); a gene promoter which is expressed mid-pregnancy and throughout lactation (Pittius et al., 1988). Over expression of maspin by the WAP promoter during these stages inhibited alveolar development and differentiation during pregnancy, indicating that the regulation of maspin expression is vital to proper development of the mammary gland during pregnancy (Zhang et al., 1999).

1.6.3.2 Development

To explore the role of Maspin in normal embryonic development, maspin knockout and heterozygous mice were developed. Maspin knockout resulted in embryonic lethality at the peri-implantation stage due to disruption of the endodermal layer, however this was not reported in heterozygous maspin models (Gao et al., 2004). Heterozygous knockout models appeared morphologically normal after birth but later presented a defect in mammary gland and ovarian development at puberty; supporting the crucial role of maspin in early embryonic development. Male heterozygous maspin knockout mice models displayed aberrant prostate development and hyperplastic lesions; implicating maspin in the epithelial development of the prostate (Shao et al., 2008). Maspin is not strictly an embryonic gene as it is expressed in adult cell types such as myoepithelial cells of the breast (Bodenstine et al., 2012). To this end, maspin functioning is diverse and further investigation is required to explore the roles maspin plays in regulating development.

1.6.3.3 Cell behaviour and tumour suppression

Maspin was first recognised as a tumour suppressor gene over 25 years ago when Zou et al. (1994) utilised subtractive hybridisation to identify candidate tumour suppressor genes that were defective in breast carcinomas. Decreased expression of maspin was identified in mammary tumour cells. Structural alterations to the maspin gene were not found in the tumour cells indicating that decreased expression in these tumours was due to changes in regulation. Following this discovery, various studies have explored the role of maspin in cell behaviours which are altered during cancer development and progression. These behaviours include proliferation, angiogenesis, apoptosis, cell migration and invasion.

1.6.3.3.1 Angiogenesis

Maspin is a known inhibitor of angiogenesis; the process in which new blood and lymphatic vessels are formed to enable growth and development. Angiogenesis is also a fundamental step in cancer and the transition of tumours from benign to malignant (reviewed in Nishida et al. (2006)). Formation of new vessels provide tumour cells with the vital nutrients and oxygen required for growth. Cells are able to metastasize to other sites in the body by penetrating the vessels and circulating through the intravascular system. *In vitro* studies have demonstrated reduced angiogenesis in cultured endothelial cells exposed to recombinant maspin produced in *Escherichia coli* as a recombinant glutathione S-transferase (GST) fusion protein. Recombinant maspin inhibited cell migration induced by basic fibroblast growth factor and vascular endothelial growth factor. *In vivo*, angiogenesis was blocked in rats implanted with rat corneas and non-inflammatory pellets containing Maspin. Maspin derivatives with mutant RCL were unable to inhibit migration but were still able to block angiogenesis *in vitro* and *in vivo*; implying that the RCL of maspin does not affect angiogenesis (Zhang et al., 2000a). The same group utilized an athymic mouse xenograft model to determine if the ability of maspin to inhibit angiogenesis plays a role in its anti-tumour activity. They implanted LNCaP cells into the mice and monitored tumour growth and angiogenesis following treatment with exogenous maspin. Maspin-treated tumours presented reduced microvessel density compared to control tumours. (Zhang, 2004). Injection of maspin-transfected DU145 cells into the human bone microenvironment has also been shown to

limit angiogenesis; suggesting that maspins effect on angiogenesis is not limited to primary tumours (Cher et al., 2003).

1.6.3.3.2 Apoptosis

Maspin also plays a role in apoptosis. It is the only pro-apoptotic member of the serpin family and its effects are specific to pathological or pharmacological apoptotic stimuli (Liu et al., 2004).

Jiang et al. (2002) provided the first evidence that maspin re-expression in breast cancer cells is not sufficient to induce apoptosis *in vitro*. Endogenous expression of maspin sensitises cells to staurosporine (STS)-induced apoptosis and is characterised by increased DNA fragmentation, PARP and caspase-8 and 3. It was reported in breast and prostate cancer cells that the apoptosis-sensitising effect of maspin occurs in response to increased expression of bax; a pro-apoptotic member of the Bcl-2 family. Following exposure to bax siRNA, maspin-transfected cells became resistant to drug-induced apoptosis. The link between maspin and bax up-regulation in these tumours may explain why maspin is often deficient in invasive tumour cells (Liu et al., 2004). Intracellular maspin as an active inducer of apoptosis and bax up-regulation has also been identified in endothelial cells. The pro-apoptotic effect of maspin was also found to be dependent on an intact RCL (Li et al., 2005). A further study found that maspin limits tumour progression via the mitochondrial apoptosis pathway (Latha et al., 2005). These findings demonstrate a role for maspin in the regulation of cell death and suggest that maspin may be used as a target for apoptosis-based therapies.

1.6.3.3.3 Migration and invasion

Maspin as an inhibitor of cell migration and invasion was first reported in breast and prostate cancer cells exposed to recombinant maspin (rMaspin). Time-lapse microscopy demonstrated that rMaspin blocks cell motility leading to reduced cell invasion and metastasis (Sheng et al., 1996). A later study demonstrated that maspin exerts its inhibitory effects on both tumour and vascular smooth muscle cell (VSMC) migration in the absence of protease inhibition. Despite this, maspin may also indirectly influence the cell-surface plasminogen system which may contribute to its tumour suppressing capabilities (Bass et al., 2002). The group also reported that the inhibitory effects of maspin on cell migration in VSMC's was mediated by binding to $\beta 1$ integrins on the

cell surface (Bass et al., 2009). Other studies have explored the anti-invasion functions of maspin *in vivo*. Implantation of TM40D mammary tumour cells into mice mammary glands were found to be highly invasive. A significant reduction of cell invasion and metastasis was reported in TM40D cells which were transfected with maspin (Shi et al., 2001). The same group delivered maspin/*SERPINB5* DNA to female mice bearing mammary tumours. Primary tumour growth and metastasis was significantly inhibited, and this was correlated with increased apoptosis (Shi et al., 2002). Maspin has also been found to suppress tumour growth, invasion and metastasis *via* inhibition of histone deacetylases (Bernardo et al., 2011, Dzinic et al., 2014).

1.6.4 Maspin in cancer

The role of maspin in cancer progression is conflicting as its expression is down-regulated in cancers of the breast, prostate, stomach and skin but up-regulated in cancers of the pancreas, colon, gallbladder and thyroid. Different expression patterns between tumours may be explained by the subcellular location of maspin in cancer cells and epigenetic modifications (reviewed in Berardi et al. (2013)).

1.6.4.1 Subcellular localisation of maspin

Maspin is primarily a cytoplasmic protein but may also localise in the nucleus and is secreted. Nuclear expression of maspin is required for its tumour suppressor function and is associated with improved cancer survival in various tumours including those of the breast, ovaries, head and neck. Cytoplasmic expression is associated with aggressive behaviour and poor prognosis (Solomon et al., 2006, Goulet et al., 2011). Nuclear expression of maspin is associated with aggressive behaviour and poorer prognosis in cancers of the stomach, rectum and colon (Bettstetter et al., 2005, Berardi et al., 2013, Gurzu et al., 2016). The tumour suppressive function of maspin is dependent on subcellular localisation and the organ in which it is expressed. More studies are required to understand how maspin is regulated by microenvironment of different tumours.

1.6.4.2 Epigenetic effects of maspin

Maspin is epigenetically regulated in a tissue-specific manner and changes to gene expression are implicated in cancer progression.

Studies have reported aberrant cytosine methylation and chromatin configuration at the *maspin* promoter in several progressive tumours deficient in maspin. Treatment of aberrantly methylated, maspin null breast cancer cell lines with the DNA demethylating agent, 5-aza-2'-deoxycytidine (5-aza-dC) was shown to reactivate maspin gene expression in a dose dependent manner (Domann et al., 2000). Immunohistochemistry studies have also demonstrated that aberrant methylation of the *maspin* promoter occurs *in vivo* during breast carcinogenesis and is associated with loss of maspin expression (Futscher et al., 2004). These results support that aberrant methylation of the *maspin* promoter is implicated in maspin gene silencing and cancer progression.

Maspin has also been shown to regulate the acetylation state of various transcription factors and proteins by interacting and inhibiting histone deacetylase 1 (HDAC-1). HDAC-1 hydrolyses *N*-acetyl lysine residues in histone and other proteins, leading to chromatin condensation, reduced binding of transcription factors to DNA and consequently suppression of gene expression. A yeast two-hybrid screen study confirmed the role of maspin as a negative regulator of HDAC-1 activity in prostate tissues. The study reported a downregulation of maspin and upregulation of HDAC-1 in prostate tumour cells, leading to epigenetic changes in favour of dedifferentiation and resistance to cell death. These findings support the role of maspin in tumour suppression, cell cycle arrest and improved prognosis in cancers (Li et al., 2006).

1.6.4.3 *Maspin in prostate cancer*

Maspin is expressed in normal prostate cells but is often downregulated during tumour development and progression. Studies that have explored the role of maspin in prostate cancer are detailed below in Table 1.4. Re-activation of maspin expression in prostate tumours is an attractive therapeutic target to reduce primary risk of metastasis.

Table 1.4: Maspin expression in prostate cancer

Cancer sample	Maspin expression	Key study findings	Reference
Prostate cancer cell lines	Maspin downregulation	Cells treated with recombinant maspin exhibited inhibitory effects on cell invasion and migration	(Sheng et al., 1996)

Prostate tumour specimens	Maspin downregulation	Maspin expression was inversely correlated with gleason score and positively correlated with lower tumour stage.	(Riddick et al., 2005)
Prostate tumour specimens	Maspin downregulation	Maspin expression in benign tissues, slightly in grade 3 tumours and absent in grade 4/5 tumours.	(Chen et al., 2003)
Prostate cancer cell lines	Maspin downregulation	Maspin transfection decreased tumour growth, reduced osteolysis and decreased angiogenesis.	(Cher et al., 2003)
Prostate tumour specimens	Maspin downregulation	Loss of maspin expression correlated to higher tumour stage, increasing histologic dedifferentiation and increased p53 mutation.	(Machtens et al., 2001)
Prostate tumour specimens	Maspin downregulation in primary prostate cancers	Loss of maspin expression in prostate tumours. Upregulation of maspin in response to androgen ablation suggesting a role for maspin in growth inhibition and/or apoptosis of prostate cancer cells during androgen ablation.	(Zou et al., 2002)

1.6.4.4 Maspin in other cancers

The expression patterns of maspin in other cancers are presented in Table 1.5. As mentioned above in section 1.6.4 and 1.6.4.1, maspin expression is variable between tumour types and this is in part due its subcellular location.

Table 1.5: Maspin expression in other cancers.

Cancer sample	Maspin expression	Key study findings	Reference
Breast- Maspin is lost in cancer			
Mammary epithelial cells	Maspin downregulation in mammary cancer cells	Loss of maspin occurred most frequently in advanced cancers. Transfection of mammary carcinoma cells with maspin reduced cells ability to induce tumours and metastasise.	(Zou et al., 1994)

Mammary tumour specimens	Maspin downregulation	Decreased maspin levels correlated with tumour progression. Maspin downregulation associated with increased risk of distant metastasis.	(Maass et al., 2001)
Invasive breast carcinoma specimens	Maspin downregulation	Nuclear maspin = good prognosis, Cytoplasmic maspin = poor prognosis	(Mohsin et al., 2003)
Lung- Maspin is lost in cancer			
Non small-cell lung cancer specimens	Maspin downregulation	Nuclear maspin expression = Better prognosis/increased survival. Cytoplasmic maspin expression = Poorer prognosis	(Berardi et al., 2013)
Non small-cell lung cancer specimens	Maspin downregulation	Loss of maspin contributed to invasion and metastasis.	(Wu et al., 2012)
Non small-cell lung cancer specimens	Maspin downregulation	Enhanced maspin expression was associated with favourable prognosis	(Takanami et al., 2008)
Gastric- Maspin is lost in cancer			
Gastric cancer specimens	Maspin downregulation	Systematic meta and bio-informatic analysis of databases revealed down-regulated maspin in gastric cancers compared to normal mucosa and dysplasia. Higher levels associated with increased survival.	(Zheng and Gong, 2017)
Gastric cancer specimens	Maspin downregulation in tumour samples	Cancer samples expressed reduced levels of maspin compared to normal mucosa and dysplasia. Maspin expression was negatively associated with invasive depth and metastasis but correlated with expression of Caspase-3	(Wang et al., 2004)
Gastric cancer specimens	Maspin expression inversely correlated with histological grade	Patients with both nuclear and cytoplasmic maspin expression survived longer than cytoplasmic expression alone. Expression is inversely correlated with mutant p53 expression.	(Lee et al., 2008)

Melanoma- Maspin is lost in cancer			
Melanoma specimens	Maspin downregulation in tumour specimens	Maspin expression was absent in most tumour samples (87.5 %). Aberrant expression of maspin in some cells occurs due to epigenetic modification.	(Wada et al., 2004)
Metastatic Melanoma specimens	Maspin expression lost in the transition from radial growth to vertical growth phase	Maspin correlated with decreased angiogenesis and tumour thickness; supporting its role as a tumour suppressor.	(Chua et al., 2009)
Pancreas- Maspin is expressed in cancer			
Pancreatic tissue specimens	Maspin upregulation in tumours	Maspin was absent in normal pancreatic ducts and low-grade precancerous lesions. 90% of ductal carcinoma samples and high-grade precancerous lesions expressed maspin.	(Liu et al., 2012)
Human pancreatic carcinoma cell lines	Maspin upregulation during pancreatic carcinogenesis	Pancreatic carcinoma cells acquire maspin expression through epigenetic de-repression of the maspin locus.	(Fitzgerald et al., 2003)
Colon- Maspin is expressed in cancer			
Inflammatory bowel disease (IBD) specimens	Maspin overexpression	IBD and invasive colorectal cancers expressed increased maspin compared to inactive IBD and normal colonic mucosa	(Cao et al., 2005)
Colorectal adenocarcinoma	Maspin overexpression	Maspin correlated with depth of invasion and high-grade tumour budding.	(Umekita et al., 2006)
Gallbladder- Maspin is expressed in cancer			
Gallbladder specimens	Increased expression of maspin in gallbladder tumours	Maspin was not expression in normal mucosa or adenoma. Maspin was expressed in 60% of gallbladder tumour and this increased from dysplasia to carcinoma suggesting that maspin may play a role in early steps of carcinogenesis	(Kim et al., 2010a)
Cholelithiasis and gallbladder cancer patients	Increased maspin expression in metaplasia and carcinoma	Maspin expression was increased in patients with cholelithiasis compared to those without. Expression also correlated with metaplasia and expression may increase susceptibility to gallbladder carcinoma development.	(Maesawa et al., 2006)

1.7 Histone deacetylase

Histone deacetylases (HDACs) are a family of enzymes that have a crucial role in biological processes, largely transcriptional gene repression. There are 18 mammalian HDAC enzymes which are categorised into two groups; The class III HDACs which comprise the NAD⁺ dependent sirtuins 1-7 and the classical HDAC enzymes. Classical HDACs fall into two phylogenetic classes, class 1 and 2 (de Ruijter et al., 2003). HDAC-1, a member of the class 1 classical HDAC family, was the first protein shown to have histone deacetylase activity (Taunton et al., 1996). It is a ubiquitous protein located in the cell nucleus and it plays a role in the regulation of cell proliferation and survival. HDAC-1 has also been implicated in the regulation of cancer cell proliferation and survival (Senese et al., 2007).

1.7.1 HDAC-1 structure and function

HDAC-1 is a homolog of the yeast protein Rpd3. It is an enzyme that catalyses the removal of acetyl residues from core histones and non-histone proteins, leading to chromatin structure condensation and transcriptional repression (Seto and Yoshida, 2014). It shares an almost identical catalytic core domain and conserved C-terminal tail with HDAC2. The HDAC catalytic domain is formed by a stretch of more than 300 amino acids and it partially overlaps an N-terminal HDAC association domain (HAD) which is essential for homo- and heterodimerisation. The C-terminus of HDAC-1 contains a lysine-rich sequence that is crucial for nuclear localisation of the enzyme (Taplick et al., 2001).

Mice studies have demonstrated a crucial role for HDAC-1 in normal mammalian development and proliferation. *HDAC-1* gene knockout in mice results in embryonic lethality at day 10 due to proliferation and developmental retardation. HDAC-1 deficient embryonic stem cells have also presented aberrant cell proliferation and reduced viability. Upregulation of cyclin-dependent kinase p21 and p27 expression in these deficient models highlighted an essential role of HDAC-1 in the regulation of cell proliferation via the repression of cell cycle inhibitors (Lagger et al.,

2002). Other studies have also reported decreased cell viability in HDAC deficient cells (Yamaguchi et al., 2010, Jamaladdin et al., 2014).

1.7.2 HDAC-1 in cancer initiation

HDAC-1 has been implicated in cancer initiation and progression due to its role in the negative regulation of genes such as cell cycle inhibitors, tumour suppressor genes, apoptotic and differentiation factors. This brings about changes to cell proliferation, adhesion, migration and invasion; enabling characteristics of cancer development (Parbin et al., 2014).

HDAC inhibitors have emerged as anti-cancer therapies that induce cell cycle arrest, apoptosis and differentiation, and inhibit cell proliferation and angiogenesis (Min et al., 2015). These therapies have also been shown to down-regulate DNA repair pathways and enhance cell sensitivity to DNA damaging agents. For example, HDAC inhibition downregulates the expression of genes associated with HR repair including *BRCA1/2* and *RAD51*; leading to sustained DNA damage signalling and defective DNA repair (Kachhap et al., 2010). The potential of HDAC inhibitors will be discussed further in section 1.7.3.

1.7.2.1 HDAC-1 in prostate cancer

HDAC-1 is frequently upregulated in prostate cancers and is associated with an aggressive phenotype that contributes to tumour progression. Immunohistochemical analysis of HDAC-1 in prostate carcinoma specimens reported high expression of class 1 HDAC proteins and this correlated with tumour dedifferentiation and higher proliferative fractions (Weichert et al., 2008b). These findings were in line with *in vitro* studies that utilised a panel of PC cell lines and prostate tissues to investigate the expression profile of HDAC-1 and its role in tumour development. They reported increased HDAC-1 protein expression in pre-malignant and malignant lesions; particularly in hormone refractory prostate tumours. To support the human tissue data the group examined the correlation between androgen manipulation and HDAC-1 expression in mouse models. Castration resulted in HDAC-1 upregulation compared to untreated control; highlighting a potential dependence of HDAC-1 on the hormone environment (Halkidou et al., 2004).

The tumour suppressor maspin influences the acetylation of transcription factors and other proteins by interacting and endogenously inhibiting HDAC-1 in tumour cells and tissues; including those derived from the prostate (Kaplun et al., 2012). To this end, reduced maspin and increased HDAC-1 expression during prostate cancer progression (discussed in 1.6.4.2) may be due to a maspin/HDAC-1 interaction in which HDAC-mediated protein deacetylation is regulated by maspin. Chemical HDAC inhibitors as inducers of maspin re-expression are an attractive potential target for cancer patients with aggressive tumours deficient in maspin.

1.7.2.2 HDAC-1 in other human cancers

Aberrant expression of HDAC-1 has been implicated in various human cancer types (Table 1.6) and the overexpression of HDACs, particularly HDAC-1, is associated with poor prognosis due to repression of important growth suppressive genes.

Table 1.6: Expression of HDAC-1 in human cancers.

Cancer type	HDAC-1 expression	Reference
Lung	HDAC-1 is overexpressed in lung cancer and correlates with poor prognosis. Overall survival was better in lung cancer patients with low HDAC-1 expression.	(Minamiya et al., 2011, Cao et al., 2017)
Colon	HDAC-1 expression is enhanced in highly proliferating and dedifferentiated colorectal tumours. High expression significantly reduced survival.	(Weichert et al., 2008c, Stypula-Cyrus et al., 2013)
Breast	HDAC-1 expression is increased in breast cancer cells compared to normal epithelial breast cells. HDAC-1 knockdown suppressed proliferation and migration of breast cancer cells.	(Tang et al., 2017)
Ovarian	High expression of HDAC-1 is associated with poor prognosis in ovarian carcinomas. HDAC-1 overexpression is associated with chemotherapeutic resistance. HDAC-1 silencing enhances response to therapy.	(Weichert et al., 2008a, Liu et al., 2018)
Liver	HDAC-1 is upregulated in human hepatocarcinoma and liver cancer cell lines. Inactivation of HDAC-1 results in reduced cell proliferation and increased apoptosis.	(Xie et al., 2012, Buurman et al., 2012)

1.7.3 HDAC inhibitors for cancer therapy

The role of HDAC in cancer progression has led to the development of HDAC inhibitors (HDACi) as potential anti-cancer therapies. HDACis can counteract the abnormal acetylation status of

proteins in cancer cells, leading to the reactivation of tumour suppressors and consequently induction of apoptosis, cell differentiation and inhibition of tumour cell migration and invasion (Li and Seto, 2016). HDAC inhibitors also exacerbate DNA damage by inducing the accumulation of ROS and downregulating DNA repair proteins involved in DSB repair (reviewed in Marks (2010). ROS accumulation following HDAC inhibition may occur *via* the inhibition of ROS scavengers. For example, the HDAC inhibitor SAHA has been shown to upregulate TBP2, an inhibitor of the ROS scavenger thioredoxin (Xu et al., 2006).

The HDAC inhibitory activity of the naturally occurring compounds Butyrate and Trichostatin A (TSA) was discovered in the late 1970s and early 1990s, respectively (Riggs et al., 1977, Yoshida et al., 1990). These studies demonstrated the efficacy of these compounds as inducers of cell differentiation, cell cycle arrest, and inhibitors of cell growth and survival in transformed cells; attributable to the inhibition of the HDAC enzymes. There are now a range of natural and synthetic chemical compounds that target HDAC and they are comprised of four main structural classes: Hydroxamic acids, short-chain fatty acids, cyclic peptides and benzamides. These molecules possess varied specificity, pharmacokinetic properties and toxicological characteristics (Walkinshaw and Yang, 2008). Vorinostat (sub-eroylanilide hydroxamic acid/SAHA) is structurally similar to TSA and was the first FDA-approved HDAC inhibitor for the treatment of lymphoma. Over 15 class I HDAC inhibitors have been tested or are under pre-clinical and clinical studies to date (Reviewed by Li and Seto (2016)).

The studies carried out for submission of this thesis utilised the pan HDAC inhibitor Trichostatin A (TSA). For this reason, this drug will be discussed in further detail below.

1.7.3.1 *Trichostatin A*

The organic anti-fungal antibiotic TSA is produced by *Streptomyces hygroscopicus* and is a derivative of a primary hydroxamic acid (Tsuji et al., 1976). It is a potent and specific inhibitor of HDAC that alters gene expression by reversibly interacting with the HDAC catalytic site to inhibit substrate binding; leading to increased histone acetylation and accumulation of acetylated histones in the cell (Yoshida et al., 1990). TSA exerts its anti-cancer effects at nanomolar concentrations in tumours cells by enhancing the expression of apoptosis-related genes to induce

cell differentiation and growth arrest. Various *in vitro* and *in vivo* studies have demonstrated the efficacy of TSA as a potent inhibitor of proliferation and inducer of apoptosis in tumours including those from the breast, bone, lung and prostate (Vigushin et al., 2001, Roh et al., 2004, Kim et al., 2006a, Zhang et al., 2015). Increasing concentrations of TSA were shown to suppress the proliferation of metastatic prostate cell line PC3 in a time dependent manner. Further evaluation revealed increased cell cycle arrest at G1 phase, upregulation of the apoptotic proteins caspase-3, caspase-9 and downregulation of bcl-1 (Zhang et al., 2015). TSA has also been shown to induce the reversal process of epithelial-mesenchymal transition in PC3 cells; leading to attenuated cell invasion and migration capabilities (Wang et al., 2015b). TSA is currently only used in laboratory experiments due to its high potency and toxicity. However, it is a cheap and effective HDAC inhibitor for preliminary proof of principle experiments (reviewed in Eckschlager et al. (2017)).

1.8 Combined PARP and HDAC inhibition as a potential cancer therapy

Combination therapy is gaining prominence in cancer therapeutics as multiple defective cellular components are often involved in tumorigenesis. Many reports have shown that HDAC inhibitors sensitise tumour cells to PARP inhibitors for cancer therapy. For example, prostate cells exposed to the HDACi SAHA in combination with the PARPi Olaparib have shown a synergistic decrease in cell viability. This coincided with increased apoptosis and DNA damage which concomitantly downregulated DNA repair proteins associated with HR (Chao and Goodman, 2014). Glioblastoma studies have also reported down-regulation of the DNA response following inhibition of HDAC and sensitisation to PARP inhibition (Rasmussen et al., 2016). The efficacy of PARP and HDAC inhibitor co-targeting has also been explored in triple negative breast cancers. Co-treatment inhibited cell proliferation, particularly in BRCA mutated cell lines (Marijon et al., 2018). These results demonstrate a rationale to combine a HDACi with a PARPi to limit DNA repair and sensitise aggressive tumours to PARP inhibition.

1.9 Rationale and hypothesis

Studies have explored the potential of HDAC and PARP inhibitors as co-targeting agents for cancer therapy, but they have not yet explored the effects of NF- κ B and maspin on cell sensitivity

to HDACi and PARPi co-treatment. Downregulation of Maspin has been associated with constitutive activation of NF- κ B activation in PC. Constitutive activation of NF- κ B is common in many cancers and correlates with increased metastatic potential and therapeutic resistance (Xia et al., 2014).

IKK α , an activator of NF- κ B signalling, exerts its pro-metastatic effects in tumours by repressing transcription of the maspin gene; leading to gene silencing and tumour exacerbation (Luo et al., 2007). Inhibition of IKK α has been shown to enhance maspin expression in prostate tumours, resulting in reduced tumour invasiveness (Mahato et al., 2011, Leopizzi et al., 2017). Thus, inhibition of NF- κ B with a PARPi represents an attractive target for therapeutic exploitation.

One of the most interesting concepts of combining PARP inhibitors is to induce synthetic lethality by combining them with agents that hinder DNA repair by HR, such as HDAC inhibitors which have been shown to mimic a HR-deficient phenotype by downregulating the expression of major DNA repair signalling HR proteins (reviewed in Groselj et al. (2013)). Studies have linked NF- κ B to HDAC, showing that the transactivation function of NF- κ B is in part regulated through its association with HDAC 1 and 2 corepressor proteins (Ashburner et al., 2001). Maspin interacts and endogenously inhibits HDAC-1 (Kaplan et al., 2012) and chemical inhibition of HDAC-1 has been found to prevent activation of NF- κ B (Place et al., 2005). Studies using PC cells and clinical specimens have demonstrated the re-expression of maspin following inhibition of HDAC-1 (Abbas and Gupta, 2008).

These studies, along with experimental interactions and text mining on the STRING database (Figure 1.10), show a link between PARP-1, NF- κ B, maspin and HDAC. The STRING database aims to collect and integrate data of all functional interactions between expressed proteins in a large number of organisms (Szklarczyk et al., 2017). Despite known interactions between these molecules, the exact mechanisms have not yet been explored.

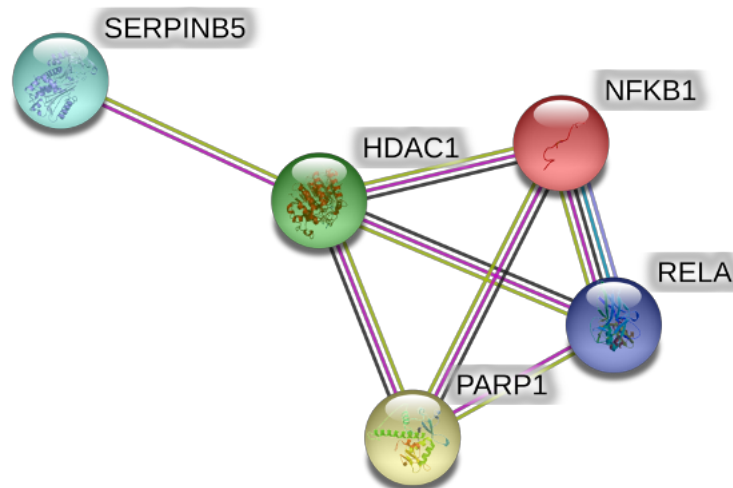


Figure 1.10: STRING network visualisation of PARP-1, HDAC-1, SERPINB5/Maspin and NF-kB protein-protein interactions.

The interaction network highlights the predicted associations with proteins of interest. The network nodes are proteins and the edges connecting each protein together signify the predicted functional associations. Each coloured line represented different types of evidence which supports the protein-protein interaction (Pink: experimental determined interactions, Green: text mining, Black: co-expression, Light blue: database evidence and Purple: protein homology).

It is hypothesised that constitutively activated NF-kB down regulates maspin leading to a more aggressive phenotype and resistance to cancer therapy. Inhibition of constitutively active NF-kB with the PARP inhibitor Rucaparib will enhance maspin expression and sensitise PC cancer cells to therapy. This sensitisation will be increased following combination treatment of Rucaparib with the HDAC inhibitor Trichostatin A (TSA). The interplay between these molecules and the potential effects of PARP-1 and HDAC-1 inhibition is depicted in the schematic presented below in Figure 1.11.

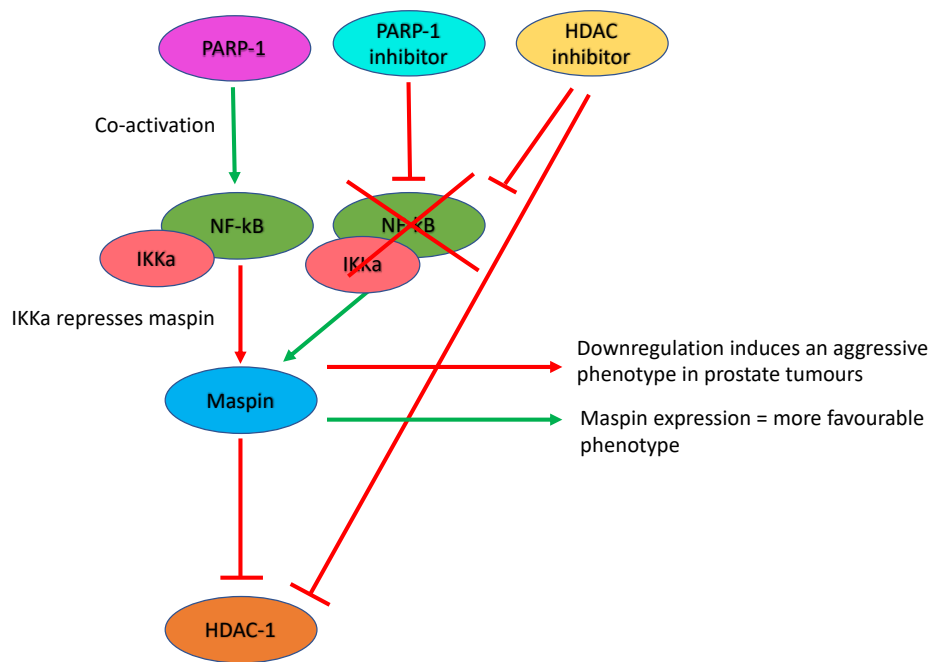


Figure 1.11: Potential interplay between PARP-1, NF-kB, IKK α , HDAC-1 and maspin molecules and the hypothetical effects of PARP and HDAC inhibitors on the expression and regulation of these molecules.

PARP-1 is a known co-activator of NF-kB. Constitutive activation of NF-kB is an unfavourable phenotype in cancer and is associated with increased metastatic potential and tumour progression. Downregulation of the tumour suppressor maspin is also an unfavourable phenotype in cancer and such downregulation is associated with increased expression of IKK α ; an activator of NF-kB. Inhibition of NF-kB with a PARP-1 inhibitor may enhance expression of maspin leading to a more favourable phenotype. Maspin is an endogenous inhibitor of HDAC-1 and inhibition of HDAC-1 limits activation of NF-kB. Thus, combined inhibition of PARP-1 and HDAC-1 limit NF-kB and upregulate maspin to sensitise tumours to cancer therapies. Green arrows represent upregulation, red arrows represent downregulation and flat arrowheads represent inhibition.

1.10 Aims

The general aim of this thesis is to investigate the effect of PARP-1 and HDAC-1 on cell behaviours in prostate cell models of varied maspin expression. More specifically, the studies presented in this thesis aim to:

1. Confirm a relationship between NF-kB and maspin in prostate cells.
2. Investigate cell viability, growth, survival and DNA damage in response to PARP and HDAC inhibitors in prostate cells of varied maspin status.
3. Investigate the combined effects of PARP and HDAC inhibitors on cell viability, growth, survival and DNA damage in prostate cells of varied maspin status.

4. Investigate the combined effects of PARP and HDAC inhibitors on cell migration in prostate cells of varied maspin status.

5. Investigate the role of maspin and NF- κ B in cell survival with use of maspin and PARP-1 siRNA, alone and in combination with PARP and HDAC inhibitors; with a view to show mechanism between maspin and NF- κ B in tumour progression.

Chapter Two

Materials and methods

2.1 Materials and reagents

Essential experimental chemicals were obtained from Sigma Aldrich (Poole, Dorset, UK) unless otherwise stated in the text. Sterile plasticware for cell culture experiments was supplied by CellStar (Greiner Bio-One, Gloucester). Cell culture media and components were supplied by Life Technologies (Paisley, UK). All other lab equipment was from Eppendorf (Stevenage, UK) or Sigma Aldrich, unless otherwise stated. Primary antibodies used for Western blotting and Immunofluorescence were obtained from various sources (Table 2.3). Secondary antibodies for Western blotting (Table 2.4) were supplied from Dako (Cambridgeshire, UK), and those used for Immunofluorescence were from Thermo Fisher Scientific (Waltham, MA USA).

Table 2.1: Buffers and solutions

Buffer/solution	Preparation
1% Acetic acid	10ml Acetic acid in 1 litre distilled water.
1% BSA /PBS blocking agent (BSA/PBS block)	100mg Bovine Serum Albumin (w/v) in 10ml 1x PBS.
10 X PBS	80g NaCl, 2g KCl, 6.1g Na ₂ HPO ₄ and 2g KH ₂ PO ₄ in 1 litre distilled water.
SDS-PAGE running buffer	2.4g Tris, 14.4g Glycine and 10% SDS (w/v) in 1 litre distilled water.
Carnoy's fixative	30% Acetic acid (v/v) in 70% Methanol (v/v).
PBS/0.5% Tween 20 (PBS-T)	500µl Tween 20 in 1 litre 1x PBS
PBS/0.05% Tween 20/5 % milk powder (PBS-MT)	5% milk powder in 100ml 1X PBS-T.
Total protein extraction buffer (RIPA)	300µl 5M NaCl, 100µl 0.5M EDTA, 500µl 1M Tris, 100µl Triton-X, 100µl 10% Sodium Deoxycholate, 100µl 10% SDS and one complete EDTA free PIC tablet in 8.4ml distilled water.
SDS-PAGE 10% resolving gel	3.3ml Acrylamide (30%, 37.5:1 Acrylamide: Bis-Acrylamide), 2.5ml

	1.5M Tris-HCl pH 8.8, 100µl SDS (10%), 100µl APS (10%) and 5µl TEMED in 4ml distilled water.
SDS-PAGE stacking gel	1ml Acrylamide (30%, 37.5:1 Acrylamide: Bis-Acrylamide), 2.5ml 0.6M Tris-HCl pH6.8, 100µl SDS (10%), 100 µl APS (10%), 5µl TEMED in 3.2ml distilled water.
SRB solution	4% SRB (w/v) in 1% Acetic acid in 500ml distilled water
Transfer buffer	2.9g Glycine, 5.8g Tris, 0.37g SDS and 200ml Methanol to 1 litre in distilled water.
Lysis solution	2.5M NaCl (146.1g), 0.1M EDTA (37.2g), 10mM Tris (1.21g) in 1 litre distilled water. pH 10 with concentrated 10M NaOH.
Alkaline electrophoresis solution	0.3M NaOH (12g) and 1 mM EDTA (0.37g) in 1 litre distilled water.
Neutralising buffer	0.4M Tris (12g) in 1 litre distilled water. pH 7.5 with concentrated HCL.

APS, ammonium persulfate; BSA, bovine serum albumin; PBS, phosphate buffered saline; SDS, sodium dodecyl sulphate; SDS-PAGE, polyacrylamide gel electrophoresis; SRB, Sulforhodamine B; TEMED, N,N,N',N'-Tetramethylethylenediamine; Tris, Tris(hydroxymethyl)aminomethane; EDTA, Ethylenediaminetetraacetic acid; PIC, protease inhibitor cocktail .

The cell lines utilised in the in vitro experiments described in this thesis are presented in Table 2.2.

DU145 cells harbour two mutations in the tumour suppressor p53 gene; one on either allele. PC3 cells do not express p53 due to a base pair deletion of one allele and a frame shift mutation in the other. PNT1A cells are wildtype for p53 (Chappell et al., 2012). The *PTEN* tumour suppressor gene is also mutated in DU145 cells. PC3 cells do not express *PTEN* due to a loss of function in both gene alleles. *PTEN* (phosphatase and tensin homolog) is involved in the regulation of cell behaviours such as growth, survival and migration. Function is frequently lost in cancer development; leading to increased cell proliferation and reduced cell death (Song et al., 2012).

Table 2.2: Cell summary and culture conditions

Cell line	Media components	Tissue	Disease	p53 status	PTEN status
DU145	RPMI 1640, 10% FCS (v/v), 100U/ml penicillin and 1mg/ml streptomycin	Prostate tissue derived from brain metastasis	Carcinoma	mutant	mutant
PC3	RPMI 1640, 10% FCS (v/v), 100U/ml penicillin and 1mg/ml streptomycin	Prostate tissue derived from bone metastasis	Grade IV Adenocarcinoma	null	null
PNT1A	RPMI 1640, 10% FCS (v/v), 100U/ml penicillin and 1mg/ml streptomycin	Normal prostatic epithelial cells transfected with a plasmid containing SV40 genome with a defective replication origin. Primary cells were obtained from a 35-year-old male at post-mortem.	Normal prostate epithelial cells.	wildtype	wildtype
MEF	DMEM, 10% FCS (v/v), 100U/ml penicillin and 1mg/ml streptomycin	Mouse embryonic fibroblast	-	-	-

DMEM; Dulbecco's modified eagle medium, FCS; heat inactivated foetal calf serum, MEM 1X; Minimum essential medium, NEAA; non-essential amino acids, RPMI; Roswell park memorial institute.

Table 2.3: Primary antibodies used for western blotting and Immunofluorescence

Primary antibody	Species	Concentration used for Western Blotting	Concentration used for Immunofluorescence	Lot number/ Reference	Company
Maspin	Goat	0.1µg/ml	-	KUV03101	Bio-technie
Maspin	Mouse	-	1:50	554292	BD Pharmingen

NF-kB p50	Mouse	1:1000	1:100	E1513	Santa Cruz Biotechnology Inc
NF-kB p65	Mouse	1:1000	1:100	K1814	Santa Cruz Biotechnology Inc
PARP-1	Rabbit	1:1000	1:100	K0614	Santa Cruz Biotechnology Inc
IkB- α	Rabbit	1:1000	1:100	B1315	Santa Cruz Biotechnology Inc
IKK α	Rabbit	1:1000	1:100	C0514	Santa Cruz Biotechnology Inc
RelB	Mouse	1:1000	1:100	C2515	Santa Cruz Biotechnology Inc
Anti-actin	Mouse	1:10000	-	AC-40 A3853	Sigma Aldrich
Negative control igG	Mouse	-	1:100	X0931	Dako
RAD51	Rabbit	1:2000	-	PC130	Merck
γ H2AX	Mouse	-	1:500	AB26350	Abcam

Table 2.4: Secondary antibodies used for western blotting and Immunofluorescence

Secondary antibody	Species	Concentration used for western blotting	Concentration used for Immunofluorescence	Lot number/ Reference	Company
Anti-Mouse HRP conjugated	Goat	1:1000	-	P0447	Dako
Anti-Rabbit HRP conjugated	Goat	1:1000	-	P0448	Dako
Anti-Goat HRP conjugated	Rabbit	1:1000	-	P0449	Dako

Anti-Mouse Alexa Fluor 488	Donkey	-	1:1000	1113537	Life Technologies
Anti-Rabbit Alexa Fluor 568	Donkey	-	1:1000	1134929	Life Technologies

2.1.1 PARP Inhibitor AG014699

The PARP inhibitor used throughout this thesis was AG014699, otherwise known as Rucaparib. It was the first PARP inhibitor entered into clinical trials as a chemo-potentiator. It was obtained from Stratech Scientific Ltd (Suffolk, UK) and stored at -20°C as a 10mM stock solution in Dimethyl Sulfoxide (DMSO). The drug was diluted in DMSO to make stock concentrations, and further diluted in appropriate media so that the DMSO concentration was 0.5% (v/v) when added to cells. The chemical structure of Rucaparib is presented in Figure 2.1.

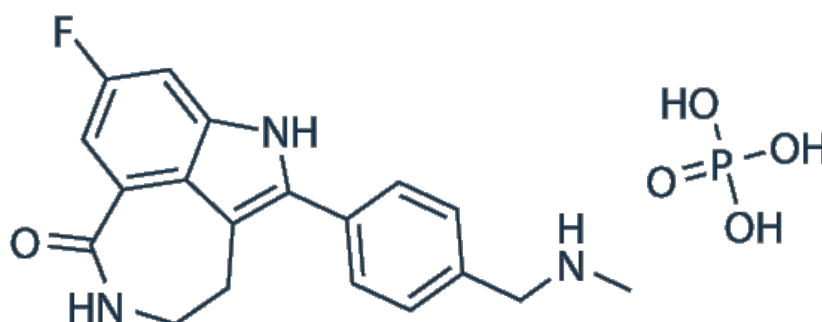


Figure 2.1: Chemical structure of the potent PARP inhibitor Rucaparib.
Obtained from: <http://www.selleckchem.com/>

2.1.2 Histone deacetylase inhibitor Trichostatin A

The histone deacetylase (HDAC) inhibitor selected for use was Trichostatin A (TSA). It was obtained from Sigma Aldrich (Poole, Dorset, UK) and stored at -20°C as a 1mM stock solution in DMSO. The chemical structure of TSA is presented in Figure 2.2.

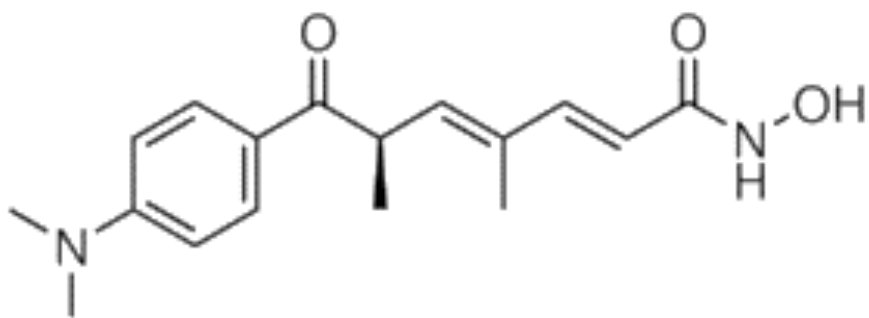


Figure 2.2: The chemical structure of HDAC inhibitor Trichostatin A.
Obtained from: <http://www.sigmaaldrich.com/>

2.2 General methods

2.2.1 Mammalian cell culture

Immortalised prostate and mouse embryonic fibroblast (MEF) cell lines were selected for *in vitro* experiments. Prostate cells were kindly provided by Dr Luke Gaughan, Newcastle UK. Cell lines are summarised below and in Table 2.2 to assist with interpretation of results.

- **PNT1A:** Normal prostate epithelial cells established by transfection with a plasmid containing SV40 genome with a defective replication origin (Sigma Aldrich) . Primary culture was obtained from a 35-year old male.
- **DU145:** Epithelial prostate cancer cells isolated from brain metastasis (Stone et al., 1978b). They are AR- and express negligible amounts of endogenous maspin (Ma et al., 2012).
- **PC3:** Grade 4 prostatic adenocarcinoma cells isolated from bone metastasis. Highly aggressive cells that express maspin. They are androgen receptor (AR) - and prostate specific antigen (PSA) - (Tai et al., 2011).
- **MEF p65^{+/+}:** Immortalised MEF cells derived from primary cells.
- **MEF p65^{-/-}:** Immortalised MEF cells. Knockout for NFκB p65.
- **MEF IKKα^{-/-}:** Immortalised MEF cells. Knockout for IKKα.

2.2.1.1 Resurrection of cryopreserved cell lines from frozen storage

Cell lines were resurrected from long-term storage at -150°C by warming at 37°C to thaw the cell suspension which was diluted in freezing media (80% v/v complete medium, 10% (v/v) FCS and 10% (v/v) DMSO). Traces of DMSO were removed from the cell suspension via centrifugation at 1200rpm, and cell pellets were re-suspended in fully supplemented growth media (Table 2.2) in sterile tissue culture flasks.

2.2.1.2 Routine culture of cell lines

Mammalian cell lines were cultured as monolayers in plastic tissue culture flasks and maintained in exponential growth at 37°C in a humidified incubator (5% CO_2 and 95% O_2). Cells were assigned their own growth reagents (Table 2.2) under sterile conditions in class II tissue culture hoods.

During routine sub-culture, and in experiments, media was removed from the flasks and the cells were briefly washed in sterile 1X PBS. A 2ml volume of 1X 0.5% (v/v) Trypsin/PBS was added, and the cells were incubated in the trypsin solution for 5 minutes. When cells were detached from the flask surface, trypsin was inactivated by the addition of an equal volume of fully supplemented media. Cells were seeded into new flasks at their optimum growing densities, as identified by cell proliferation assays. Seeding densities were calculated by counting the cells in the original cell suspension using a haemocytometer, as later described.

2.2.1.3 Cell counting using a haemocytometer

In the cell studies described in this thesis, a haemocytometer was used to count cells.

2.2.1.3.1 Principle

A haemocytometer is a thick glass microscope slide containing two flat chambers of known depth with a grid of perpendicular lines etched onto the surface. The slide is prepared by breathing over it and sliding a glass cover slip over the chambers. Each chamber is comprised of 9 large 1mm^2 squares of 0.1mm depth, which are further divided into 16 smaller squares (see figure). The volume of each large square is 0.1mm^3 . It is known that 1mm^3 is equal to $1\mu\text{l}$, and the conversion factor for 1ml is $\times 10^4$.

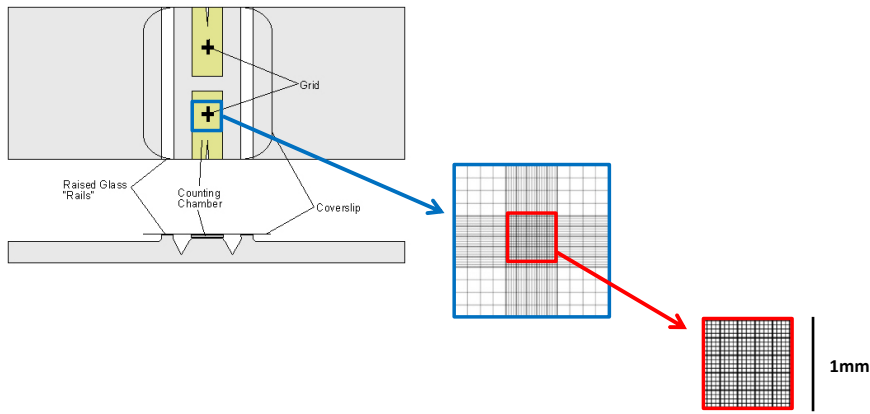


Figure 2.3: Chamber layout of a haemocytometer

2.2.1.3.2 Method

The cell suspension was mixed thoroughly and 10 μ l was pipetted on to the edge of the haemocytometer chamber where it was drawn under the coverslip by capillary action. Using a 40X objective under the microscope, cells lying within the four 1mm² corner squares were counted; including those lying on the top and left-hand lines. The following formula was applied to calculate cells/ml x 10⁴:

$$\frac{\text{Cell count}}{\text{Number of squares}} = \text{cells per ml} \times 10^4$$

2.2.1.4 Preparing cell stocks for long term freezer storage

Exponentially growing cells were removed from culture flasks with 1X 0.5% (v/v) Trypsin/PBS as previously described in 2.2.1.2. The cell pellet was re-suspended in freezing media (80% v/v complete medium, 10% (v/v) FCS and 10% (v/v) DMSO) to a concentration of 1 x 10⁶ cells/ml and transferred to cryovials. Cell suspensions were stored overnight at -80^oc and then transferred to a -120^oc freezer for long term storage.

2.2.1.5 Mycoplasma testing

2.2.1.5.1 Principle

A major problem in cell culture laboratories is mycoplasma contamination. Mycoplasmas are not detectable by morphological changes to the cell or visual presence in the cell culture medium.

They induce changes to the cell such as: altered protein and nucleic acid synthesis, altered cell metabolism, viability and growth (Drexler and Uphoff, 2002). A quick and cost-effective way to check for mycoplasma contamination is to stain cells with 4',6-Diamidino-2-Phenylindole, Dihydrochloride (DAPI). DAPI is an indirect nucleic acid stain which binds to DNA and forms strong fluorescent DNA-DAPI complexes which fluoresce blue under a fluorescent microscope. Uncontaminated cultures stained with DAPI will highlight the cell nuclei, however cultures which are contaminated with mycoplasma will also show discreet fluorescent filaments over the cytoplasm and occasionally in intercellular spaces (Nikfarjam and Farzaneh, 2012b). The DAPI staining technique can produce false positive or false negative results, and therefore the gold standard is to confirm findings with a rapid and sensitive detection method such as polymerase chain reaction (PCR). Cell cultures were tested for mycoplasma contamination by routine testing using the PCR based Venor™GeM Mycoplasma detection kit (Cambio, Cambridge, UK) alongside DAPI staining, on a three-monthly basis.

2.2.1.5.2 Method

Cells were grown on to sterile circular glass coverslips (22 mm diameter, 1mm thickness) in wells of a sterile 24 well plate. After a 72-hour incubation period, cells were fixed with Carnoys fixative (Table 2.1), briefly washed with PBS and then mounted onto microscope slides with Vectorshield hard set mounting medium with DAPI (Vector laboratories; Peterborough, UK). Images of cells in a fixed state were captured at a 40X magnification using a confocal microscope (Leica Microsystems Ltd, UK). For PCR based mycoplasma screening, 100µl of cell culture supernatant was taken from a 90% confluent flask of cells, heated for 5 minutes at 95°C and centrifuged at 13000 rpm for 2 minutes. PCR reaction tubes were set up containing 2µl of centrifuged supernatant and 23µl of PCR mastermix. For positive control, 2µl of positive control DNA was added to the positive control reaction tube. PCR was set up and carried out for 1 cycle at 94°C for 2 minutes, 39 cycles of 94°C for 30 seconds, 55°C for 1 minute and 72°C for 30 seconds. Products were then ran on a 1.5% agarose gel for 20 minutes at 100v alongside positive and negative controls, and bands were visualised on the G: Box chemo xx6 imaging system (Syngene, Cambridge, UK). Positive samples will have a band at 270 base pairs (BP).

2.2.2 Assessment of cell and nuclear morphology

2.2.2.1.1 Principle

Examining the morphological characteristics of cells in culture such as their shape, structure and form, is essential for successful cell culture experiments. Regular assessment of cell morphology by microscopy enables detection of contamination, but also cell deterioration, detachment and death. Assessment of cell morphology is often carried out alongside cytotoxicity experiments to evaluate the effects of cytotoxic drugs on cell health. It is also important to assess nuclear morphology in response to cytotoxic agents, as this can give a good indication to the mode of cell death. For example, cells undergoing apoptosis display characteristic nuclear alterations such as: chromatin condensation, nuclear fragmentation and formation of apoptotic bodies.

2.2.2.1.2 Method

To assess cell morphology, cells were seeded onto 6 well plates at 2.5×10^4 /ml and then incubated for 24 hours to enable cell adherence. The morphology of the cells was then visualised by eye and images were captured on a Leica optical microscope at a 10X magnification. For detection of nuclear morphology, cells were seeded on to circular coverslips (22 diameter, 1mm thickness) in wells of a sterile 24 well plate at the same density. Following the incubation period cells were washed twice with PBS and fixed with 100% methanol at -20°C for 10 minutes. Cells were then washed with PBS and mounted onto microscope slides with Vectorshield hard set mounting medium with DAPI (Vector laboratories; Peterborough, UK). Fluorescent images were captured using a Leica DMI8 inverted confocal microscope (Leica Microsystems Ltd, UK) at a 40X magnification. For cytotoxicity experiments, cells were exposed to appropriate drugs alone, and in combination for 72 hours prior to any fixing and imaging steps.

2.2.3 Proliferation and cytotoxicity assays

2.2.3.1 WST-1 assay

2.2.3.1.1 Principle

WST-1 reagent is a tetrazolium salt that measures metabolic activity of the cell and therefore cellular proliferation and viability in culture. The assay is based on the ability of viable cells to

cleave the tetrazolium salt and produce an orange formazan dye (Figure 2.4). The formazan dye is soluble and can be quantified by spectrophotometry at an absorbance of 450nm. The amount of formazan dye formed is proportional to the number of metabolically active cells within the sample, which directly correlates with cell viability.

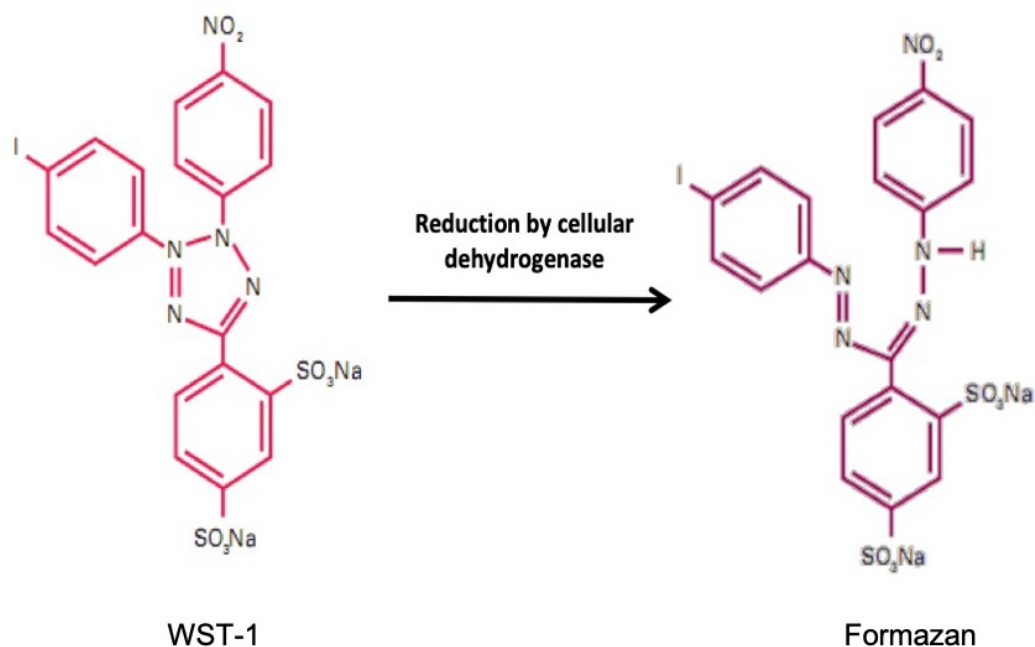


Figure 2.4: WST-1 is metabolised to a soluble formazan product which is indicative of cell viability.

2.2.3.1.2 Method

Cells in exponential growth were harvested, centrifuged (1200 rpm for 6 minutes) and re-suspended in appropriate growth medium (Table 2.2). To assess cell proliferation, a series of cell suspensions at various concentrations (1×10^5 , 5×10^4 , 2.5×10^4 , 1.2×10^4 , and 0.5×10^4 cells/ml) were prepared and 100 μ l was then pipetted into the wells of a 96 well plate in triplicate. Media was added to outer wells of the plate to account for a phenomenon known as the “edge effect” (Lundholt et al., 2003). This phenomenon is when the media around the perimeter of the plate evaporates, leading to discrepancies with results. Three plates were set up for each cell line and one plate was incubated in 10 μ l/well WST-1 reagent for two hours daily, at 24-hour intervals for a total of 72 hours. Absorbance was measured at 450nm using a FLUOstar OMEGA microplate reader (BMG LABTECH Ltd, Buckinghamshire, UK).

The WST-1 method was also employed to assess the effects of drugs on cell viability. Cells were seeded at their optimum density for proliferation and then returned to incubation (37°C, 5% CO₂) for 24 hours to allow cells to adhere. Media was aspirated and replaced with fresh media containing increasing concentrations of drugs. As drugs were dissolved in DMSO, each well contained 0.5% DMSO, including untreated controls. Cells were returned to incubation for 72 hours before WST-1 was applied.

2.2.3.1.3 Analysis

Mean absorbance data was plotted against time graphically on an x-y plot. When drugs were added to cells the concentration required to inhibit cell growth by 50% (GI₅₀) was calculated for each cell line in each independent experiment. Each assay contained three replicates and results presented represent data from three independent experiments. GraphPad PRISM software was used to produce point to point graphs, calculate cell doubling time and perform appropriate statistical analysis.

2.2.3.2 Sulforhodamine B (SRB) colorimetric assay for cell growth inhibition

2.2.3.2.1 Principle

Cell growth inhibition in response to drug treatment was investigated using the Sulforhodamine B (SRB) protein dye assay. This assay is a rapid, sensitive and cost-effective technique to determine cell density by measuring cellular protein content. Colour intensity at an absorbance of 570nm is directly proportional to the amount of protein and subsequently cell mass.

2.2.3.2.2 Method

Cells were seeded onto 96 well plates at their optimum growing densities. Medium was added to the outer wells of the plates to compensate for the “edge effect”, as previously described in section 2.2.3.1.2. After a 24-hour incubation period to allow cells to adhere, media was aspirated and replaced with 100µl of media containing relevant concentrations of drug in 0.5% (v/v) DMSO. Once drug was added to the cells, an additional plate of control cells was fixed with 25µl of Carnoys fixative (Table 2.1) to measure the cell density at time 0. Cells were exposed to the drug for 72 hours at 37°C, fixed in Carnoys fixative and briefly washed in distilled water. When dry,

cells were stained with 0.4% SRB solution (diluted in 1% acetic acid) for 30 minutes, washed in 1% acetic acid to remove unbound dye and solubilised in 10mM Tris (pH 10.5) for 20 minutes. Absorbance of SRB was measured at 570nm using the Spark™ 10M multimode microplate reader (Tecan group Ltd, Switzerland) to determine cell density.

2.2.3.2.3 Analysis

Mean absorbance data was plotted graphically, and the drug concentration required to inhibit cell growth by 50% (GI₅₀) was calculated for each cell line in each independent experiment. Each assay contained ten replicates for each drug concentration and results presented represent data from three independent experiments. GraphPad PRISM software was used as described in 2.2.3.1.3.

2.2.3.3 Cell counting assay

Cells were seeded into 6 well plates at 2.5×10^4 /ml and returned to incubation for 24 hours. Media was replaced with fresh media containing appropriate concentrations of cytotoxic drugs, alongside an untreated control with equivalent 0.5% DMSO (1% DMSO for drug combination experiments). After 72 hours cells were washed with PBS, trypsin was applied and then cells were counted as described in section 2.2.1.3.

2.2.3.4 Resazurin (Alamar blue) cell viability assay

2.2.3.4.1 Principle

Resazurin is a cell permeable redox indicator used to assess cell viability and mitochondrial metabolic activity. The assay is based on the ability of viable and metabolically active cells to reduce resazurin into a pink, fluorescent, Resorufin product Figure 2.5. The Resorufin product can be quantified by spectrophotometry at an absorbance of 560nm. The amount of resorufin formed is proportional to the number of metabolically active cells within the sample, which directly correlates with cell viability.

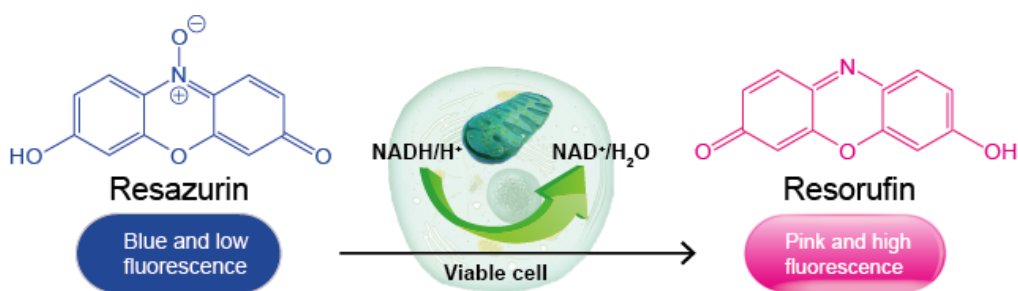


Figure 2.5: Resazurin is reduced to a resorufin product by metabolically active cells.

Obtained from: <https://www.creative-bioarray.com/support/resazurin-cell-viability-assay.html>

.

2.2.3.4.2 Method

Cells were harvested and seeded into 96 well plates as described in section 2.2.3.2, dosed with appropriate drugs and cultured for 72 hours. 10µl of resazurin sodium salt solution (1mg/ml in PBS) was then added to each well and the plates were placed into incubation for a further 2 hours at 37°C. Absorbance was measured at 570nm using a FLUOstar OMEGA microplate reader (BMG LABTECH Ltd, Buckinghamshire, UK).

2.2.3.4.3 Analysis

Data was analysed as described in 2.2.3.1.3.

2.2.4 Protein expression analysis

2.2.4.1 Preparation of whole cell extracts

Whole cell lysates were prepared by re-suspending harvested cell pellets in an appropriate volume of ice cold RIPA lysis buffer (Table 2.1) and EDTA-free complete protease inhibitors (Roche Applied Science, Burgess Hill, UK) at 1X concentration. Samples were then vortexed and placed on ice for 30 minutes to achieve lysis. Lysate samples were centrifuged at 1200 rpm for 5 minutes to remove cell debris and the supernatant was transferred to clean 1.5ml eppendorf's for quantification.

2.2.4.2 Protein quantification by BCA assay

2.2.4.2.1 Principle

The Pierce bicinchoninic acid (BCA) protein assay kit (Thermo Fisher Scientific Inc, IL, USA) measures the total protein concentration of a lysate sample against a known protein standard. The assay is a colorimetric technique based on the reduction of Cu^{+2} to Cu^{+1} by protein in an alkaline medium. BCA chelates to Cu^{+1} in a ratio of 2:1 to form a purple-coloured reaction product. Absorbance of this product is measured at 570nm using a FLUOstar OMEGA microplate reader (BMG LABTECH Ltd, Buckinghamshire, UK).

2.2.4.2.2 Method

Bovine serum albumin (BSA) standards of various concentrations were prepared as shown in Table 2.5. Lysate samples, diluted 1:10 in RIPA lysis buffer, were loaded in quadruplicate onto a 96 well plate in 10 μ l volumes. Standards were loaded alongside each lysate sample. 190 μ l of BCA working reagent was prepared as per the manufacturer's instructions and added to each well. After a 30-minute incubation period at 37 $^{\circ}$ c, absorbance was measured at 570nm on the SparkTM 10M multimode microplate reader (Tecan group Ltd, Switzerland). Known concentrations of each BSA standard were plotted against mean absorbance, and linear regression analysis was carried out using GraphPad PRISM to calculate unknown protein concentrations. Results were then multiplied by 10 to account for initial sample dilutions.

Table 2.5: Preparation of diluted BSA standards

BSA standard (mg/ml)	Vial	Volume of RIPA lysis buffer (μ l)	Volume and source of BSA (μ l)
2	A	0	300 of BSA stock
1.5	B	125	375 of BSA stock
1	C	325	325 of BSA stock
0.75	D	175	175 of vial B dilution
0.5	E	325	325 of vial C dilution
0.25	F	325	325 of vial E dilution

0.125	G	325	325 of vial F dilution
0.025	H	400	100 of vial G dilution
0	I	400	0

2.2.4.3 Preparation of protein samples for gel electrophoresis

Cell lysate samples were diluted to 20µg protein, unless otherwise stated, as per BCA assay calculations, in 2X laemmli sample buffer at a 1:1 ratio. Diluted samples were centrifuged (1400 RPM for one minute) and placed onto a heat block for 5 minutes at 100°C to enable protein denaturation and epitope exposure.

2.2.4.4 Separation of proteins by SDS- polyacrylamide (PAGE) gel electrophoresis

2.2.4.4.1 Principle

Sodium dodecyl sulphate-polyacrylamide gel electrophoresis (SDS-PAGE) is a method used to separate proteins under denaturing conditions according to their molecular weight. PAGE is based upon the principle that a charged molecule will migrate in a negative to positive direction through a gel towards an electrode when an electric field is applied. SDS, a detergent, denatures the proteins and reduces them to linear molecules with uniform charge. This allows the proteins to migrate through the gel according to their molecular weight.

2.2.4.4.2 Method

SDS PAGE gels were made using 10% resolving and stacking gels (Table 2.1). A 10% gel was selected due to the weight of the proteins of interest. Combs were added to the stacking gel to form wells for protein loading. Gels were placed into a Bio-Rad mini-PROTEAN® tetra cell tank (Bio-Rad; Hertfordshire, UK) and the inner and outer reservoirs were filled with SDS running buffer (Table 2.1) according to the manufacturer's instructions. Protein samples were loaded into the wells of the stacking gel alongside a protein molecular weight marker (Bio-Rad; Hertfordshire, UK). Proteins were separated by electrophoresis at 100V for two hours.

2.2.4.5 Western Blotting

2.2.4.5.1 Principle

Separated proteins are transferred from SDS-PAGE gels onto nitrocellulose membranes by application of an electrical current. Protein transfer to nitrocellulose membrane is followed by immunodetection by specific antibodies.

2.2.4.5.2 Method

Two mini-PROTEAN® transfer pads (Bio-Rad; Hertfordshire, UK), two filter paper sheets (Bio-Rad; Hertfordshire, UK) and one Protran premium 0.45 nitrocellulose membrane (Amersham Biosciences; Buckinghamshire, UK) cut to 8cm x 6cm, were soaked in transfer buffer for 30 minutes (Table 2.1). The apparatus was set up and the blotting cassette was put together as shown in Figure 2.6. Proteins were transferred from the gel to the membrane (Table 2.1) for 1 hour at 100V on ice. When transfer was complete the membranes were removed from the transfer cassette and prepared for immuno-detection.

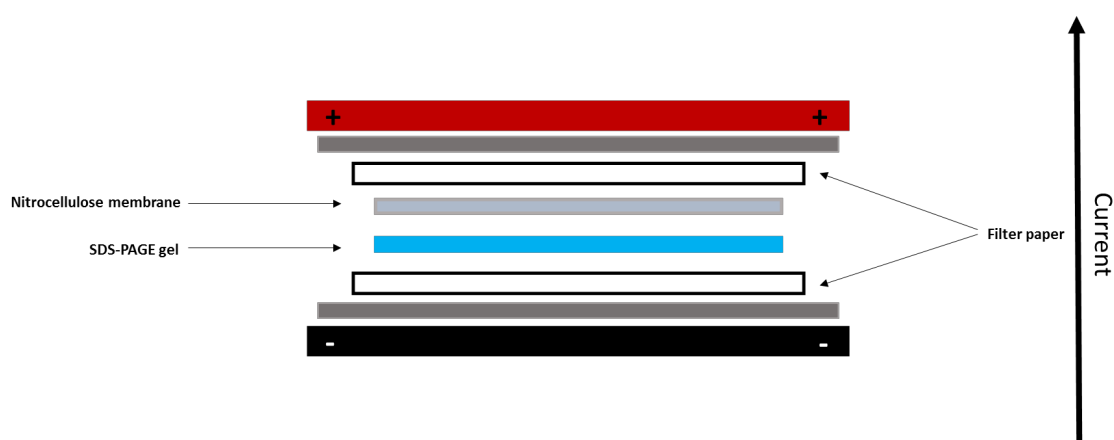


Figure 2.6: Set up of the blotting cassette for protein transfer (Bio-Rad mini-PROTEAN® tetra cell system).

2.2.4.6 Immuno-detection

The membrane was blocked in 10ml of PBS-MT (Table 2.1) at room temperature for 1 hour to prevent non-specific antibody binding. After blocking, the membrane was incubated overnight at 4°C in appropriate primary antibody, specific to the protein of interest, diluted in PBS-MT (Table 2.3). The next day the membrane was washed in PBS-T three times for 5 minutes, and then

incubated in appropriate secondary antibody (Table 2.4) diluted in PBS-MT for one hour at room temperature. Following incubation of the secondary antibody, four 20-minute washes in PBS-T were carried out before detection of protein by enhanced chemiluminescence (ECL).

2.2.4.7 *Enhanced chemiluminescence (ECL) protein detection*

2.2.4.7.1 Principle

ECL is a light emitting system that requires the oxidation of luminol in the presence of an enhancer under alkaline conditions by horseradish peroxidase (HRP). Chemical enhancers increase the light intensity and prolong the duration of light emission so that peak emission occurs between 2- and 30-minutes following incubation with chemiluminescent reagents. Light emission is proportional to protein quantity and can be measured using a G:Box chemi XX6 imaging system and Genesys capturing software (Syngene, Cambridge, UK).

2.2.4.7.2 Method

ECL prime detection fluid was used as described in the manufacturer's instructions (GE Healthcare; Buckinghamshire, UK). Luminol enhancer and peroxide reagents were applied to the nitrocellulose membrane at a 1:1 ratio and left for 1 minute. Excess ECL reagent was removed and the membrane was placed protein side up in the G:Box chemi XX6 imaging system. Images were captured with an exposure of the appropriate time.

2.2.4.7.3 Analysis

Protein levels were assessed visually by comparing between expression bands. On some occasions differences between expression bands were difficult to detect by eye, and so the bands were also quantified using Image J software and then standardised to a loading control. Quantitative data was plotted graphically in GraphPad PRISM.

2.2.5 Immunofluorescence

2.2.5.1.1 Principle

Immunofluorescence is a technique used to visually assess the presence and subcellular localisation of target molecules in a cell sample. The technique involves the use of a primary

antibody which specifically binds to a molecule of interest, and a secondary antibody which is chemically conjugated to a fluorescent dye. When the secondary antibody is bound to the primary antibody, the molecule of interest can be located and visually assessed by fluorescent confocal microscopy. The nucleus of each cell can also be visualised by combining a DAPI DNA counterstain.

2.2.5.1.2 Method

Cells were seeded at a density of 1×10^4 /ml on to sterile circular glass coverslips (22 mm diameter, 1mm thickness) in wells of a sterile 24 well plate. Following a 48-hour incubation at 37°C, cells were washed in ice cold PBS and fixed with 100% methanol at -20°C for 10 minutes. Excess fixing agent was washed away with PBS and wells were blocked for 30 minutes in 500µl bovine serum albumin (BSA) blocking buffer (1% BSA in 1X PBS). Cells were then incubated at 4°C overnight in 100µl of appropriate primary antibodies diluted in BSA blocking buffer (Table 2.1). Following incubation with primary antibodies, cells were washed in 500µl PBS/0.1% Tween and then incubated in the dark for 1 hour at room temperature in secondary fluorescent antibody diluted in BSA blocking buffer. Cells were washed with distilled water and mounted onto microscope slides with Vectorshield hard set mounting medium with DAPI (Vector laboratories; Peterborough, UK).

2.2.5.1.3 Analysis

Images of cells in a fixed state were captured at 40X magnification using a Leica DMi8 inverted confocal microscope (Leica Microsystems Ltd, UK). Images were merged together, with LAS X software (Leica Microsystems Ltd, UK), so that the expression location of the proteins of interest could be visualised alongside the cell nucleus.

2.2.6 Quantifying single DNA breaks

2.2.6.1 *Quantifying DNA single strand breaks by Alkaline single cell gel electrophoresis assay (comet assay)*

2.2.6.1.1 *Principle*

The alkaline comet assay is a technique used to assess DNA damage caused by SSBs. Cells are encapsulated in low melting point agarose and pipetted onto pre-coated slides. Cells are then lysed under alkaline conditions to unwind the DNA, allowing it to migrate out of the cell in structures resembling comets during electrophoresis. To determine the extent of DNA damage the DNA is visualised using Vectorshield hard set mounting medium with DAPI (Vector laboratories; Peterborough, UK). Cells that have accumulated DNA breaks appear as fluorescent comets with tails of fragmented DNA. The intensity of the comet tail relative to the head is a reflection of the number of DNA breaks, as described by (Collins et al., 1995) and presented in Figure 2.7 .

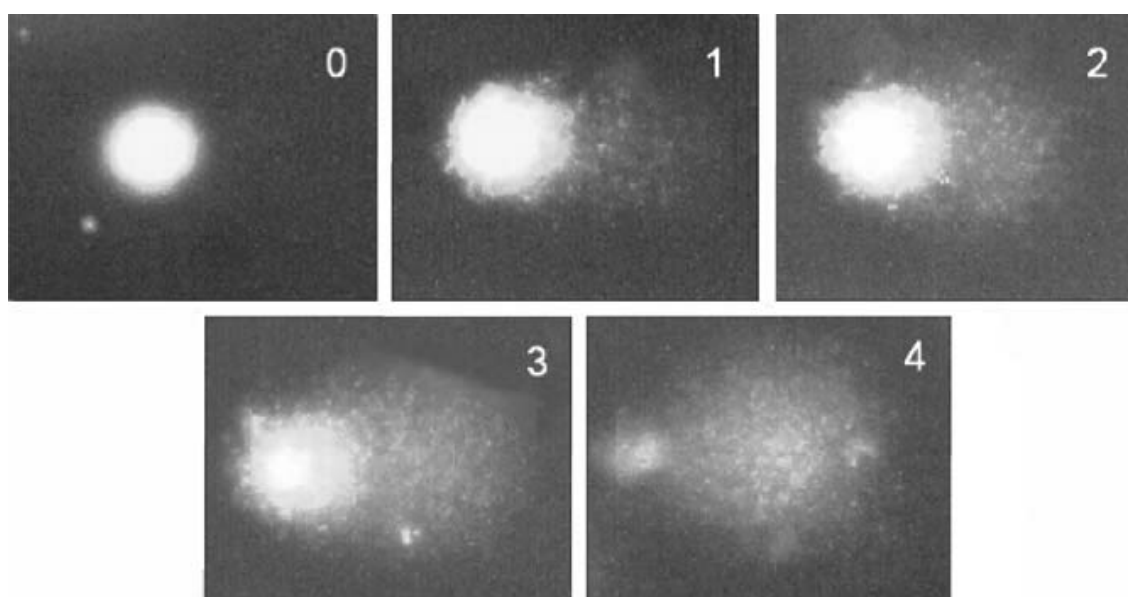


Figure 2.7: Comet visual classification (0-4) following staining with DAPI.

2.2.6.1.2 *Method*

Glass microscope slides were pre-coated in 1% agarose and left to dry. Meanwhile, cells which were exposed to drugs for 72 hours were harvested at a density of 5×10^4 , centrifuged (1500 rpm for 3 minutes) and re-suspended in ice cold PBS. Cells were then mixed with 70 μ l of 1% low

melting point (LMP) agarose at 37°C, pipetted onto the dry pre-coated glass slides and refrigerated at 4°C for 10 minutes. Once set, the slides were incubated in comet lysis solution (Table 2.1) at 4°C for one hour in the dark, to prevent DNA repair and protect from further DNA damage. Slides were then placed into a wide electrophoresis tank and immersed in cool alkaline electrophoresis solution for 40 minutes to unwind the DNA, before electrophoresis at 21V in the dark for 40 minutes. The slides were then washed in neutralising buffer, at 5 minutes intervals for 15 minutes at 4°C. A drop of Vectorshield hard set mounting medium with DAPI (Vector laboratories; Peterborough, UK) was added to the slides to stain the comets and then a coverslip was applied in readiness for visualisation and quantification.

2.2.6.1.3 Analysis

A Leica DMI8 inverted confocal microscope and associated LAS X software (Leica Microsystems Ltd, UK) was used to visualise comets and capture images at 40X magnification. Fifty comets were scored visually based upon the 5 recognisable classes of comet, with 0 being undamaged, and 4 being maximally damaged (Figure 2.7).

2.2.7 Quantifying DNA double strand breaks

2.2.7.1 γ H2AX immunofluorescence assay

2.2.7.1.1 Principle

H2AX is a histone H2A variant that is ubiquitously expressed throughout the genome and plays a key role in the cellular response to DNA damage. DNA double strand breaks (DSBs) prompt rapid phosphorylation of H2AX at serine 139 to form γ H2AX foci. The number of γ H2AX foci has been shown to correspond with the number of DSBs within the cell nucleus. Increased levels of γ H2AX foci have been observed in a number of human cancer cell models including cervical, breast, ovarian and melanoma (reviewed in Palla et al. (2017)) and are associated with tumour progression and poor prognosis. γ H2AX foci are also a useful biomarker for monitoring the efficacy of DNA damaging agents in tumour cells (Ivashkevich et al., 2012).

This assay detects γ H2AX foci in cell nuclei by binding a specific γ H2AX primary antibody with a fluorescently tagged secondary antibody to enable visual identification of foci by microscopy.

2.2.7.1.2 *Method*

PNT1A, DU145 and PC3 cells were seeded onto sterile circular glass coverslips in wells of a sterile 24 well plate, as described in section 2.2.5. Following a 24-hour incubation period to allow cell adherence, culture medium was removed and replaced with medium containing GI₅₀ concentrations of Rucaparib and TSA, alone and in combination. GI₅₀ drug concentrations required for each cell line are presented in Chapter Four, section 4.3.7, Table 4.3. Following a 72-hour incubation period at 37°C, cells were washed in ice cold PBS and fixed with 100% methanol at -20°C for 10 minutes. Excess fixing agent was washed away with PBS and wells were blocked for 30 minutes in 500 μ l bovine serum albumin (BSA) blocking buffer (1% BSA in 1X PBS). Cells were then incubated at 4°C overnight in 100 μ l of primary mouse monoclonal γ H2AX antibody diluted in BSA blocking buffer (Table 2.1). Following incubation with the primary antibody, cells were washed in 500 μ l PBS/0.1% Tween and then incubated in the dark for 1 hour at room temperature in secondary fluorescent antibody Alexa Fluor goat anti-mouse (Dako) diluted in BSA blocking buffer. Cells were washed with distilled water and mounted onto microscope slides with Vectorshield mounting medium with DAPI to counterstain the DNA.

2.2.7.1.3 *Analysis*

Images of cells were captured at 63X magnification using a Leica DMI8 inverted confocal microscope (Leica Microsystems Ltd, UK). γ H2AX foci were manually quantified in 20 nuclei from each treatment slide. Graphs were produced and data was statistically analysed using GraphPad prism software.

2.2.8 **Scratch assay**

2.2.8.1.1 *Principle*

The *in vitro* scratch assay, otherwise known as wound healing assay, is a simple and inexpensive method used to measure cell migration. An artificial “wound” is created by scratching down the

centre of a culture dish containing a confluent cell monolayer. Microscopic images of the scratch are captured over time, at regular intervals, to monitor closure of the gap as cells migrate.

2.2.8.1.2 Method

Cells were seeded into six well plates at a density of 1×10^5 /ml and incubated for 24 hours to allow formation of a confluent monolayer. A p200 pipette tip was then used to gently scratch across the centre of the cell monolayer to create a cell free “wound”. Cells were washed with PBS to remove cell debris and then appropriate drugs, diluted in fresh fully supplemented media, were added to the wells. Cells were visualised at 10X magnification and images of the scratch wound were taken following the addition of drugs, and every 24 hours thereafter for a total of 72 hours.

2.2.8.1.3 Analysis

Wound closure over time was assessed visually and quantitatively. Image J software was used to assess wound closure by tracing the wound parameter to generate a numerical value (pixels) of the wound area. Percentage wound closure was calculated from the raw data to produce graphs in GraphPad prism.

2.2.9 xCELLigence real-time cell analyser (RTCA)

The xCELLigence RTCA system uses micro electric biosensor technology to analyse and quantify cellular events in a non-invasive label free, real time manner. The system measures electrical impedance across micro-electrodes which are integrated across the bottom of specially designed microtiter plates. The impedance measurement is presented as cell index (CI) and is used to quantify cell status. CI is a dimensionless parameter and cell status may be viability, migration or invasion depending on the type of assay used. The xCELLigence system was used to investigate cell migration in the studies described in this thesis.

2.2.9.1 Cell migration CIM-Plate assays

2.2.9.1.1 Principle

The CIM-plate 16 is an electronically integrated Boyden chamber which is used to assess cell migration. It is comprised of an upper and lower chamber which snap together. The lower chamber has 16 wells whereby appropriate chemoattractant is added as a reservoir for cells in the

corresponding upper chamber. The upper chamber has 16 wells which are sealed with a polyethylene terephthalate (PET) microporous membrane. Cells are seeded into the upper chamber of the plate and pass through the microporous membrane onto gold impedance electrodes towards chemoattractant in the lower chamber. The impedance signal produced by cell movement from the upper chamber to the lower chamber enables a quantitative kinetic measurement representative of cell migration.

2.2.9.1.2 Method

Transwell CIM-plates (ACEA Biosciences, Inc, USA) were assembled for migration assays as per manufacturer's instructions. Initially, 160µl (10% FCS, 1% pen/strep) and 50µl (serum starved) of media was added to the lower and upper chambers of the plate which were then locked together and placed into the xCELLigence RTCA DP device for 30 minutes (37°C, 5% CO₂ and 95% O₂) to allow plates to reach equilibrium. Following incubation, a baseline measurement was taken, and cells were seeded at their optimum seeding densities into wells of the upper chamber. Plates were incubated for a further 15 minutes to allow cells to settle onto the membrane. Cell migration through the 8µM pore membrane was measured by a microelectrode on the underside of the membrane, giving a cell index value based on impedance. Cell migration was measured every 5 minutes for 72 hours in the xCELLigence DP system according to the manufacturer's instructions.

2.2.9.1.3 Analysis

Raw data was acquired and analysed with the RTCA software (version 1.2.1, ACEA Biosciences Inc). GraphPad PRISM software was then utilised to produce graphical representations.

2.2.10 Transient small interfering ribonucleic acid (siRNA) transfection

2.2.10.1.1 Principle

Ribonucleic acid (RNA) interference (RNAi) is a common tool used to silence any gene by inactivation of the corresponding mRNA. The most common way to knockdown gene expression by RNAi technology is with use of small interfering RNA (siRNA). siRNA is double stranded RNA (dsRNA) that is cleaved by the RNase III enzyme DICER to produce 2 nucleotide overhangs

at the 3' end of the dsRNA. The cleaved siRNA, along with dicer and argonaute-2 (Ago-2) proteins, forms a complex known as the RNA-induced silencing complex (RISC); which uses the siRNA as a guide to target and cleave mRNA. The cleaved mRNA becomes degraded, leading to a loss of RNA transcript and therefore gene silencing. The mechanism of gene silencing is presented below in Figure 2.8.

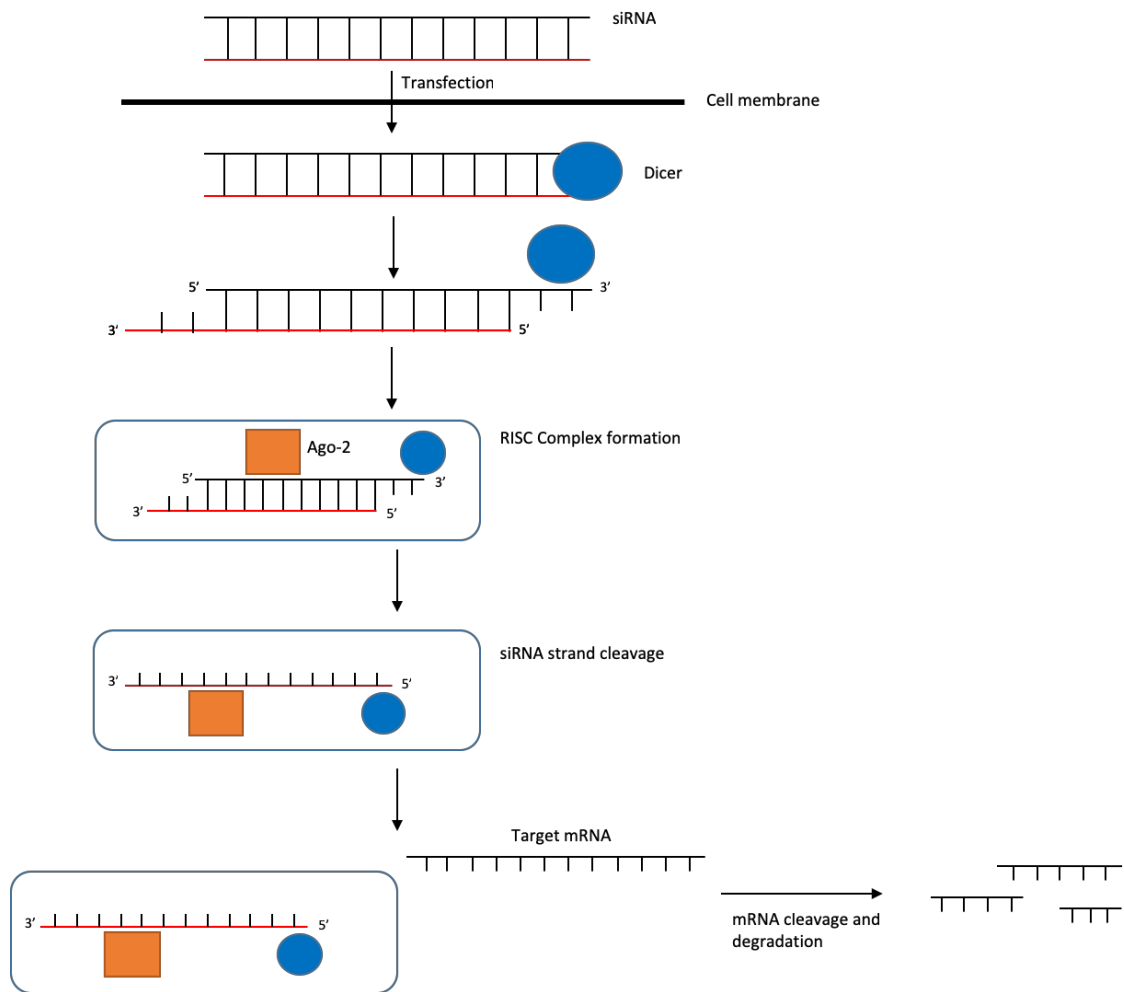


Figure 2.8: siRNA gene silencing mechanism.

siRNA is transfected into the cell and enters the cytoplasm where it becomes cleaved by the RNase III enzyme dicer to produce a 2-nucleotide overhang at the 3' end of the dsRNA. Cleaved siRNA forms a RISC complex with dicer and Ago-2. One of the siRNA strands is cleaved by dicer and removed from the complex. The remaining strand in the RISC can bind to the complementary target mRNA sequence. Ago-2 binds both the siRNA and target mRNA, resulting in mRNA cleavage and consequently gene silencing.

This technique relies on siRNA being imported into the cell by transfection. Lipid transfection is the most common method of transfection and is the method employed in this thesis. Lipid transfection reagents couple a nucleic acid to a cationic lipid to produce a liposome that interacts with the cell membrane and enables transportation of the nucleic acid into the cell.

Five siRNA molecules were used in this thesis; two were used to knockdown the expression of human Maspin, one to knockdown human PARP-1 and two were used as control/non-specific siRNAs. Maspin and PARP-1 siRNA target sequences were obtained from the theses of group members Dr Louise Brown and Dr Jill Hunter, respectively. The siRNA target sequences are presented below in Table 2.6.

Table 2.6: Human Maspin and PARP-1 siRNA target sequences

Target gene	siRNA number	Product Name	Supplier	siRNA sequence
<i>Maspin/SERPINB5</i>	1	Hs_SERPINB 5_6	Qiagen (Manchester, UK)	GCCGTTGATCTGTTC AAACAA
<i>Maspin/SERPINB5</i>	2	Hs_SERPINB 5_1	Qiagen (Manchester, UK)	TCAGATCAACAACCT CAATTAA
<i>PARP-1</i>	-	PARP-1	Dharmacon (Cramlington, UK)	AAGCCUCCGCUCCUG AACAAU

2.2.10.1.2 Method

Maspin siRNA was obtained from Qiagen and reconstituted in 100µl sterile, RNase-free water to make a stock concentration of 10µM. Corresponding control siRNA was reconstituted to a 20µM concentration. PARP-1 and control siRNA was purchased from Dharmacon and reconstituted in 1x siRNA buffer to make 20µM stock concentrations. All siRNA oligos were stored at -20°C in aliquots until required for transfection.

Cells were seeded into 6 well plates and incubated at 37°C/5% CO₂ for 24 hours prior to transfection to enable cell adherence. Cells were then transfected with either 10nM Maspin or control siRNA, or 50nM PARP-1 or control siRNA. In sterile conditions, siRNAs were incubated in serum free RPMI media for 5 minutes and then mixed with Hiperfect siRNA transfection reagent (Qiagen, UK). Transfection mixes were briefly vortexed and incubated at room temperature for 30 minutes, to allow the siRNA molecules to form complexes with the Hiperfect, and then added directly to the cell culture plate containing cells in a dropwise manner. Cells were returned to incubation for 6 hours, before aspirating the media and replacing with fully

supplemented media for a desired time period at 37°C/5% CO₂. Samples were harvested, lysed and then protein knockdown was assessed by Western blotting, as described in 2.2.4.

2.2.11 Statistical Analysis

All statistical tests presented were carried out using GraphPad Prism software. The statistical tests used throughout this thesis are described below and are specified, as appropriate, in each chapter.

2.2.11.1 One-way analysis of variance (ANOVA)

The one-way ANOVA is a hypothesis-based test that determines whether there are any statistically significant differences between the means of three or more independent groups whilst considering only one independent variable. If at least two group means are statistically different from each other the test returns a statistically significant result. In this instance, a post hoc test is carried out to determine which specific groups differ from each other. Tukey's with multiple comparisons is a common post hoc test and was the post hoc test selected for use in this thesis. It compares the means of all treatments to the mean of every other treatment to allow identification of groups that significantly differ.

2.2.11.2 Two-way ANOVA

The two-way ANOVA test is an extension of one-way ANOVA. It compares the mean differences between the means of three or more independent groups of data that have been split in to two independent variables. Like one-way ANOVA, a post hoc test such as Tukey's with multiple comparisons may be carried out if a significant difference is identified between groups.

2.2.11.3 Independent T-test

The independent t-test (unpaired t-test) compares the means of two independent groups, assuming that the values follow a gaussian (normal) distribution, to determine if there is a significant difference.

Chapter Three

In vitro studies to characterise a panel of immortalised cell lines.

3.1 Introduction

This chapter presents the characterisation of prostate and Mouse Embryonic Fibroblasts (MEF) cell lines used throughout this thesis. Additionally, it explores the effect of maspin protein expression on the levels and localisation of PARP-1 and NF- κ B subunits.

3.1.1 Cell lines

Immortalised cell lines are used in medical research to study biological processes at the cellular and molecular level. They are cost effective, provide an unlimited supply of cells and bypass ethical issues associated with the use of animal and human tissue (Kaur and Dufour, 2012).

The cell lines selected for study throughout this thesis are summarised in 2.2.1 and Table 2.2. DU145 and PC3 human prostate cancer cells are two of the most commonly used androgen-independent cell lines used in prostate cancer research (Sampson *et al.*, 2013). The PNT1A cell line was selected for use as a non-cancerous control. The MEF cells used throughout this thesis are isogenic immortalised mouse embryonic fibroblasts engineered from primary cells through the introduction of a targeted gene mutation. MEF p65^{+/+} and p65^{-/-} cells are proficient and deficient in the *NF- κ B p65/RelA* gene, respectively. MEF IKK α ^{-/-} cells are deficient in the IKK α gene. These cell models provide a system for the study of NF- κ B genes and their role in cellular processes and drug response. Any differences between the isogenic MEF cells in the studies presented in thesis provide functional validation attributed to the presence or absence of the NF- κ B p65 and IKK α genes.

3.1.2 Cell line authentication

Cell line authentication is important to confirm that you are working with cells that are not cross contaminated or misidentified and to add stringency in research results. Despite a rise in cell line authentication to meet the demands of high impact journals, many cell lines remain unidentified; and there are still an unknown number of publications reporting on misidentified cell lines.

Misidentified cell lines impact study reproducibility and validity in research data (Almeida et al., 2016). To this end, many published articles have been retracted (Clement-Schatlo et al., 2012, He et al., 2015, Zhang et al., 2013). HeLa cells are a cervical cancer cell line that have been widely documented as a contaminant of tissue culture. The immortalised cell line was derived from the cervical cancer cells of Henrietta Lacks, a patient who died of cancer in 1951 (Masters, 2002). HeLa were the first immortalised human cancer cell line and are still the most commonly used human cell line in biomedical research. HeLa cell contamination is a common problem in tissue culture research due to rapid proliferation and lack of contact inhibition. The controversy surrounding HeLa cell contamination began in the 1960's when Gartler (1967) demonstrated that the epidermoid carcinoma KB cell line identified by Harry Eagle in 1955 was misidentified and was in fact HeLa. Strikingly, the original stocks of KB given to the ATCC by Harry Eagle, after 50 years of testing, still show no authentic material. Vaughan et al. (2017) explored the impact of HeLa cell misidentification on scientific literature to highlight the need for journals to require cell line authentication testing as a condition of publication. Using the PubMed database, they identified 631 journal articles between the years 2000-2014 that stated the use of KB. Only 57 of these articles correctly acknowledged that KB were in fact HeLa.

Short tandem repeat (STR) profiling is the gold standard technique for human cell line authentication to the individual gene level. It adheres to a strict standard (ASN-0002) for human cell line authentication set out by the American National Standards Institute (ANSI) and the American Type Culture Collection (ATCC) (Almeida et al., 2016). STR profiling is an analytical DNA technique that utilises primers to identify repeated sequences of DNA (STR loci) that are typically 2 to 6 base pairs long. The STR profile generated from a given test sample is compared to a parental cell line on the ATCC database to confirm authenticity (Nims et al., 2010). Authentication of non-human cell lines is less clear and is burdened by the lack of development in testing, databases and accepted STR standards.

3.1.3 Mycoplasma

Mycoplasma is a prokaryotic organism that is a frequent contaminant of cell cultures. The presence of mycoplasma compromises host cell line physiology by altering gene expression,

inducing chromosomal abnormalities and changing cell growth characteristics; consequently hindering the results and conclusions of any experiment (Nikfarjam and Farzaneh, 2012a). For example, Zhang et al. (2000b) investigated the effects of mycoplasma on gene expression in immortalised cervical and prostate cell lines. They measured the transcripts of 38 cytokine genes before and after mycoplasma contamination; finding that 55-74% of the cytokine genes expressed in the two cell lines were altered. Other studies have also reported changes to gene expression and cell growth following Mycoplasma contamination (Miller et al., 2003, Liu and Shou, 2011).

The main sources of mycoplasma contamination vary from personnel to materials and equipment used in the tissue culture laboratories. It is important that laboratories adhere to strict rules for aseptic technique to limit contamination, and test cell stocks for potential contamination on a regular basis. DNA staining and PCR based methods are the most common techniques used to detect mycoplasma contamination.

3.1.4 Cell proliferation

Cell proliferation is defined as an increase in cell number secondary to cell growth and division (Romar et al., 2016). Assessment of cell proliferation is crucial to cell studies as it provides information about general cell health and maintenance. The traditional way to assess cell proliferation in cultured cells is by cell counting with a haemocytometer. It is low cost and a direct measure of cell number; it is also time consuming and relies on thorough training to minimise human error (Morten et al., 2016). Various multiwell-plate assays have been developed to measure cell proliferation; each of which monitor different parameters such as protein content, DNA synthesis and metabolic activity (Reviewed in Riss et al. (2004) and Orellana and Kasinski (2016)). The type of multiwell-plate assay used is dependent on personal preference, the nature of the study, cost and the equipment available. The assays are easy to use and are able to assess cell proliferation on a large scale, in less time and with increased sensitivity. There are some disadvantages to the use of multiwell plate assays for the assessment of cell proliferation. Spectrophotometers are only accurate in a linear range and do not discriminate between the sample of interest and contaminants that absorb at the same wavelength. Spectrophotometer results may also be influenced by temperature, pH and impurities (Geisler, 2015).

3.1.5 Cell morphology

Regular assessment of cell morphology is important when carrying out cell culture work to ensure that cells are healthy and free from contamination. Cell deterioration and change to normal morphology may occur for a variety of reasons, such as contamination of the culture, cellular stress and cytotoxicity. Changes to cell morphology include change in cell shape, size and viability.

3.1.6 Protein expression and localisation

Proteins are versatile macromolecules and they are involved in virtually every cellular process. The expression of proteins within a cell provides insight into complex biological processes.

Investigating the expression levels of specific proteins is important for cell characterisation but also for their roles in disease and progression (Ponten et al., 2009). Many proteins play a role in disease and its progression; making them suitable targets for therapeutic exploitation. For example, PARP-1 is overexpressed in many different tumours and is associated with disease deterioration, metastasis and therapeutic resistance (as discussed in Chapter one, section 1.4). To this end, PARP inhibitors have been developed to selectively target PARP-1 with an aim to overcome drug resistance and improve disease outcome (Wang et al., 2017).

Identifying the sub-cellular localisation of a protein within a cell is also an essential step towards understanding its function, interaction partners and potential roles in functional biological networks. Changes to protein subcellular localisation alters normal cell functioning, behaviour and regulation which contributes to the development and progression of human disease, including cancer (Hung and Link, 2011).

3.2 Chapter aims

The aim of this chapter was to characterise the cell lines used throughout this thesis, to validate cell lines, identify optimal conditions for exponential cell growth and seeding, and to assess differences in protein expression and localisation for subsequent investigations. The following parameters were explored:

- Cell line authentication

- Mycoplasma
- Cell proliferation rates
- Cellular morphology
- Expression and localisation of PARP-1, NF-kB p50, NF-kB p65, IKK α , IKB α , RelB, Maspin and HDAC-1 proteins in prostate cell line models by Western Blotting and Immunofluorescence.

3.3 Results

3.3.1 Authentication of cell lines by DNA STR analysis

Human cell lines were authenticated by Northgene (Newcastle, UK) to confirm the identity of the cell lines and to ensure the validity of research findings. Cell samples were collected using an FTA card sample collection kit provided by NorthGene.

Briefly, cells were harvested, centrifuged and resuspended in fresh fully supplemented media to create a cell suspension of 5×10^5 /ml. 50 μ l of the cell suspension was pipetted on to the centre of an FTA card; chemically treated filter paper that is designed for the collection and preservation of biological samples for subsequent DNA analysis. Cell samples were then sent to NorthGene in plastic bags with a desiccant for testing and analysis.

The DNA STR profiles of each cell line were authenticated using markers provided by the ASN-0002 standard. The STR profile for each cell line was compared against the STR profiles of the parental cell lines on the ATCC DNA STR database and a matching percentage was calculated. DU145 and PC3 cells were successfully authenticated with a 95% and 94% match, respectively. PNT1A was not successfully authenticated as a full allelic reference profile could not be obtained on the ATCC database in accordance with the ASN-0002 standards. The STR profile for PNT1A was unique and did not match with any samples on the database. A reference STR profile for the PNT1A cell line was found online on the ExPASy Bioinformatics resource portal and two STR loci that fit the ASN-0002 standard criteria, vWA and Amelogenin, matched with the PNT1A cell line. The other Locus identified were not comparable against the criteria. Mouse embryonic fibroblasts were not authenticated as these cell lines are not derived from a human source.

Table 3.1: PNT1A cell allelic data.

Genotypes were identified by STR analysis and could not be matched to a profile on the ATTC database. Two comparable STR locus were matched online.

STR Locus	Genotypes: PNT1A (cell sample)	Genotypes: PNT1A (Online database sample)	Match vs. Mis-Match
D5	12 12	-	-
D13	11 11	-	-
D7	10 10	-	-
D16	10 11	-	-
vWA	17 19	17 19	Match
Amelogenin	X Y	X Y	Match
TPOX	8 8	-	-
CSF1PO	12 12	-	-
THO1	6 6	-	-

Table 3.2: DU145 cell allelic data.

STR Locus	Genotypes: DU145 (cell sample)	Genotypes: DU145 Prostate Carcinoma Human (ATTC database sample)	Match vs. Mis-Match
D5	10 1	10 1	Match
D13	12 14	12 13 14	Mis-Match
D7	7 10 11	7 10 11	Match
D16	11 13	11 13	Match
vWA	17 18 19	17 18 19	Match
Amelogenin	X Y	X Y	Match
TPOX	11 11	11 11	Match
CSF1PO	10 11	10 11	Match
THO1	7 7	7 7	Match

Table 3.3: PC3 cell allelic data.

STR Locus	Genotypes: PC3 (cell sample)	Genotypes: PC3 Prostate Adenocarcinoma Human (ATTC database sample)	Match vs. Mis-Match
D5	13 13	13 13	Match
D13	11 11	11 11	Match
D7	8 8	8 11	Mis-Match
D16	11 11	11 11	Match
vWA	17 17	17 17	Match
Amelogenin	X X	X X	Match
TPOX	8 9	8 9	Match
CSF1PO	11 11	11 11	Match
THO1	6 7	6 7	Match

3.3.2 Mycoplasma screening

All of the cell lines used throughout this thesis were screened for mycoplasma using the PCR based Venor GeM Mycoplasma Detection Kit, as described in section 2.2.1.5. All prostate and MEF cell lines were negative for Mycoplasma contamination, as shown in Figure 3.1.

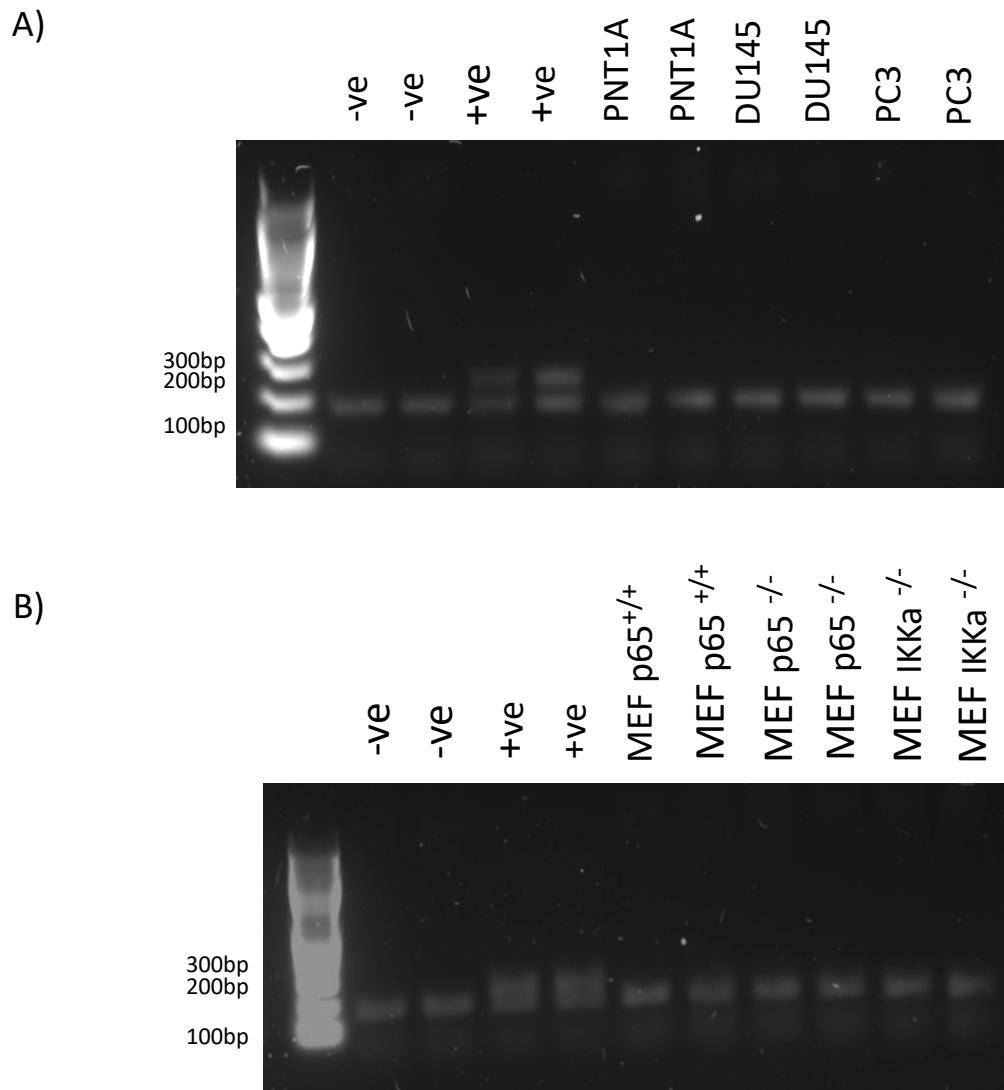


Figure 3.1: Mycoplasma testing of (A) Prostate and (B) Mouse embryonic fibroblast (MEF) cell lines by PCR using the Venor®GeM OneStep detection kit.

DNA products were visualised by gel electrophoresis through a 1.5% agarose gel containing SYBR™safe (ThermoFisher Scientific, Cramlington, UK). A positive result for mycoplasma gives rise to a band ~270bp. All samples tested were negative for mycoplasma contamination (191bp).

Prostate cells were also fixed and stained with DAPI for identification of mycoplasma. Briefly, cells were seeded onto glass coverslips in 6-well plates and then fixed with ice cold methanol when in exponential growth. Fixed cells were washed in PBS and then mounted onto microscope slides with Vectorshield mounting medium containing DAPI. Cell nuclei were visualised by confocal microscopy to confirm the presence or absence of mycoplasma contamination. Presence of a dotted stain around the cell nuclei is an indicator of mycoplasma contamination. The image

presented below in Figure 3.2 is representative of mycoplasma contaminated cells stained with DAPI.

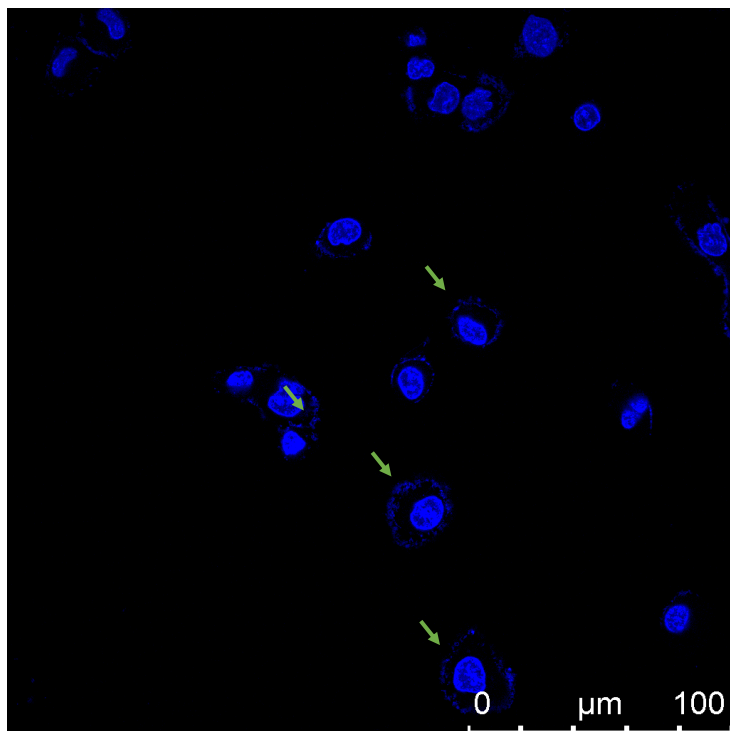
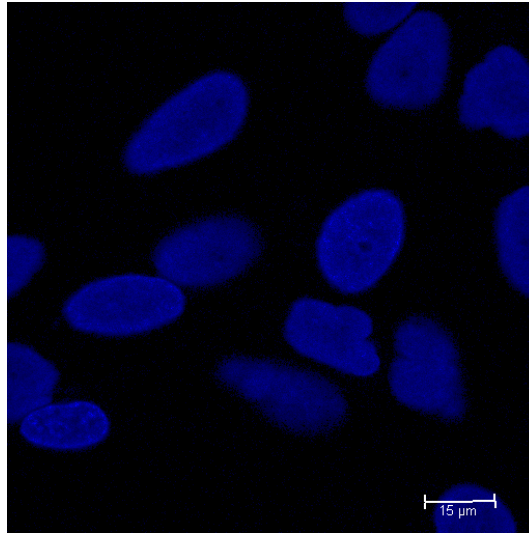


Figure 3.2: DAPI staining of cells contaminated with mycoplasma.

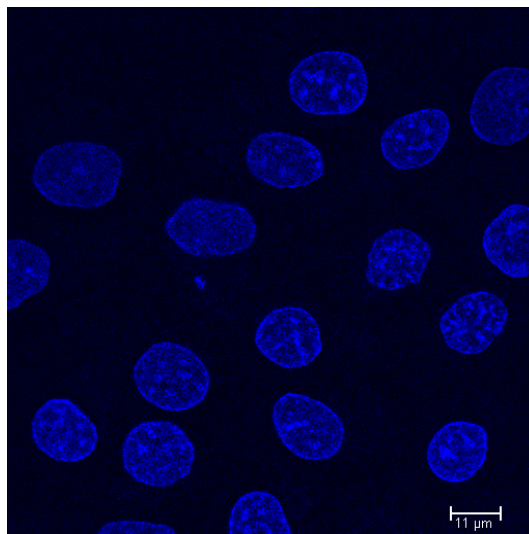
The DAPI image demonstrates fluorescence of the eukaryotic cell nuclei and the extra nuclear prokaryotic DNA (green arrows).

In line with the PCR data presented in Figure 3.1, the representative DAPI images presented below in Figure 3.3 confirm the absence of mycoplasma contamination in all prostate cell lines.

A)



B)



C)

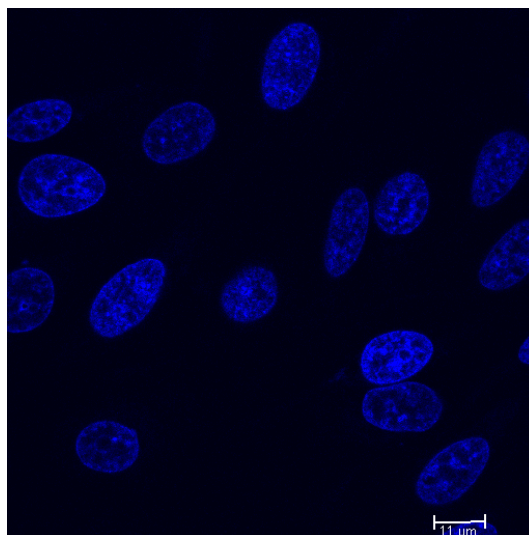


Figure 3.3: DAPI staining of prostate cells to confirm the absence of Mycoplasma contamination. (A) PNT1A, (B) DU145 and (C) PC3 cell nuclei were stained with DAPI and visualised by confocal microscopy at x63 magnification.

3.3.3 Proliferation rates of cell lines

The cell proliferation rate and optimal cell density required for exponential growth was identified by WST-1 assay for each cell line, as described in section 2.2.3.1. Prostate cell lines cells proliferated exponentially at a cell density of 2.5×10^4 /ml for 72 hours (Figure 3.4 and Figure 3.5).

MEF p65^{+/+}, MEF p65^{-/-} and MEF IKK α ^{-/-} cells proliferated exponentially at a cell density of 0.5×10^4 /ml for 72 hours. A mean doubling time of 34 +/-1hr was observed for all prostate cell lines when seeded at their optimum densities. A mean doubling time of 21 +2hr was observed from all MEF cell lines when seeded at their optimum densities for exponential growth (Table 3.4).

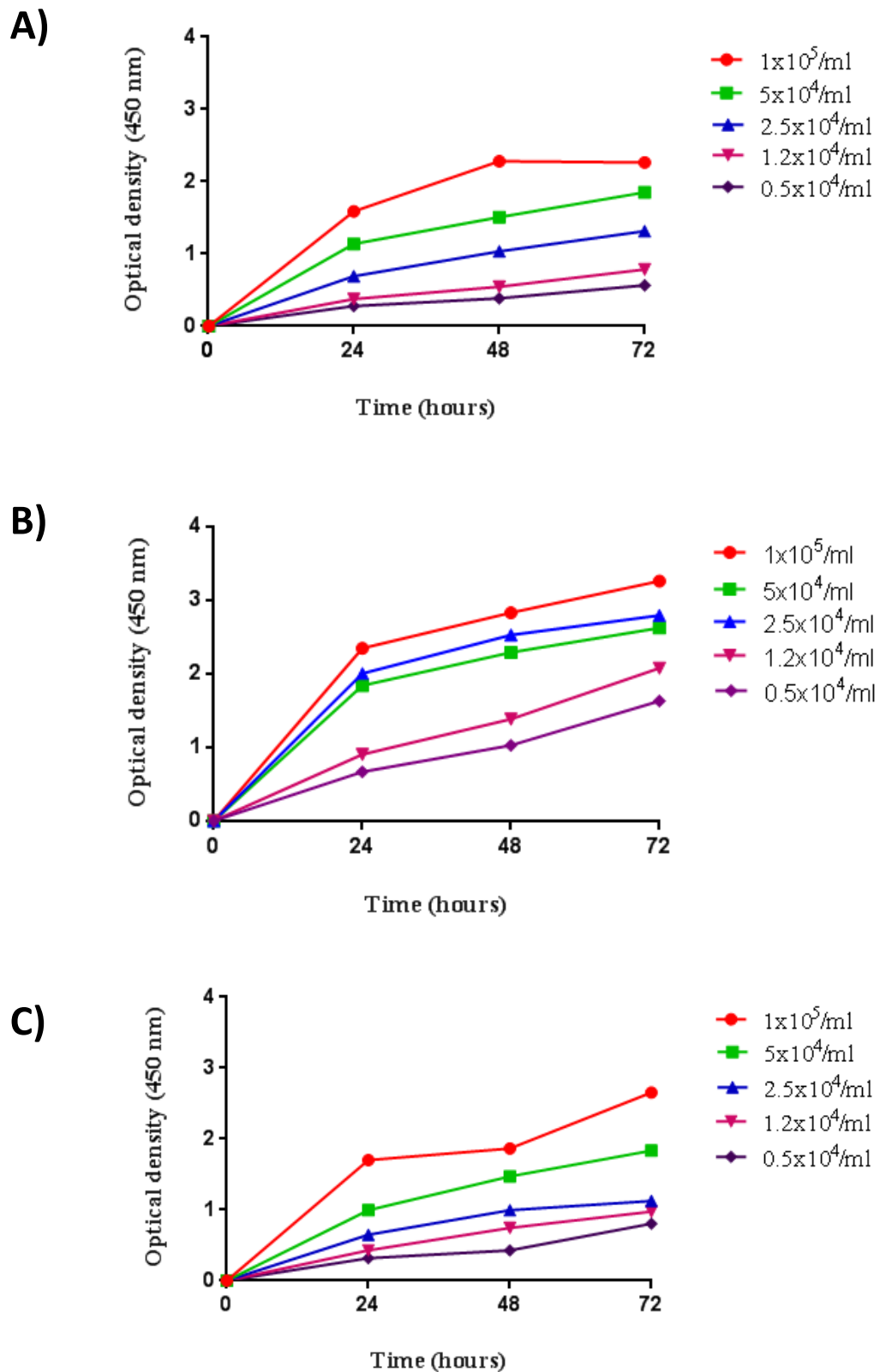


Figure 3.4: Representative growth curves to show cell proliferation of prostate cells. (A) PNT1A, (B) DU145 and (C) PC3 cells were seeded at various densities ranging from $1 \times 10^5/\text{ml}$ to $0.5 \times 10^4/\text{ml}$. Proliferation was measured via cleavage of the WST-1 tetrazolium salt at 24-hour intervals, for 72 hours.

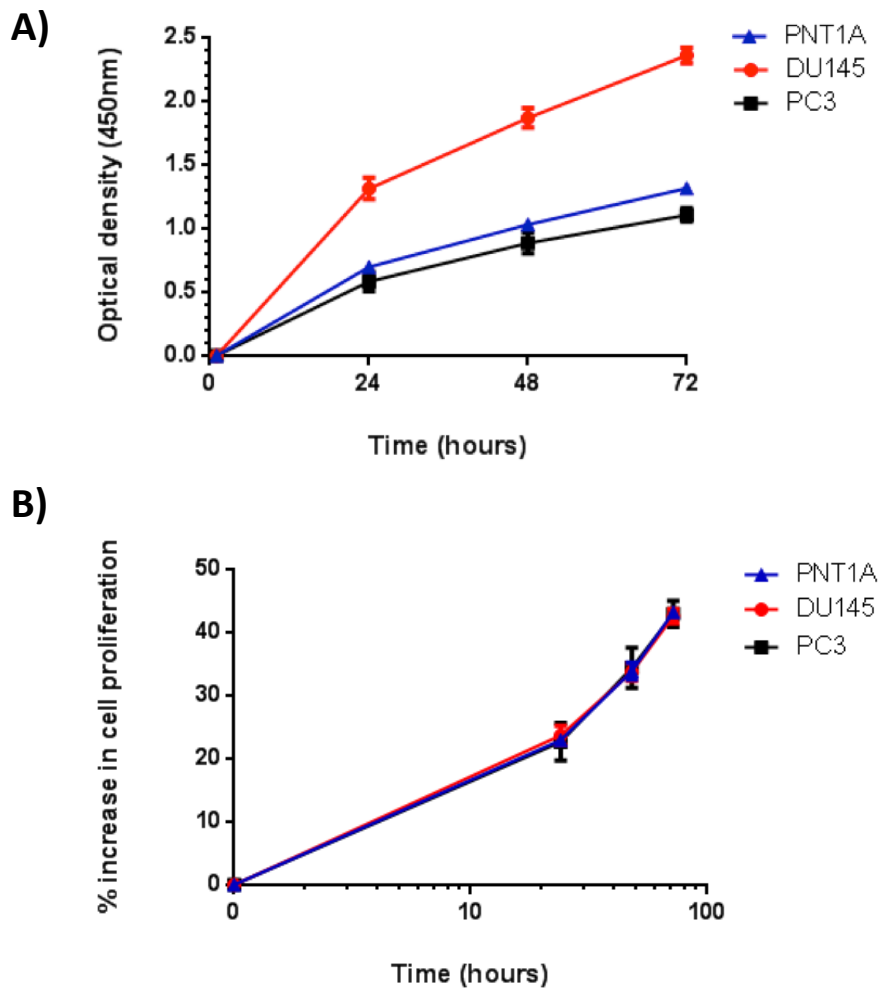


Figure 3.5: PNT1A, DU145 and PC3 cells proliferate exponentially at a density of 2.5×10^4 /ml.

(A) A cell seeding density of 2.5×10^4 /ml was selected as the optimum seeding density for all experiments, unless otherwise stated, to ensure at least 1-2 cell doublings within the exponential growth phase. Error bars represent standard error of the mean (SEM). (B) Normalised graph to show the percentage increase in cell proliferation over 72 hours at a density of 2.5×10^4 /ml. There was no significant difference in cell proliferation between DU145, PC3 and PNT1A cells (One-way ANOVA, $p=1.0000$). Data are the average of at least three independent experiments and error bars represent standard error of the mean (SEM).

Table 3.4: Optimum cell densities and doubling times.

Cell proliferation rates were measured by WST-1 assay and doubling times were calculated by non-linear regression of the curve of log absorbance against time in GraphPad PRISM. Data represents the mean of at least three independent experiments +/- SD.

Cell line	Optimum seeding density for exponential growth	Mean doubling time (hours)	Standard Deviation (SD)
PNT1A	2.5×10^4 /ml	34	1.23
DU145	2.5×10^4 /ml	35	2.81
PC3	2.5×10^4 /ml	34	5.61
MEF p65 ^{+/+}	0.5×10^4 /ml	23	0.06
MEF p65 ^{-/-}	0.5×10^4 /ml	21	0.12
MEF IKK α ^{-/-}	0.5×10^4 /ml	21	0.15

3.3.4 Cell morphology

Cell morphology was assessed during routine subculture and during experiments by light microscopy. Cells were seeded at their optimum growing densities and images were captured using a Leica optical microscope 24 hours later, when cells had adhered to the surface of culture flasks.

Prostate cell lines presented epithelial-like morphology, appeared polygonal in shape and attached to the surface of the culture flasks in discrete patches (Figure 3.6). There were visible differences in morphology between the three different prostate cell lines. Normal PNT1A prostate cells are larger than the cancerous DU145 and PC3 prostate cells. PNT1A and PC3 appeared to be more elongated than DU145 cells.

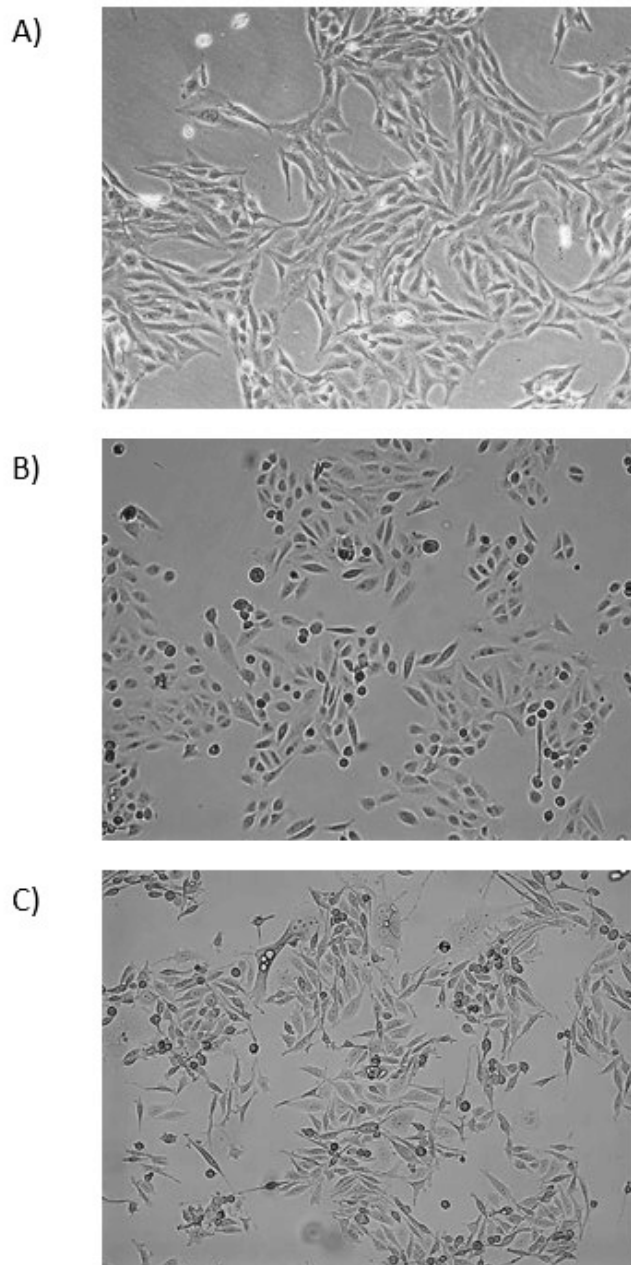


Figure 3.6: Cell morphology of (A) PNT1A, (B) DU145 and (C) PC3 prostate cells in culture. Cells were seeded at 2.5×10^4 /ml. Images were captured 24 hours after seeding by Brightfield microscopy, X10 magnification.

MEF cells presented a fibroblast-like morphology, as shown in Figure 3.7. MEF $IKK\alpha^{-/-}$ knockout cells were larger and more elongated than the $p65^{+/+}$ and $p65^{-/-}$ MEF cells which were compact.

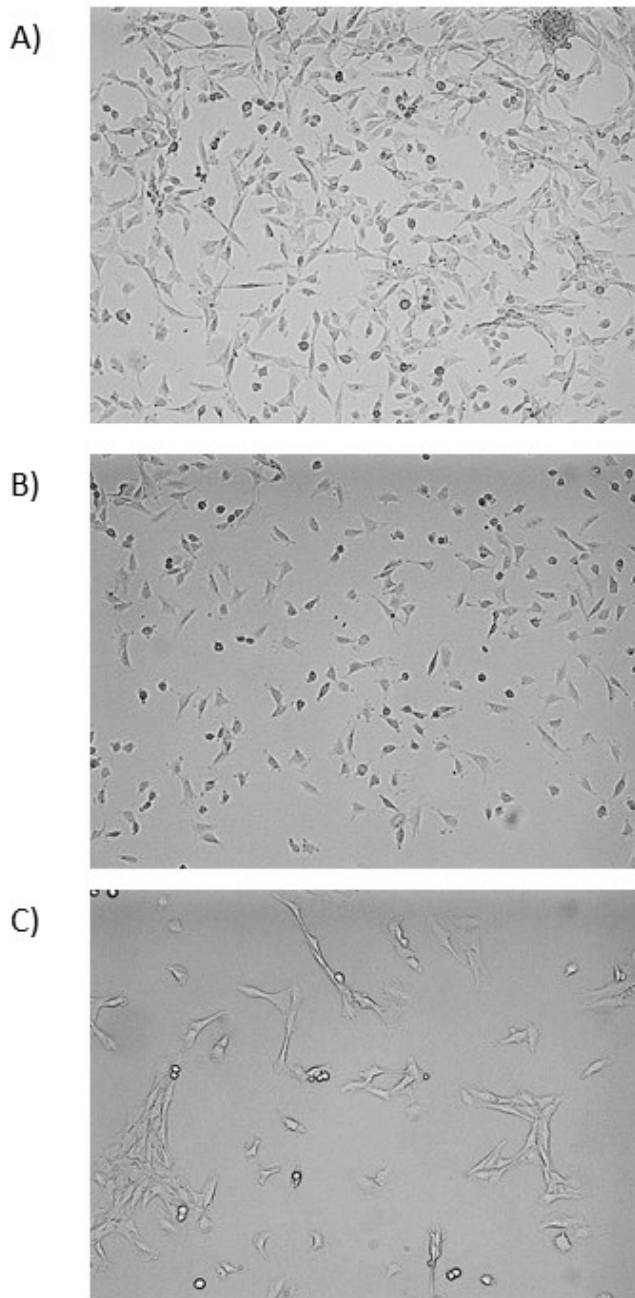


Figure 3.7: Cell morphology of MEF cells (A) $p65^{+/+}$, (B) $p65^{-/-}$ and (C) $IKK\alpha^{-/-}$ in culture. Cells were seeded at 2.5×10^4 /ml. Images were captured 24 hours after seeding by Brightfield microscopy, X10 magnification.

3.3.5 Protein expression and subcellular localisation

The expression levels of PARP-1, NF- κ B p50, NF- κ B p65, IKK α , IKB α , RelB, maspin and HDAC-1 proteins were visualised in PNT1A, DU145 and PC3 prostate cells by Western blotting (Figure 3.8). Briefly, exponentially growing cells were harvested, cell lysates were prepared and loaded onto 10% SDS-PAGE gels prior to protein separation by gel electrophoresis; as described

in section 2.2.4. Separated proteins were electro-transferred onto nitrocellulose membrane and probed for the proteins of interest using specific antibodies (Table 2.3 and Table 2.4). The house keeping protein, Anti-Actin, was used as a loading control. This loading control was chosen due to its general expression across all eukaryotic cells. It must be acknowledged that the protein expression data for PNT1A cells are from a different experiment and therefore the protein levels in these cells are subjective and the best estimates.

PARP-1 protein levels were higher in PNT1A and PC3 cells than DU145 cells. Interestingly, DU145 cells expressed higher levels of NF-kB p50 protein but lower levels of NF-kB p65 and RelB when compared to PNT1A and PC3 prostate cells. IKK α protein expression levels were also higher in DU145 cells. Expression of IKB α appeared equal in all cells lines relative to loading control. As expected, maspin levels were less in DU145 cells than that observed in PNT1A and PC3 cells. HDAC-1 levels were higher in PNT1A and PC3 cells than DU145 cells, relative to loading control.

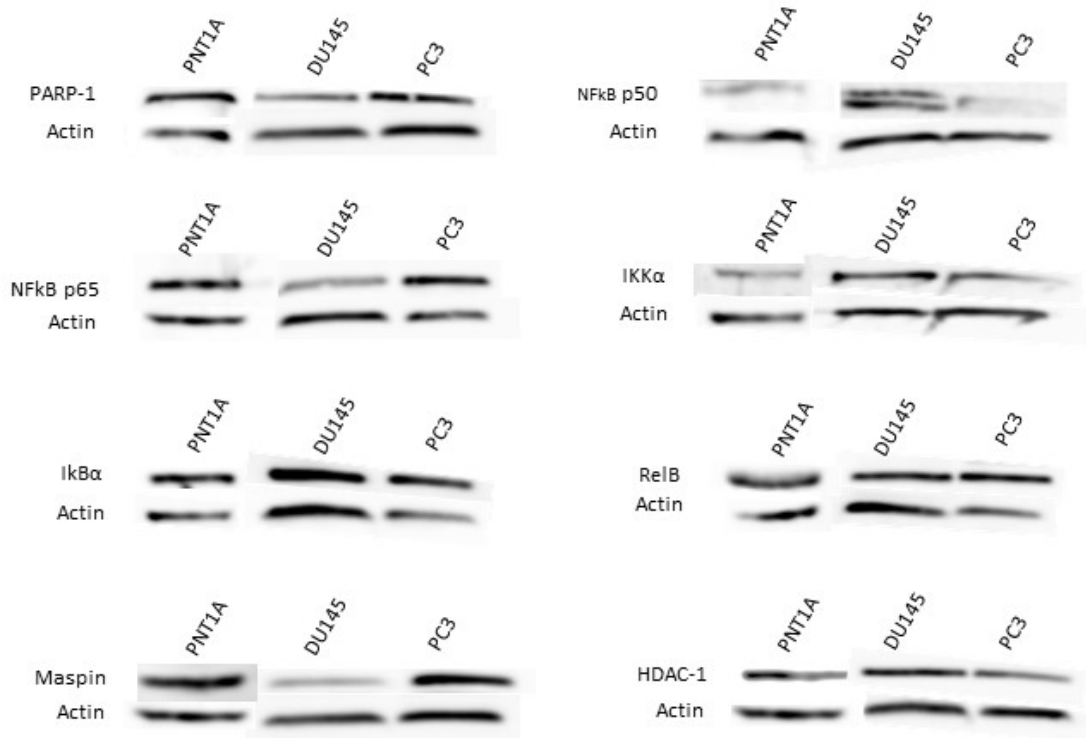


Figure 3.8: Representative Western blots of whole PNT1A, DU145 and PC3 prostate cell protein extracts.

Blots were probed using antibodies against: PARP-1, NF-kB p50, NF-kB p65, IKK α , I κ B α , RelB, maspin, HDAC-1 and Anti-Actin.

Protein expression levels were normalised to Anti-Actin loading controls and quantified using ImageJ densitometry software. This produced semi-quantitative measurements of protein expression which enabled standardised comparison of proteins between each cell line. This data is presented in Figure 3.9. Significant differences in the expression levels of proteins were determined by one-way ANOVA analysis followed by Tukey's multiple comparisons test. The mean semi-quantified expression data mirrored the visual expression results presented in Figure 3.8, whereby the expression of IKK α was inversely proportional to maspin expression (Figure 3.9 D and G). PARP-1 expression (A) correlated with NF-kB p65 (C) and maspin (G) expression. PARP-1 and maspin expression was inversely proportional to HDAC-1 (H).

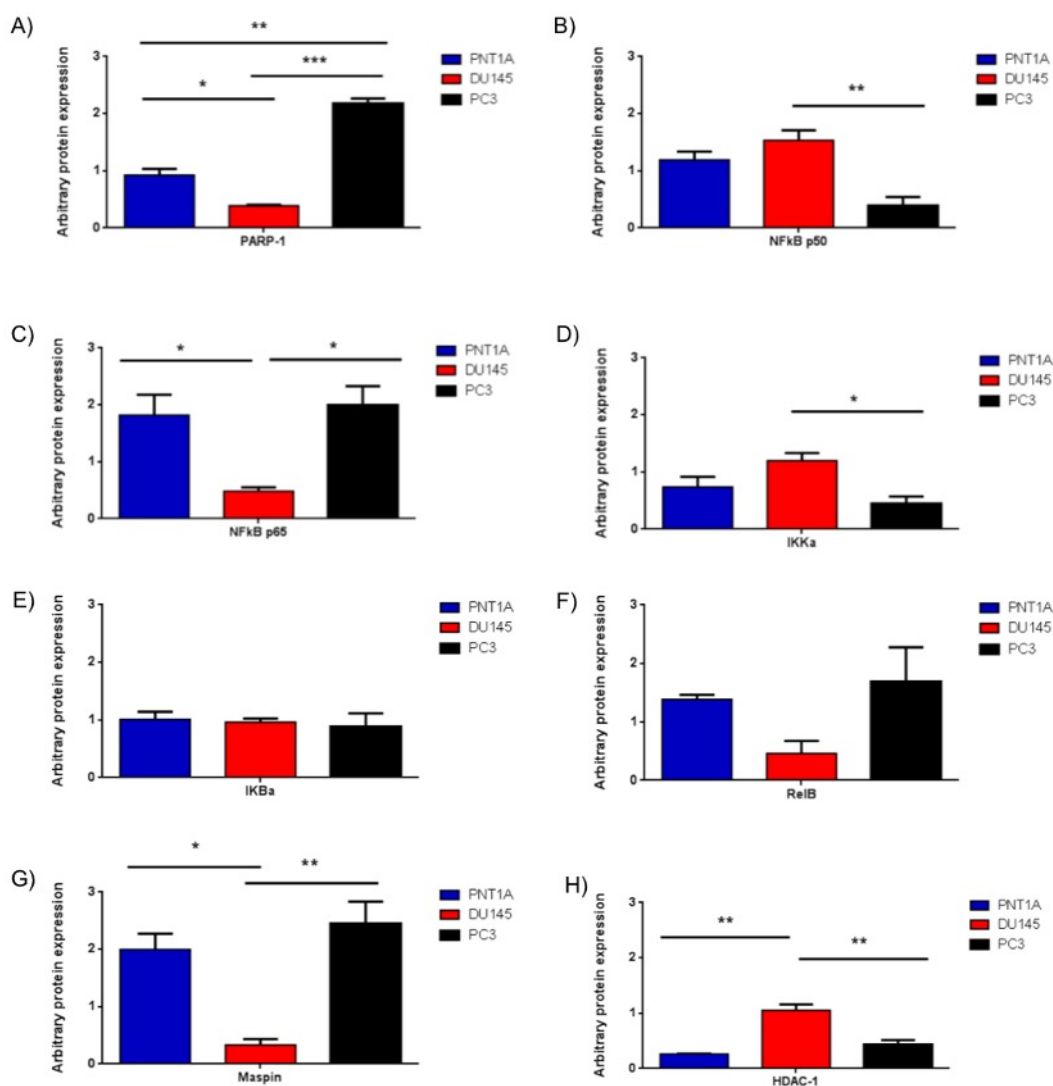


Figure 3.9: Semi-quantitative expression of proteins in prostate cell lines.

(A) PARP -1, (B) NF-kB p50, (C) NFkB p65, (D) IKK α , (E) IKB α , (F) RelB, (G) Maspin and (H) HDAC-1 protein expression in PNT1A, DU145 and PC3 cell lines was quantified with ImageJ densitometry software. Expression data were normalised to β -actin and expressed as mean + SEM (n = 3). Significant differences were determined by one-way ANOVA analysis followed by Tukey's multiple comparison test. *P < 0.05, **P < 0.01 and ***P < 0.001.

The results presented below (Figure 3.10-Figure 3.12) display the expression levels of the proteins investigated in each cell line along with immunofluorescence results to show their subcellular localisation. For immunofluorescence experiments, cells were grown on to glass coverslips for 48 hours, fixed in 100% ice cold methanol, incubated with appropriate primary and secondary antibodies (Table 2.3 and Table 2.4) and then visualised with confocal microscopy, as described in section 2.2.5.

The expression of PARP-1 protein was less than the expression of maspin ($P < 0.05$) in PNT1A cells. This could indicate that the maspin antibody worked better than the PARP-1 antibody for the immunofluorescence technique. HDAC-1 and IKK α expression levels were both reduced in the presence of maspin ($P < 0.05$). Interestingly, there were higher levels of NF-kB p65 than NF-kB p50 (Figure 3.10a). PARP-1 and HDAC-1 expression was confined to the nucleus of PNT1A cells. Maspin, NF-kB p65 and NF-kB p50 was confined to the cytoplasm. Expression of NF-kB p50 was low in comparison to NF-kB p65, in line with Western blotting results. IKK α , IKB α and RelB was expressed in both the nucleus and cytoplasm (Figure 3.10b).

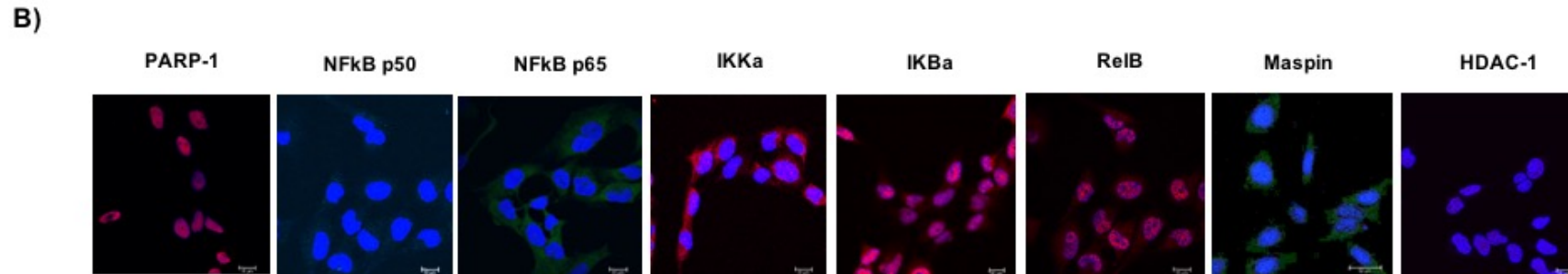
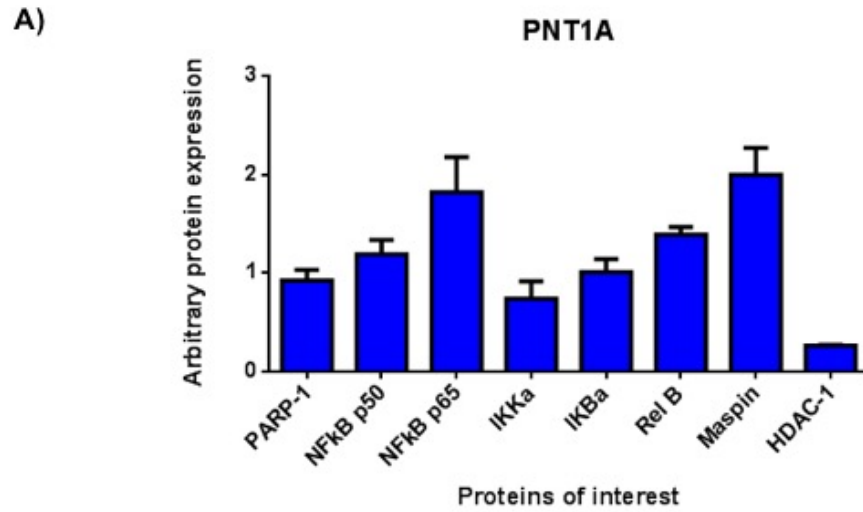


Figure 3.10: Protein quantification and Immunofluorescence staining of PNT1A cells.

(A) Protein quantification of PARP-1, NFkB p50, NFkB p65, IKK α , IKB α , RelB, Maspin and HDAC-1 normalised to β -actin. Data presented are the mean \pm SEM of at least three independent experiments. **(B)** Immunofluorescence staining to show protein expression and localisation in PNT1A cells. Proteins were detected using Alexa Fluor 488 (green) and Alexa Fluor 568 (red) conjugated antibodies. Nuclei were counterstained with DAPI (blue). Scale bar = 18 μ m.

The expression of PARP-1 protein was low in DU145 cells; significantly less than the expression of NF- κ B p50 ($P < 0.001$), IKK α ($P < 0.01$), IKB α and HDAC-1 ($P < 0.05$). There was no significant difference in the expression of PARP-1 and maspin. Maspin expression was lower than the expression of IKK α ($P < 0.01$) and HDAC-1 ($P < 0.05$). The expression levels of NF- κ B p50 were higher than NF- κ B p65, RelB and maspin. IKK α expression levels were higher than those of NF- κ B p65 ($P < 0.05$) (Figure 3.11a). PARP-1 and HDAC-1 expression was confined to the nucleus. Maspin subcellular localisation was not apparent. NF- κ B p65 and NF- κ B p50 was confined to the cytoplasm. IKK α , IKB α and RelB was expressed in both the nucleus and cytoplasm (Figure 3.11b).

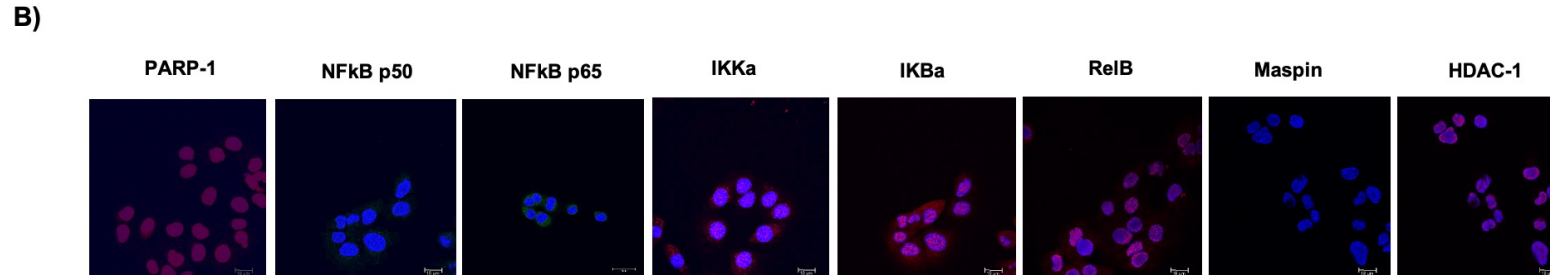
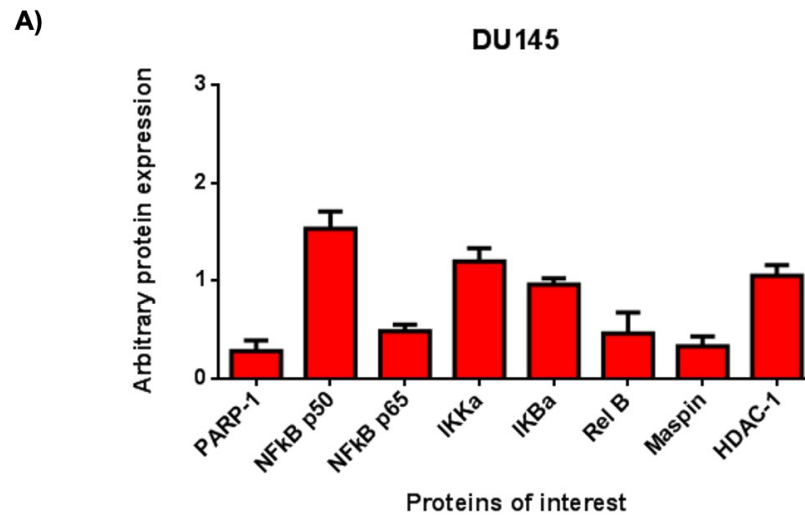


Figure 3.11: Protein quantification and Immunofluorescence staining of DU145 cells.

(A) Protein quantification of PARP-1, NF- κ B p50, NF- κ B p65, IKK α , IKB α , RelB, Maspin and HDAC-1 normalised to β -actin. Data presented are the mean \pm SEM of at least three independent experiments. (B) Immunofluorescence staining to show protein expression and localisation in DU145 cells. Proteins were detected using Alexa Fluor 488 (green) and Alexa Fluor 568 (red) conjugated antibodies. Nuclei were counterstained with DAPI (blue). Scale bar = 18 μ m.

There was no significant difference in the expression levels of PARP-1, NF-kB p65, RelB and maspin in PC3 cells. NF-kB p65 levels were higher than those of NF-kB p50. Maspin expression levels were higher than the expression levels of both IKK α and HDAC-1 ($P < 0.05$) (Figure 3.12a). PARP-1, HDAC-1 and RelB expression was confined to the nucleus of PC3 cells, however, NF-kB p65 and NF-kB p50 was confined to the cytoplasm. Maspin is expressed in both the nucleus and cytoplasm. IKK α and IKB α also localised to both subcellular locations. RelB expression was confined to the nucleus (Figure 3.12).

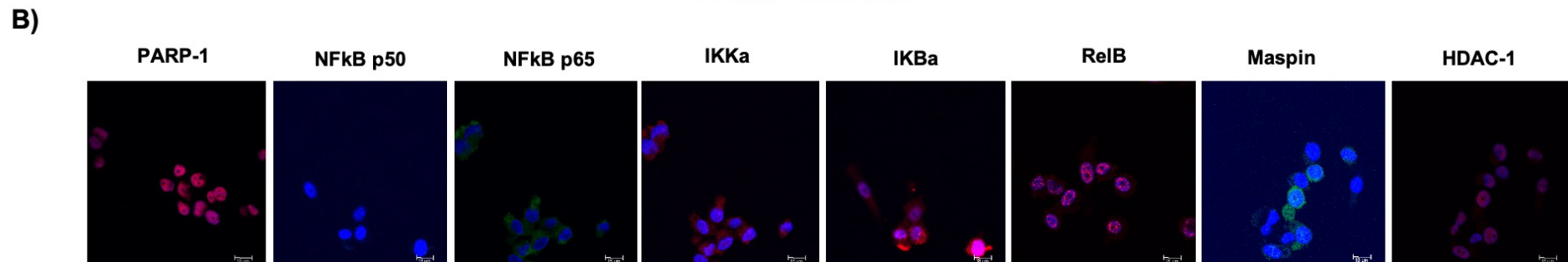
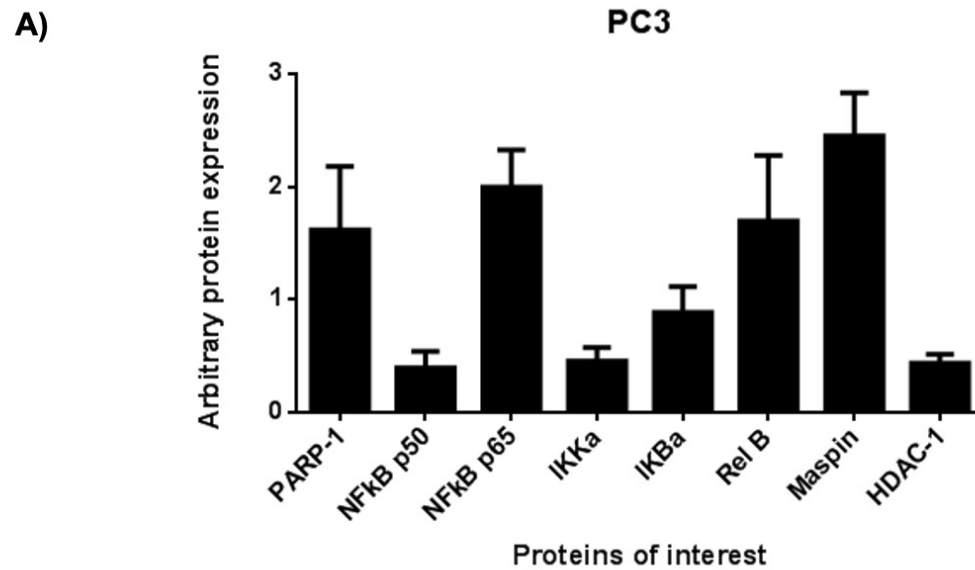


Figure 3.12: Protein quantification and Immunofluorescence staining of PC3 cells.

(A) Protein quantification of PARP-1, NF- κ B p50, NF- κ B p65, IKK α , IKB α , RelB, Maspin and HDAC-1 normalised to β -actin. Data presented are the mean \pm SEM of at least three independent experiments. (B) Immunofluorescence staining to show protein expression and localisation in PC3 cells. Proteins were detected using Alexa Fluor 488 (green) and Alexa Fluor 568 (red) conjugated antibodies. Nuclei were counterstained with DAPI (blue). Scale bar = 18 μ m.

In summary, PARP-1 protein expression levels were inversely correlated to the expression of HDAC-1 ($P < 0.05$) and IKK α ($P < 0.01$) proteins in DU145 cells, and vice versa in PNT1A and PC3 cells. PARP-1 and NF- κ B p65 protein levels were higher in cell lines expressing increased levels of maspin; when compared to the cells which expressed low levels of maspin. In PNT1A cells NF- κ B p50 expression levels were lower than NF- κ B p65 levels. This pattern was increasingly evident in PC3 cells, in DU145 cells NF- κ B p65 protein expression was significantly higher than NF- κ B p50 ($P < 0.001$). An expression pattern between maspin, HDAC-1 and IKK α was observed. IKK α and HDAC-1 correlate each other, and their expression is inversely correlated to the expression of maspin ($P < 0.05$). Maspin, PARP-1 and NF- κ B p65 correlate one another.

PARP-1 was expressed in the nucleus of all prostate cells but was most intense in PNT1A and PC3 cells, in line with the total protein expression data (Figure 3.8 and Figure 3.9). NF- κ B p50 was expressed at low levels in the cytoplasm of PNT1A and DU145 cells but not in PC3 cells. PC3 cells have the least whole NF- κ B p50 protein expression and the lack of expression by immunofluorescence may be that the antibody doesn't work as well in Immunofluorescence. NF- κ B p65 was expressed in the cytoplasm of all cell lines and was most intense in PNT1A and PC3 cells. Maspin was expressed in the cytoplasm of PNT1A cells and, interestingly, in both the cytoplasm and nucleus of PC3 cells. DU145 cells were not found to express maspin. IKK α was expressed in the cytoplasm and nucleus of all cell lines, however expression was more apparent in the nucleus of DU145 cells. Immunostaining of the HDAC-1 protein was most intense in DU145 and, interestingly, PC3 cell lines.

The protein expression levels of maspin, NF- κ B p65 and IKK α proteins were also visualised in MEF cell lines (Figure 3.13). MEF p65^{+/+} cells did not express maspin, MEF p65^{-/-} cells expressed negligible levels of maspin. Maspin expression levels were highest in MEF IKK α ^{-/-} cells. These results correlate with the prostate cell protein expression data in Figure 3.9; whereby NF- κ B p65 inversely correlated with IKK α protein expression. IKK α expression is also inversely correlated with the expression of maspin. PARP protein expression levels were not assessed but previous studies carried out by Hunter et al. (2012) have shown comparable levels of PARP-1 between the MEF cell lines.

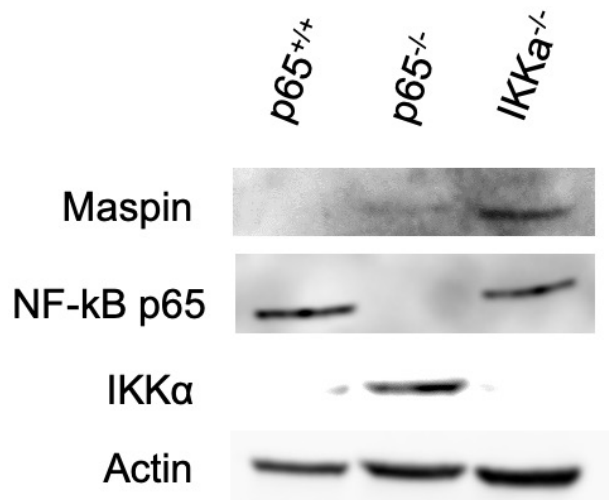


Figure 3.13: Western Blots of whole MEF cell protein extracts.

Blots were probed using antibodies against: Maspin, NF-kB p65 and IKKα. Anti-Actin was used as loading control.

3.4 Discussion

The aim of this chapter was to authenticate and characterise the cell lines for *in vitro* use throughout this thesis.

3.4.1 Cell line authentication and mycoplasma screening

To overcome any potential contamination often seen in research (Capes-Davis et al., 2010), it is common practise to authenticate cell lines and routinely test for mycoplasma contamination as the consequences of widespread contamination and misidentification are vast. All human cell lines used throughout this thesis were tested for authenticity by STR analysis in accordance with ASN-0002 standards set out by the ATCC. DU145 and PC3 cell line STR profiles had >93% matching with the parental cell lines from the ATCC database. A range of 80-100% for cell line authenticity is due to cell line instability; resulting from a loss of heterozygosity or issues relating to their ploidy. Stresses such as extensive passage, microbial contamination and exposure to drugs are all factors which contribute to “genetic drift” or a loss of heterozygosity in cell lines (Marx, 2014). The effects of genetic drift were controlled as far as possible throughout the experiments presented in this thesis by ensuring that fresh cell stocks were raised, and cell culture incubators were cleaned at regular intervals. A match <80% requires further investigation and analysis to

confirm cell line authenticity. The STR profile for the PNT1A cell line was not matched to a DNA profile that fits the ASN-0002 standard criteria. Two STR locus that meet the ASN-0002 standard were found on the ExPASy Bioinformatics resource portal and matched to the PNT1A cell sample. The MEF cells used in this thesis were not authenticated as methods for non-human cell line authentication are not well established (Almeida et al., 2016).

All samples tested negative for mycoplasma contamination. The positive control showed a band ~270 base pairs and this band was not present in the negative control or any of the cell line samples. No speckled dots around the cell nuclei were apparent following DAPI staining of prostate cells which confirmed that cells were negative. Routine testing for mycoplasma contamination ensured that any cell behaviours identified throughout experiments were due to the experimental variables rather than the presence of mycoplasma.

3.4.2 Cell proliferation rates and morphology

Cell proliferation experiments enabled identification of cell doubling times and optimum seeding densities, to ensure exponential growth for at least two cell doublings over 72 hours in future experiments. Cell doubling times followed the same trend in each independent experiment despite inter-assay variability. Normal prostate cells might be expected to proliferate at a slower rate than those of malignant origin; which are characterised by cell cycle acceleration. Nevertheless, we found all prostate cell lines to proliferate at the same rate +1hr regardless of their malignant status. PNT1A, DU145 and PC3 cells used throughout this thesis had mean doubling times of 34, 35 and 34 hours, respectively. Doubling times can vary between cell passage number and methods employed to assess proliferation. The doubling times identified were in line with those found in other studies (Berthon et al. (1995), Stone et al. (1978a) and Kaighn et al. (1979)). These studies used manual counting methods to assess cell proliferation, but results were comparable to the data obtained from the WST-1 assays.

MEF NF- κ B p65^{+/+} cells proliferated 1.7-fold faster than the p65^{-/-} and IKK α ^{-/-} MEF cells. As these cell lines are isogenic, it is evident that the presence of NF- κ B affects cell proliferation rate. NF- κ B is well known to affect the hallmarks of cancer and inflammatory disease by regulating the genes that control cell proliferation, inflammatory signalling and cell survival (Park and Hong,

2016). This was supported by a reduction in HeLa cell proliferation and malignant transformation following repression of NF- κ B p65; highlighting a role for NF- κ B in cell proliferation and tumour development Kaltschmidt et al. (1999). The effect of NF- κ B expression on normal mouse mammary epithelial cell proliferation has also been investigated (Brantley et al., 2001); cells deficient in the I κ B α gene, an inhibitor of NF- κ B, were found to proliferate faster than cells with the I κ B α gene. These results, along with our findings, show that NF- κ B can positively influence both normal and cancerous cell proliferation.

The morphology of the prostate cell lines matched those presented on the ATCC database. The ATCC is a global biological materials resource and standards organisation that acquires, authenticates, preserves and distributes standard reference cell lines and other materials. Changes to cell morphology generally coincide with changes to cell proliferation rates. For example, cells that are seeded at a high-density reach confluence quickly and begin to lose their shape. Cell proliferation slows down, cells become round and detached and eventually die. Regular assessment of these parameters ensures that cells are behaving correctly; providing confidence in the results obtained from our experiments. Changes to cell morphology and growth are associated with senescence, contamination, cellular stress and death; which may consequently hinder experiments. Cells entering a state of senescence become larger, lose their original shape and their cytoplasm appears flattened (Ben-Porath and Weinberg, 2004). Additionally, cells which are stressed lose contact with neighbouring cells, appear shrunken or swollen, elongated and display “blebbing” before their eventual death via apoptosis or necrosis. For example, Ratushnyy (2017) treated mesenchymal stem cells with hydrogen peroxide to assess the functional state and morphology of cells following exposure to oxidative stress. In addition to reduced cell viability and growth, cells appeared enlarged with granular cytoplasm; both of which are morphological features of cellular stress which indicate a likelihood of cell death. All of these morphological features can of course be harnessed as markers of cell death and damage following treatment with specific compounds.

MEF cells have a relatively uniform morphology, appearing elongated and spindle-shaped with clear edges (Mackley et al., 2006). MEF I κ K α ^{-/-} cells appeared larger and more elongated

compared to MEF p65^{+/+} and MEF p65^{-/-} cells in culture (Figure 3.7); demonstrating the effects of gene manipulation on cell morphology and function.

3.4.3 Protein expression and localisation

PARP-1 expression has been shown to be increased in a number of cancers and is associated with disease progression and poor prognosis. Studies have provided an extensive *PARP-1* mRNA expression profile in human primary cancers and normal tissues; reporting increased *PARP-1* gene and protein expression in several malignant tissue types. PARP-1 expression levels were found to be 1.14-fold higher in prostate adenocarcinomas compared to normal prostate tissue (Ossovskaya et al., 2010). Other studies have demonstrated a significant correlation between increased PARP-1 expression and tumorigenesis. For example, Salemi et al. (2013) reported increased PARP-1 expression in prostate cancer tissues compared to normal prostate tissues. They concluded that PARP-1 overexpression in cancers correlates with increased PARP-1 activity in tumours in response to increased DNA damage. Increased expression in tumours may also relate to its close functional relationship with pro-apoptotic factors. In line with these findings, our data revealed high expression of PARP-1 protein in the highly metastatic PC3 cell line. Interestingly, “normal” prostate PNT1A cells expressed more PARP-1 than the moderately metastatic DU145 prostate cancer cells. Albeit expression was significantly less than PC3 cells which are most aggressive. Increased expression of PARP-1 protein in PC3 cells compared to DU145 cells was also reported by Yin and Glass (2006). The low expression of PARP-1 in the DU145 cells may be due to less basal PARP activity compared to the other cell lines. Some studies have correlated PARP-1 activity with PARP-1 protein expression levels (Tentori et al., 2006) whereas others have reported no correlation between PARP-1 activity and PARP-1 protein levels (Zaremba et al., 2009). These contentions highlight the complexity of PARP-1 regulation. Phenotypic and behavioural changes within the cell clearly implicate PARP-1 regulation more than genotype or protein expression. PARP-1 is a nuclear protein used for cell cycle regulation, DNA repair and metabolic regulation. It was therefore not surprising that PARP-1 expression was located in the nucleus of the prostate cell lines.

As PARP-1 is a known co-activator of NF- κ B (Hassa and Hottiger (2002), Martín-Oliva et al. (2004)) we expected levels of NF- κ B to correspond to the expression of PARP-1. We found this to be the case for the NF- κ B p65 subunit but not p50. A study by Weichert et al. (2007) found that high expression of NF- κ B p65 was associated with activation of NF- κ B signalling and poor prognosis in pancreatic cancer. Other studies have also observed overexpression of cytoplasmic and/or nuclear NF- κ B p65 in cancers of the liver (Tai et al., 2000), cervix (Tilborghs et al., 2017) and prostate (Shukla et al., 2004). NF- κ B p65 expression levels were higher in PNT1A cells than DU145 cells and this may be in part due to the expression of maspin. There is a clear correlation between maspin and NF- κ B that needs exploring. Lessard et al. (2003) investigated NF- κ B subcellular localisation and its prognostic significance in prostate cancer. They utilised tissue specimens to compare nuclear localisation with Gleason score and patient outcome. Nuclear localisation of the p65 NF- κ B subunit was specific to cancer tissue. These comparisons were used to generate risk categories and stratify patients into low and high-risk categories of cancer progression. We found expression of p65 to be cytoplasmic in all of the prostate cell lines, suggesting that NF- κ B is not constitutively activated. This may be due to a heterodimer vs homodimer balance. Dimerisation is required for NF- κ B binding to DNA and different dimers are held in the cell cytoplasm by interaction with specific inhibitors. The NF- κ B p65/p50 is the most abundant dimeric complex. The NF- κ B p50 subunit lacks a transcriptional activation domain and forms homodimers with no ability to activate transcription. It can form heterodimers with the NF- κ B p65 subunit to enable translocation to the nucleus where they function as potent activators of gene expression (Siebenlist et al., 1994).

Cytoplasmic and nuclear expression of I κ B α in the prostate cancer cell lines suggests that NF- κ B may be constitutively active. I κ B α is located in the nucleus where it prevents NF- κ B activation and nuclear translocation. It is only when I κ B α is phosphorylated and degraded that NF- κ B is able to translocate to the nucleus and become activated (Wan and Lenardo, 2010). Cytoplasmic and nuclear expression of I κ B α in our cells (Figure 3.10-Figure 3.12) suggests partial degradation of I κ B α ; an enabling characteristic of NF- κ B nuclear translocation and consequential activation. As the NF- κ B p65 and p50 subunits associated with canonical activation

of NF- κ B were not found to be constitutively active in our cell lines, the expression and localisation of RelB, an NF- κ B subunit associated with the non-canonical NF- κ B pathway, was investigated.

RelB expression results were analysed and total protein levels were highest in PC3 cells. High expression levels of RelB in PNT1A cells, compared to DU145 cells, was not expected. High RelB expression is associated with oncogenic transcription and tumour progression. High expression of RelB in metastatic PC3 cells is in line with other studies that have correlated increased levels of RelB with tumour progression. For example, immunohistochemistry analysis of laryngeal cancer samples showed increased expression of RelB with increased tumour stage and grade; establishing RelB as a useful biomarker of prognosis (Giopanou et al., 2017). The immunofluorescence data (Figure 3.10-Figure 3.12) shows nuclear localisation of RelB in DU145 and PC3 cells. These results indicate that RelB is active in the prostate cancer cell lines irrespective of their total protein expression. Expression is nuclear and cytoplasmic in PNT1A cells, and therefore high total protein expression in these cells is not indicative of increased activation. Xu et al. (2009) investigated the role of RelB and the non-canonical NF κ B pathway in prostate cancer progression. They reported a reduction in tumour growth in PC3 cells following inhibition and silencing of RelB. Wang et al. (2016) also reported a significant reduction in DU145 cell migration and invasion following knockdown of RelB. RelB complexes were frequently detected in the nucleus of prostate cancer tissue and were directly correlated to Gleason score. These results highlight a tumour-supportive role of RelB following activation via the non-canonical NF- κ B pathway.

IKK α , an IKK kinase complex, is a core molecule in both canonical and non-canonical NF- κ B activation and signalling (Israel, 2010). All prostate cell lines expressed the IKK α protein but expression levels were highest in DU145 cells which express the least maspin; highlighting a potential link between IKK α and maspin. High IKK α expression levels correlated to low expression maspin, and low IKK α expression correlated to increased maspin expression. These results are in line with a study carried out by Luo et al. (2007). Using a transgenic mouse model, they showed that IKK α plays a role in inflammation and metastasis by repressing the transcription

of tumour suppressor gene maspin. Inactive IKK α in mice was found to slow down prostate cancer growth and this correlated with increased expression of maspin. Additionally, nuclear expression of IKK α correlated with metastatic progression and maspin repression. An inhibitory effect on cell invasion was observed in breast cancer cells following knockdown of IKK α ; however the relationship with maspin was not explored (Merkhofer et al., 2010). IKK α shuttles between the cytoplasm and nucleus; and when localised to the nucleus, the maspin gene is repressed. We showed nuclear expression of IKK α in all of our prostate cell lines but expression was greatest in low maspin expressing DU145 cells. We demonstrated increased expression of maspin in mouse embryonic cells deficient in IKK α (Figure 3.13). Leopizzi et al. (2017) found that nuclear translocation of IKK α stimulated maspin production. Hepatocarcinoma studies also reported increased expression of maspin and suppression of tumour metastasis following the downregulation of IKK α (Jiang et al., 2010). As NF-kB signalling is controlled by IKK α , the group also examined the expression of other NF-kB regulators and target genes to determine whether NF-kB was activated. Increased nuclear expression of NF-kB p65, typical of constitutive NF-kB activation, was found in tumour tissues expressing high levels of IKK α compared to normal liver tissue. This suggests that overexpression of IKK α drives NF-kB signalling and consequently, inflammatory signalling and tumour progression. The increased nuclear expression of IKK α in our DU145 cells suggests that these cells are more active in terms of NF-kB; and therefore, we would expect this cell type to be more aggressive. The results show that NF-kB p65 and NF-kB p50 resides in the cytoplasm and are therefore not constitutively activated. The non-canonical NF-kB subunit RelB is active in both DU145 and PC3 cells. The literature suggests that PC3 cells are more aggressive than DU145 cells (Ravenna et al., 2014). Nevertheless, both cell lines are metastatic, and it is important to explore other molecular markers which may contribute to the difference in IKK α expression between cell lines; such as maspin and HDAC.

As previously mentioned, inhibition of the tumour suppressor gene maspin has been associated with increased cell migration and metastatic progression. The DU145 cells express the lowest levels of maspin protein from the panel of cell lines, but interestingly PC3 cells express high levels; greater than those of the normal PNT1A prostate cells. These expression levels inversely

correlate to the expression levels of IKK α and NF-kB p65. The MEF cell expression studies have also evidenced negligible expression of maspin in MEF p65 knockout cells, and high expression of maspin in MEF IKK α knockout cells. These results further support the inverse correlation between maspin and IKK α , and NF-kB p65 and IKK α .

The literature suggests that normal cells should express much higher levels of maspin in comparison to cancerous cells. For example, Zhang (2004) investigated the expression pattern of maspin in human breast cell lines. Maspin was highly expressed in normal mammary epithelial cells, down regulated in primary breast tumours and deficient in metastatic tumour cells. The group also studied maspin gene expression in several human normal and prostate tumour cell lines. Maspin was highly expressed in CF3, CF91 and MLC normal cell lines compared to LNCaP, PC3 and DU145 tumour cells. Other studies have also reported high expression of maspin in benign prostate tissue samples compared to well-differentiated prostate carcinoma samples (Zou et al., 2002). McKenzie et al. (2008) compared basal expression levels of maspin in DU145, PC3, LNCaP prostate cells and normal BPH-1 prostate epithelial cells. In line with the protein expression data presented in Figure 3.9, maspin gene expression levels were higher in PC3 cells than DU145 cells and normal BPH-1 cells.

As expected, expression of the maspin protein is confined to the cytoplasm of PNT1A cells but interestingly, it is expressed in both the cytoplasm and nucleus of PC3 cells. Maspin is predominantly expressed in the cytoplasm (<95%) of normal tissues, it may also be expressed in the nucleus (Pemberton et al., 1997). There are contentions in the literature with regards to nuclear expression of maspin and disease prognosis. Nuclear expression of maspin in breast, prostate and ovarian cancers has been associated with well-differentiated phenotype and improved survival, in colorectal cancers nuclear expression it is associated with poor disease outcome (Berardi et al., 2013). Increased expression of maspin in both the cytoplasm and nucleus of PC3 cells, compared to DU145 cells, may be a more favourable phenotype in these cells despite being more aggressive. Goulet et al. (2011) demonstrated that nuclear localisation of maspin is required for its tumour suppressing function. They examined several potential maspin-regulated genes, showing that at least two genes crucial to breast cancer progression were negatively regulated by nuclear maspin.

To this end, the cytoplasmic and nuclear expression of maspin in PC3 cells may be due to an interaction with various genes. Another factor which may explain contentions in results of maspin localisation could be cell line identification. The PC3 cells used throughout this thesis have been thoroughly authenticated and therefore the results can be validated. The significance of nuclear maspin localisation remains unclear and warrants further investigation but is beyond the scope of this thesis.

Protein expression and localisation results support previous studies which demonstrate that maspin interacts and endogenously inhibits histone deacetylase 1 (HDAC-1) (Li et al., 2006). HDACs regulate a range of proteins and processes and are key elements in the regulation of gene expression, differentiation and homeostasis (Ropero and Esteller, 2007). Increased levels of HDACs are associated with prostate cancer progression (Wang et al., 2009b) and class 1 HDACs have been implicated in DNA damage signalling and repair; enabling characteristics of cancer development (Munshi et al. (2005) and Kim et al. (2003)). Histone deacetylation influences the expression of genes involved in cancer initiation and progression such as those involved in cell cycle, apoptosis, angiogenesis and migration (Glozak and Seto, 2007). High expression of HDAC-1 in DU145 cells compared to PNT1A and PC3 cells suggests that these cells are more aggressive and prone to DNA damage. Wang et al. (2009b) examined the levels of HDAC-1 mRNA and total protein in a panel of prostate cancer cell lines, including the DU145 and PC3 cells used throughout this thesis. They found HDAC-1 mRNA and protein expression levels to be high in androgen-independent cell lines; particularly PC3 cells. Halkidou et al. (2004) also showed upregulation of HDAC-1 expression in androgen independent prostate cancers; contributing to aggressive phenotype and metastatic potential. The group reported similar expression levels of HDAC-1 in DU145 and PC-3M cells. PC-3M cells are a metastasis-derived variant of PC3 with enhanced distant organ metastasis, and therefore we would expect the PC3 cells to express less HDAC-1 than the more metastatic PC-3M variant. Despite contentions in literature, we can be confident that the findings presented in Figure 3.8 are valid.

Ashburner et al. (2001) evidenced that HDAC-1 interacts with the NF- κ B p65 subunit and inhibits its expression. This is in line with the protein expression results obtained for DU145 cells;

showing increased expression of HDAC-1 and low expression of NF-kB p65 and maspin. Chemical inhibition of HDAC has been shown to increase the expression of various DNA repair proteins, transcription factors and NF-kB. Studies have shown that exposure of cells to HDAC inhibitors results in the acetylation of NF-kB p65 on lysine residues; leading to IKK activation, I κ B α degradation and increased nuclear binding and transactivation of NF-kB p65 (Dai et al., 2005, Kim et al., 2006b). Interestingly, expression of IKK α was greatest in the DU145 cells which expressed the highest levels of HDAC-1. The expression of HDAC-1 was localised to the nucleus of all cell lines, as would be expected for a nuclear protein (Kim et al., 2010b). Expression was less visible in the maspin expressing cell lines, which supports the protein expression results obtained from western blotting and the findings presented by Li et al. (2006).

Figure 3.14 summarises the main findings from the protein expression data presented in this chapter; highlighting clear inverse correlations between the expression of PARP-1 and IKK α , IKK α and maspin, and maspin and HDAC-1 proteins in prostate tumour cells.

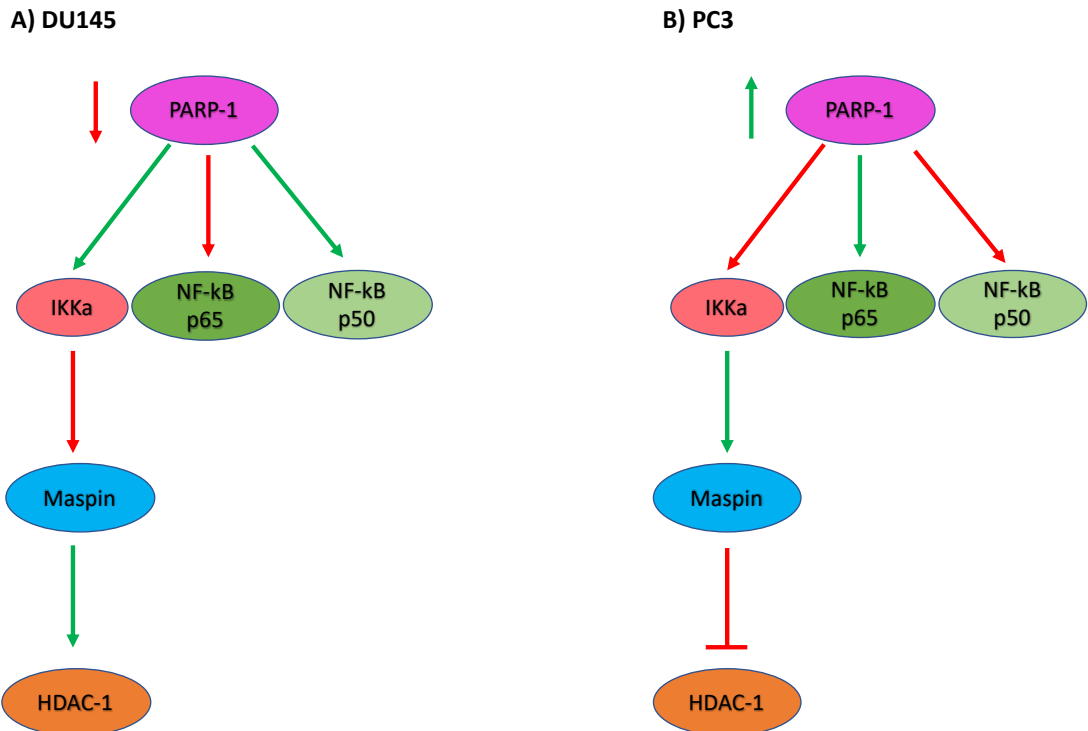


Figure 3.14 Schematic to summarise the expression of proteins in DU145 and PC3 cells.

A) Reduced expression of PARP-1 in DU145 cells is associated with reduced expression of NF-kB p65 but increased expression of NF-kB p50 and IKKa. Maspin protein expression is reduced when IKKa is expressed and this is associated with reduced levels of HDAC-1. **B)** Increased expression of PARP-1 in PC3 cells is associated with increased expression of NF-kB p65 but reduced expression of NF-kB p50 and IKKa. Maspin protein expression is increased when IKKa levels are low and this is associated with increased levels of HDAC-1. Red arrows represent reduced expression and green arrows represent increased expression. Flat arrowheads indicate inhibition.

3.5 Summary

The studies presented in this chapter have shown that:

- Cell lines are of the correct genotype and phenotype.
- Maspin expression does not affect prostate cell proliferation rate.
- IKK α protein expression is inversely correlated with the expression of maspin in prostate and MEF IKK α ^{-/-} cell lines, and increased maspin expression is inversely correlated to the expression of HDAC1.
- Knockout of NF-kB p65 and IKK α subunits in MEF cells reduces proliferation rate.

3.6 Future work

Future work could include expanding the panel of cell lines and include patient samples to identify similar patterns in other cancer cells. It would also be beneficial to develop isogenic prostate

cancer cell lines proficient and deficient for maspin, IKK α and PARP-1 genes to further explore potential mechanisms between these molecules. It would be interesting to see whether knockout, inhibition or silencing of IKK α enhances maspin in the cancer cells; and if this would result in decreased cell survival following exposure to treatments. Future experiments, beyond the scope of this thesis, could be to assess PARP and NF-kB activity and investigate the effects of PARP inhibition on cells with varied expression of NF-kB and maspin. PARP activity could be determined by measuring the formation of PAR polymer chains which are synthesised by PARP-1 using NAD⁺ as a substrate. This could be achieved by immunocytochemistry or Western blot. NF-kB activity could be measured by luciferase gene reporter assay followed by bioluminescence. A reporter gene is an exogenous coding region joined to a promotor sequence in an expression vector. Protein expression data could also be compared to patient sample and omics data from various sources such as the human protein atlas to verify our findings.

Chapter Four

Investigating the effects of PARP-1 and HDAC-1 inhibitors on cell growth and survival in cell lines with varied maspin expression.

4.1 Introduction

This chapter investigates the sensitivity of prostate and mouse embryonic fibroblast cell lines (proficient and deficient for NF- κ B p65 and IKK α) to the PARP-1 inhibitor Rucaparib (AG014699) and HDAC-1 inhibitor Trichostatin A (TSA). Combined effects of these drugs were assessed in terms of cell growth, proliferation, morphology and protein expression relative to the expression levels of maspin and NF- κ B.

4.1.1 Choice of inhibitors

Olaparib is currently the best studied PARP inhibitor (Chen and Du, 2018). In 2014 it was the first PARP inhibitor to be approved by the European medicines agency and the US food and drug administration (FDA) for the treatment of ovarian cancer. Rucaparib is a potent PARP inhibitor that was developed by researchers at Newcastle University. It was the first PARP inhibitor to enter anticancer human clinical trials in 2003. The trial assessed the safety and efficacy of Rucaparib in combination with the cytotoxic agent temozolomide in patients with advanced solid tumours (Plummer et al., 2008). In 2015 it was granted FDA approval for clinical use as a monotherapy in ovarian cancer patients with somatic and/or germline BRCA mutations (Drew et al., 2016). It was approved for use on the NHS in 2019. Rucaparib is currently in clinical development for the treatment of metastatic AR independent prostate cancer (Cancer Research) and for this reason it was selected for *in vitro* use throughout this thesis.

HDAC inhibitors are a class of anti-cancer agents that play a role in epigenetic modification, cell death, apoptosis and cell cycle arrest in cancer cells (Kim and Bae, 2011). These roles are in part due to the downregulation of DNA repair pathways, leading to the persistence of DNA damage and increased sensitivity to DNA damaging agents. For example, the HDAC inhibitor TSA was shown to impair radiation-induced repair of DNA damage in head and neck squamous carcinoma

and breast cancer cell lines (Zhang et al., 2007). HDAC inhibitors have also been shown to downregulate DNA repair proteins and induce phosphorylated histone γ H2AX, a marker of DNA double strand breaks, in normal and transformed cells (Lee et al., 2010).

Trichostatin A (TSA) is a potent and specific inhibitor of class I and II HDAC activity. Maspin interacts and inhibits HDAC-1, therefore TSA was selected for use in the studies presented in this thesis. TSA was the first natural hydroxamate found to inhibit HDAC's which are overexpressed in various cancers. Since its discovery in 1990 (Yoshida et al., 1990) studies have demonstrated a link between the inhibition of HDAC-1 and 2, and the suppression of tumour cell growth and survival (Vigushin et al., 2001, Chang et al., 2012).

Both PARP and HDAC inhibitors prevent homologous recombination DNA repair and studies have explored the efficacy of these drugs as single and combined agents for cancer therapy (Chao and Goodman, 2014, Rasmussen et al., 2016, Marijon et al., 2018). Studies have not explored the role of maspin in treatment response. A proposed working model of Rucaparib and TSA co-treatment in prostate cells of varied maspin expression is presented below.

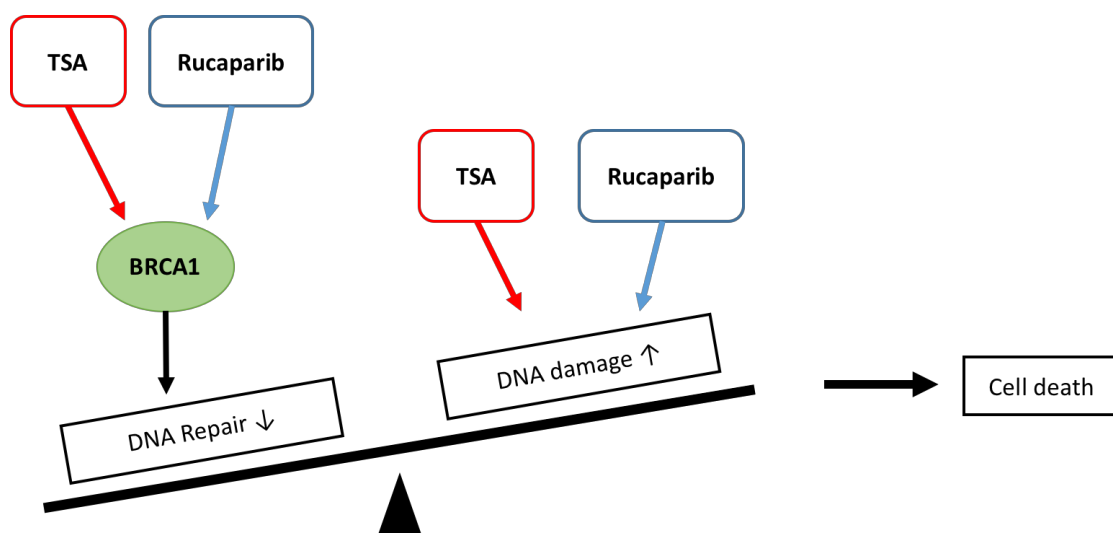


Figure 4.1 Proposed working model of TSA and Rucaparib co-treatment.

Co-treatment will enhance anticancer efficacy by two mechanisms: Impairing DNA repair and inducing DNA damage, leading to enhanced cell cytotoxicity. Figure adapted from (Yin et al., 2018).

4.1.2 Sensitivity to inhibitors and selection of methodology

In vitro cytotoxicity assays are essential for determining the sensitivity of normal and cancerous cells to therapeutic agents. The clonogenic survival assay is considered the gold standard, however, the assay disregards the impact of cell-to-cell communication as the cells are seeded at very low densities (Mirzayans et al., 2007). Alternative, and frequently used, cytotoxicity testing assays include cell counting, SRB, WST-1 and Resazurin. These assays are based on biochemical events specific to living cells, such as protein content and metabolic activity (Assay principles are outlined in Chapter 2).

It has been well documented that cellular cytotoxicity results vary depending on the method used (O'Donovan, 2012). Assays measure different endpoints such as protein binding, metabolism and physical growth. Therefore, different assays produce different results based on the variables that they are measuring. Haibe-Kains et al. (2013) analysed data from two large-scale pharmacogenomic studies: The Cancer Genome Project (CGP) (Garnett et al., 2012) and the Cancer Cell Line Encyclopaedia (CCLE) (Yoshida et al., 1990). Both studies presented gene expression profiles and drug sensitivity assays for over 700 cell lines and 138 drugs, and over 1000 cell lines and 24 drugs, respectively. Comparison of gene expression profiles highlighted good concordance between the two studies, however drug sensitivity results did not. This was likely due to use of different cytotoxicity assays between the two studies; CGP measured dehydrogenase activity whereas CCLE measured cellular ATP (Weinstein and Lorenzi, 2013). An earlier study demonstrated that measurement of ATP levels better reflected cell viability compared to dehydrogenase inhibition. ATP levels were extensively depleted in non-viable cells, but dehydrogenase activity remained at 24% of untreated control cells (Maehara et al., 1987).

Assessment of several methods is vital to enable selection of a single methodology; particularly for drug combination cytotoxicity studies, to ensure that results obtained from sequential data are directly comparable.

4.1.3 Assessment of cell morphology in the presence and absence of Rucaparib and TSA.

Cells exposed to treatments are generally susceptible to nuclear and morphological changes which differ from their normal state; such as pseudopodial protrusions, nuclear condensation,

fragmentation, blebbing and swelling. Assessment of cell morphology following treatment enables identification of cell stress and cytotoxicity; but also assists in the identification of cell death pathway in which treatments induce.

4.1.4 Protein expression levels in the presence of Rucaparib and TSA.

Previous studies have explored changes to the expression levels of proteins following exposure to PARP and HDAC inhibitors, alone and in combination. For example, Chao and Goodman (2014) and Rasmussen et al. (2016) both reported decreased expression levels of key DNA repair proteins, BRCA1 and RAD51, in prostate and glioblastoma cells, respectively; following PARP and HDAC inhibition alone. Combination treatment led to a decrease in HDAC-1 and PARP-1 protein levels. These findings provide a rationale for assessment of protein expression levels as biomarkers to predict clinical response, and for the use of combined PARP and HDAC inhibitors in the treatment of cancers. Increased PARP-1 and HDAC-1 is implicated in tumour progression and reduced expression of these molecules may enhance patient survival. PARP and HDAC inhibitors limit DNA repair and enhance cell death, therefore the combination of the two inhibitors enhances anticancer efficacy by decreasing metastatic progression and improving patient prognosis. Changes to protein expression levels following PARP and HDAC inhibition, relative to the presence of NF-kB and maspin proteins have not previously been investigated, this is an interesting area of study as NF-kB activation *via* IKK α has been implicated in tumour progression *via* the repression of maspin. As discussed in Chapter 1, maspin repression is thought to enhance cell proliferation, apoptosis, migration and invasion; enabling characteristics of cancer development.

4.2 Chapter aims

This chapter investigates the effects of Rucaparib and TSA, alone and in combination, on cell growth and survival; relative to the expression of NF-kB and maspin. It is hypothesised that TSA will enhance the effects of Rucaparib in DU145 and PC3 cell lines; particularly DU145 cells which are depleted in maspin and are therefore more susceptible to DNA damage and resistant to

apoptosis. It is expected that co-treatment will reduce protein expression levels of NF-kB and PARP-1; resulting in increased maspin expression. The aims of this chapter are detailed below:

- To investigate the effect of Rucaparib and TSA, alone and in combination, on cell growth and survival with use of multiple cytotoxicity assays such as manual cell counting, WST-1, SRB and Resazurin; to optimise methodology for co-treatment studies.
- To investigate the combined effects of Rucaparib and TSA on cell survival, relative to maspin expression.
- To assess the effects of Rucaparib and TSA, alone and in combination, on cell and nuclear morphology in prostate cells.
- To examine the effects of Rucaparib and TSA treatment, alone and in combination, on the protein expression levels of PARP-1, maspin and NF-kB subunits in prostate cells.
- To investigate the Rucaparib and TSA sensitivity in MEF cell models.

4.3 Results

4.3.1 The effects of Rucaparib on prostate cell growth and survival and selection of methodology for future experiments.

To assess prostate cell growth and survival, following exposure to Rucaparib, a series of cell growth and proliferation assays were conducted. WST-1, Resazurin, SRB and counting methods (see section 2.2.3 for assay protocols) were selected for comparison of effect and outcome; to identify a single methodology for later experiments (Figure 4.2). Cells were exposed to Rucaparib for 72 hours up to 50 μ M.

A low dose (3 μ M) hormetic response to Rucaparib was identified by WST-1 assay in DU145 and PC3 cell lines (Figure 4.2B and C, respectively) but not PNT1A cells (Figure 4.2A). Cell viability was reduced in a dose dependent manner at drug concentrations >3 μ M, however GI₅₀ (the concentration of drug required for 50% inhibition of cell growth) was not reached at 50 μ M in PNT1A and PC3 cells indicating reduced sensitivity to Rucaparib compared to DU145 cells. Resazurin assay results also displayed a low dose hormetic response to Rucaparib in DU145 cells

but not PC3 and PNT1A cells. Interestingly, Resazurin data showed that that PC3 cells were most sensitive to Rucaparib (GI_{50} 8.8 μ M) and PNT1A cells were least sensitive (GI_{50} >50 μ M).

Assessment of growth inhibition by SRB assay and cell counting in response to drug treatment did not show a low dose stimulation to Rucaparib in any of the cell lines; but rather a dose dependent inhibition of cell growth (Figure 4.2). DU145 cells with lower levels of basal maspin were most sensitive to Rucaparib (GI_{50} 8.2 μ M) compared to PC3 and PNT1A cells (GI_{50} 15.7 μ M and 27.5 μ M, respectively).

Mean Rucaparib GI_{50} concentrations were calculated and compared between growth and survival assays (Table 4.1). It was not possible to obtain GI_{50} Rucaparib concentrations for PNT1A and PC3 cells by WST-1 assay, and PNT1A cells by Resazurin assay.

Table 4.1: Comparison of Rucaparib GI_{50} concentrations between different growth and survival assays in prostate cell lines.

Data are the mean values (SD) from at least three independent experiments.

Cell line	GI_{50} (μ M)			
	SRB	Counting	WST-1	Resazurin
	Mean \pm standard deviation			
PNT1A	27.45 \pm 5.11	17 \pm 1.85	>50	>50
DU145	8.2 \pm 1.46	8.7 \pm 0.95	37.3 \pm 2.51	38.84 \pm 6.31
PC3	15.7 \pm 3.29	13.3 \pm 2.75	>50	8.8 \pm 1.62

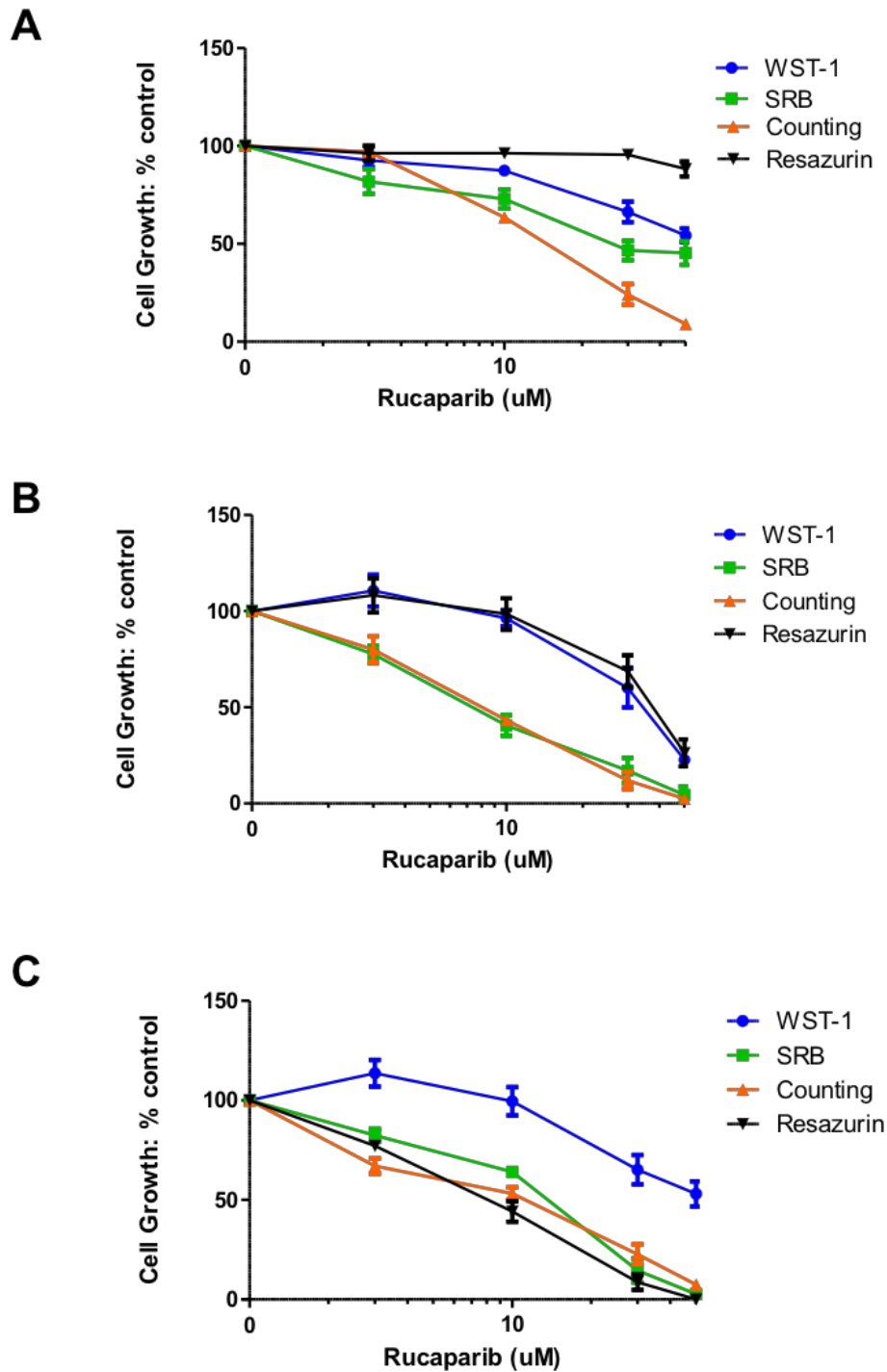


Figure 4.2: Comparison of growth inhibition by Rucaparib using WST-1, SRB, Resazurin and counting in Prostate cell lines. (A) PNT1A, (B) DU145 and (C) PC3 cells were treated with Rucaparib at various concentrations for 72 hours and cell number was determined. Data shown are the average of at least three independent experiments and error bars represent SEM.

The graphs presented in Figure 4.3 compared the differences in prostate cell survival between the growth and survival assays carried out following treatment with 10 μ M Rucaparib. A 10 μ M

concentration was selected as it is an approximate dose that is equitoxic in all cell lines with ~50% cell death by cell counting after 72 hours.

After 72 hours there was no significant difference in cell response to drug treatment between SRB and cell counting methods in all cell lines (Figure 4.3). WST-1 results were significantly different to SRB and counting results but not to Resazurin assay in PNT1A and DU145 cells (Figure 4.3A and B). WST-1 results were significantly different to all methods carried out in PC3 cells (Figure 4.3C).

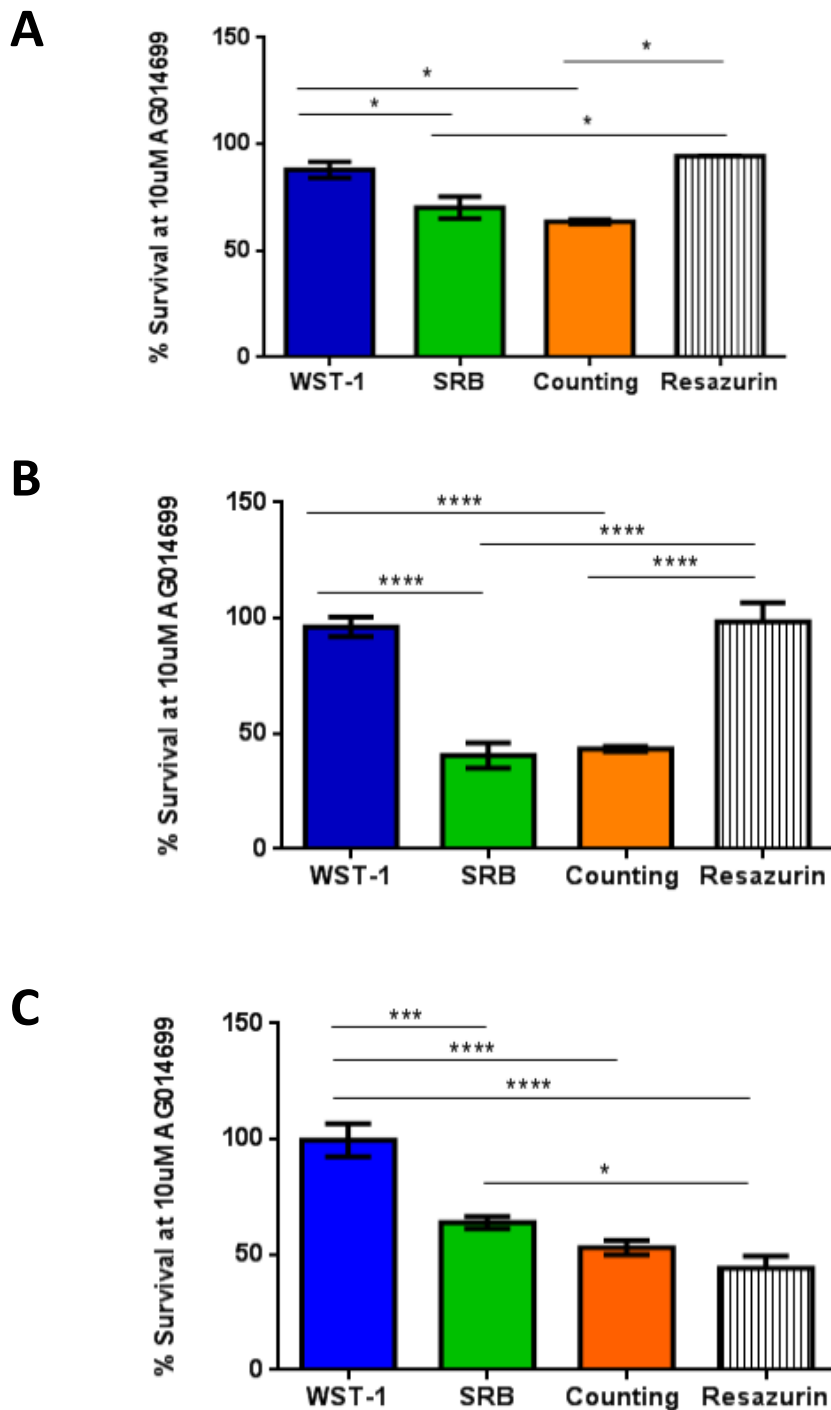


Figure 4.3: Effect of 10µM Rucaparib on survival and growth of prostate cells, as measured by WST-1, SRB, Counting and Resazurin assays. (A) PNT1A, (B) DU145 and (C) PC3 cells were exposed to Rucaparib for 72 hours and cell growth or viability was assessed. One-way ANOVA analysis with multiple comparisons was carried out to provide statistical significance (*p<0.05, ***P<0.001 and ****p<0.0001).

In summary, Maspin depleted DU145 cells were most sensitive to Rucaparib in all of the methods assessed other than the Resazurin cell viability assay. Comparative assessment of the four growth and survival assays demonstrate that a single methodology is essential to ensure that results obtained in later studies are directly comparable. SRB was selected as the methodology of choice

due to its simplicity, reproducibility and concordance with cell counting. The GI_{50} concentrations obtained from SRB experiments which are presented in Table 4.1 were taken forward in drug combination experiments described later in this chapter.

4.3.2 The effects of Rucaparib on prostate cell morphology.

PNT1A, DU145 and PC3 cells were exposed to various concentrations of Rucaparib for 72 hours to investigate changes to cell morphology and growth. Morphology was assessed by light microscopy, as described in 2.2.2.

All cell lines showed prominent morphological change and decrease of cell number in a concentration dependant manner in comparison to untreated controls (Table 4.4). PNT1A cells were less sensitive to Rucaparib treatment and their morphology was only affected by drug concentrations $>30\mu\text{M}$. Rucaparib concentrations $>10\mu\text{M}$ induced fibroblast-like morphology and pseudopodial protrusions, indicative of cellular stress, in both DU145 and PC3 cell lines. A drug concentration $>30\mu\text{M}$ was cytotoxic to the cancerous cell lines but not to the normal prostate cells. At the GI_{50} dose (identified by SRB as shown in Table 4.1) cell morphology indicated a reduced confluence which was comparable to the growth inhibitory data.

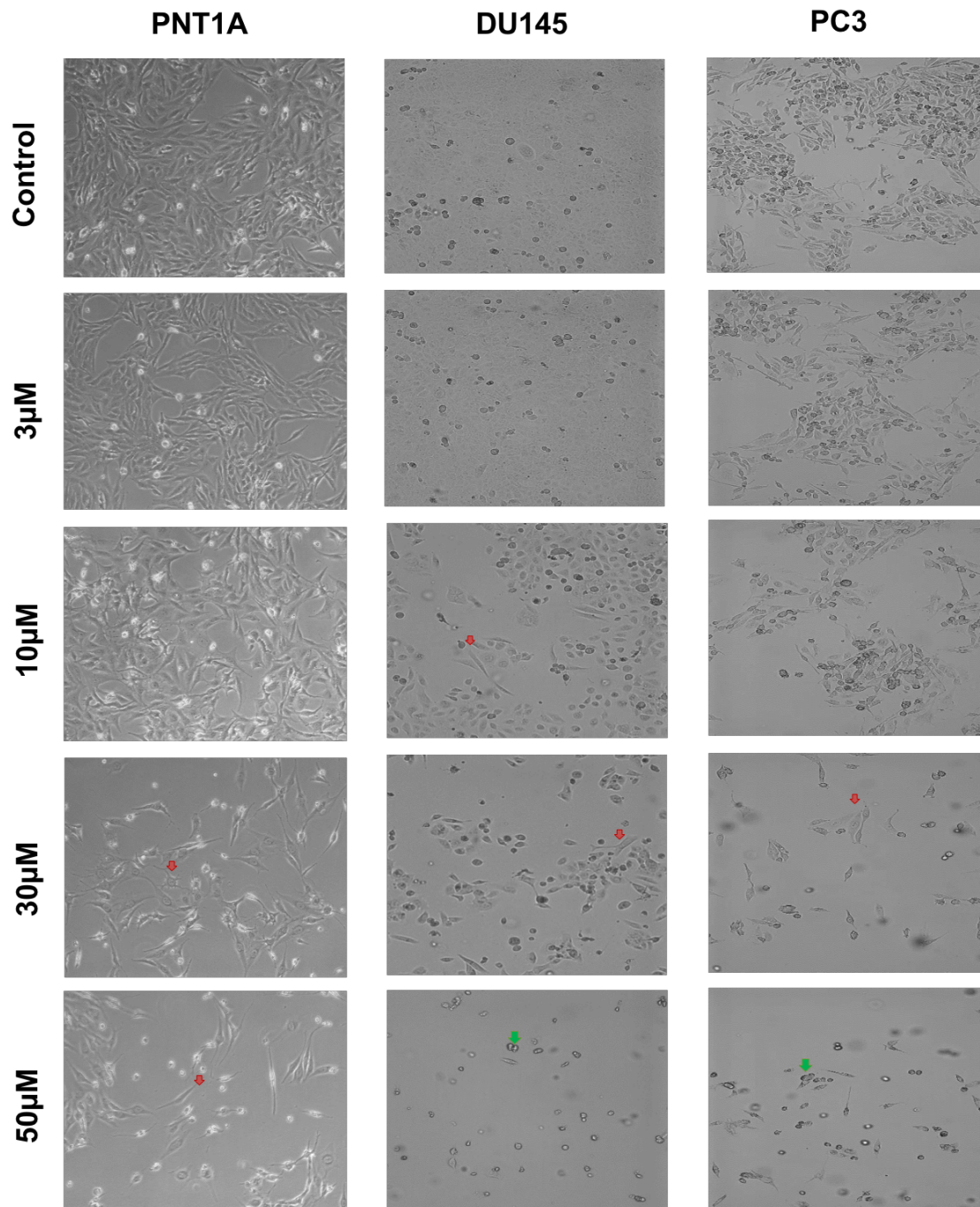


Figure 4.4: The assessment of cell morphology in response to Rucaparib by brightfield microscopy. DU145, PC3 and PNT1A cells were exposed to various concentrations of Rucaparib for 72 hours. Images are representative of three independent replicates. Red arrowheads indicate changes to morphology and green arrowheads indicate cell death. Images captured at X10 magnification.

4.3.3 The effects of Rucaparib on prostate cell nuclear morphology.

Changes to nuclear morphology following exposure to Rucaparib for 72 hours was assessed, as described in section 2.2.2. Briefly, cells were fixed to glass coverslips and then stained with DAPI to enable visualisation of the cell nucleus by confocal microscopy.

Changes to nuclear morphology in response to increasing concentrations of Rucaparib were apparent in all prostate cell lines; particularly the cancerous cell lines (Figure 4.5). DU145 and PC3 cells exposed to 3 μ M Rucaparib presented with nuclear blebbing and fragmentation. Nuclear condensation was also apparent in response to increasing concentrations of Rucaparib in these cell lines. Exposure to Rucaparib appeared to cause nuclear swelling in the PC3 cells but not in the DU145 cells. PNT1A cells presented changes to nuclear morphology such as nuclear condensation membrane blebbing in response to Rucaparib despite reduced sensitivity in cytotoxicity assays. Cell nuclei were not affected by treatment with 3 μ M Rucaparib but nuclear condensation, fragmentation and membrane blebbing was apparent in concentrations $\geq 10\mu$ M.

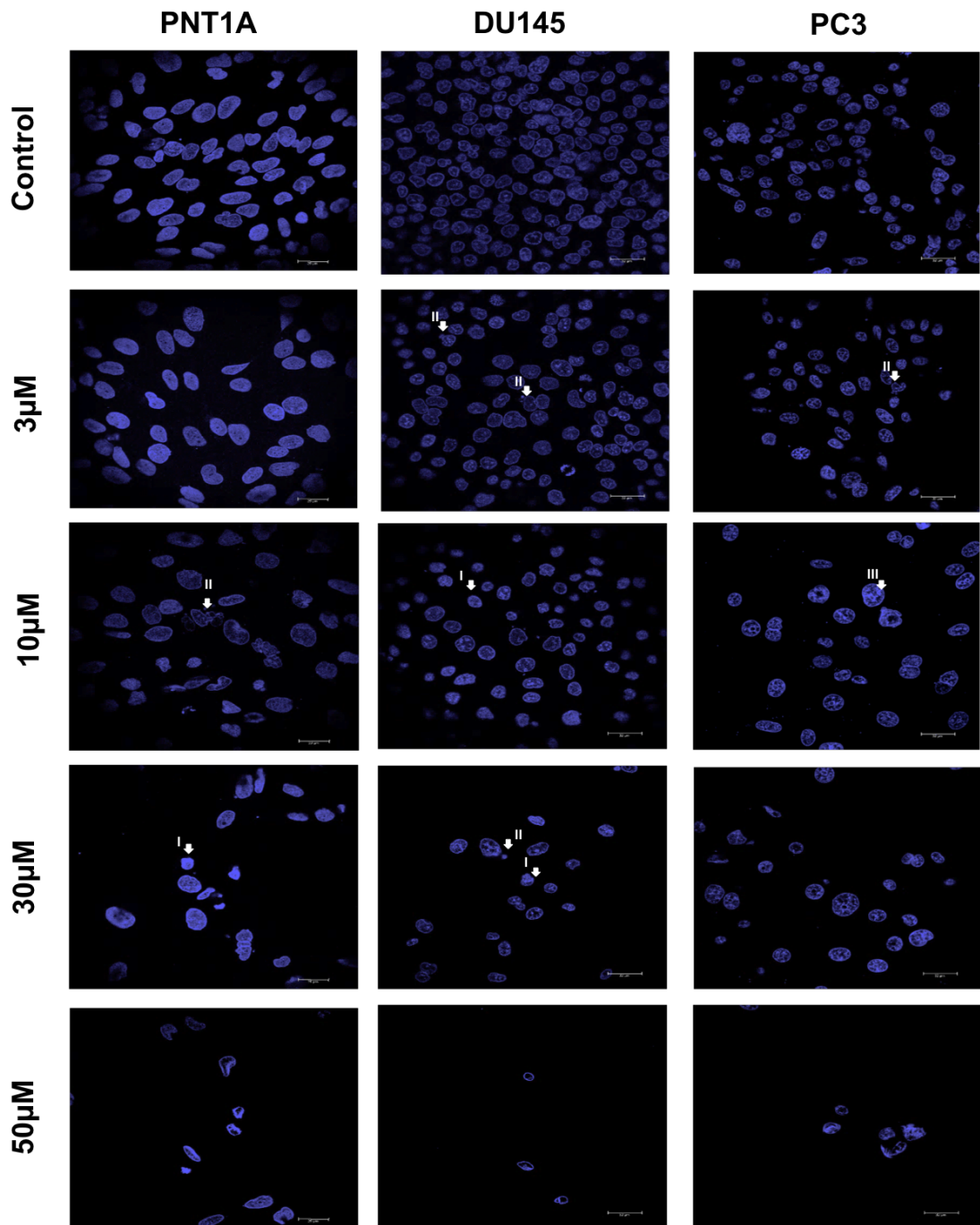


Figure 4.5: The assessment of nuclear morphology in response to Rucaparib using DAPI staining and fluorescence microscopy.

DU145, PC3 and PNT1A cells were exposed to various concentrations of Rucaparib for 72 hours. Images are representative of three independent replicates. Arrowheads indicate: (I) Nuclear condensation, (II) membrane “blebbing” and (III) cell swelling; all of which are features of cell death. Images were captured at X40 magnification. Scale bar= 32μM.

To quantify changes to nuclear morphology following Rucaparib exposure, twenty cells were scored for each sample based on their nuclear morphology (Nuclear condensation, Nuclear fragmentation/membrane blebbing and cell swelling). The scoring criteria used was normal nuclear morphology, and indicators of cell death: chromatin condensation, nuclear condensation,

nuclear fragmentation and cell swelling. Scores were expressed as a percentage of the twenty cells assessed in each sample, as shown in Figure 4.6.

In line with the representative images displayed in Figure 4.5, a decline in normal nuclear morphology was apparent with increasing Rucaparib concentration. The normal nuclear morphology of PNT1A and PC3 cells was reduced 4 and 5-fold following exposure to 50 μ M Rucaparib compared to untreated controls, respectively. An 11-fold decrease in normal nuclear morphology of DU145 cells treated with 50 μ M Rucaparib highlighted an enhanced sensitivity of this cell line to a PARP inhibitor; in line with cytotoxicity data presented in section 4.3.1.

Cell samples treated with Rucaparib presented increased nuclear condensation and fragmentation, representative of apoptosis, in a dose dependent manner. Treated DU145 cells had the highest percentage of cells with nuclear fragmentation compared to PNT1A and PC3 cell lines. At a 10 μ M concentration ~50% of the DU145 cells presented fragmented nuclei compared to PNT1A and PC3 cells, where only ~20% and ~10% of nuclei were fragmented, respectively. Approximately 5% of DU145 cells exhibited cell swelling, a morphological feature of cell necrosis, following a 10 μ M exposure to Rucaparib. Cells did not present swelling at Rucaparib concentrations below and in excess of 10 μ M. PNT1A and PC3 cells were subject to ~5% cell swelling following exposure to Rucaparib at 30 μ M. At a cytotoxic 50 μ M concentration, cell swelling was only apparent in the PNT1A cells.

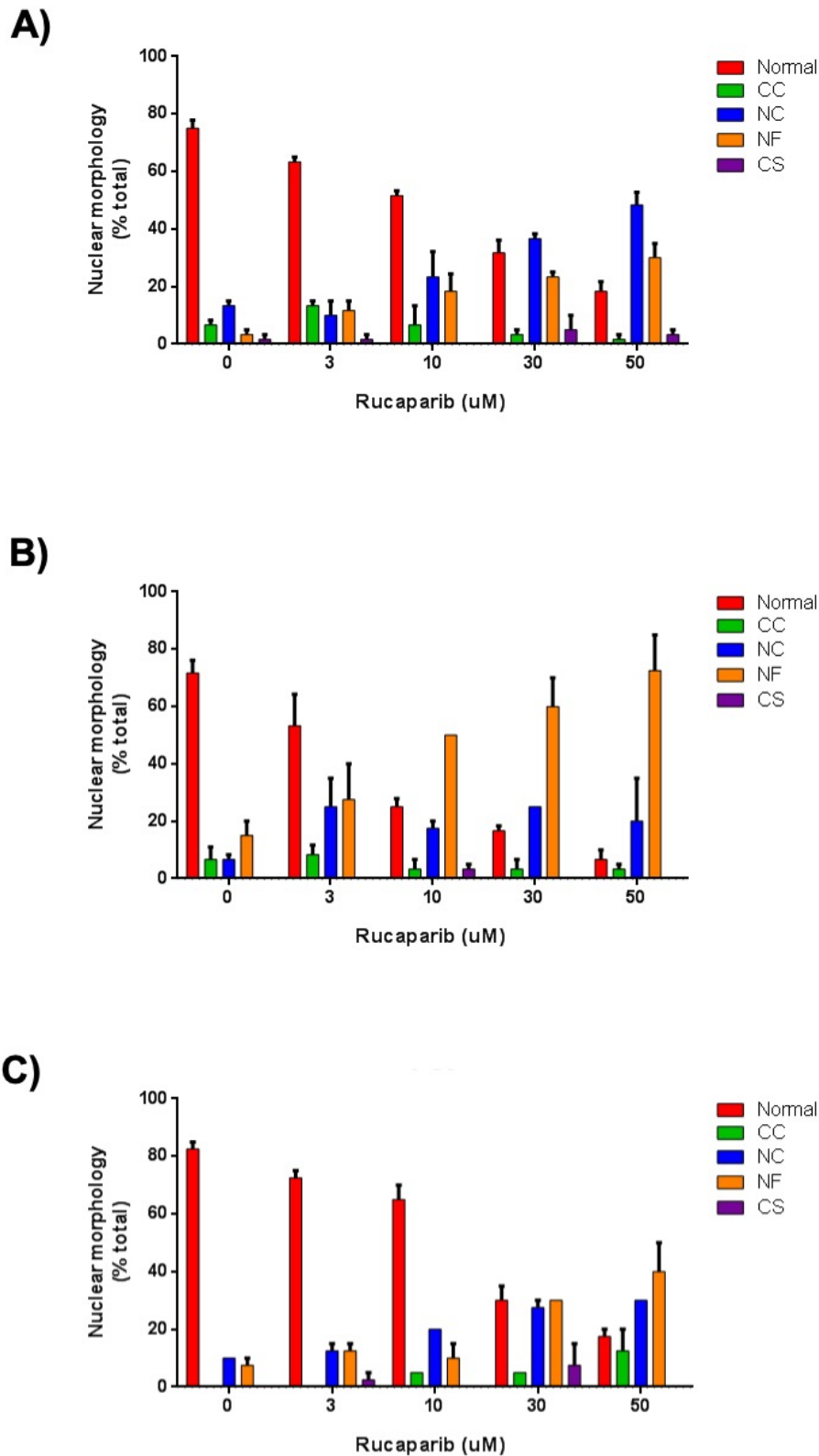


Figure 4.6: Quantification of changes to nuclear morphology following a 72-hour exposure period to Rucaparib.

Epifluorescence was used to assess the changes to nuclear morphology in (A) PNT1A, (B) DU145 and (C) PC3 cells treated with increasing doses of Rucaparib for 72 hours. Twenty cells were scored per dose and results are the mean of at least two independent experiments. CC= chromatin condensation, NC= Nuclear condensation, NF= Nuclear fragmentation and CS= cell swelling.

4.3.4 The effects of Trichostatin A on prostate cell growth and survival and selection of methodology.

Prostate cell growth and survival was assessed following 72-hour exposure to the HDAC inhibitor Trichostatin A (TSA) using the methods outlined in 2.2.3.

Assessment of cell viability by WST-1 assay, following exposure to increasing concentrations of TSA revealed a hormetic response up to 10nM in PC3 cells (Figure 4.7C). This response was not apparent in PNT1A and DU145 cells (Figure 4.7A and B). Cell viability was reduced in a dose dependent manner at drug concentrations >10nM in PNT1A and DU145 cells, and \geq 40nM in PC3 cells. The cell viability of PNT1A and PC3 cells was not inhibited by 50% at the highest concentrations of TSA used (100nM).

Assessment of growth inhibition by SRB assay and cell counting in response to TSA did not show a hormetic response and cell growth declined in a dose dependent manner (Figure 4.7). Both SRB and counting methods found the prostate cancer cells to be more sensitive to TSA, in comparison to the normal PNT1A cells. Cell growth following exposure to TSA was variable between the SRB and counting methods in PNT1A cells. At a 100nM TSA concentration, cell viability was reduced 2.2-fold when measured by counting than SRB assay (Figure 4.7A).

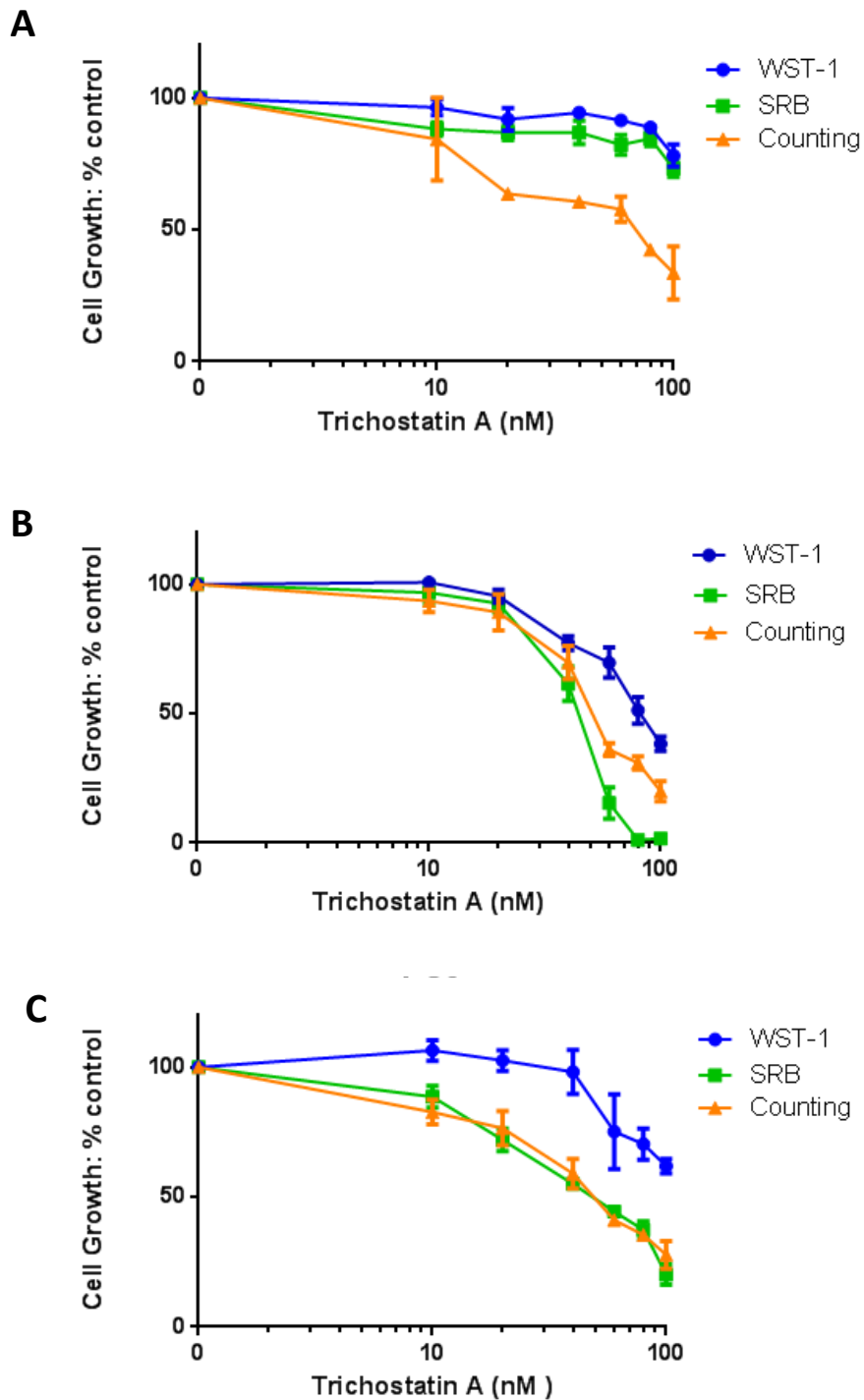


Figure 4.7: Comparison of growth inhibition by Trichostatin A using WST-1, SRB and counting methods in Prostate cell lines.

(A) PNT1A, (B) DU145 and (C) PC3 cells were treated with Trichostatin A at various concentrations (0-100nM) for 72 hours and cell number was determined. Data shown are the mean of at least three independent experiments and error bars represent SEM.

The graphs presented in Figure 4.8 highlight the differences in prostate cell survival between the growth and survival assays carried out following treatment with 60nM TSA, for 72 hours. A

60nM concentration was selected as this concentration inhibited DU145 and PC3 cell growth by >50% (SRB and cell counting data).

There was a significant difference in percentage cell survival between WST-1 and SRB ($p < 0.001$) methods, and WST-1 and cell counting ($p < 0.001$ and $p < 0.01$ in DU145 and PC3 cells, respectively); in DU145 and PC3 cells (Figure 4.8B and C). Percentage cell survival between WST-1 and cell counting data, and SRB and cell counting data differed in PNT1A cells (Figure 4.8D). Interestingly, there was no significant difference in PNT1A cell survival between WST-1 and SRB methods; following treatment with TSA.

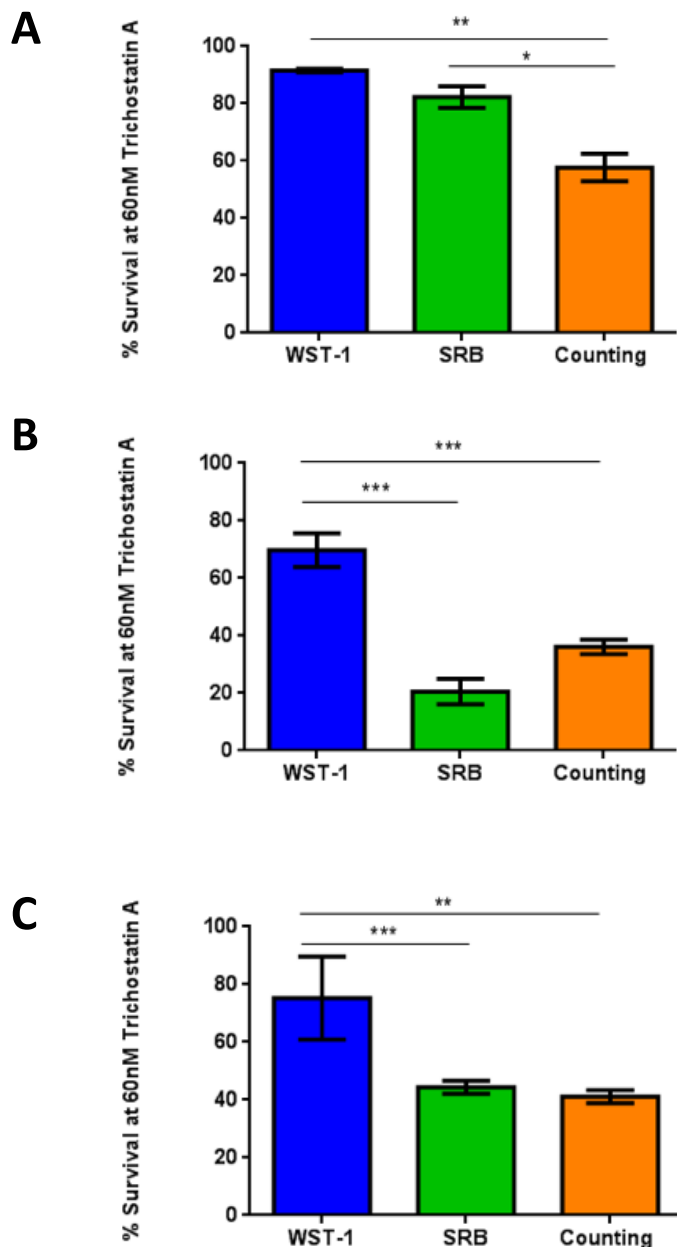


Figure 4.8: Comparison of percentage growth and survival inhibition using WST-1, SRB and Counting in prostate cells treated with 60nM Trichostatin A.

(A) PNT1A, (B) DU145 and (C) PC3 cells were exposed to Trichostatin A for 72 hours and cell growth and viability was assessed. One-way ANOVA analysis with multiple comparisons was carried out to provide statistical significance (* $p < 0.05$, ** $p < 0.01$ and *** $P < 0.001$).

Mean TSA GI_{50} concentrations were calculated and compared between growth and survival assays (Table 4.1). A GI_{50} concentration for TSA could not be obtained for PNT1A and PC3 cells at the highest dose (100nM) by WST-1 assay. Therefore, additional WST-1 assays were carried out in these cell lines using increased drug concentrations (200nM and 300nM), to establish a drug concentration which would limit cell viability by 50%.

Table 4.2: Comparing cytotoxicity to Trichostatin A in prostate cell lines by proliferation assays.
Data are the mean values (SD) from at least three independent experiments.

Cell line	GI ₅₀ (nM)		
	SRB	Counting	WST-1
	Mean ± standard deviation		
PNT1A	188 ± 21.5	70 ± 5.93	215 ± 2.94
DU145	45 ± 5.17	52 ± 5.08	82 ± 11.29
PC3	49 ± 5.39	50 ± 13.29	214 ± 6.13

In summary, data from SRB and cell counting showed that PNT1A cells were 4.1-fold and 3.8-fold less sensitive to TSA than DU145 and PC3 cells, respectively (Table 4.2). There was no significant difference in drug sensitivity between DU145 and PC3 cells. Cytotoxicity data from WST-1 assays was not consistent with the data obtained from SRB and counting methods. DU145 cells were 2.6-fold more sensitive to TSA than PNT1A and PC3 cells. Despite a difference in drug sensitivity for PNT1A cells between SRB and cell counting methods, SRB was selected as the methodology of choice due to its reproducibility and simplicity. The TSA GI₅₀ concentrations obtained from SRB experiments (Table 4.2) were be combined with Rucaparib GI₅₀ concentrations (Table 4.1) in order to assess the effects of the drugs in combination on cell growth and survival.

4.3.5 Trichostatin A affects prostate cell morphology in a dose dependent manner

Prostate cells were exposed to increasing concentrations of TSA for 72 hours to investigate changes in cell morphology and growth. Morphology was assessed by light microscopy, as described in 2.2.2. Images are presented in Figure 4.9.

In line with the findings presented in 4.3.4, PNT1A cells were less sensitive to TSA treatment and consequently, cell morphology was unaffected by exposure to the drug at concentrations up to 100nM. Cells exposed to 100nM TSA presented pseudopodial protrusions; indicating cellular stress. Cell detachment was also apparent with increasing drug concentration, indicating cell death. DU145 and PC3 cells showed increased sensitivity to TSA treatment and changes to normal morphology were apparent in cells that were exposed to TSA concentrations ≥ 40 nM (Figure 4.9). A number of cells displayed an elongated fibroblast-like morphology when exposed to 40nM TSA. TSA concentrations >40 nM induced cell detachment and death in a dose dependent manner.

100nM TSA was not completely cytotoxic to the prostate cancer cell lines but a significant deterioration in cell health was apparent.

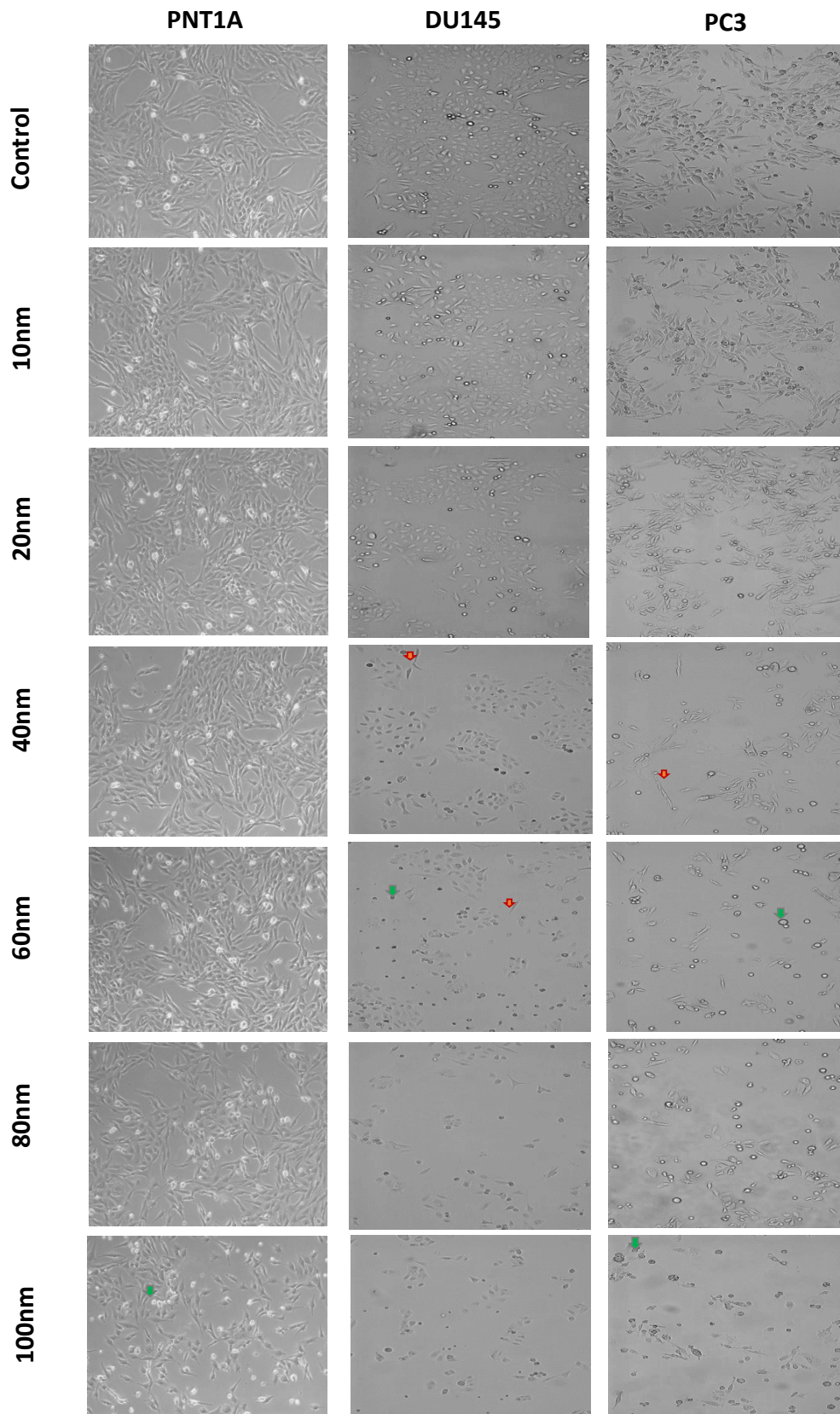


Figure 4.9: The assessment of cell morphology in response to Trichostatin A by brightfield microscopy.

DU145, PC3 and PNT1A cells were exposed to various concentrations of Trichostatin A for 72 hours. Images are representative of three independent replicates. Red arrowheads indicate changes to morphology and green arrowheads indicate cell death. Images captured at X10 magnification.

4.3.6 Trichostatin A affects prostate cell nuclear morphology in a dose dependent manner.

Changes to nuclear morphology following exposure to TSA for 72 hours was assessed by epifluorescence, as described in section 2.2.2.

Changes to nuclear morphology and a decline in cell number in response to increasing concentrations of TSA was apparent in all prostate cell lines; particularly the cancerous cell lines (Figure 4.10). Cells were less sensitive to TSA concentrations <40nM. Cells exposed to 40nM and 60nM TSA exhibited signs of nuclear condensation. An 80nM drug concentration induced features of apoptosis such as nuclear blebbing and fragmentation in PNT1A and DU145 cells. Interestingly, PC3 nuclei exposed to 80nM TSA exhibited signs of swelling; a morphological characteristic of the necrosis death pathway. A visible decline in cell number was apparent following exposure to 100nM TSA in DU145 and PC3 cells. PNT1A cells were least sensitive to morphological change following drug exposure, but a limited number of cells presented signs of nuclear swelling.

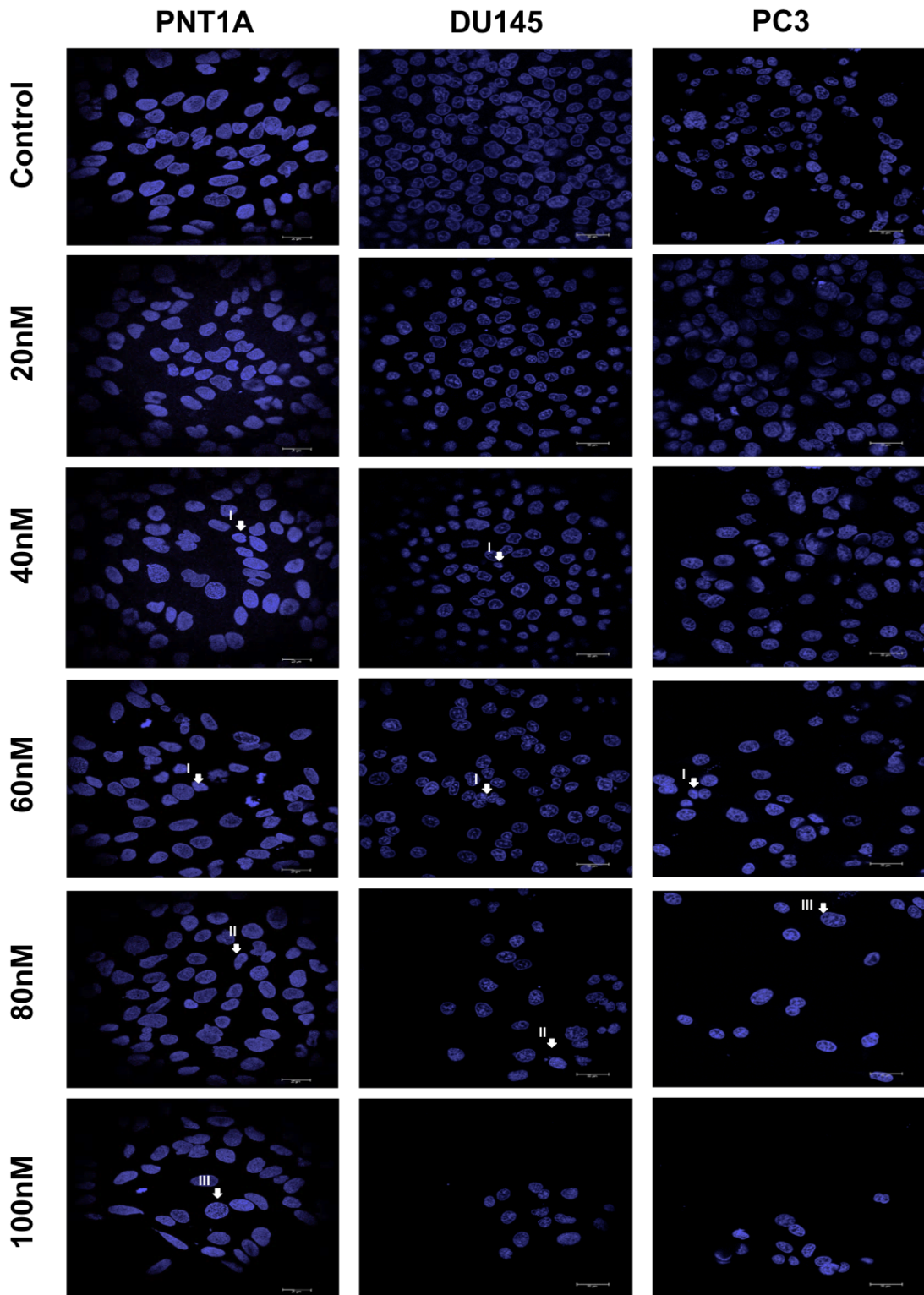


Figure 4.10: The assessment of changes to nuclear morphology in response to Trichostatin A using DAPI staining and fluorescence microscopy.

PNT1A, DU145 and PC3 cells were exposed to various concentrations of Trichostatin A for 72 hours. Images are representative of three independent replicates. Arrowheads indicate: (I) Nuclear condensation, (II) membrane “blebbing” and (III) cell swelling; all of which are features of cell death. Images captured at X40 magnification. Scale bar= 32 μ M.

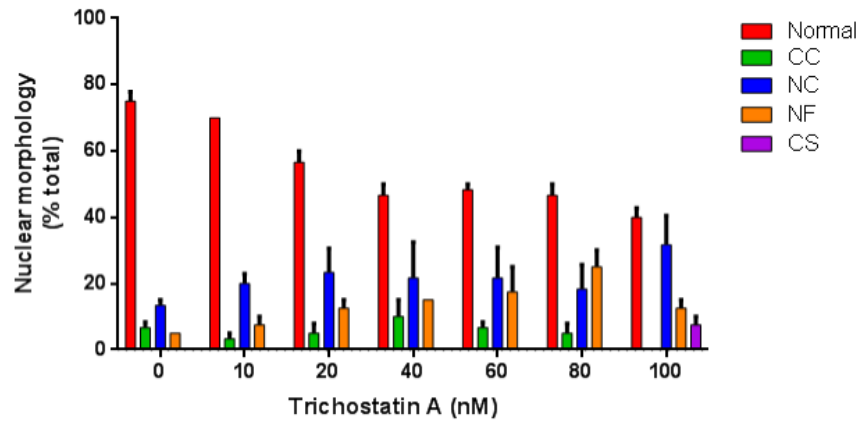
To quantify changes to nuclear morphology following treatment with TSA, twenty cells were scored for each sample based on nuclear morphology and then split into a percentage, as previously described in section 4.3.3.

In line with the representative images displayed in Figure 4.10, there was a dose dependent decrease in normal cell nuclear morphology; particularly in the prostate cancer cell lines, as depicted in Figure 4.11. From the DU145 and PC3 cells scored, there was a 2.5 and 4-fold reduction in normal nuclear morphology in DU145 and PC3 cells exposed to 60nM TSA (a drug concentration growth inhibitory by >50% in these cell lines), compared to untreated cells. Normal nuclear morphology was further reduced 3.3 and 5.5-fold in DU145 and PC3 cells exposed to the highest TSA concentration (100nM), respectively. There was a 2-fold decrease in normal nuclear morphology in PNT1A cells exposed to 100nM TSA, compared to untreated controls.

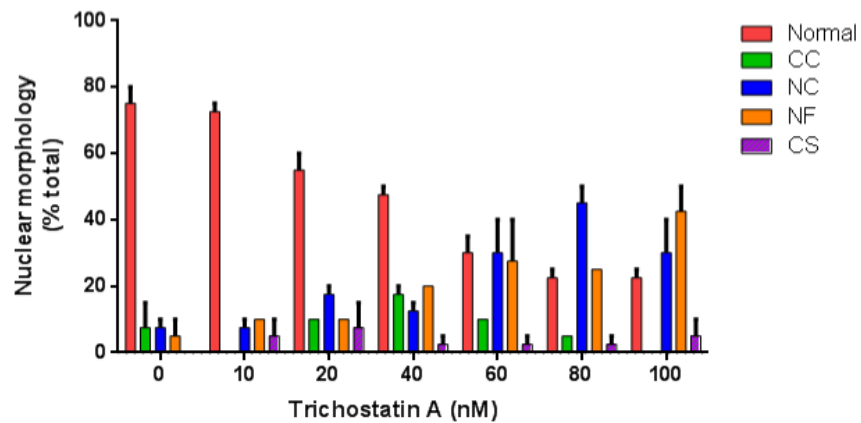
All of the prostate cell lines treated with TSA presented increased nuclear condensation and fragmentation, representative of apoptosis, in a dose dependent manner. A reduction in nuclear fragmentation was apparent in PNT1A cells following treatment with 100nM TSA. In DU145 cells, there was a reduction in nuclear condensation following treatment with 100nM TSA. However, increasing TSA concentration did not correlate with increased chromatin condensation in any of the prostate cell lines. At 60nM, a drug concentration that is growth inhibitory (>50%) in DU145 and PC3 cells, approximately 28% of DU145 and 40% of PC3 cells presented nuclear fragmentation; compared to PNT1A cells whereby ~17% of the cells scored presented fragmented nuclear morphology. Cell swelling was apparent at low levels in the DU145 and PC3 cell samples exposed to drugs, however there was no correlation between cell swelling and increasing TSA concentration. PNT1A cells exhibited cell swelling following exposure to TSA at a concentration of 100nM.

These data highlight increased nuclear sensitivity to DU145 and PC3 cells exposed to TSA, compared to PNT1A cells.

A)



B)



C)

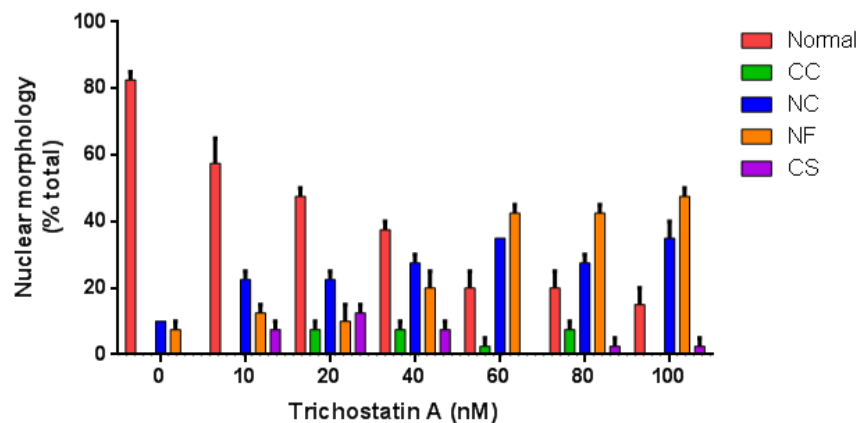


Figure 4.11: Quantification of changes to nuclear morphology following a 72 hour exposure period to Trichostatin A.

Epifluorescence was used to assess the changes to nuclear morphology in (A) PNT1A, (B) DU145 and (C) PC3 cells treated with increasing doses of Trichostatin A for 72 hours. Twenty cells were scored per dose and results are the mean of at least two independent experiments. CC= chromatin condensation, NC= Nuclear condensation, NF= Nuclear fragmentation and CS= cell swelling.

4.3.7 Evaluation of the combined effects of Rucaparib and Trichostatin A on prostate cell survival by SRB assay.

Having optimised the methodology for assessment of cell growth inhibition, the sensitivity of prostate cells to Rucaparib and TSA in combination was determined by SRB assay. The respective GI₅₀ concentrations of Rucaparib and TSA identified by SRB assay in previous studies (detailed in sections 4.3.1 and 4.3.4) are presented in Table 4.3 below. A GI₅₀ concentration is used to measure the effects of treatments on whole cell growth. The choice to use SRB, and therefore GI₅₀, came from the Northern Institute for Cancer Research, who use this as their primary screen, and from my data which shows that results from the SRB method are consistent with manual cell counting. It is important to acknowledge that in a purified enzyme system use of IC₅₀ (half maximal inhibitory concentration) would be much lower than the GI₅₀ used in a whole cell system. We did not look at the effects of treatments on PARP-1 and HDAC-1 activity in these studies and therefore GI₅₀ concentration was favoured.

Table 4.3: GI₅₀ concentrations of Rucaparib and Trichostatin A identified by SRB assay in prostate cell lines of varying maspin expression.

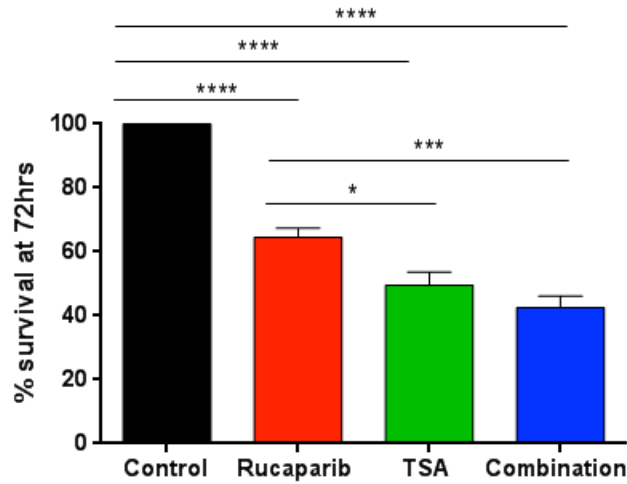
Cell line	Mean GI ₅₀ ± SD	
	Rucaparib (μM)	Trichostatin A (nM)
PNT1A	27.45 ± 5.11	188 ± 21.5
DU145	8.2 ± 1.46	45 ± 5.17
PC3	15.7 ± 3.29	49 ± 5.39

These drug concentrations were used to evaluate the combined effects of Rucaparib and TSA on cell survival after 72 hours. They were also used in other drug combination studies which are discussed throughout this chapter. The level of growth inhibition was normalised to Rucaparib, TSA and 1% DMSO alone controls.

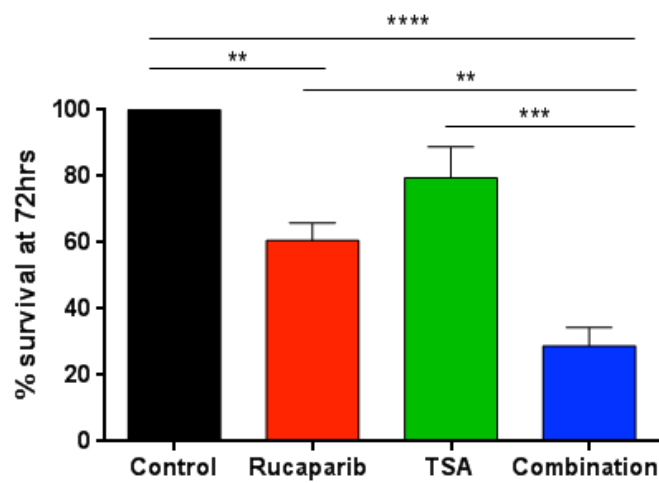
The results presented in Figure 4.12 show that prostate cells exposed to combination treatment for 72 hours are significantly more sensitive than cells exposed to Rucaparib or TSA alone. DU145 and PC3 cells were 1.5-fold more sensitive to the combination treatment than PNT1A cells; demonstrating increased efficacy of the drug combination in cancer cell lines. The GI₅₀ concentration of TSA applied to both DU145 and PC3 cell lines did not significantly differ. The

GI₅₀ Rucaparib concentration for PC3 cells was ~2-fold higher than the concentration required to achieve GI₅₀ in DU145 cells (Table 4.3).

A)



B)



C)

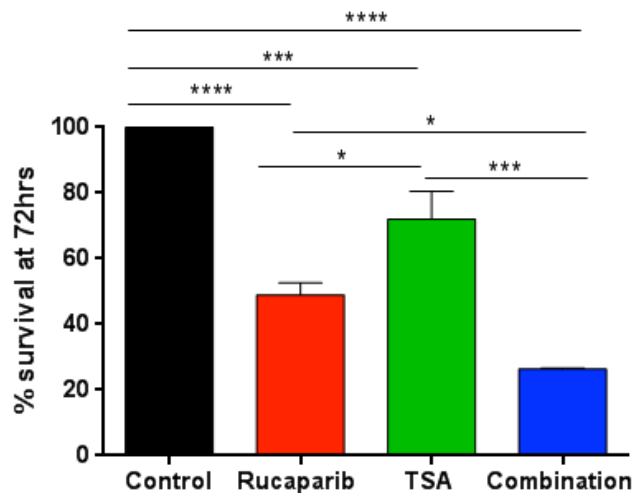


Figure 4.12: Combined treatment of Rucaparib and Trichostatin A enhances growth inhibition in prostate cell lines.

(A) PNT1A, (B) DU145 and (C) PC3 prostate cell lines were exposed to Rucaparib and TSA, alone and in combination at their GI_{50} concentrations for 72 hours. Combination treatment is significantly more effective than Rucaparib alone in all cell lines (two-way ANOVA followed by Tukey's multiple comparison test, * $p < 0.05$, ** $p < 0.01$, *** $p < 0.001$). The data presented are percentage of untreated controls and are the mean \pm SEM of at least three independent experiments.

4.3.8 Trichostatin A enhances the effects of Rucaparib on cellular and nuclear morphology in prostate cell lines.

The effects of combined treatment on cell morphology relative to single agent treatment was assessed after 72 hours. Cells cultured in media containing 1% DMSO without the addition of drugs were used as control. The representative images presented in Figure 4.13 show changes to normal cell morphology and increased cell death following treatment with Rucaparib and TSA alone and in combination.

Untreated cells were intact and had reached ~80-90% confluence following 72 hours in culture. Cells treated with TSA and Rucaparib at their respective GI_{50} concentrations, and cells treated with a combination began to lose adherence from the cell surface; a feature which is typical of cellular stress and death. Rucaparib induced the appearance of cell elongation and pseudopodia; particularly in the DU145 and PC3 cells, as previously described. Following combination treatment with Rucaparib and TSA, reduced cell density, death and changes to morphology were extensive (Figure 4.13-Figure 4.15). PNT1A and PC3 cells presented pseudopodia and a number of PC3 cell nuclei appeared fragmented. DU145 cells did not display pseudopodia or fragmentation, but rather cell elongation and cell death; which was characterised by cell detachment and debris. The results presented in Figure 4.13-Figure 4.15 demonstrate that Rucaparib and TSA co-treatment enhances cell cytotoxicity in these cell lines; particularly the maspin depleted DU145 cells.

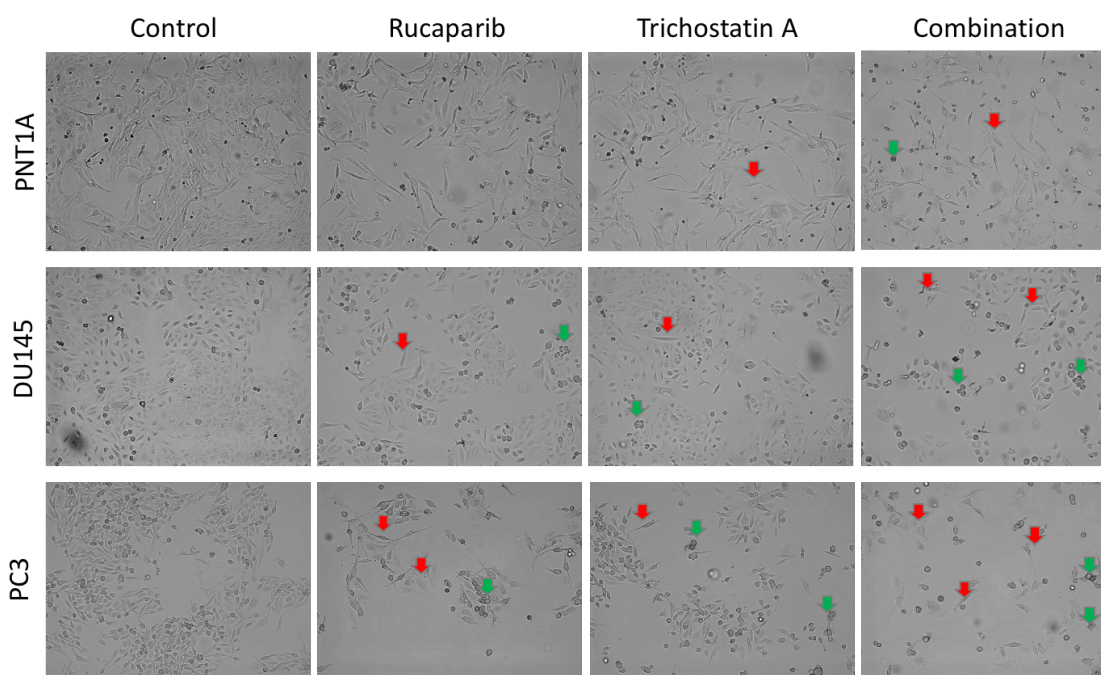


Figure 4.13: The assessment of cell morphology in response to Rucaparib and Trichostatin A, alone and in combination, by brightfield microscopy.

PNT1A, DU145 and PC3 cells were exposed to various concentrations of Rucaparib and Trichostatin A, alone and in combination at GI_{50} concentrations, for 72 hours. Images are representative of three independent replicates. Red arrowheads indicate changes to morphology and green arrowheads indicate cell death. Images captured at X10 magnification.

The effects of combined Rucaparib and TSA treatment on nuclear morphology relative to single agent treatment, at their respective GI_{50} concentrations, was examined after 72 hours using fluorescence microscopy and DAPI staining. Cell nuclei were examined to identify changes to morphology and characteristic features of cell death by apoptosis and necrosis. Representative images are displayed in Figure 4.14. Nuclear fragmentation and membrane blebbing, features of apoptosis, were identified in all prostate cells following treatment with Rucaparib. A number of PNT1A and DU145 nuclei appeared smaller and condensed; another feature commonly identified in cell death by apoptosis. Interestingly, a number of PC3 cell nuclei appeared swollen following treatment with Rucaparib, suggesting that these cells may be subject to cell death by necrosis following PARP inhibition.

PNT1A, DU145 and PC3 cells exposed to TSA presented nuclear condensation. DU145 cells also displayed nuclear fragmentation and membrane blebbing. The combined treatment of Rucaparib and TSA had an increased effect on the nuclear morphology of all cell lines; particularly DU145

and PC3 cells. These cells displayed increased amounts of nuclear fragmentation, membrane blebbing and apoptotic bodies compared to cells exposed to each treatment alone. A limited number of PC3 cells were also swollen in response to combined treatment. The effects of combined treatment on PNT1A cells did not enhance changes to nuclear morphology compared to Rucaparib and TSA as single treatments.

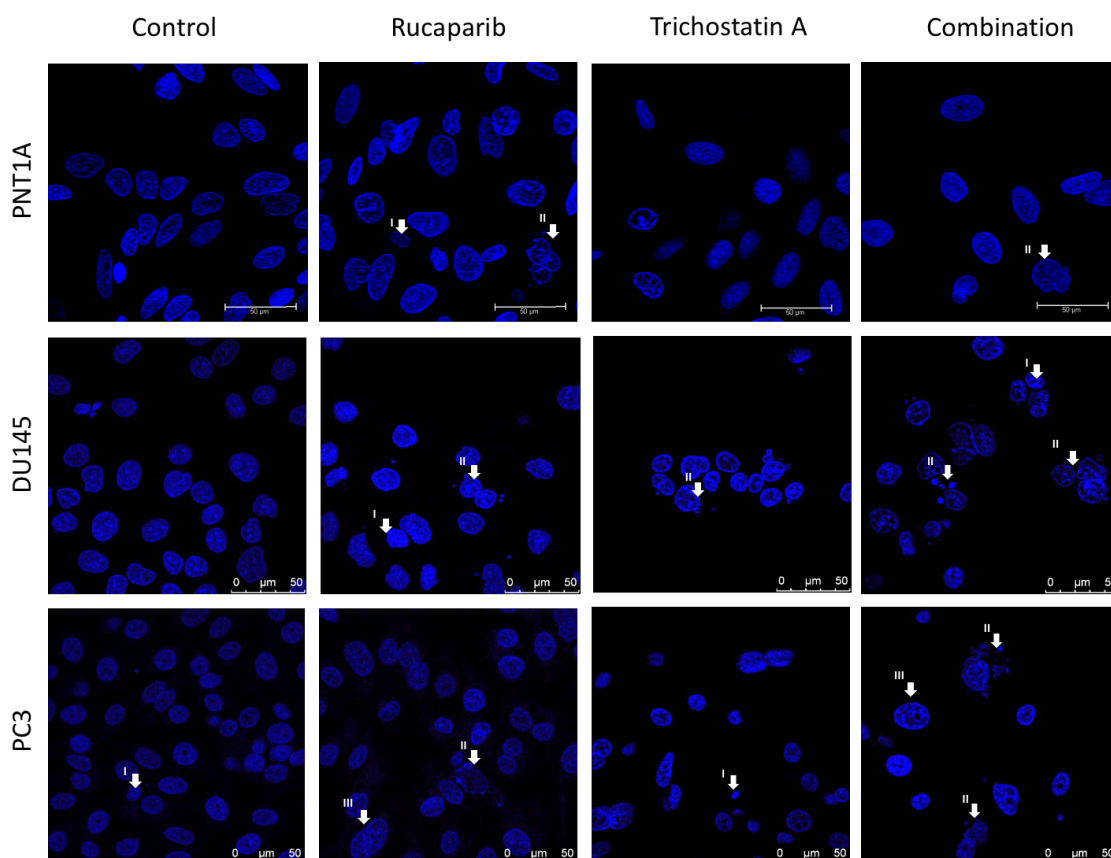


Figure 4.14: The assessment of nuclear morphology changes in response to Rucaparib and Trichostatin A in combination using DAPI staining and fluorescence microscopy.

PNT1A, DU145 and PC3 cells were exposed to Rucaparib and Trichostatin A, alone and in combination at GI_{50} concentrations, for 72 hours. Images are representative of three independent replicates. Arrowheads indicate: (I) Nuclear condensation, (II) membrane “blebbing” and (III) cell swelling; all of which are features of cell death. Images captured at X63 magnification. Scale bar= 50 μ M.

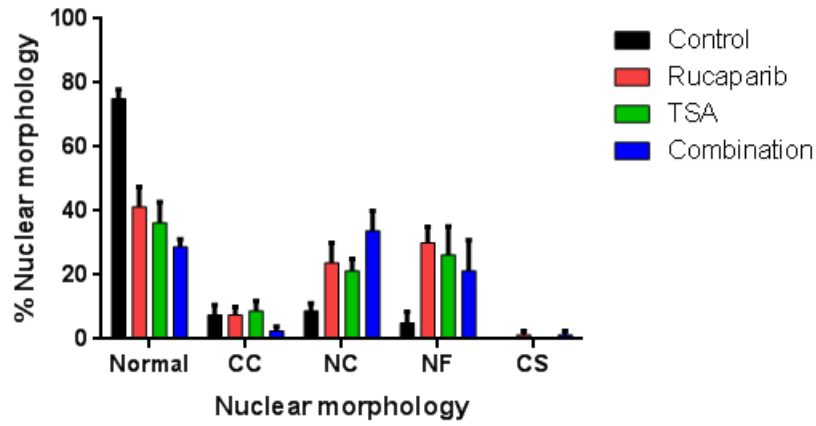
As previously described in section 4.3.3, the changes to nuclear morphology following treatment with Rucaparib and TSA, alone and in combination, at their respective GI_{50} concentrations was quantified (Figure 4.15).

Quantitative analysis of multiple PNT1A cell samples exposed to treatments highlighted a significant reduction in normal nuclear morphology compared to untreated controls ($p \leq 0.001$), as

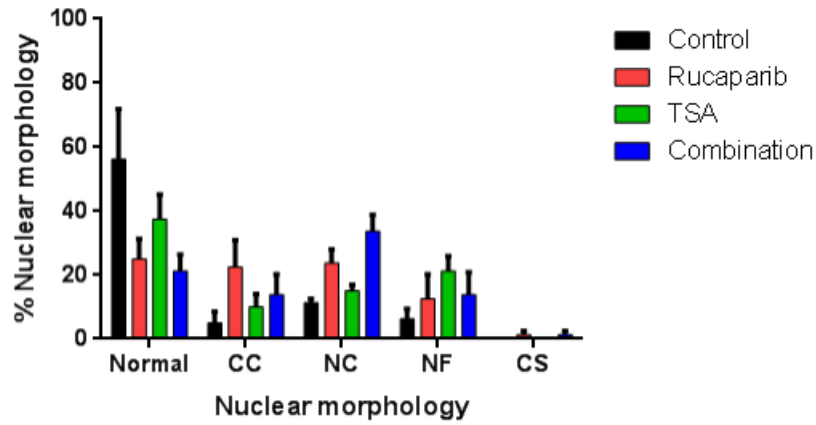
shown in Figure 4.15A. Rucaparib and TSA alone did not significantly affect the normal nuclear morphology of DU145 cells, however, a significant reduction in normal nuclear morphology was apparent following co-treatment ($p=0.05$). There was no significant reduction in the normal nuclear morphology of PC3 cells following exposure to treatments alone and in combination. However, there is a visible reduction in the normal nuclear morphology of DU145 and PC3 cells exposed to treatments (Figure 4.15). The lack of statistical significance is a result of variation between repeated experiments.

The difference in percentage normal nuclear morphology between cells exposed to treatments as single agents and in combination was not significant in all prostate cell lines; suggesting that co-treatment is no more effective than Rucaparib alone. Despite this, a 1.4-fold increase in nuclear condensation was identified in co-treated PNT1A and DU145 cells, compared to cells treated with Rucaparib. The effects of Rucaparib and co-treatment on DU145 cell nuclear fragmentation was not significant. A 1.4-fold decrease in PNT1A cell nuclear fragmentation was identified following co-treatment. In PC3 cells, nuclear condensation and fragmentation levels were not enhanced by Rucaparib and TSA co-treatment, compared to cells exposed to Rucaparib alone. An increase in cell swelling following treatment was not apparent in these cells.

A)



B)



C)

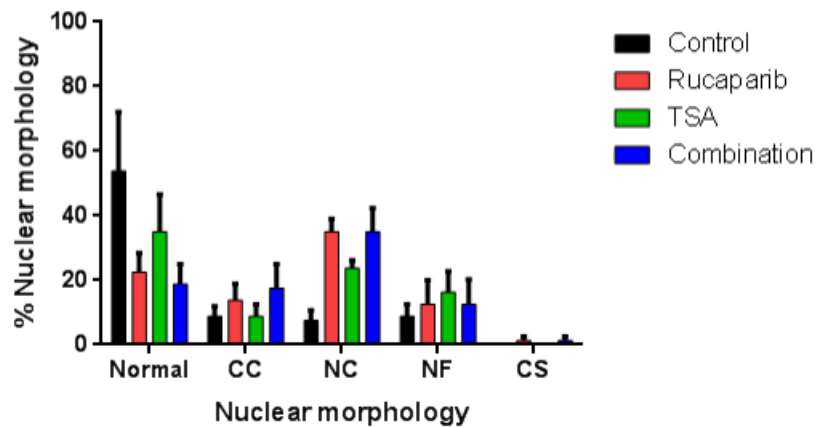


Figure 4.15: Quantification of changes to nuclear morphology following a 72 hour exposure period to Rucaparib and Trichostatin A, alone and in combination.

Epifluorescence was used to assess the changes to nuclear morphology in (A) PNT1A, (B) DU145 and (C) PC3 cells treated with Rucaparib and Trichostatin A, alone and in combination at their GI₅₀ concentrations, for 72 hours. Twenty cells were scored per dose and results are mean of at least two independent experiments. CC= chromatin condensation, NC= Nuclear condensation, NF= Nuclear fragmentation and CS= cell swelling.

4.3.9 The effects of Rucaparib and TSA, alone and in combination on whole protein expression.

The expression levels of PARP-1, Maspin, NF- κ B p65, IKK α and IKB α proteins were visualised by Western blotting in PNT1A, DU145 and PC3 prostate cell samples which were exposed to Rucaparib and TSA, alone and in combination, for 72 hours. Briefly, cells were exposed to treatments at their respective GI₅₀ concentrations. Cells were then harvested, lysates were prepared and loaded onto SDS-PAGE gels for protein separation; prior to electro-transfer, antibody probing and chemiluminescent detection (as described in section 2.2.4). Anti-Actin was used as a loading control alongside Ponceau-S staining. Ponceau-S staining was carried out to ensure that the drug treatments did not affect the expression of the Anti-actin loading control.

The expression of proteins in PNT1A cells exposed to drug treatments are presented in Figure 4.16. Anti-Actin protein bands were not clear and consistent in the PNT1A samples. Consequently, Ponceau-S staining was carried out and used as loading control. The stain highlighted a variance in protein loading between samples, particularly in the TSA treated sample. PARP-1 protein levels were reduced in PNT1A cells exposed to combination treatment, relative to untreated control and Ponceau-S staining. Expression was not affected by single agent treatment. Similarly, Maspin and NF- κ B p65 expression levels were significantly lower in PNT1A cells exposed to combination treatment. Expression of IKK α was reduced following TSA exposure; however, it is not possible to determine whether this is a true result, or rather a fault with chemiluminescent detection. A repeat of this experiment was not completed due to time constraints. Rucaparib and TSA treatment reduced expression levels of IKB α and levels were further reduced with co-treatment; relative to controls.

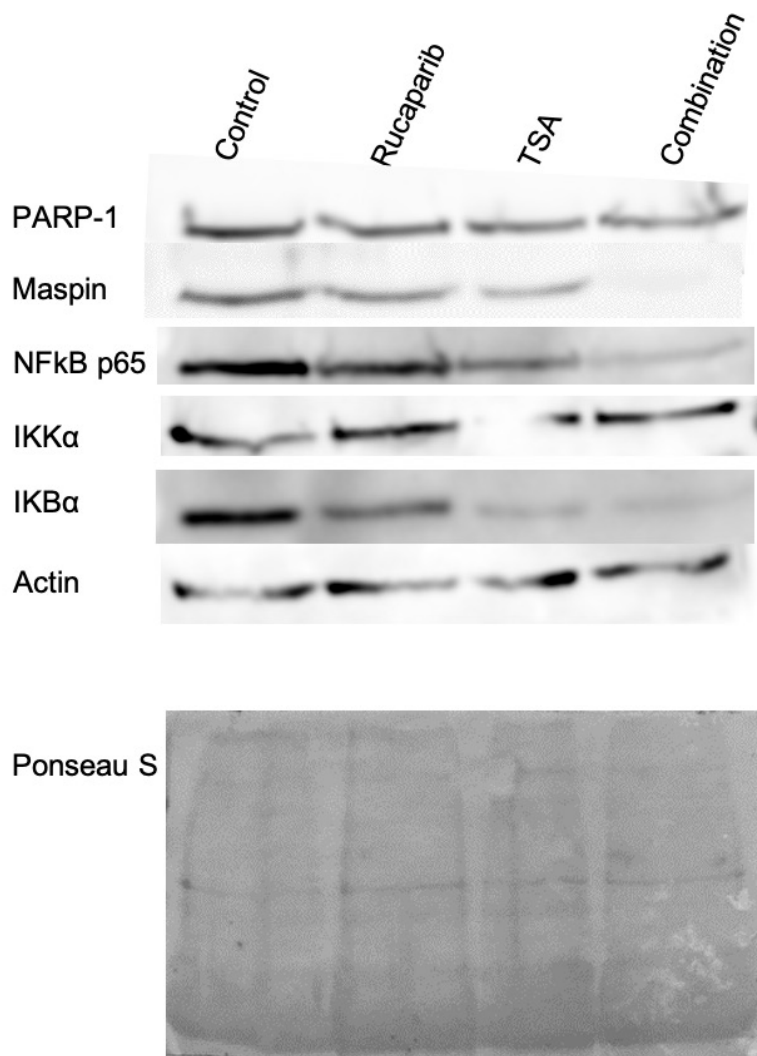


Figure 4.16: PNT1A protein expression following exposure to treatments.

Western blot of whole cell extracts of PNT1A cells at 72 hours after treatment with Rucaparib and TSA, alone and in combination. Blots were probed using antibodies against: PARP-1, Maspin, NF-kB p65, IKK α , IKB α , RelB and Anti-Actin. Blots were stained with Ponceau-S as additional load control. Results from a single experiment.

Treated DU145 cell protein expression results (Figure 4.17) highlight a reduction in PARP-1 expression following co-treatment, but not with single agents alone. Interestingly, TSA and c-treatment reduced maspin expression at 72 hours. Rucaparib treatment has no effect on the expression of maspin and NF-kB p65, however expression is reduced in DU145 samples exposed to TSA. There is an increase in maspin and NF-kB p65 protein levels following co-treatment, compared to TSA alone, but not greater than the expression levels of untreated control and Rucaparib treated cell samples. Rucaparib reduces the expression of IKK α , however TSA has a

greater effect. IKK α protein expression was also reduced in the presence of co-treatment, relative to loading control. Rucaparib and TSA reduce IKB α expression and co-treatment enhances this effect. Anti-Actin loading control suggests that more protein is present in the co-treated sample, however Ponceau-S staining highlights equal loading between samples. To this end, expression results were compared to Ponceau-S loading control.

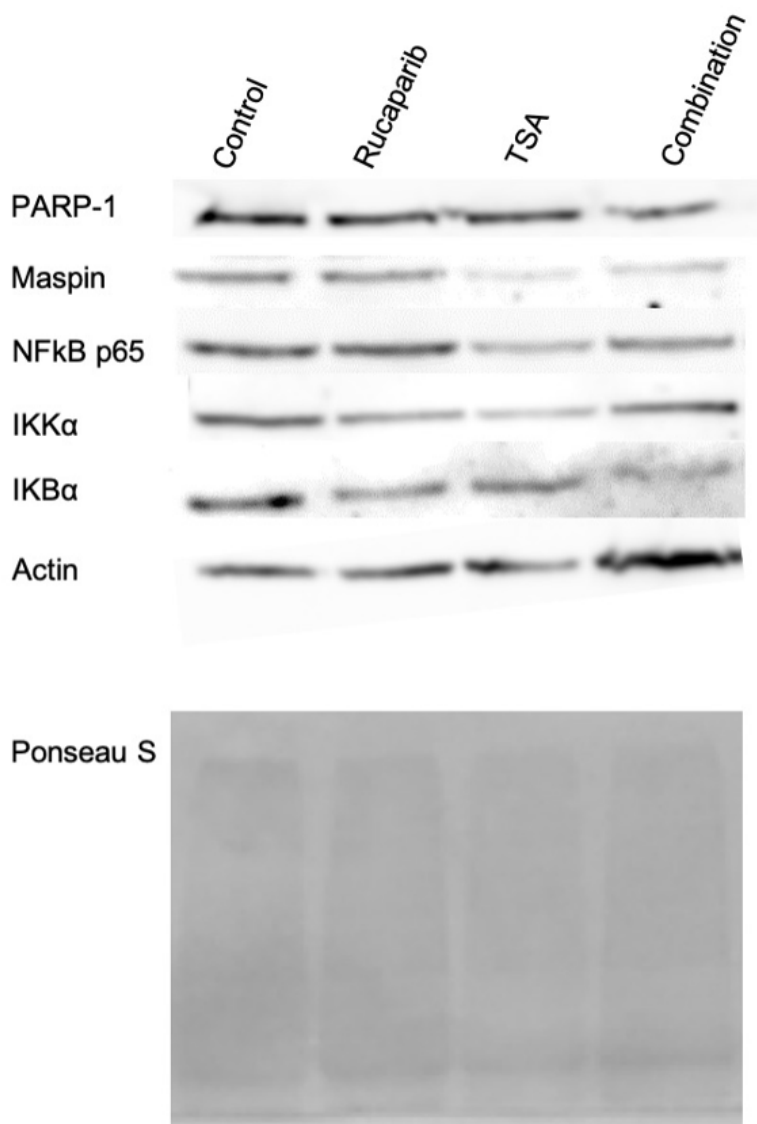


Figure 4.17: DU145 protein expression following exposure to treatments.

Western blot of whole cell extracts of DU145 cells at 72 hours after treatment with Rucaparib and TSA, alone and in combination. Blots were probed using antibodies against: PARP-1, Maspin, NF-kB p65, IKK α , IKB α , RelB and Anti-Actin. Blots were stained with Ponceau-S as additional load control. Results from a single experiment.

Rucaparib and TSA treatment alone had no effect on the expression levels of PARP-1, maspin and NF-kB p65 proteins in PC3 cells, however, expression of these proteins was reduced

following co-treatment (Figure 4.18). The expression levels of IKK α were reduced by Rucaparib and TSA. An almost loss of IKK α expression was apparent following co-treatment. Rucaparib reduced IKB α expression levels. The levels of IKB α protein expression was further reduced following co-treatment; however, exposure to TSA alone had no effect on expression levels. Anti-Actin expression shows equal loading of PC3 samples. Ponceau-S staining of proteins ensures adequate quality control.

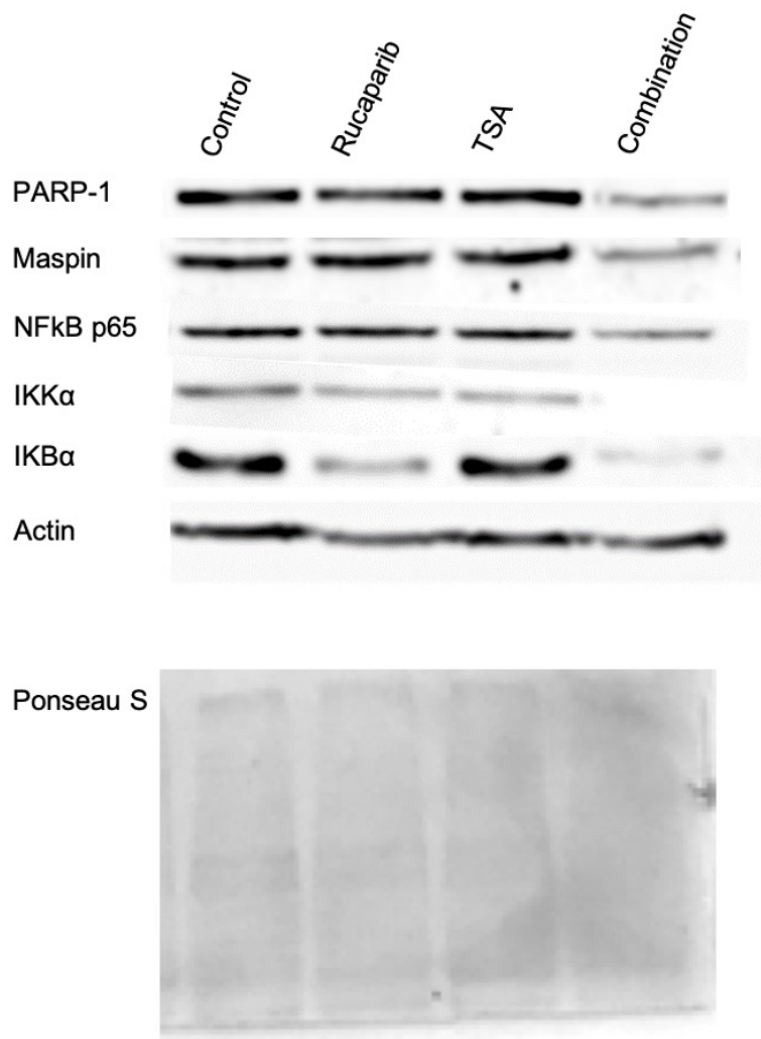


Figure 4.18: PC3 protein expression following exposure to treatments.

Western blot of whole cell extracts of PC3 cells at 72 hours after treatment with Rucaparib and TSA, alone and in combination. Blots were probed using antibodies against: PARP-1, Maspin, NFkB p65, IKK α , IKB α , RelB and Anti-Actin. Blots were stained with Ponceau-S as additional load control. Results from a single experiment.

In summary, the above protein expression results indicate that Rucaparib and TSA treatment, alone and in combination, do not enhance the expression of maspin. TSA treatment reduces

maspin expression in PNT1A and DU145 cells but not PC3 cells. Maspin expressed in all cell lines following co-treatment. Co-treatment also reduces the expression of PARP-1 and NF- κ B p65 expression in all cell lines.

4.3.10 NF κ B affects Rucaparib sensitivity in MEF cells.

In support of the findings presented in section 3.3.5 and 4.3.1, MEF cells were used to investigate sensitivity to Rucaparib relative to the presence, or absence, of NF- κ B subunits. Growth inhibition assays were carried out with p65^{+/+}, p65^{-/-} and IKK α ^{-/-} MEF cells exposed to increasing concentrations of Rucaparib (Figure 4.19). As expected, MEF p65^{-/-} cells were significantly more sensitive to Rucaparib than p65^{+/+} and IKK α ^{-/-} cells (one-way ANOVA with Tukey's multiple comparisons test. $p \leq 0.001$ and $p \leq 0.01$, respectively). The growth of p65^{+/+} and IKK α ^{-/-} cells was not suppressed by >50% at the highest concentration of Rucaparib used; indicating reduced drug sensitivity in these cell lines.

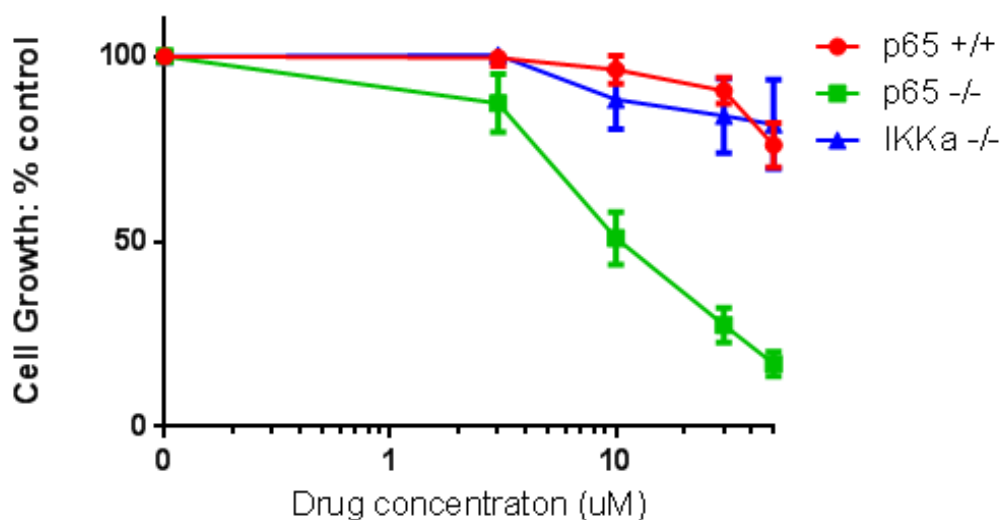


Figure 4.19: Cytotoxicity to Rucaparib in Mouse embryonic fibroblast cell lines by SRB assay.

MEF cells were treated with Rucaparib at various concentrations for 72 hours and cell number was determined. Data shown are the average of at least three independent experiments and error bars represent SEM.

Mean Rucaparib GI₅₀ concentrations for MEF cells were calculated (Table 4.4). Due to a lack of sensitivity, it was not possible to obtain GI₅₀ Rucaparib concentrations for MEF p65^{+/+} and IKK α ^{-/-} cells.

Table 4.4: MEF GI₅₀ values following exposure to Rucaparib for 72 hours.

Cell line	Mean GI ₅₀ (μM) ± SD
MEF p65 ^{+/+}	-
MEF p65 ^{-/-}	11 ± 11.39
MEF IKKα ^{-/-}	-

These findings in addition to the experiments carried out in prostate cells highlight a link between NFκB p65 and PARP inhibitor sensitivity. MEF p65^{-/-} cells, which express low levels of maspin and high levels of IKKα, are most sensitive to Rucaparib treatment. These findings correlate to the protein expression data for maspin depleted DU145 cells; low expression of NF-κB p65 and maspin and high expression of IKKα. IKKα^{-/-} cells, which were not sensitive to Rucaparib, expressed NF-κB p65 and maspin. (Expression data presented in Chapter three, section 3.3.5).

4.3.11 NF-κB p65 enhances TSA resistance in MEF cells.

MEF cell sensitivity to TSA was also investigated by SRB assay (Figure 4.20). Cell growth was inhibited by TSA concentrations >40nM in all MEF cells; in a dose dependant manner. TSA concentrations ≤40nM were not growth inhibitory to p65^{+/+} cells. p65^{-/-} and IKKα^{-/-} MEF cells were significantly more sensitive to TSA than p65^{+/+} cells (one-way ANOVA with Tukey's multiple comparisons p≤0.01). There was no significant difference between the sensitivity to TSA in MEF p65^{-/-} and IKKα^{-/-} cells (p>0.669, unpaired t-test).

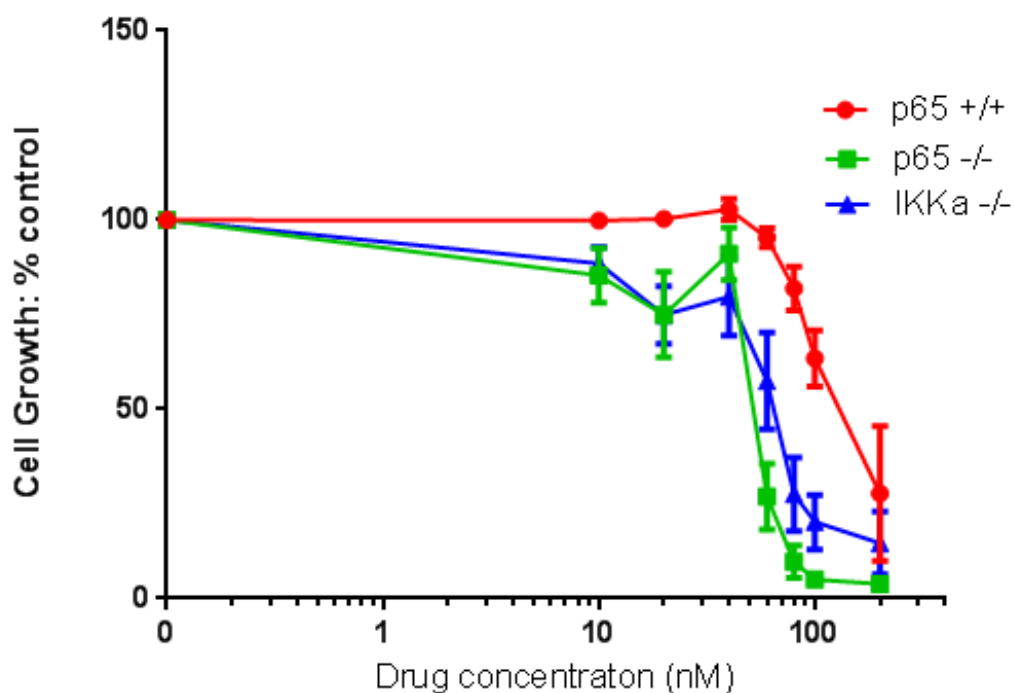


Figure 4.20: Cytotoxicity to Trichostatin A in Mouse embryonic fibroblast cell lines by SRB assay. MEF cells were treated with Trichostatin A at various concentrations for 72 hours and cell number was determined. Data shown are the average of at least three independent experiments and error bars represent SEM.

Mean TSA GI₅₀ concentrations for MEF cells were calculated (Table 4.5). The concentration of TSA required to inhibit growth by 50% in MEF p65^{+/+} cells was 2.6-fold and 2.1-fold higher than the doses required for p65^{-/-} and IKKα^{-/-} cells, respectively.

Table 4.5: MEF GI₅₀ values following exposure to TSA for 72 hours.

Cell line	Mean GI ₅₀ (nM) ± SD
MEF p65 ^{+/+}	138 ± 16.05
MEF p65 ^{-/-}	53 ± 4.3
MEF IKKα ^{-/-}	65 ± 9.4

Analysis of the data indicate that the absence of NF-κB p65 or IKKα leads to increased sensitivity to TSA. These findings do not correspond with the TSA sensitivity data for prostate cells. The data shows no significant difference in sensitivity to TSA in DU145 and PC3 cells; despite variance in NF-κB p65 and IKKα expression levels DU145 expressed low levels of NF-κB p65

compared to PC3 cells and expression was inversely correlated to the expression levels of IKK α (Figure 3.9 and Table 4.3).

4.4 Discussion

The studies presented in this chapter evaluate the effects of Rucaparib and Trichostatin A, as single agents and in combination, in a panel of prostate and mouse embryonic fibroblast (MEF) cell lines of varied maspin and NF- κ B expression.

4.4.1 The effects of Rucaparib on prostate and MEF cell survival

The cell viability of DU145 and PC3 cells exposed to low dose Rucaparib (3 μ M) was increased 10% and 13% by WST-1 assay (Figure 4.2), respectively. This may be due to a biphasic dose response stimulation otherwise known as hormesis. The hormesis phenomenon has been observed in a range of biological systems and is well characterised in cancer therapeutics. It describes the drug action of low dose stimulation, arising due to homeostatic adaptation, followed by high dose inhibition (Bhakta-Guha and Efferth, 2015). A hormetic response following exposure to Rucaparib was cancer cell specific, indicating a PARP inhibitory effect on cancer cell metabolism. The WST-1 assay is a bio-reduction reaction dependent on the glycolytic production of NAD(P)H in viable cells, and therefore, the low dose stimulation observed in DU145 and PC3 cells could be attributable to enhanced mitochondrial metabolism following PARP inhibition. This suggestion is in line with a previously published study by Almeida et al. (2017), where PARP inhibition in colorectal and ovarian cancer cell lines resulted in an increase in NAD⁺ concentration. Similarly, Bhute and Palecek (2015) reported a reverse in NAD depletion in breast cancer cells following exposure to the PARP inhibitor Veliparib. Enhanced mitochondrial bioenergetics is considered a hallmark of cancer (Hanahan and Weinberg, 2011) and this could explain why a low dose stimulation was not observed in the normal prostate cells. The reduction in cell viability following exposure to higher concentrations of Rucaparib than 3 μ M is likely due to increased DNA damage, NAD⁺ depletion and consequently cellular stress and cytotoxicity.

To investigate the biphasic response trend further, WST-1 data was compared to results obtained from cell counting, SRB and Resazurin assays. A biphasic dose response stimulation was not

observed by SRB and cell counting methods. These methods do not measure mitochondrial activity; they quantify live cell number and bind to protein components of the cell which are directly proportional to cell mass, respectively. The findings support that the low dose stimulation to Rucaparib identified by WST-1 is due to changes to mitochondrial metabolism. Resazurin, another measurement of metabolic activity, also presented a low dose stimulation to Rucaparib (8%) in DU145 cells, but not PC3 cells. The reason for variance between WST-1 and Resazurin findings in PC3 cells is unclear but are likely to be attributed to variances in cell health and cell cycle stage between experiments. This could be tested carrying out cell growth and viability tests between each experiment. Cell cycle could be assessed by measuring DNA content by flow cytometry. Overall, the chemical reduction of WST-1 and Resazurin assays is impacted by changes in intracellular metabolic activity rather than cytotoxicity, and because PARP can alter levels of NAD^+ , the effects of PARP inhibition in these assays is a result of changes in metabolic processes rather than cell death. Deregulated metabolism is an enabling characteristic of cancer development and warrants further investigation, however, was beyond the scope of this thesis. As the sensitivity to Rucaparib did not significantly differ between SRB and cell counting methods in prostate cells, the SRB method was selected for use in experiments with MEF cells and treatment combinations. The method has a stable endpoint, is fast and cost effective. Use of a single methodology is essential in pharmacological studies to ensure standardisation of response measurement (Haibe-Kains et al., 2013).

Within the panel of cell lines studied, DU145 cells were 2 and 3.3-fold more sensitive to Rucaparib than PC3 and PNT1A cells, respectively (fold-change based on SRB data). Studies have demonstrated that PARP-1 is an essential mediator of NF- κ B activation, which in turn is an essential mediator of resistance to DNA damaging agents (Veuger et al., 2009). Later studies from the same group highlighted the importance of NF- κ B status in tumours; showing that inhibition of NF- κ B signalling using PARP inhibitors can sensitise breast cancer cells to IR and chemotherapeutic agents (Hunter et al., 2012). Nakagawa et al. (2015) also supported the role of NF- κ B signalling in PARP inhibitor sensitivity. They generated PARP-inhibitor resistant breast and ovarian cancer cell lines and measured upstream effectors and downstream products of NF-

kB by polymerase chain reaction; to show upregulation of NF-kB signalling in PARP inhibitor resistant cells. The non-canonical NF-kB p65 subunit mediated sensitivity to PARP inhibition; knockdown of p65 was found to enhance PARP inhibitor sensitivity in PARP inhibitor-resistant cell lines. These studies support the data presented in Figure 3.9 that shows increased expression levels of NF-kB p65 protein in PC3 and PNT1A cells, compared to DU145 cells. However, DU145 cells were most sensitive to PARP inhibition and expressed reduced levels of the PARP-1 protein. Investigation into DU145 cell PARP-1 activity is required; to elucidate that the increased sensitivity to Rucaparib is due to reduced NF-kB p65 signalling rather than reduced PARP activity. Cytotoxicity studies with MEF cells (Figure 4.19) revealed increased sensitivity to Rucaparib in p65^{-/-} cells compared to MEF p65^{+/+} cells; further supporting the role of NF-kB in reducing PARP inhibitor sensitivity. MEF IKK α ^{-/-} cells were less sensitive to PARP inhibition. DU145 cells, which are most sensitive to Rucaparib, expressed increased levels of IKK α and reduced levels of NF-kB p65 protein compared to the other prostate cell lines which were less sensitive; strengthening a link between NF-kB and PARPi sensitivity.

Prostate cell cytotoxicity data also highlights a potential role of maspin expression and PARPi sensitivity. The literature has explored a correlation between NF-kB and the expression of maspin, however, it is yet to investigate the role of maspin in relation to PARP inhibitor sensitivity. Luo et al. (2007) showed that prostate cell metastasis is regulated by the NF-kB subunit IKK α ; which downregulates maspin and promotes a metastatic phenotype. Using transgenic mice models, they showed that inhibition of IKK α limited prostate cancer growth and progression; which correlated to increased expression of maspin. A more recent study examined cutaneous squamous cell carcinoma samples (+/- metastasis) by immunohistochemistry to measure the association of active IKK α and maspin with cancer behaviour. IKK α inversely correlated with maspin levels, and samples depleted in maspin were found exclusively in those derived from metastasis (Toll et al., 2015). A series of studies carried out by Shukla et al, with the use of a natural compound apigenin, showed that increased levels of maspin were associated with reduced IKK α activity and nuclear expression of NFkB p65 (Shukla, 2008). Recently, they demonstrated that apigenin enhances maspin expression via p53 upregulation and downregulation of HDAC activity in prostate cancer

cells (Shukla, 2015). These findings support our data which shows low expression of maspin and increased expression of IKK α in DU145 cells, and high expression of maspin and low expression of IKK α in PC3 cells. MEF IKK α ^{-/-} cells expressed increased levels of maspin compared to MEF p65^{+/+} and p65^{-/-} cells lines. As PARP is a known transcriptional co-activator of NF-kB (Hassa et al., 2001), inhibition of NF-kB by Rucaparib may enhance maspin expression. Our data showed that Rucaparib reduced the expression of IKK α in DU145 and PC3 cells (Figure 4.17 and Figure 4.18) but there was no change to the expression of maspin at the 72-hour time point that was tested suggesting inhibition of maspin activity rather than protein levels.

The enhanced sensitivity of DU145 cells to Rucaparib may also be due to genetic mutation; including mutated BRCA1. BRCA deficient and/or mutated cancers are exquisitely sensitive to PARP inhibition through the mechanism of synthetic lethality. PARP inhibition compromises SSB repair, and cells lacking functional HR mechanisms, such as BRCA, are subject to double strand breaks (DSB). Consequently, these cells are then damaged beyond repair (Farmer et al., 2005). BRCA1 interacts with p65 leading to NF-kB activation, and NF-kB acts as a mediator of BRCA1-induced chemo-resistance. Therefore, the reduced sensitivity to Rucaparib seen in PNT1A and PC3 cell lines may be due to functional BRCA1 and high NF-kB p65 protein expression. The increased sensitivity to Rucaparib in DU145 cells could be in part due to dysfunctional BRCA1 which attributes to increased IKK α and therefore activation of NF-kB. Additionally, dysfunctional BRCA1 induces an HR deficient repair phenotype; a major cause of hypersensitivity to PARP inhibition. The cytotoxicity results presented in this chapter support previously published studies which demonstrate selective cytotoxicity to PARP inhibitors in BRCA mutated and deficient models; confirming the concept of synthetic lethality (Farmer et al., 2005, Bryant et al., 2005).

4.4.2 Rucaparib has increased effect on cell morphology and death in maspin depleted prostate cancer cells.

Changes to prostate cell morphology following Rucaparib treatment were consistent with cell survival data from SRB assays. Changes to cell morphology representative of cell stress were greater in DU145 and PC3 cells, compared to PNT1A cells; demonstrating the efficacy of

Rucaparib in selectively targeting tumour cells. Assessment of nuclear morphology by DAPI assisted in the identification of cell death pathway. Apoptosis occurs in the vast majority of physiological cell deaths and is a common response to PARP inhibition in a variety of cancers (Shi et al., 2014). Features of apoptosis were apparent in all cell lines, particularly DU145 cells, which presented a high percentage of nuclear fragmentation and cell shrinkage. Interestingly, PNT1A and PC3 cells also presented signs of cell swelling in response to Rucaparib; suggesting that cell necrosis may also contribute to loss of cell viability in these cell lines. A potential reason for both apoptotic and necrotic features in these cells may be secondary necrosis; a process of cell elimination occurring when apoptotic cells are not cleared by scavengers (Silva, 2010). Further investigation is required to confirm the modes of cell death in these cells, whether it be apoptosis or necrosis, to enhance the understanding of molecular events taking place up to Rucaparib-induced cell death.

4.4.3 The effects of TSA on cell survival in prostate and MEF cells.

HDAC inhibition has been reported to reduce the expression of proteins involved in HR DNA repair; resulting in impaired DSB repair and “*BRCAness*”. To this end, HDACi has emerged as a therapeutic strategy to pharmacologically manipulate HR repair for sensitisation to PARP inhibitors (Kachhap et al., 2010, Ha et al., 2014). Prior to combination studies with Rucaparib, the effects of the HDAC inhibitor, TSA, as a single agent were assessed.

SRB and counting data confirmed that prostate cancer cells are significantly more sensitive to TSA than immortalised prostate cells; suggesting the possibility of a therapeutic window. However, there was no difference in sensitivity to TSA between DU145 and PC3 cell lines despite variances in the expression of maspin. Maspin is the only endogenous HDAC inhibitor that has been identified so far, and the biological effects of maspin are similar to those of pharmacologic HDAC inhibitors. Li et al. (2006) demonstrated that binding of maspin to HDAC1 did not block the action of the synthetic pharmacologic HDAC inhibitor M344. The group also reported increased maspin expression in both DU145 and PC3 cells following synthetic HDAC inhibition; demonstrating that the inhibitory effect of maspin on synthetic HDAC inhibition positively

feedbacks on maspin expression, and therefore contributes to tumour suppression. With this in mind, we would have expected TSA to have the greatest effect on PC3 cells.

Assessment of cell viability by WST-1 assay revealed a 2.6-fold increase in DU145 cell sensitivity to TSA, compared to PC3 and PNT1A cells that were equally as sensitive. Walton et al. (2008) also assessed the effects of TSA on cell viability and metabolism in prostate cell lines. In line with our findings, they reported increased sensitivity to TSA treatment in DU145 cells. These findings indicate that TSA has a greater effect on DU145 cancer cell metabolism, despite no significant difference in cell cytotoxicity between PC3 cells. The reason for such effect is unknown. Higgins et al. (2009) investigated metabolic phenotypes in prostate cancer cell lines; including DU145 and PC3. They demonstrated a reduced reliance on oxidative phosphorylation in these cells, compared to less invasive LNCaP cells, due to mitochondrial dysfunction and therefore reduced mitochondrial enzyme activity. Despite this, the mRNA levels of mitochondrial enzymes were 5-fold higher in DU145 cells. This finding may explain the different effects on the cellular metabolism and viability of DU145 and PC3 cells exposed to TSA. The increased effect of TSA on DU145 cell metabolism may also be attributed to epigenetic status and expression of the *maspin* gene. Metabolic enzyme expression impacts the methylation and acetylation of DNA and histone proteins, driving vital biological outcomes such as cancer. Maspin specifically inhibits HDAC-1; a histone deacetylase commonly upregulated in malignancy. DNA methylation leads to recruitment of HDACs to promotor regions, leading to the repression of genes. Class 1 HDAC inhibitors reverse promotor methylation and gene silencing (Sarkar et al., 2011). Therefore, a loss of HDAC inhibition, when maspin is downregulated, may increase DNA methylation and epigenetic gene silencing. *In vitro* models of human breast cancer have reported a loss of maspin expression, and this was often a result of aberrant methylation of the *maspin* promotor (Futscher et al., 2004). Inhibition of HDAC, by TSA, in maspin depleted DU145 cells may therefore override repressive histone modifications; leading to the upregulation of genes which may be associated with enhanced sensitivity to pharmacological HDAC inhibitors (Li et al., 2006). HDAC is endogenously inhibited by the presence of maspin in PNT1A and PC3 cells,

and these cells may therefore be metabolically less sensitive to pharmacological HDAC inhibition; compared to DU145 cells whereby HDAC is not endogenously inhibited.

MEF p65^{+/+} cells were 2.6 and 2.1- fold less sensitive to TSA than MEF p65^{-/-} and MEF IKK α ^{-/-} cells, respectively. These findings support the findings of Mayo et al. (2003), whereby NF-kB was identified as a mediator of HDACi resistance. They demonstrated that inhibition of NF-kB facilitated apoptosis in response to HDAC inhibition, concluding that the ineffectiveness of HDAC inhibitors to induce apoptosis may be attributed to the ability of tumour cells to respond to these treatments by up-regulating NF-kB. These results do not correspond with the prostate cell data, where there is no significant difference in TSA sensitivity between DU145 and PC3 cells at GI₅₀; despite variations in the expression of NF-kB p65 and IKK α . Resistance to TSA in MEF p65^{+/+} cells could also be due to maspin deficiency. This link was not identified in the prostate cell lines, however, the MEF cells are isogenic and therefore we cannot rule it out. The expression of maspin in the MEF cells correlated to TSA sensitivity (Figure 3.13), with high maspin expressing IKK α ^{-/-} cells being most sensitive. Exact mechanisms contributing to variances in TSA sensitivity between MEF cells are unclear and warrant further investigation, but the data highlights an interesting difference in TSA sensitivity that is likely dependent on the presence of NF-kB p65. A combined molecular targeting that inhibits both NF-kB and HDAC, such as PARP and HDAC inhibitors, may provide a significant anti-cancer therapy.

4.4.4 TSA- cell morphology and death

Assessment of cell and nuclear morphology following TSA treatment support the findings from SRB cytotoxicity assays; whereby DU145 and PC3 are equally as sensitive to TSA. Our data reinforces the known selectivity of TSA to cancer cells, as the treated PNT1A cells are visibly resistant to morphological change. In line with the studies by Walton et al. (2008), TSA induced increased nuclear condensation, blebbing and fragmentation in the cell lines; suggesting that TSA is important in apoptotic signalling. PNT1A cells presented signs of apoptosis following treatment with higher concentrations of TSA but were significantly less sensitive to cell death than the other cell lines. It has been reported that various HDAC inhibitors, including TSA, arrest cell cycle progression leading to apoptosis. Cell cycle analysis was not carried out in the studies presented

in this thesis, however Choi et al. (2013) reported an accumulation of DU145 and PC3 cells in the sub-G1 phase of the cell cycle following treatment with the HDACi A248. Increased nuclear condensation and fragmentation was also observed, highlighting the importance of A248 in apoptotic signalling.

Studies have also reported increased DNA damage signalling in cancerous cells following HDAC inhibition. Zhang et al. (2007) discovered that squamous carcinoma cells treated with TSA and IR exhibited delayed DNA repair compared to cells exposed to IR alone. They postulated that this response was due to suppression of genes and proteins associated with DNA repair such as BRCA1. Indeed, TSA was found to suppress *BRCA1* gene expression, therefore driving a HR phenotype and enhancing sensitivity to Rucaparib, implicating *BRCA1* as a molecular target of TSA treatment. Of the prostate cell lines studied throughout this thesis, only DU145 cells are BRCA1 mutated. As there is no significant difference in TSA sensitivity between DU145 and PC3 cells, we cannot conclude that TSA contributes to apoptosis and DNA damage in these cell lines through suppression of *BRCA1*. These findings show that exposure to TSA alone is no more effective in maspin depleted cell lines. However, treatment may show promise in sensitising these cells to PARP inhibition by exacerbating DNA damage and death. The effects of TSA on DNA damage are explored in Chapter Six.

4.4.5 Pharmacological inhibition of HDAC by TSA synergises prostate cancer cells to the PARP-1 inhibitor Rucaparib.

A number of studies have shown that HDAC inhibitors synergise with PARP inhibitors in the treatment of cancers (Chao and Goodman, 2014, Marijon et al., 2018, Rasmussen et al., 2016) by preventing HR DNA repair and inducing “*BRCAness*”. However, the effect of these drugs in combination relative to NF- κ B and maspin has not yet been explored. Studies by Hassa et al. (2005) suggested that PARP-1 interacts and is de-acetylated by HDAC-1. They showed that PARP-1 dependent activation of NF- κ B is negatively regulated by HDACs 1-3; suggesting that acetylation of PARP-1 is vital for its role as a transcriptional coactivator. In support of these studies, our data revealed increased levels of HDAC-1, and consequently, reduced levels of PARP-1 and NF- κ B in maspin depleted DU145 cells. The enhanced sensitivity to PARP inhibitors

in these cells may be further potentiated by HDAC inhibitors due to increased NF- κ B signalling and DNA damage. Both drugs are reported to down-regulate BRCA1, and so we would expect co-treatment to have significantly greater effect on BRCA1 mutant DU145 cells. The findings presented in Figure 4.12 demonstrate that TSA enhances the effects of Rucaparib to inhibit cell growth; particularly in cancer cell lines. Unexpectedly, there was no difference in sensitivity to combination treatment, at respective GI₅₀ concentrations, between DU145 and PC3 cells; suggesting that response to combined treatment is independent of maspin or BRCA1 status. However, it is important to note that the required Rucaparib GI₅₀ concentration for DU145 cells is ~2-fold less than the concentration required for PC3 cells, and therefore we would expect DU145 cells to be significantly more sensitive to combination treatment if the GI₅₀ concentration for PC3 cells was used. CalcuSyn software is a popular tool used to quantitatively measure the dose-effect relationship of drugs alone, and in combination, to determine drug synergy. Use of this software applies a non-subjective method to drug interaction and enables standardised interaction classifications (Bijnsdorp et al., 2011).

In line with cytotoxicity data, co-treatment had an enhanced effect on cell and nuclear morphology in all cell lines, compared to treatments alone. Normal prostate cells were less sensitive to the combined effects of HDAC and PARP inhibition. DU145 and PC3 cells exposed to co-treatment exhibited increased cellular stress, increased nuclear condensation and fragmentation; representative of apoptosis. PC3 cells also presented cell swelling following co-treatment suggesting that a different mode of cell death is responsible for loss of cell viability and changes to morphology. As this response was also identified in cells exposed to Rucaparib alone, we can conclude that Rucaparib is responsible for the mechanism of cell death induced in these cells. Chao and Goodman (2014) reported non-apoptotic cell death in PC3 cells co-treated with the HDAC inhibitor SAHA and PARP inhibitor Olaparib; concluding that autophagy may be a potential mechanism of cell death. Further investigation into the mode of cell death in PC3 cells following treatments is required but is beyond the scope of this thesis.

4.4.6 Western blot analysis of Maspin, NF-kB and PARP-1 expression in prostate cell lines treated with Rucaparib, TSA as single agents and in combination.

To investigate the potential mechanism involved in the sensitivity of prostate cancer cell lines to Rucaparib and TSA, alone and in combination, the expression levels of maspin, NF-kB and PARP-1 proteins were studied. Tables 4.6 and 4.7 summarise the changes to expression of these proteins in DU145 and PC3 cells exposed to Rucaparib and TSA, respectively.

Table 4.6: The effects of Rucaparib on the expression levels of maspin, PARP-1, NF-kB p65 and IKKa proteins in DU145 and PC3 cells.

	Maspin	PARP-1	NF-kB p65	IKKa
DU145	no effect	no effect	no effect	reduced
PC3	reduced	reduced	reduced	reduced

Table 4.7: The effects of TSA on the expression levels of maspin, PARP-1, NF-kB p65 and IKKa proteins in DU145 and PC3 cells.

	Maspin	PARP-1	NF-kB p65	IKKa
DU145	reduced	no effect	reduced	reduced
PC3	no effect	no effect	no effect	reduced

We expected to see a reduction in NF-kB, and an increase in maspin protein expression following treatments; however, this was not the case. Rucaparib had no effect on the expression of maspin in any of the prostate cell lines, indicating that inhibition of NF-kB with a PARP inhibitor does not enhance maspin. TSA had no effect on the expression of maspin in PC3 cells, however, a reduction in maspin expression was apparent in PNT1A and DU145 cells. Previous studies have reported an increase in maspin expression following TSA treatment (Abbas and Gupta, 2008) and therefore, further investigation is required to elucidate why our findings are different. A possible reason could be changes to DNA methylation following inhibition of HDAC; leading to the epigenetic silencing of genes that may affect the expression of downstream proteins. Interestingly, Rucaparib and TSA co-treatment further reduced the expression of maspin in all cell lines. TSA and Rucaparib single agents did not affect the expression of maspin in PC3 cells, therefore the reduction of maspin following co-treatment is an effect of the treatment combination.

IKK α protein levels were reduced following Rucaparib treatment in DU145 and PC3 cells, and expression levels were reduced further when combined with TSA. Treatment did not affect the expression of IKK α in PNT1A cells, demonstrating a cancer specific affect. Increased expression of IKK α has been implicated in prostate cancer progression via down-regulation of maspin. Goktuna et al. (2014) evidenced protection against tumour development in mice which were deficient in IKK α ; highlighting the potential of IKK α as a therapeutic target in cancers of the colon. Luo et al. (2007) revealed that active IKK α repressed transcription of the *maspin* gene and correlated with metastatic progression. We did not find an inverse correlation between maspin and IKK α protein expression in our treatment studies and the reason for this is unknown. The expression studies were carried out with use of cell samples exposed to treatments for 72 hours, additional time-points may have revealed a change to maspin expression. Gene expression of NF- κ B and maspin, and activity of PARP and NF- κ B were not assessed in our studies due to time constraints. These studies may provide further insight into the interplay between IKK α and maspin in cancer progression. A recent study by Mahato et al. (2011) investigated the role of IKK α in PC3 cell invasiveness; reporting upregulation of maspin in prostate cancer following IKK α silencing by siRNA. These findings are in line with the expression data obtained in our studies with MEF IKK α ^{-/-} cells; whereby maspin expression levels are higher compared to MEF cells which were not deficient for IKK α .

The expression of NF- κ B p65 was reduced following PARP inhibition in normal PNT1A cells but not in DU145 and PC3 cells. This may be attributable to the increased inflammatory signalling in tumour cells. Reduced levels of IKK α expression following PARP inhibition in these cell lines suggest that NF- κ B may not be constitutively activated despite expression. However, the protein expression data is representative of total protein expression and further investigation into the cytoplasmic and nuclear expression of NF- κ B subunits following PARP inhibition is warranted to elucidate NF- κ B constitutive activation. Interestingly, TSA treatment reduced the protein expression levels of NF- κ B p65 in PNT1A and DU145 cells, but not PC3 cells. Rucaparib and TSA co-treatment significantly reduced the expression levels of NF- κ B p65 in PNT1A, DU145 and PC3 cell lines. These findings demonstrate that the reduction of NF- κ B p65 is dependent on

HDAC inhibition in PNT1A and DU145 cells. In PC3 cells reduced expression of NF-kB p65 is dependent on Rucaparib and TSA co-treatment.

As PARP-1 is a known coactivator of NF-kB, the expression levels of PARP-1 following treatment were also investigated. Rucaparib and TSA as single agents had no effect on the expression levels of PARP-1, however expression was reduced following co-treatment in the cancerous cell lines. A possible explanation for the aforementioned is PARP trapping. In addition to the inhibition of PARP-1 catalytic activity, PARP inhibitors trap PARP at DNA breaks; preventing DNA SSB repair leading to the development of cytotoxic DSB's and cell death. Various PARP inhibitors, including Rucaparib, have been reported to trap PARP in a number of cancer studies (Shen et al., 2015, Murai et al., 2014, Rouleau et al., 2010, Murai et al., 2012). Studies have also reported acetylation of PARP-1 following HDAC inhibition. For example, Robert et al. (2016) showed increased acetylation of PARP-1 in leukaemia cells exposed to TSA. They evidenced increased PARP-1 binding to DSB's in chromatin, a mechanism similar to the PARP-1 trapping mechanism observed following PARP inhibition. The same group reported increased PARP trapping following combined HDAC and PARP inhibitor treatment. However, the ability of these drugs to trap PARP in chromatin is dependent on their cytotoxicity, and the reduced expression of PARP-1 following co-treatment in our cell lines correlates with cell cytotoxicity data. Combined HDAC and PARP inhibitor treatment has also been shown to decrease PARP-1 expression in other cancer studies, including the prostate (Rasmussen et al., 2016, Yin et al., 2018). PARP-1 protein expression does not reflect the activity of PARP and therefore measurement of activity may provide further insight into the effects of PARP and HDAC inhibition.

Overall, the protein expression data from treated cell samples show that maspin expression is not increased following combined PARP and HDAC inhibition. Co-treatment does reduce the expression of PARP-1 and NF-kB expression in DU145 and PC3 cell lines and therefore is an attractive therapeutic target.

4.5 Summary

The studies presented in this chapter have shown that:

- Rucaparib induces a low dose hormetic response that is specific to tumour cells.
- SRB assay is the best technique to assess cell sensitivity to Rucaparib and TSA treatment. The technique provides a stable endpoint and correlates to data obtained from manual cell counts.
- Maspin depleted cells are significantly more sensitive to Rucaparib treatment than maspin proficient cells.
- Cells expressing reduced levels of PARP-1 and the NF- κ B subunit p65 are most sensitive to Rucaparib; supporting the role for PARP-1 as a mediator of NF- κ B activation which promotes resistance to DNA damaging agents.
- NF- κ B p65 knockout MEF cells are more sensitive to Rucaparib than NF- κ B p65 proficient MEF cells.
- TSA enhances cell sensitivity to Rucaparib in DU145 and PC3 cells, underlining a promising strategy for tumour sensitisation. Response to co-treatment was not significantly different between DU145 and PC3 cells at GI₅₀, suggesting that the differential expression of maspin does not affect sensitivity.
- The expression of maspin is not affected by Rucaparib and TSA co-treatment in prostate cells.
- PARP-1, IKK α and NF- κ B p65 protein expression is reduced in DU145 and PC3 cells exposed to Rucaparib and TSA co-treatment.

4.6 Future work

Future work could be to assess PARP-1 activity in DU145 cells to confirm that an increased sensitivity to Rucaparib is due to reduced NF- κ B signalling rather than reduced PARP-1 levels. It would also be useful to look at protein localisation by immunofluorescence in cells exposed to treatments as this would confirm whether Rucaparib and TSA, alone and in combination, affect NF- κ B activity. Identification of a hormetic response by WST-1 assay in DU145 and PC3 cells

exposed to low doses of Rucaparib (section 4.3.1) highlighted a need for further investigation into the effects of Rucaparib on cancer cell metabolism and bioenergetics. Further investigation could include use of the Agilent Seahorse platform to directly measure live cell metabolic pathways in response to treatments. This system would enable identification of the metabolic pathway that the tumour cells are relying on and what effects Rucaparib are having on the pathway. To strengthen the nuclear and cellular morphology data assays could be carried out to confirm the mode of cell death that is induced following exposure to Rucaparib and TSA, alone and in combination. For example, the Caspase-Glo assay system from Promega measures the activity of caspase 3 and 7 could be carried out to confirm cell death by apoptosis. Other commercial kits are also available to measure cell apoptosis and necrosis such as Apoptosis/necrosis assay kit from Abcam; this system simultaneously detects cell apoptosis, necrosis and healthy cells by flow cytometry or fluorescence microscopy.

Chapter Five

Investigating the effects of PARP-1 and HDAC-1 inhibitors on cell migration in prostate cells with varied maspin expression.

5.1 Introduction

5.1.1 Cell migration

Cell migration is the directed movement of cells and is fundamental to the development and maintenance of multicellular organisms. Dysregulated cell migration contributes to pathologies such as tumour development and metastasis (Trepatt et al., 2012). Acquisition of invasive phenotypes such as a loss of cell-cell adhesion promotes the migration of tumours from their initial site of tumour growth to surrounding tissues and distant sites (Yilmaz and Christofori, 2010).

The main cause of death in cancer patients is organ failure due to uncontrolled tumour progression and metastasis. Metastatic tumour cells invade healthy tissues and distant organs, starving them of the nutrients and space required for normal function (Seyfried and Huysentruyt, 2013). Assessment of cell migration and the development of drugs which target migration are of paramount importance in cancer research. Inhibition of cell migration has the potential to limit cell metastasis; holding promise for a viable alternative means of therapy (Palmer et al., 2011). Various molecules play a role in the regulation of cell migration such as chemokines, cytokines, integrins and growth factors (Ilina and Friedl, 2009). Maspin is a known endogenous inhibitor of cell migration and is often downregulated in cancers (Maass et al. (2001), Ravenhill et al. (2010)). To this end, the development of treatments to induce re-expression of these molecules may limit cell migration and improve disease outcome.

5.1.2 Assessment of cell migration in the presence and absence of Rucaparib and TSA.

The traditional way to assess cell migration is by scratch assay. It is a simple, low cost technique that allows the observation of 2D cell migration in confluent cell cultures (Liang et al., 2007); however, the method is time consuming and relies on a large amount of cells. It is also difficult

to standardise this method and there are potential issues around effects of debris from damaged cells (Cormier et al., 2015). The xCELLigence cell analyser platform quantitatively measures cell migration in real-time. It is a non-invasive assay requiring limited quantities of cell culture.

This chapter ascertains the effects of Rucaparib and TSA treatment, alone and in combination, on the migration of prostate cell models using two different techniques. The xCELLigence real time cell analyser system was used in addition to a traditional scratch assay technique with time lapse microscopy.

5.2 Chapter aims

It is hypothesised that Rucaparib and TSA co-treatment will reduce cell migration in cancerous cell lines lacking maspin by reducing IKKa. It is expected that DU145 cells will have higher migration potential due to maspin depletion and increased IKKa. The aims of this chapter are detailed below:

- To examine the effects of Rucaparib and TSA treatment, alone and in combination, on migration in PNT1A, DU145 and PC3 cells.
- To investigate how the presence of maspin affects the migration of cells when exposed to Rucaparib and TSA treatments, alone and in combination.

5.3 Results

5.3.1 Real-time effects of Rucaparib and TSA treatment, alone and in combination, on prostate cell migration.

The xCELLigence analyser measured prostate cancer cell migration exposed to treatments for 72 hours. Briefly, cells were seeded into a specialised xCELLigence CIM-Plate as outlined in section 2.2.9.1. Following an overnight incubation period, drugs were applied to the wells containing cells and cell impedance, representative of cell migration, was measured in real-time over a 72-hour period. Cell impedance increased over the duration of the experiment in both cell lines. PC3 cells were less migratory than DU145 cells at all time points in all treatment conditions (Figure 5.1A and B).

DU145 cell migration was reduced by all treatment conditions, particularly cells exposed to Rucaparib as a single agent. There was no difference in DU145 cells exposed to TSA and co-treatment at any time point (Figure 5.1A and C). The migration of PC3 cells was reduced in all treatment conditions. Rucaparib had the greatest effect on cell migration compared to TSA. PC3 cell migration was further reduced following exposure to co-treatment (Figure 5.1B and D).

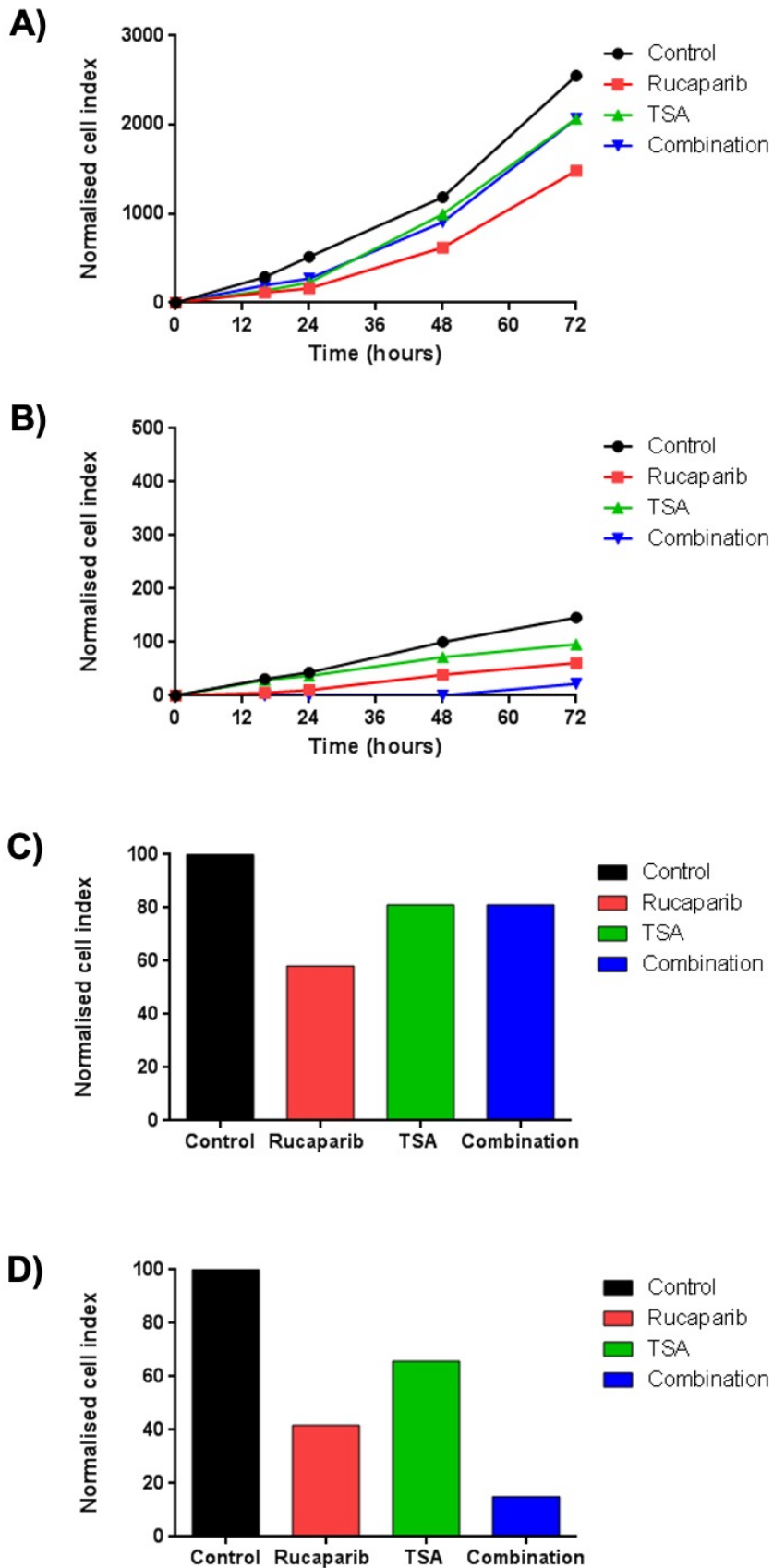


Figure 5.1: Real-time analysis of prostate cell migration in response to Rucaparib and TSA, alone and in combination, using the xCELLigence system.

(A) DU145 and (B) PC3 prostate cell lines were exposed to Rucaparib and TSA, alone and in combination at their GI50 concentrations for 72 hours. The migration of (C) DU145 and (D) PC3 cells following exposure to treatments for 72 hours was compared against untreated controls. Data is representative of a single experiment.

5.3.2 The effects of Rucaparib and TSA treatment, alone and in combination, on prostate cell migration by scratch assay

Scratch assays were carried out in addition to xCELLigence experiments to enable visual assessment of cell migration over time. As outlined in section 2.2.8, cells were seeded into sterile tissue culture plates and incubated overnight to allow cell adherence. The following day a scratch was applied through the centre of each well containing cells and drugs were applied at their respective GI₅₀ concentrations in 1% DMSO, alone and in combination. Cell migration was assessed for 72 hours, at 24-hour intervals, by microscopy. Image J densitometry was used to quantify and compare scratch closure between each treatment condition.

PNT1A cell migration was not affected by treatment conditions in the first 24 hours of the assay. At 48 hours, cells migration was increased in response to Rucaparib and TSA as single agents, compared to control. At 72 hours, cell migration had increased in all treatment conditions but there was no difference in the migration of cells exposed to treatments compared to control, indicating that the drugs did not affect PNT1A cell migration at 72 hours (Figure 5.2A). Scratch wounds incubated for 72 hours were semi-quantified (Figure 5.2B); confirming that the difference in cell migration between untreated and treated cells was insignificant.

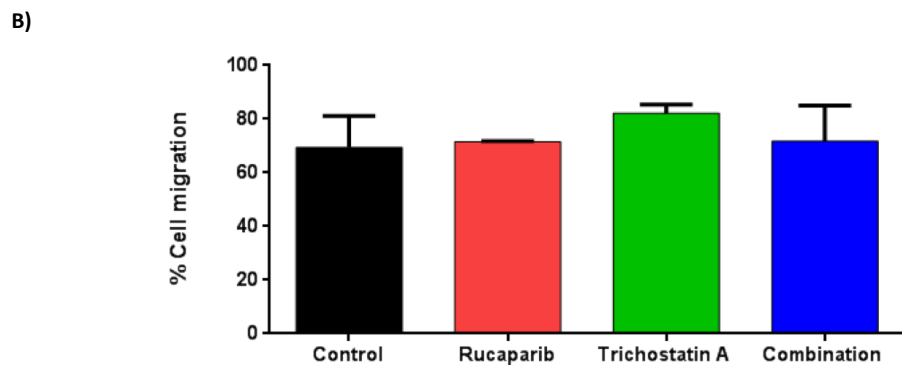
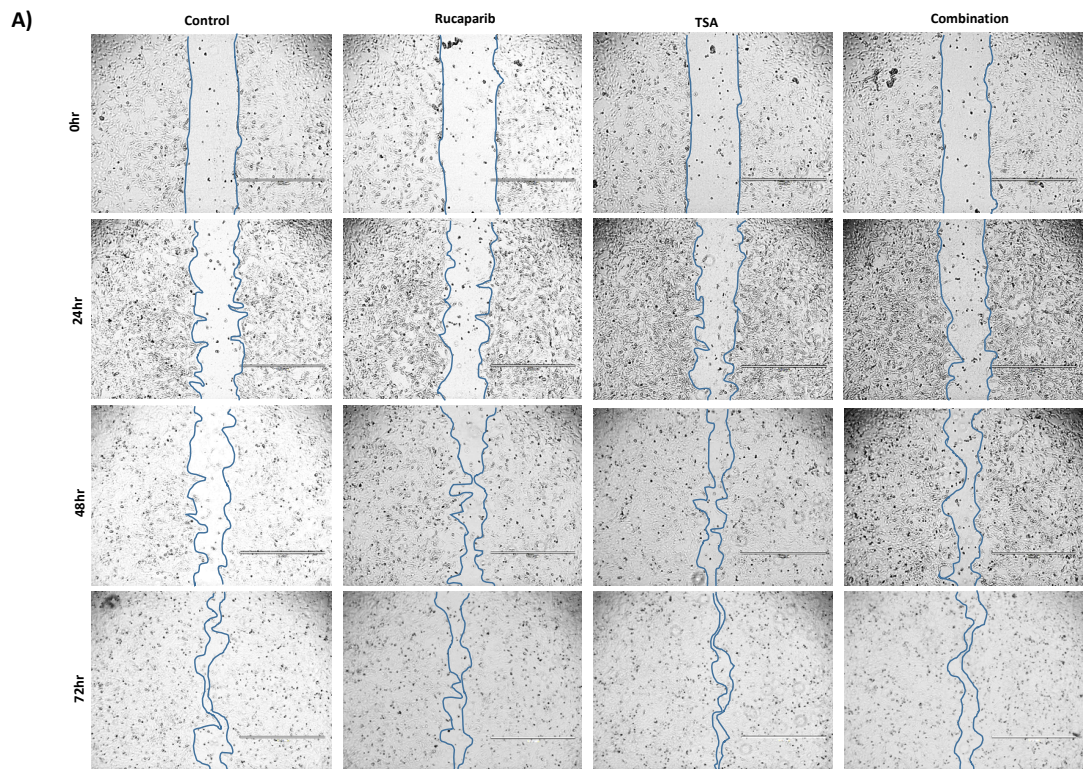


Figure 5.2: Assessment of PNT1A cell migration by scratch wound healing assay in the absence or the presence of Rucaparib and TSA, alone and in combination.

Cells were exposed to Rucaparib and TSA, alone and in combination at their GI_{50} concentrations. (A) Migration and wound closure were assessed against untreated controls at 24-hour intervals, for 72 hours. The presented images are representative of three independent experiments and solid blue lines indicate wound borders. Images were captured at a 10X magnification. Scale bar= $1000\mu\text{m}$. (B) Percentage cell migration following 72hours drug treatment. Wound closure at 72 hours following treatment was quantified using ImageJ densitometry software. Untreated cells were used as a control. Bars represent the mean of three independent experiments \pm SEM.

DU145 cells gradually migrated over a 72-hour time period in all treatment conditions (Figure 5.3A). Rucaparib did not affect cell migration at 48- or 72-hour time points. At 48 hours, TSA limited cell migration and this response was further enhanced with co-treatment. All treatments did not significantly affect cell migration at 72 hours (Figure 5.3B).

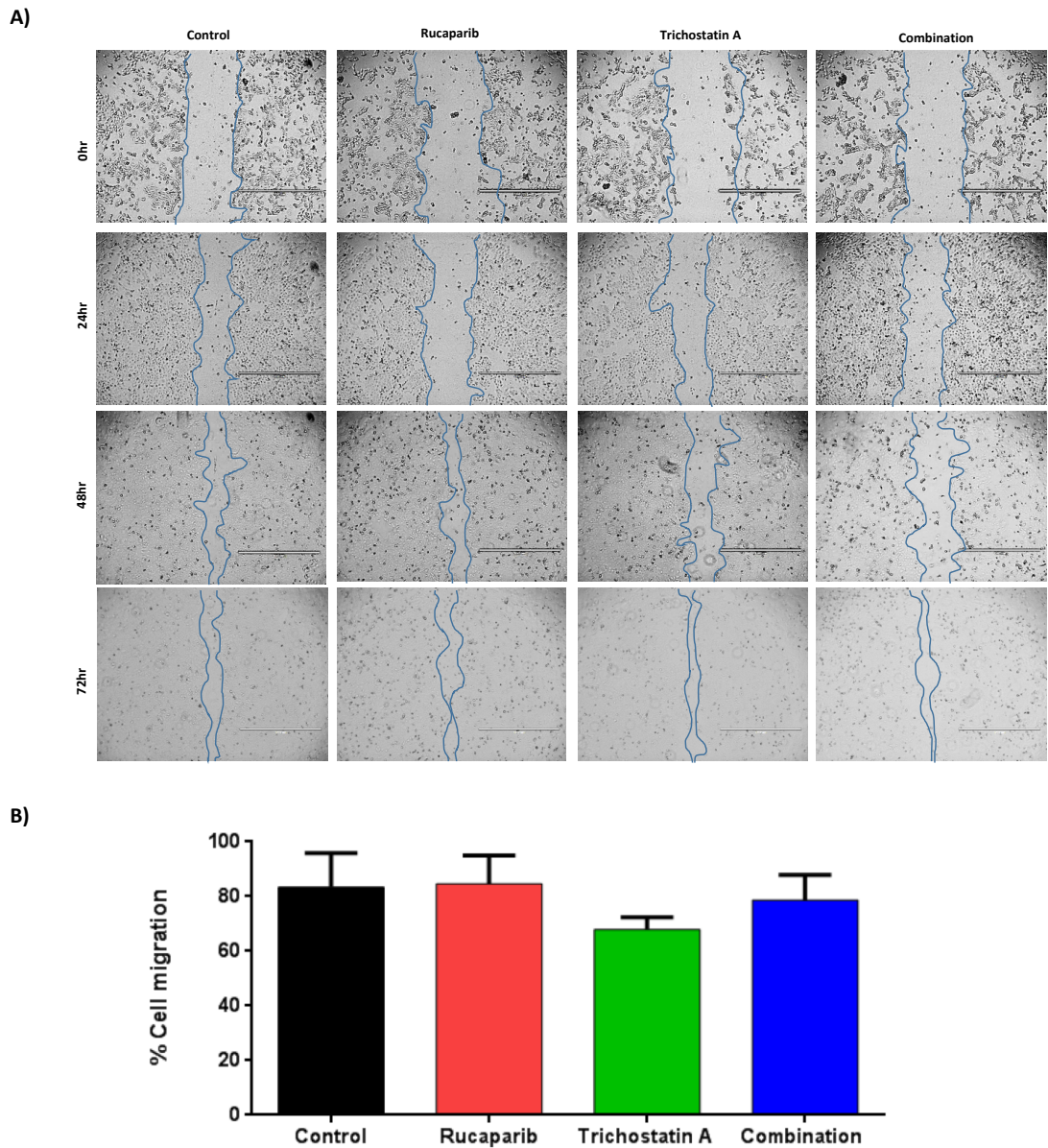


Figure 5.3: Assessment of DU145 cell migration by scratch wound healing assay in the absence or the presence of Rucaparib and TSA, alone and in combination.

Cells were exposed to Rucaparib and TSA, alone and in combination at their GI_{50} concentrations. **(A)** Migration and wound closure were assessed against untreated controls at 24-hour intervals, for 72 hours. The presented images are representative of three independent experiments and solid blue lines indicate wound borders. Images were captured at a 10X magnification. Scale bar= $1000\mu\text{m}$. **(B)** Percentage cell migration following 72hours drug treatment. Wound closure at 72 hours following treatment was quantified using ImageJ densitometry software. Untreated cells were used as a control. Bars represent the mean of three independent experiments \pm SEM.

TSA and combination treatment were inhibitory to PC3 cell migration at 48 and 72 hours, compared to control, but Rucaparib was most inhibitory to cell migration at 48 and 72 hours (Figure 5.4A). Semi-quantification of Scratch wounds exposed to treatments for 72-hours (Figure

5.4B) showed a 1.5,1.3 and 1.3 -fold reduction in cell migration following exposure to Rucaparib, TSA and co-treatment, respectively. The effect of Rucaparib on the inhibition of cell migration was significant ($P \leq 0.05$).

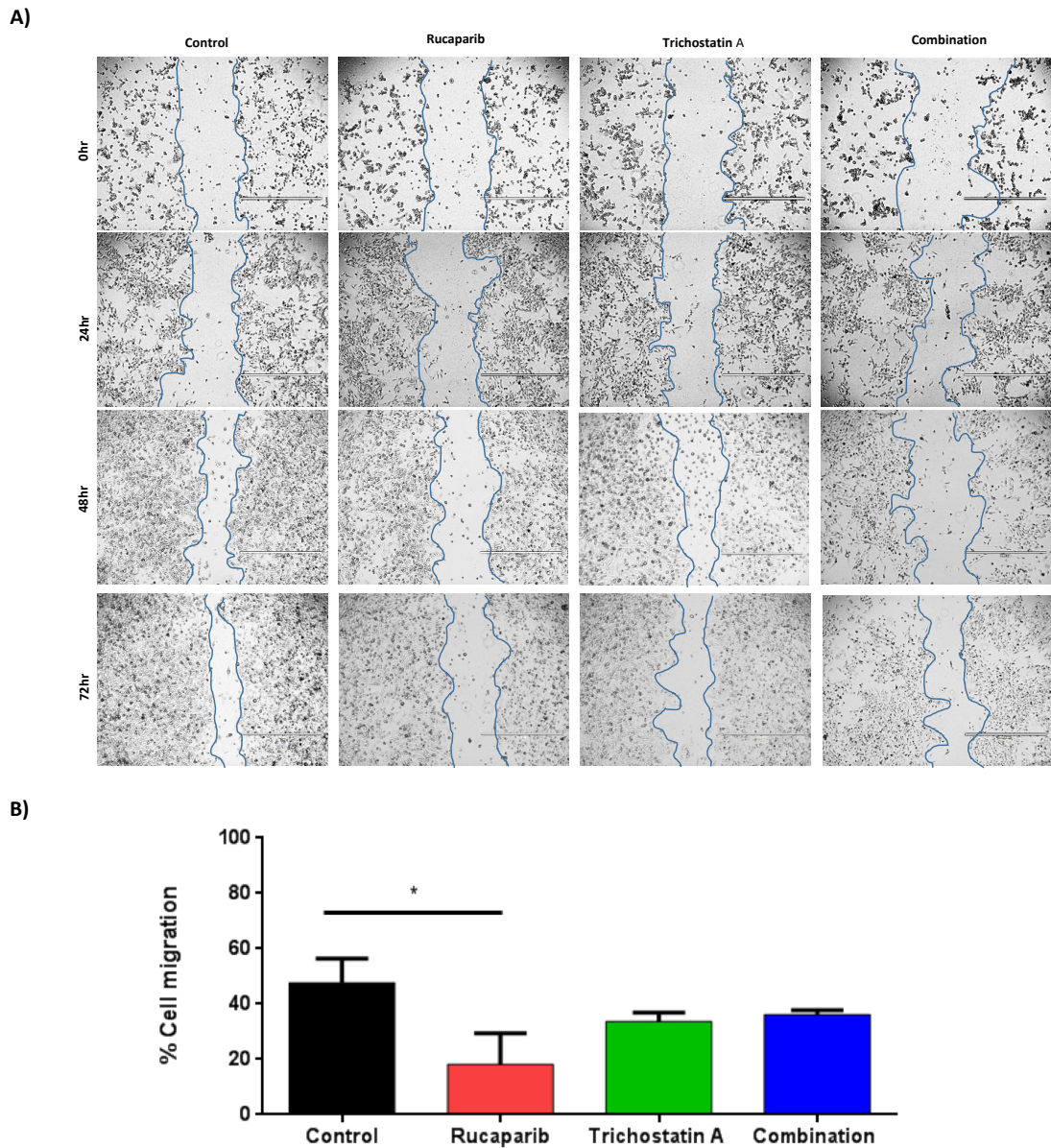


Figure 5.4: Assessment of PC3 cell migration by scratch wound healing assay in the absence or the presence of Rucaparib and TSA, alone and in combination.

Cells were exposed to Rucaparib and TSA, alone and in combination at their GI_{50} concentrations. **(A)** Migration and wound closure were assessed against untreated controls at 24-hour intervals, for 72 hours. The presented images are representative of three independent experiments and solid blue lines indicate wound borders. Images were captured at a 10X magnification. Scale bar= $1000\mu m$. **(B)** Percentage cell migration following 72hours drug treatment. Wound closure at 72 hours following treatment was quantified using ImageJ densitometry software. Untreated cells were used as a control. Bars represent the mean of three independent experiments \pm SEM.

Semi-quantified scratch migration data for each treatment condition was compared across each cell line to identify differences in treatment response. Data is presented in Figure 5.5 and results are expressed as percentage of untreated controls.

After 72-hour treatment with Rucaparib, the migration of PC3 cells was significantly less than the migration of PNT1A and DU145 cells ($P \leq 0.05$). Cell migration of both DU145 and PC3 cells was significantly less than the migration of PNT1A cells following TSA treatment. There was no significant difference in the effect of co-treatment on prostate cell migration. Collectively these data show that migration of PNT1A cells is unaffected by treatment, TSA affects DU145 and PC3 cell migration whilst Rucaparib affects PC3 cell migration only.

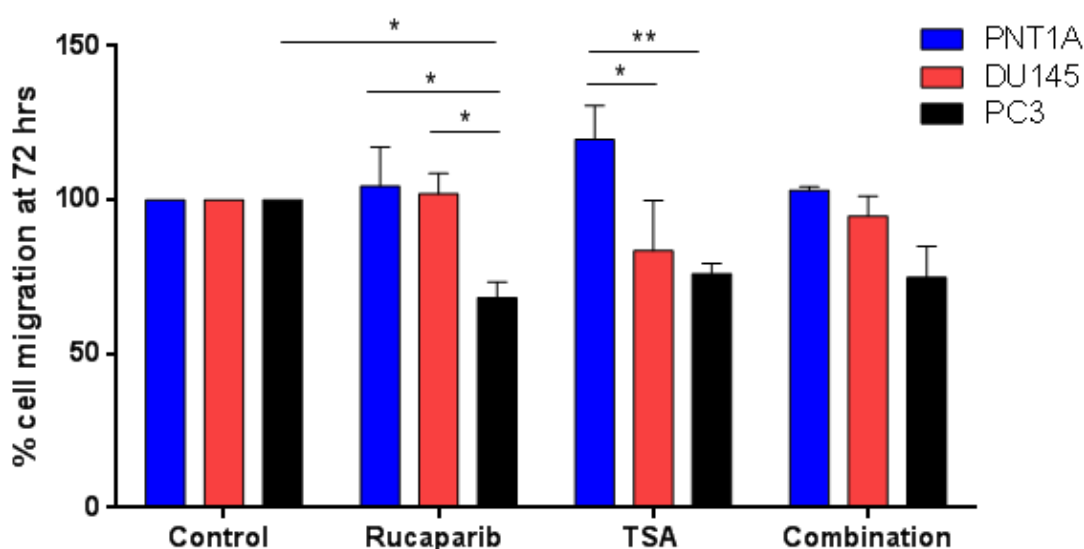


Figure 5.5: Comparison of prostate cell migration in response to Rucaparib and Trichostatin A treatment, alone and in combination.

Cell migration after 72 hours was quantified using ImageJ densitometry software. Data is expressed as % cell migration against untreated controls. Results are representative of at least two independent experiments \pm SEM.

5.3.3 The effects of maspin knockdown with siRNA on PC3 cell migration.

Results presented in 5.3.1 and 5.3.2 support the role of maspin as an inhibitor of cell migration.

To this end, the change in the migration of PC3 cells transfected with maspin siRNA sequences was investigated over a 96-hour period using xCELLigence technology. The results presented in

Figure 5.6 are from a single experiment but this preliminary data highlights an increase in PC3 cell migration, over time, following knockdown of maspin. PC3 cells transfected with maspin siRNA sequence #1 were most migratory but increased cell migration was also apparent in cells transfected with maspin siRNA sequence #2.

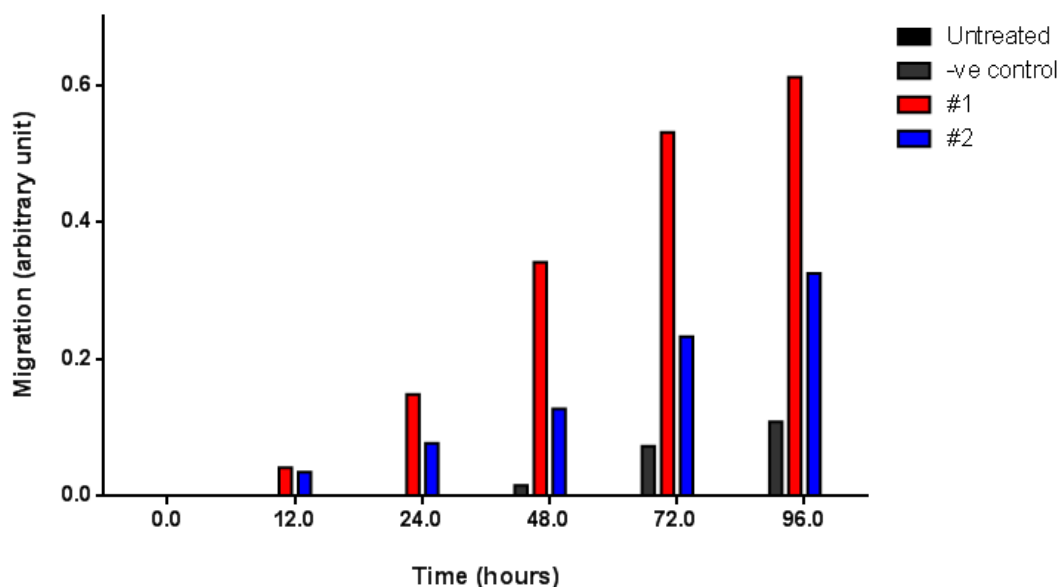


Figure 5.6: The effects of maspin siRNA on PC3 cell migration.

The migration of PC3 cells in the presence or absence of maspin siRNA was measured by xCELLigence over a 92-hour period.

5.4 Discussion

Migration experiments were carried out to confirm differences in cell migration between cancer cell lines of varied maspin status, and to explore the effects of PARP and HDAC inhibition on the migration of these cell lines. Maspin depleted DU145 cells were significantly more migratory than PC3 cells in both xCELLigence and scratch experiments. DU145 cells should be less migratory as they have less metastatic potential than PC3 cells (Ravenna et al., 2014). The metastatic potential of DU145 cells does not correlate with cell migration and maspin expression levels.

Normal prostate epithelial PNT1A cells were less migratory than DU145 cells but more migratory than PC3 cells. These findings correspond to maspin expression levels and support the role of maspin as an inhibitor of migration and invasion. Sheng et al. (1996) were the first to demonstrate the role of maspin as an inhibitor of cell invasion by blocking cell motility. They reported reduced

invasion and motility in breast and prostate cancer cells following treatment with recombinant maspin; concluding that the mechanism of action could be due to the protease inhibitory activity of maspin. A later study also demonstrated the inhibitory effect of maspin on vascular smooth muscle cell and cancer cell migration. However, they showed that the activity of maspin was independent of protease inhibition (Bass et al., 2002). The inhibitory effect of maspin on cell migration was later found to be due to binding of $\beta 1$ integrins on the cell surface (Bass et al., 2009).

Increased cell migration in PC3 cells transfected with maspin siRNA confirm that maspin acts as a tumour suppressor by inhibiting cell migration; an enabling characteristic of tumour development. Cell migration was increased 23-fold and 8.5-fold following a 48-hour exposure to maspin #1 and #2 siRNA, respectively. At 92 hours migration was increased 5.6-fold and 3-fold in the presence of maspin #1 and #2 siRNA. Other studies have also reported a role for maspin as an inhibitor of cell migration in prostate cancers. For example, stable cell lines expressing maspin derived from a prostate tumour model showed decreased metastatic potential and increased adhesion to the extracellular matrix; a negative regulator of tumour migration and invasion (Abraham et al., 2003). More recent studies have demonstrated that maspin inhibits cell migration via its G-helix; which binds to $\beta 1$ integrins on the cell surface (Ravenhill et al., 2010). The group also reported a 40% increase in PC3 cell migration following maspin silencing by siRNA; supporting a role for maspin in tumour progression.

xCELLigence studies demonstrated reduced cell migration in both DU145 and PC3 cells following treatment with Rucaparib. At 72 hours, the effect was greatest in PC3 cells compared to untreated controls. The effects of Rucaparib on cell migration were not in line with growth inhibition studies whereby DU145 cells were most sensitive to Rucaparib. Although the effects of Rucaparib being greater in PC3 cells was unexpected, the cells lines tested were not isogenic and variances in the expression of various proteins may have impacted this. Scratch assay experiments also demonstrated reduced PC3 cell migration following exposure to Rucaparib for 72 hours, however, Rucaparib had no significant effect on the migration of DU145 cells compared to untreated control. Rucaparib did not inhibit the migration of PNT1A cells at a GI_{50} drug

concentration. These data highlight a clear selective effect of Rucaparib in cancer cells in terms of cell migration. The protein expression data presented in Chapter Four, Figure 4.17 and Figure 4.18 show that maspin protein expression is unaffected by Rucaparib in tumour cells, indicating that the effects of Rucaparib on cell migration occurs *via* a mechanism independent to maspin. A proposed mechanism by which Rucaparib could be reducing migration is through the modulation of β -catenin; a key regulator of cell migration (Yang et al., 2017). The PARP inhibitor PJ34 has been shown to inhibit β -catenin signalling and limit cell migration in cervical cancers (Mann et al., 2019).

PARP-1 inhibition has been shown to limit cell migration through the modulation of other epithelial-mesenchymal transition (EMT) transcription factors such as E-cadherin and Vimentin. Endothelial and metastatic melanoma cells exposed to PARP inhibitors expressed increased levels of E-cadherin, a marker associated with reduced cell motility and invasion. PARP inhibition was found to reduce the expression of Vimentin, a marker that is over-expressed in tumours and is associated with malignant transformation (Rodriguez et al., 2013). As PARP-1 is a known co-activator of NF- κ B, it would not be unreasonable to suggest that the effects of PARP inhibition on cancer cell migration may be due to down-regulation of NF- κ B, and in-turn reversal of EMT. Positive correlations between EMT transcription factors and NF- κ B activation have been reported in several human cancers (Huber et al., 2004, Cheng et al., 2011, Taki et al., 2018). A prostate cancer study demonstrated that Transforming Growth Factor Beta (TGF- β) induced EMT was mediated by NF- κ B signalling which promotes an invasive and metastatic phenotype. Chemical inhibition of NF- κ B limited the invasive capability and expression of Vimentin in these cells, leading to reversal of EMT (Zhang et al., 2009). Breast cancer studies also reported decreased cell motility and EMT following inhibition of NF- κ B (Pires et al., 2017).

TSA treatment was inhibitory to DU145 and PC3 cell migration, but not to PNT1A cells; demonstrating a selective effect in tumour cells. This finding supports that normal cells are resistant to HDACi compared with tumour cells (Abbas and Gupta, 2008). xCELLigence studies revealed a greater effect of TSA on the inhibition of PC3 cell migration, compared to DU145 cells. Results obtained from scratch assay showed a reduction in cell migration in DU145 and

PC3 cells exposed to TSA for 72 hours, compared to control, but these results were not statistically significant. The protein expression data presented in chapter four revealed a reduction in maspin expression following TSA treatment in PNT1A and DU145 cells but not in PC3 cells, supporting the role of HDAC inhibitors as inhibitors of migration in a mechanism dependent on maspin. Reduced PC3 cell migration in the presence of TSA may be additive to the inhibitory effects of maspin on HDAC. The reason for a reduction in maspin expression following TSA treatment in PNT1A cells is unknown but may explain why TSA fails to limit cell migration in these cells. Response to TSA is cell line and target specific and it could be postulated that reduced maspin expression in PNT1A cells exposed to TSA is a result of epigenetic modification and increased histone acetylation, leading to alterations in the expression of genes. Further exploration is required to elucidate mechanisms that contribute to the differential effects of HDAC inhibition on cell migration.

There are contradictory reports on the effects of HDAC inhibition on cell migration, some which are in line with our findings and some which are not. Increased cell migration has been reported in a variety of tumours, such as those derived from the breast and lung, following treatment with HDAC inhibitors (Lin et al., 2012). Low and non-cytotoxic doses were used, allowing the conclusion that increased migration was a result of epigenetic activation of tumour-suppressive genes in HDACi treated cells, rather than the selection of cells that survived HDAC inhibitor toxicity. Combined treatment of HDAC inhibitors with other agents including protein kinase inhibitors suppressed HDACi-activated tumour progressive proteins, cell migration and tumour growth. Elsewhere, the effects of HDAC inhibitors on prostate cancer cell migration and invasion were investigated. In support of our findings, inhibition of HDAC reduced cell migration and increased the expression of E-cadherin (Kim et al., 2011).

Maspin has been associated with EMT markers such as E-cadherin. It has been shown that E-cadherin was up-regulated, alongside enhanced cell-cell migration and adhesion, in maspin-transfected MCF-7 breast cancer cells compared to controls (Ravenhill et al., 2010). This response was not reported in cells transfected with mutated maspin, suggesting that the G-helix of maspin was involved in the mechanisms in which E-cadherin expression was altered by maspin, and the

inhibitory actions of maspin on cell migration was dependent on a functional G-helix. To this end, the enhanced effects of PARP-1 and HDAC-1 inhibition on cell migration may reverse EMT via maspin and this may explain why response was 0.3-fold and 4.8-fold higher in PC3 cells expressing increased levels of maspin in scratch and xCELLigence experiments, respectively, compared to DU145 cells.

Several studies also report the effects of HDAC inhibitors on the activity of NF- κ B. For example, colon cancer cells exposed to the HDAC inhibitors Butyrate and TSA showed reduced proteasome activity and presented limited proteasome dependent degradation of I κ B α and NF- κ B activation (Place et al., 2005). Others have reported increased inflammatory signalling and activation of NF- κ B following HDAC inhibition. For example, the HDAC inhibitors MS-275 and suberoylanilide hydroxamic acid (SAHA) were found to induce NF- κ B activation via hyperacetylation of NF- κ B p65 in the cell nucleus of leukaemia cells (Dai et al., 2005). Active NF- κ B is a known driver of inflammatory signalling which promotes cancer cell migration, invasion and metastasis. Our data supports the studies of others which suggest that HDAC inhibition limits activation of NF- κ B. Data also provides rationale for the potential role of TSA as an inhibitor of cancer cell migration via suppression of NF- κ B activation. Protein expression data presented in Chapter 4 also supports this finding, highlighting reduced expression of IKK α , an activator of NF- κ B, in cancer cell lines following TSA treatment.

In view of these findings along with previous growth inhibition studies, the combined effects of HDAC and PARP-1 inhibitors on cancer cell migration were explored. The xCELLigence data highlighted a reduction in the migration of PC3 cells exposed to co-treatment, compared to single agents. The inhibition of DU145 cell migration was not enhanced by TSA and Rucaparib co-treatment compared to either treatment alone, indicating that the effects of co-treatment on cell migration are cell type specific. Protein expression data of co-treated cell samples presented in Chapter four highlighted a decrease in the protein expression levels of maspin following co-treatment in all cell lines, and a decrease in the expression of IKK α in PC3 cells. These findings suggest that Rucaparib and TSA co-treatment may inhibit NF- κ B, but such response is cell type specific. The enhanced inhibitory effects of co-treatment on PC3 cell migration are independent

to the presence of maspin but may be due to reduced expression of IKK α . Scratch assay data revealed no significant effect on cell migration following co-treatment in any of the cell lines, compared to agents alone.

Variation in results between methods are likely due to the different ways in which migration was measured between experiments. The xCELLigence method was reliant on directional cell impedance towards a chemotactic gradient to enable quantitative kinetic measurement of migration. This method requires regulated formation of lamellipodia, whereas assessment of cell migration by scratch assay is random (Petrie et al., 2009). The scratch data obtained from xCELLigence studies were from a single experiment due to the expense of materials and further experiments are required to confirm validity and reproducibility. Scratch assays are a cost effective and straightforward way to assess migration but are reliant on visual evaluation of cells and lack reproducibility. The method introduces injury to the cell, leading to cell debris and release of cellular contents into the wound area which may affect the migration process (Grada et al., 2017). The scratch protocol could be improved by using technology such as a wound makerTM; a mechanical device designed to create homogenous wounds in cell monolayers.

To add stringency to data, migration studies need to be repeated across a range of doses. Variance in GI₅₀ drug concentrations between cell lines may have contributed to the migratory affects.

5.5 Summary

The studies presented in this chapter have shown that:

- The inhibitory effects of Rucaparib on cell migration are specific to cancer cell lines, particularly PC3 cells which express increased levels of maspin and reduced levels of IKK α .
- The inhibitory effects of TSA on cell migration were greater in PC3 cells when assessed by xCELLigence. Scratch assays showed reduced cell migration in both cancerous cell's lines exposed to TSA suggesting that response was independent to the expression of maspin and NF-kB expression.

- The inhibitory effects of co-treatment on cell migration were greatest in PC3 cell lines despite a reduction in the expression of IKK α and maspin proteins.
- The effects of treatments on cell migration are variable between techniques.

5.6 Future work

xCELLigence data is representative of a single experiment due to cost implications. To add stringency to the data further xCELLigence experiments could be carried out. Scratch assays could be developed to enhance the validity and reproducibility of data. One way to do this could be use of an automated system such as the IncuCyte cell migration kit and live-cell analysis system. The IncuCyte wound maker is a mechanical device that enables accurate assessment of cell migration/wound closure by creating consistent wounds in cell cultures without damaging the cells or the underlying plasticware. Cell migration experiments could be carried out in MEF NF-kB p65 and IKK α knockout cells in the presence and absence of Rucaparib and TSA, to confirm an effect of NF-kB on cell migration. Future migration studies could also utilise prostate cells transfected with PARP-1 and IKK α siRNA to validate potential mechanisms.

Chapter Six

Investigating the effects of PARP-1 and HDAC-1 inhibitors on DNA damage in prostate cell lines of varied maspin expression.

6.1 Introduction

DNA repair inhibitors such as PARP inhibitors increase the specificity and toxicity of traditional radio- and chemotherapeutic DNA damaging agents. As stand-alone agents, PARP inhibitors limit SSB repair in cancer cells, leading to an accumulation of genetically unstable DSBs (Curtin, 2013). As tumours progress, they accumulate defects in DNA repair proteins which make them unable to repair DNA DSBs via the primary repair mechanism that is HR. These tumours are dependent on NHEJ, a backup mechanism which repairs DNA breaks in the absence of HR at the cost of genome stability. PARP inhibitors induce synthetic lethality in HR deficient tumours via targeting of the backup pathway on which these cells are dependent on (Nickoloff et al., 2017). Synthetic lethality arises when cancer cells are selectively targeted, leading to inactivation of two genes or pathways which is lethal and results in cell death (Nijman, 2011). The observation that PARP inhibitors can be used as inducers of synthetic lethality in HR repair deficient cells originated from two pivotal studies which reported that cells deficient in BRCA genes were exquisitely sensitive to single agent PARP inhibition (Bryant et al., 2005, Farmer et al., 2005). These findings were independently reported by the two laboratories using different BRCA deficient models and classes of PARP inhibitors; implying that the sensitivity of these cells was indeed due to PARP inhibition. PARP inhibition in HR-defective cells stimulates error-prone NHEJ (described in Chapter 1, section 1.3.2.1). Promotion of NHEJ results in chromosome instability and cell death; a promising target for PARP inhibitor cancer therapy by synthetic lethality (reviewed in Sunada et al. (2018)).

HDAC inhibitors (HDACi) can induce cell death via accumulation of DNA damage, by down-regulating and impairing the function of DNA repair proteins such as RAD51, BRCA, Ku70/Ku80 and MRE11. These proteins are all implicated in the repair of DNA DSBs. RAD51 and BRCA

proteins are implicated in DNA DSB repair by HR, whereas Ku heterodimers and MRE11 are implicated in DNA repair by NHEJ, as discussed in Chapter 1, sections 1.3.2.1 and 1.3.2.2.

HDAC inhibitors prevent accumulation of RAD51 and BRCA1 DNA repair proteins to the site of DNA damage by downregulating transcription factors and inducing acetylation of histones and nonhistone proteins, leading to limited DNA repair efficiency and increased DNA damage (reviewed in Newbold et al. (2016)). HDACis may also mimic synthetic lethality in tumour cells that do not harbour *BRCA* mutation; by pharmacologically inducing an HR deficient phenotype (*BRCA*ness) and sensitising cells to the lethal effects of PARP inhibitors. To this end, a number of HDAC inhibitors have been shown to induce DNA damage in cancer cells and mimic a HR-deficient phenotype. For example, the HDAC inhibitor Vorinostat has been shown to induce DSBs in normal and cancerous cell lines. Normal cells were able to repair the DSBs and cancerous prostate and lung adenocarcinoma cells were not. The cancerous cells also presented increased levels of phosphorylated H2AX (γ H2AX), a known marker of DSBs, in the presence of Vorinostat (Lee et al., 2010). Reduced DNA repair and downregulation of the HR proteins BRCA1 and RAD51 has also been reported in breast cancer cells treated with the HDAC inhibitors Vorinostat and Panobinostat (Ha et al., 2014).

These studies postulate the potential efficacy for combining the HDACi TSA with the PARPi Rucaparib to downregulate HR and enhance DNA damage by inducing synthetic lethality in tumours that are not BRCA deficient. Studies have demonstrated additive DNA damage and inhibition of DNA repair following combined PARP-1 and HDAC-1 inhibitor treatment. Prostate cancer cells exposed to the HDACi SAHA in combination with the PARPi Olaparib showed increased DNA damage which was observed by Immunofluorescence microscopy of γ H2AX foci, a marker of DSBs. Co-treatment was also shown to downregulate HR-related protein expression (Chao and Goodman, 2014). Breast cancer studies have also demonstrated synergistic inhibition of breast cancer cell growth and DNA repair following combined PARP-1 and HDAC-1 inhibitor treatment; showing enhanced γ H2AX foci and reduced expression of the HR repair protein RAD51, particularly in *BRCA* deficient cells (Marijon et al., 2018). The effects of combined

treatments on DNA damage relative to the expression of maspin or NF- κ B have not yet been explored in tumour cells.

There are several ways to assess DNA single and double strand breaks. The gold standard method for measuring DNA SSBs is single-cell gel electrophoresis under alkaline conditions, otherwise known as the alkaline comet assay (principle and method described in section 2.2.6.1). The test is simple, requires a small cell sample and enables analysis of data at the individual cell level (Speit and Hartmann, 2006). The technique is cost effective but relies on image analysis equipment and software to enable comet visualisation; which carries a cost implication. In the absence of analysis software, comet tails may be quantified manually but this process is labour intensive, and results may be subjective.

Other techniques for the detection of SSBs include terminal deoxynucleotidyl transferase (TdT) dUTP nick-end labelling (TUNEL) assay and High-performance liquid chromatography (HPLC)-electrospray mass spectrometry (MS). The TUNEL assay detects DNA breaks via the visualisation of DNA fragmentation. It relies on the ability of the enzyme TdT to incorporate nucleotide analogues, conjugated with a fluorochrome, onto the free 3'-OH of a DNA strand, enabling visualisation of nuclei containing the fragmented DNA. The assay is limited in its sensitivity and specificity as it relies on DNA damage and cell death via the apoptosis pathway and cannot differentiate between other modes of cell death. HPLC-MS involves separation of component compounds in a sample which are then fed into a MS to determine the mass of each ion. It is a sensitive method for the detection of DNA SSBs via identification and quantification of altered nucleobases. The technique requires skilled personnel and is expensive to set up and run (Figuroa-Gonzalez and Perez-Plasencia, 2017).

The γ H2AX assay (principle and method described in section 2.2.7.1) is a sensitive marker that correlates well with DSBs (Sharma et al., 2012). Identification of γ H2AX foci by immunofluorescence microscopy is a powerful tool to examine the DNA damage produced in response to DNA damaging agents in tumour cells. H2AX molecules are rapidly phosphorylated to produce γ H2AX molecules in response to DNA DSBs. These molecules surround the DSBs

and prompt recruitment and localisation of DNA damage response proteins such as MRE11 and BRCA1 (Podhorecka et al., 2010). The technique is the most sensitive assay to detect DNA damage as it enables acquisition of qualitative and quantitative data in a short timeframe (Ivashkevich et al., 2012).

Other methods of DNA DSB detection include the neutral comet assay. Comet assays carried out in neutral pH conditions limit DNA unwinding but enable detection of DNA DSBs. Cells with increased frequency of DNA DSBs are more migratory to the anode under neutral assay conditions (Ostling and Johanson, 1984).

This chapter investigates DNA damage in prostate cells following exposure to Rucaparib and TSA treatment, alone and in combination. The alkaline comet and γ H2AX immunofluorescence techniques were utilised to detect single and double strand breaks, respectively. Expression of RAD51 protein, a marker of DSB repair by HR, was also investigated.

6.2 Chapter aims

It is hypothesised that Rucaparib and TSA co-treatment will enhance DNA damage in cancer cells via the mechanism of synthetic lethality.

The aims of this chapter are:

- To examine the effects of Rucaparib and TSA treatment, alone and in combination, on DNA SSBs in PNT1A, DU145 and PC3 cells.
- To examine the effects of Rucaparib and TSA treatment, alone and in combination, on DNA DSBs in PNT1A, DU145 and PC3 cells.
- To examine the DSB repair pathway utilised by PNT1A, DU145 and PC3 cells exposed to Rucaparib and TSA treatment, alone and in combination.

6.3 Results

6.3.1 DNA single strand break formation in prostate cells treated with Rucaparib and TSA, alone and in combination.

The alkaline comet assay, described in Chapter Two, section 2.2.6.1, was used to examine the formation of DNA single strand breaks (SSBs) in PNT1A, DU145 and PC3 cells treated with Rucaparib and TSA, alone and in combination. Briefly, cells treated with Rucaparib and TSA, alone and in combination, at their respective GI₅₀ concentrations for 72 hours were embedded in agarose on a glass microscope slide, immersed in lysis solution and then exposed to an electric current to enable migration of negatively charged DNA fragments towards the anode. The migration of the broken DNA resembles a comet and the size of the comet tail represents the number of DNA SSBs. Comet tails were visualised by confocal microscopy and then 20 cells were manually scored and classified according to their tail distribution. Data was statistically analysed to identify significant difference in sensitivity between treatment groups using the two-way ANOVA with multiple comparisons test.

Results presented in Figure 6.1 highlight increased levels of DNA SSBs in PNT1A cells following Rucaparib and TSA treatment, alone and in combination, as demonstrated by fluorescent microscopy images of comet tails (Figure 6.1A). Percentage tail distribution data (Figure 6.1B) revealed a 2.5-fold increase in class 2 comet tails following exposure to Rucaparib and TSA treatment, alone and in combination ($p < 0.0001$), and a 2.8-fold increase in class 3 comet tails in cells exposed to Rucaparib. There was no significant difference in sensitivity between Rucaparib, TSA and co-treatment (two-way ANOVA with multiple comparisons), indicating that co-treatment does not enhance DNA SSBs induced by single agents.

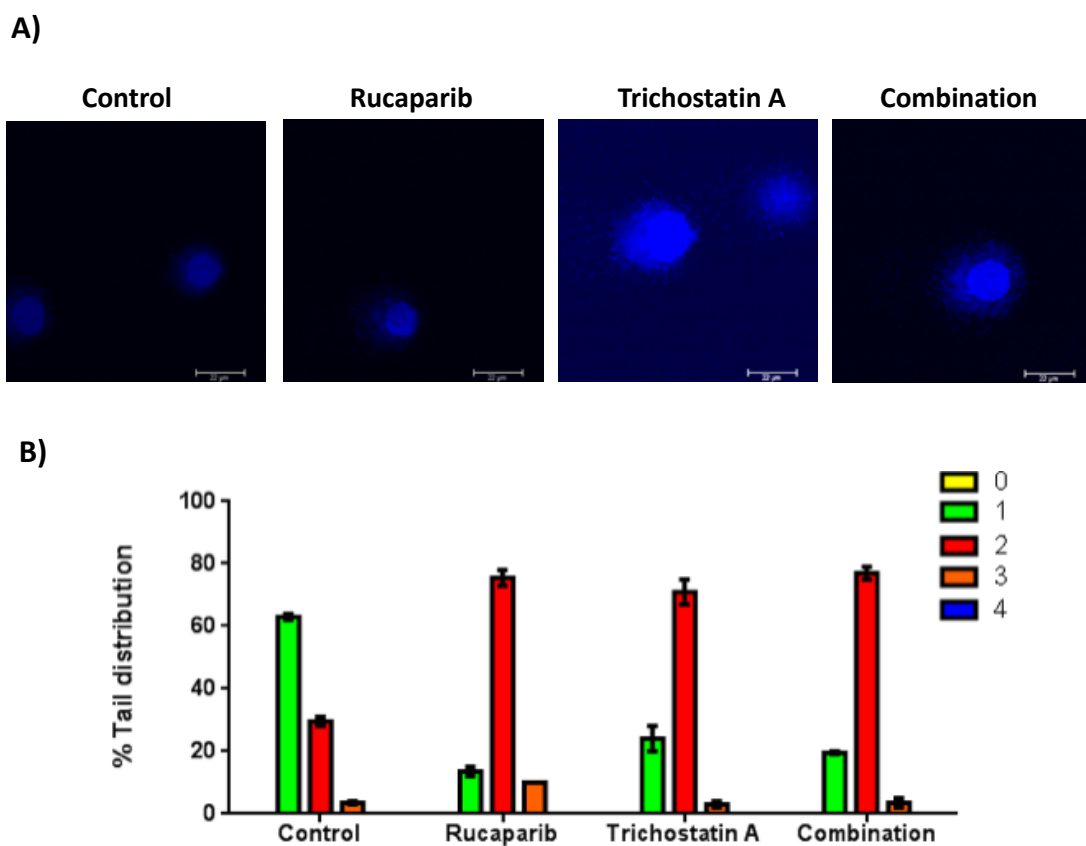


Figure 6.1: Detection of single strand DNA breaks in PNT1A cells exposed to Rucaparib and TSA, alone and in combination.

(A) Alkaline comet assay for the detection of single strand DNA breaks in PNT1A cells exposed to treatments at their GI_{50} concentrations for 72 hours. Images are representative of at least three independent experiments. Scale bar: $22\mu\text{m}$. (B) Bar graph to summarise percentage comet classes for each treatment group. Cells were assessed visually and classified 0 (undamaged) to 4 (maximally damaged), according to the size and shape of the comet tail. There is a significant increase in class 2 comet tails following treatments in comparison with control (two-way ANOVA with Tukey's multiple comparisons test, **** $p < 0.0001$), however combination treatment is not significantly more effective than Rucaparib and TSA as single agents.

The level of endogenous SSBs in DU145 cells were higher than PNT1A cells. Comet tail microscopy images presented in Figure 6.2A show increased DNA fragmentation, representative of DNA SSBs, in DU145 following Rucaparib and TSA treatment. Co-treatment increased DNA fragmentation in DU145 cells compared to Rucaparib and TSA alone, demonstrating that DU145 cells have reduced capacity to repair SSBs in the presence of co-treatment. There was a 77% and 31% increase in class 3 comet tail distribution in DU145 cells exposed to Rucaparib ($p < 0.0001$) and TSA ($p < 0.05$), respectively. Combination treatment enhanced SSBs in DU145 cells; demonstrated by a 44% increase in Class 4 comet tails ($p < 0.0001$), as shown in Figure 6.2B.

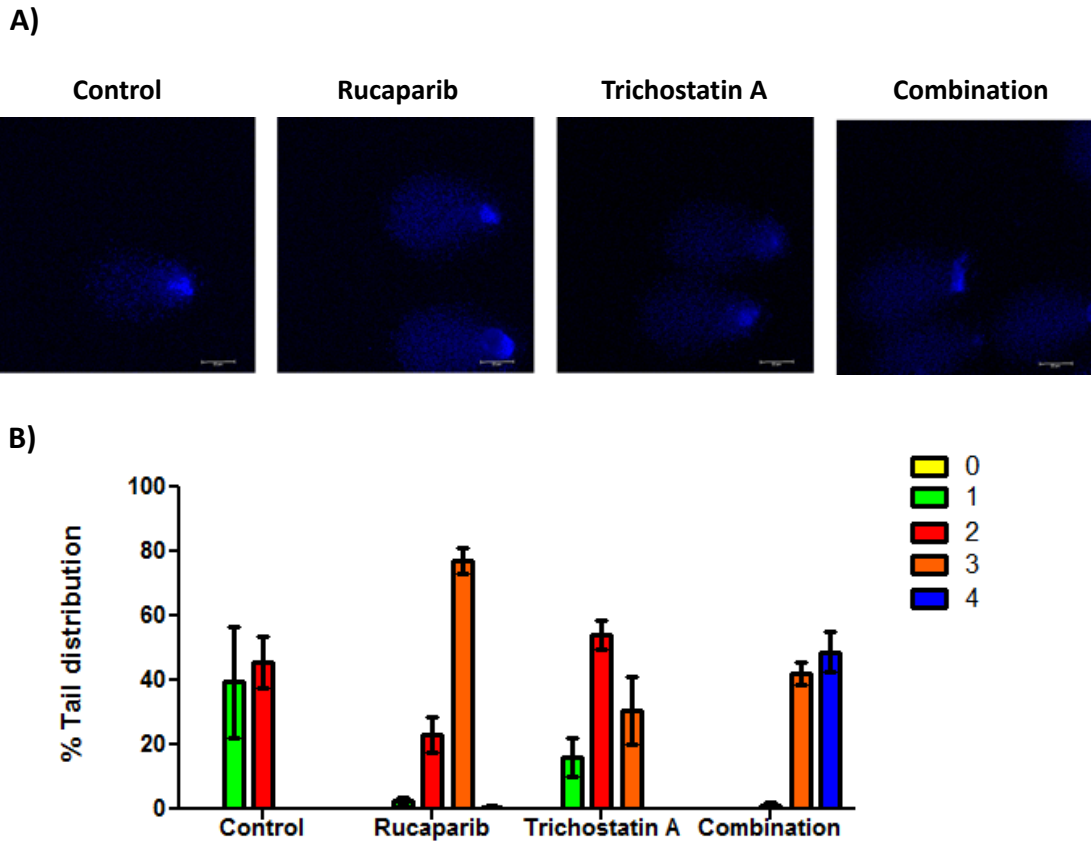


Figure 6.2: Detection of single strand DNA breaks in DU145 cells exposed to Rucaparib and TSA, alone and in combination.

(A) Alkaline comet assay for the detection of single strand DNA breaks in DU145 cells exposed to treatments at their GI_{50} concentrations for 72 hours. Images are representative of at least three independent experiments. Scale bar: $22\mu\text{m}$. (B) Bar graph to summarise percentage comet classes for each treatment group in DU145 cells. 50 cells were scored per treatment group and data is expressed as a percentage. Comet tail classification differs significantly between treatment groups ($****p<0.0001$). Cells treated with Rucaparib and TSA present higher levels of DNA breaks compared to control, however combination treatment has a significantly greater affect (two-way ANOVA with Tukey's multiple comparison test, $****p<0.0001$). (B) Bar graph to summarise percentage comet classes for each treatment group in PC3 cells. Comet tail classification differs significantly between treatment groups ($****p<0.0001$).

Rucaparib and TSA also enhanced SSBs in PC3 cells (Figure 6.3). Class 2 comet tails were 3.3-fold and 4.8-fold greater in cells exposed to Rucaparib and TSA, respectively. Class 3 comet tails were increased 3.8-fold and 2.5-fold following Rucaparib and TSA treatment, respectively. Combined treatment enhanced class 2 comet tails 1.5-fold and class 3 comet tails 5.6-fold, compared to untreated control cells (Figure 6.3B). Class 3 comet tails were increased 1.4-fold and 2.2-fold following combination treatment, compared to Rucaparib and TSA, respectively; indicating that cells exposed to combination treatment are more sensitive to single strand DNA breaks.

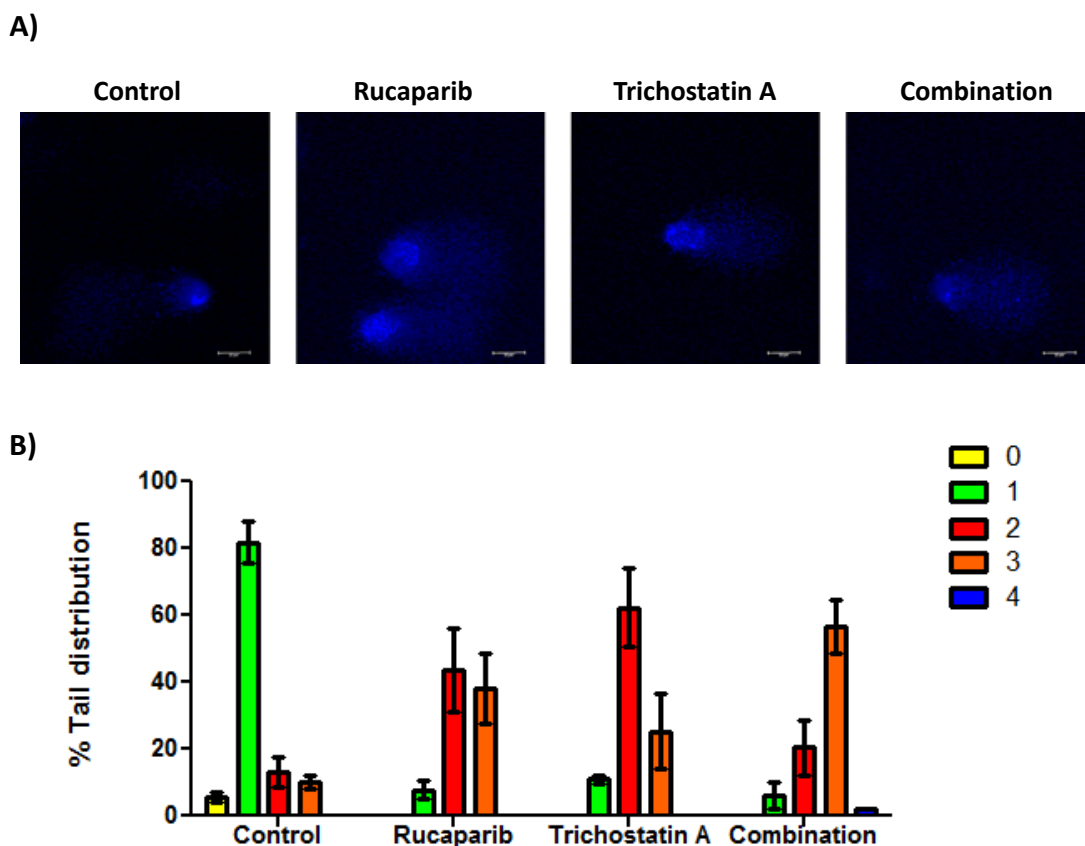


Figure 6.3: Detection of single strand DNA breaks in PC3 cells exposed to Rucaparib and TSA, alone and in combination.

(A) Alkaline comet assay for the detection of single strand DNA breaks in PC3 cells exposed to treatments at their GI_{50} concentrations for 72 hours. Images are representative of at least three independent experiments. Scale bar: $22\mu\text{m}$. (B) Bar graph to summarise percentage comet classes for each treatment group. 50 cells were scored per treatment group and data is expressed as a percentage. Comet tail classification differs significantly between treatment groups (**** $p < 0.0001$).

Comet tail classifications representative of DNA SSBs in PNT1A, DU145 and PC3 cells exposed to co-treatment, for 72 hours, were compared to determine which cells were most susceptible to SSBs (Figure 6.4). Class three comet tails were increased 14 and 18-fold in DU145 ($p < 0.01$) and PC3 ($p < 0.001$) cells exposed to treatment, compared to PNT1A cells, respectively. Class four comet tails, indicative of increased DNA damage, were increased 49 and 19-fold in DU145 and PC3 cells, compared to PNT1A cells ($p < 0.01$). These findings demonstrate increased DNA damage in DU145 and PC3 cells, as would be expected in tumour cells which are prone to genetic mutation and DNA damage. DU145 cells were significantly ($p < 0.01$) more susceptible to DNA damage following co-treatment.

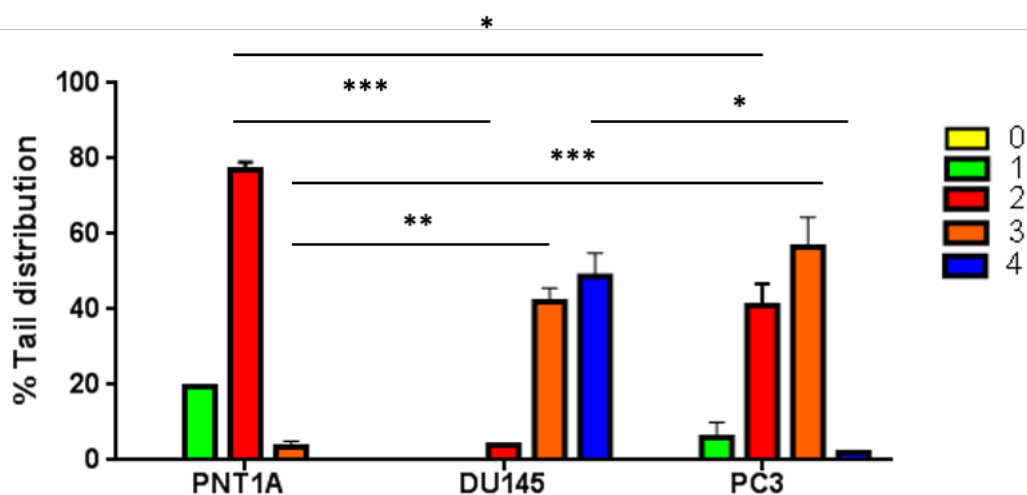


Figure 6.4: Comparison of single strand DNA breaks in prostate cells exposed to Rucaparib and TSA co-treatment.

Bar graph to summarise percentage comet classes for prostate cells exposed to co-treatment. Data is expressed as a percentage. Comet tail classification significantly differs between cell lines (* $p < 0.05$, ** $p < 0.01$, *** $p < 0.001$).

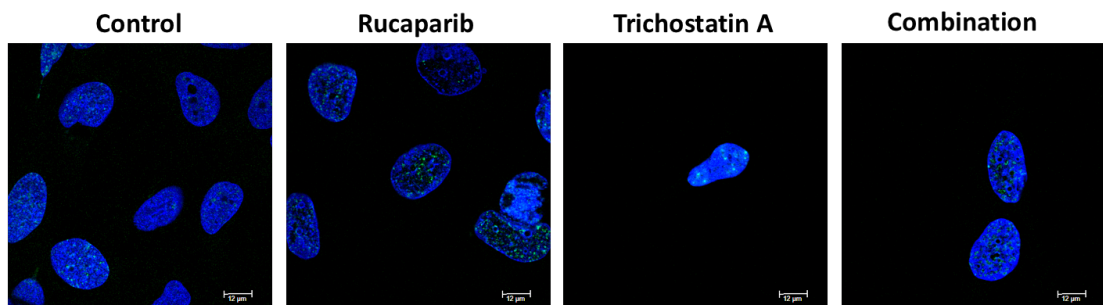
6.3.2 DNA double strand break formation in prostate cells treated with Rucaparib and TSA, alone and in combination.

To determine whether DNA double strand breaks (DSBs) accumulate following exposure to Rucaparib and TSA, DSBs were assessed using the γ H2AX immunofluorescence assay, as described in Chapter Two, section 2.2.7.1. γ H2AX foci were visualised by confocal microscopy and quantified after cells were treated with Rucaparib and TSA, alone and in combination, at their respective GI_{50} concentrations in 1% DMSO for 72 hours in culture medium. Untreated cells incubated in medium containing 1% DMSO were also quantified (negative control). Differences in sensitivity between treatment groups were statistically analysed using one-way ANOVA with multiple comparisons.

Results show an accumulation of DNA DSBs in PNT1A (Figure 6.5), DU145 (Figure 6.6) and PC3 (Figure 6.7) cells following exposure to Rucaparib, compared to their respective controls. TSA as a single agent and in combination with Rucaparib did not significantly enhance γ H2AX foci, compared to Rucaparib alone. DNA DSBs were increased in PNT1A cells and not increased in DU145 and PC3 cells exposed to TSA, compared to untreated control. The results demonstrate that cells were more susceptible to DNA damage when exposed to Rucaparib as a single agent.

PNT1A cells exposed to Rucaparib (28 μ M) for 72-hours presented 2.5-fold more DSBs ($p < 0.0001$) than untreated control cells (Figure 6.5B) and this was apparent in the fluorescent microscopy images presented in Figure 6.5A which highlight increased expression of γ H2AX foci within the cell nucleus (green dots). The levels of γ H2AX foci present in PNT1A cells exposed to TSA (188nM) were increased compared untreated control but this was not significant. γ H2AX foci were increased 2.1-fold in PNT1A cells exposed to Rucaparib and TSA in combination, compared to control. Rucaparib induced more DSBs in PNT1A cells as a single agent than in combination with TSA. This point is also visually apparent in the microscopy images presented in Figure 6.5.

A)



B)

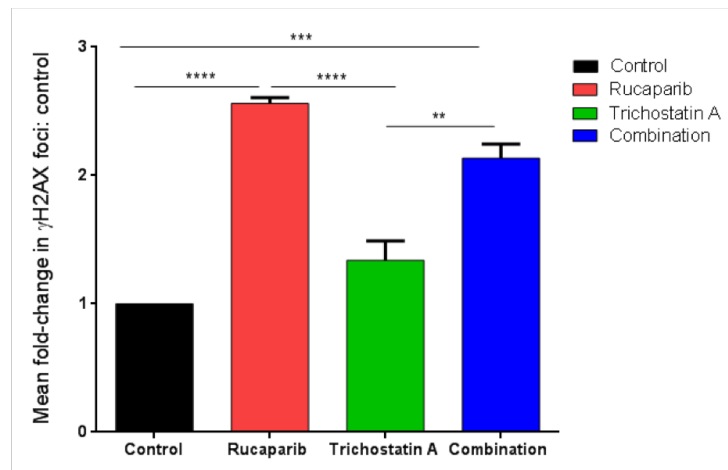
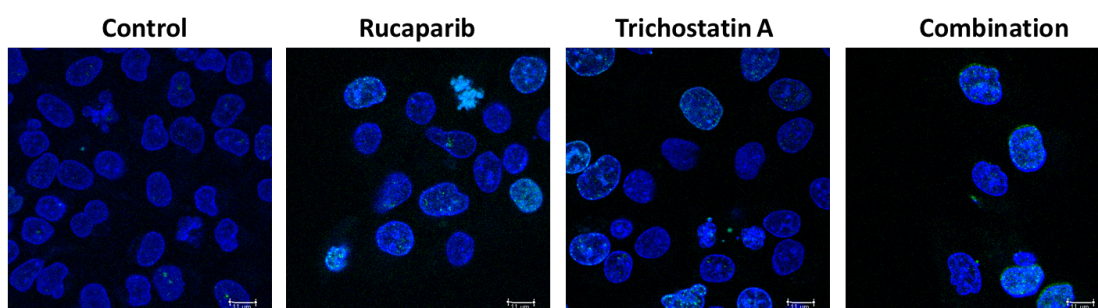


Figure 6.5: Detection of double strand DNA breaks by γ H2AX immunofluorescence assay in PNT1A cells exposed to Rucaparib and TSA, alone and in combination.

(A) Microscopy images to enable visual identification of γ H2AX foci in PNT1A cells exposed to Rucaparib and TSA for 72 hours. Images are representative of three independent experiments. Scale bar: 12 μ m. (B) Bar graph to show mean fold change in γ H2AX foci for each treatment group. γ H2AX foci were quantified in the nucleus of 20 cells per treatment group. (** $p < 0.01$, *** $p < 0.001$, **** $p < 0.0001$).

DU145 cells exposed to Rucaparib (8 μ M) for 72-hours presented 2-fold more DSBs (Figure 6.6B). than untreated control cells ($p < 0.01$). This is apparent in the fluorescent microscopy images presented in Figure 6.6A which highlight increased expression of γ H2AX foci within the nucleus of cells treated with Rucaparib, compared to control. As represented in Figure 6.6A there was a visible increase in γ H2AX foci in cells treated with TSA (45nM), however, quantitative analysis revealed no significant difference in foci between untreated cells and those exposed to TSA (Figure 6.6B). Rucaparib and TSA in combination did not significantly increase γ H2AX foci compared to Rucaparib as a single agent.

A)



B)

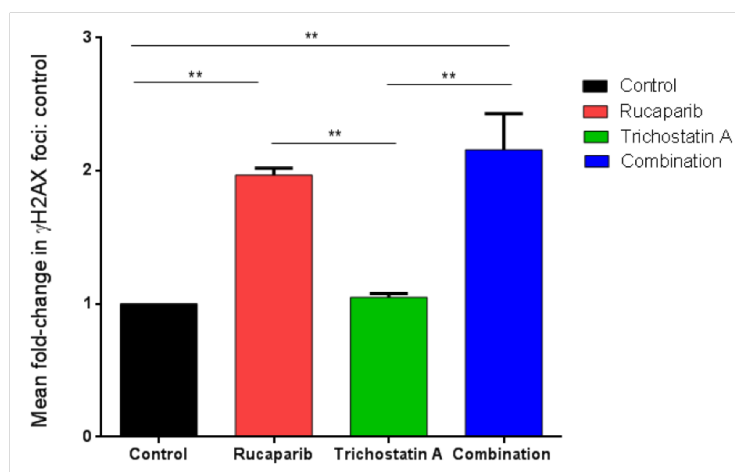


Figure 6.6: Detection of double strand DNA breaks by γ H2AX immunofluorescence assay in DU145 cells exposed to Rucaparib and TSA, alone and in combination.

(A) Microscopy images to enable visual identification of γ H2AX foci in DU145 cells exposed to Rucaparib and TSA for 72 hours. Images are representative of three independent experiments. Scale bar: 11 μ m. (B) Bar graph to show mean fold change in γ H2AX foci for each treatment group. γ H2AX foci were quantified in the nucleus of 20 cells per treatment group. (** $p < 0.01$).

The microscopy images presented in Figure 6.7 show that PC3 cells possess γ H2AX foci representative of DNA DSBs prior to drug exposure (fluorescence green dots in the cell nuclei).

Treatment with Rucaparib (16 μ M) for 72-hours significantly enhanced the expression of γ H2AX foci. Quantitative assessment confirmed this finding (Figure 6.7B), showing a significant 1.7-fold increase in DSBs ($p < 0.01$). TSA treatment (49nM) did not increase the levels of double strand breaks in PC3 cells, compared to control. There was an increase in γ H2AX foci following co-treatment compared to untreated controls but this response was not significantly greater than Rucaparib as a single agent.

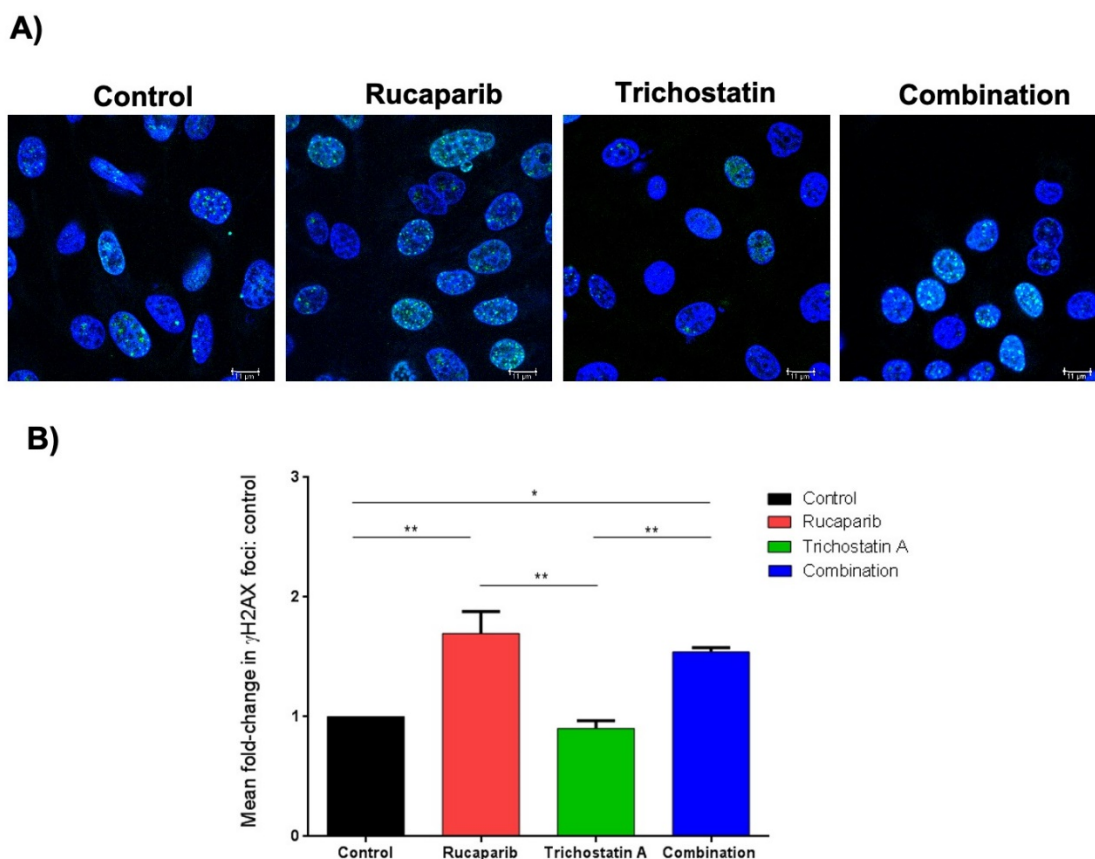


Figure 6.7: Detection of double strand DNA breaks by γ H2AX immunofluorescence assay in PC3 cells exposed to Rucaparib and TSA, alone and in combination.

(A) Microscopy images to enable visual identification of γ H2AX foci in PC3 cells exposed to Rucaparib and TSA for 72 hours. Images are representative of three independent experiments. Scale bar: 11 μ m. (B) Bar graph to show mean fold change in γ H2AX foci for each treatment group. γ H2AX foci were quantified in the nucleus of 20 cells per treatment group. (* $P < 0.05$, ** $p < 0.01$).

The graph presented in Figure 6.8A demonstrates that PNT1A cells were subject to increased levels of DNA DSBs following Rucaparib treatment at a dose inhibitory to cell growth by 50%, compared to DU145 and PC3 cells. PNT1A cells exposed to TSA expressed an increased number of γ H2AX foci than PC3 cells but not DU145 cells, as shown in Figure 6.8B. There was no significant difference in the number of γ H2AX foci between DU145 and PC3 cells following TSA

treatment. Data presented in Figure 6.8C show that PC3 cells are significantly less sensitive ($p < 0.01$) to DNA DSBs following co-treatment compared to PNT1A and DU145 cells. DU145 cells presented the highest mean increase in γ H2AX foci, relative to control, following co-treatment compared to PNT1A and PC3 cells.

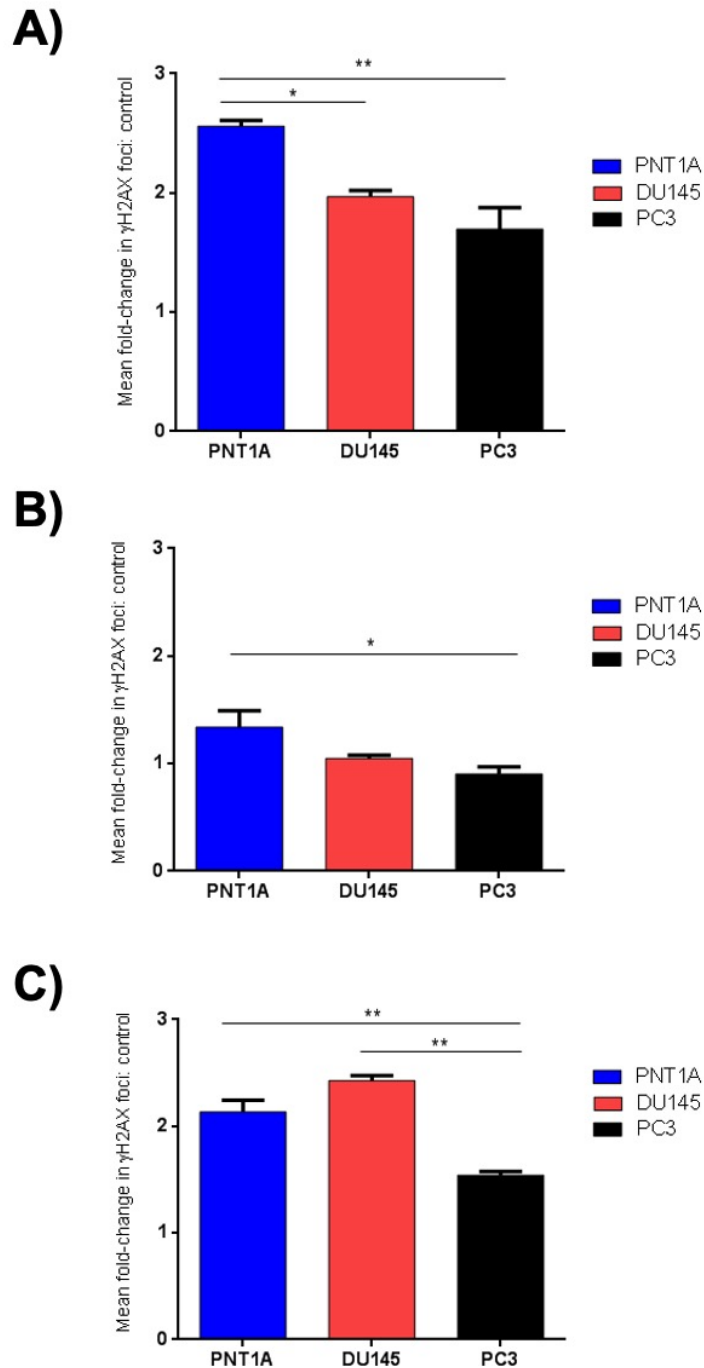


Figure 6.8: Mean fold-change in γ H2AX foci: control following continuous exposure to Rucaparib and TSA, alone and in combination, for 72 hours.

Mean γ H2AX foci: control in PNT1A, DU145 and PC3 cells following exposure to (A) Rucaparib, (B) TSA and (C) co-treatment.

6.3.3 Western blot analysis of RAD51 protein expression as a marker of Homologous recombination in prostate cancer cells exposed to Rucaparib and TSA, alone and in combination.

To determine whether DU145 and PC3 cells were able to repair Rucaparib and TSA-induced DNA DSBs by HR, the protein expression levels of RAD51 were investigated by Western blotting, as described in Chapter Two, section 2.2.4. The presence of RAD51 assists in the repair of DSB by HR. Briefly, cells were exposed to Rucaparib and TSA, alone and in combination, or no drug (negative control) at their respective GI_{50} concentrations in 1% DMSO for 72 hours in culture medium. Cells were harvested, lysates were prepared and loaded onto SDS-PAGE gels for protein separation; prior to electro-transfer, antibody probing and chemiluminescent detection.

Results show increased expression of RAD51 protein in PNT1A cells subject to Rucaparib-induced ($28\mu\text{M}$) DNA damage (Figure 6.9A). RAD51 protein expression levels were reduced in DU145 cells (Figure 6.9B) and unchanged in PC3 cells (Figure 6.9C) following exposure to Rucaparib at $8\mu\text{M}$ and $16\mu\text{M}$ GI_{50} concentrations, respectively. RAD51 expression levels were reduced in DU145 and PC3 cells but not in PNT1A cells following TSA treatment. Expression levels were further reduced in DU145 and PC3 cells exposed to Rucaparib and TSA in combination, relative to loading control, demonstrating increased DNA damage and reduced DNA repair by HR (Figure 6.9A-C).

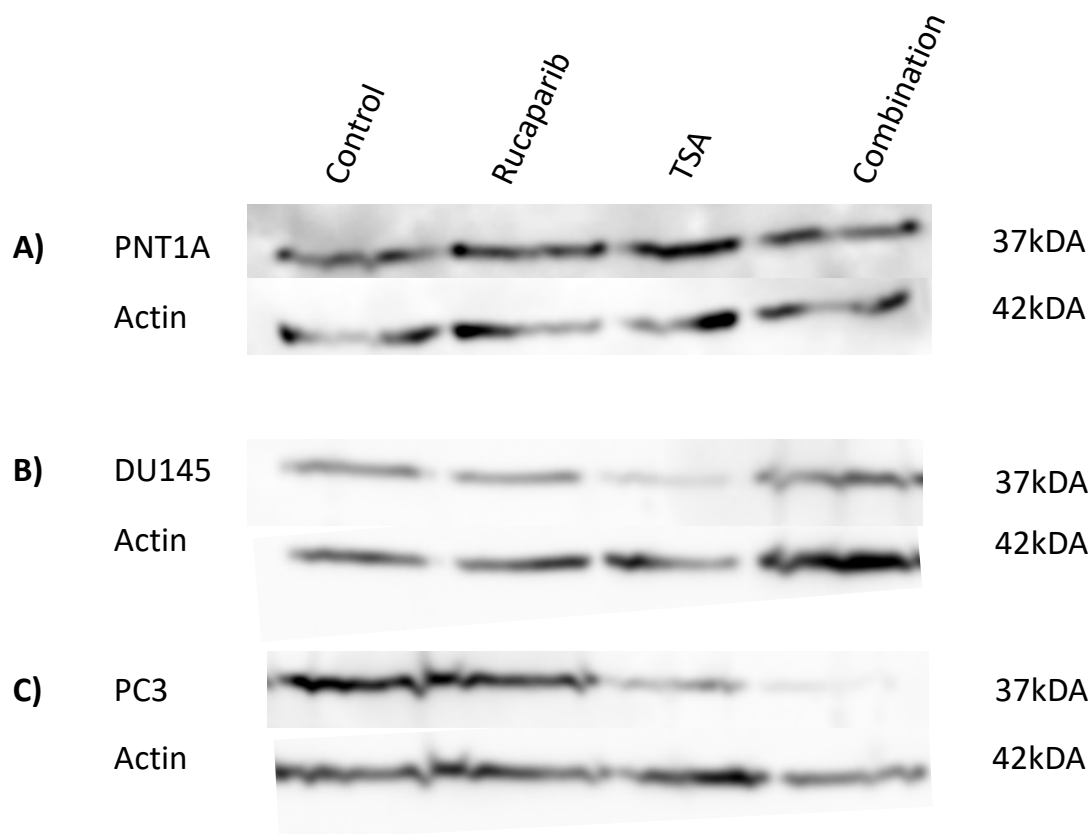


Figure 6.9: RAD51 protein expression following exposure to Rucaparib, TSA and co-treatment. Western blot of whole cell extracts of (A) PNT1A, (B) DU145 and (C) PC3 cells following 72-hour exposure to Rucaparib and TSA, alone and combination. Blots were probed using an antibody against RAD51.

6.4 Discussion

6.4.1 The effects of Rucaparib and TSA on DNA SSB formation

PNT1A, DU145 and PC3 cells exposed to Rucaparib presented increased levels of SSBs, compared to untreated controls. These findings are consistent with the known role of PARP-1 in the repair of SSB by BER (Durkacz et al., 1980). All cells were dosed at their respective GI_{50} Rucaparib concentrations however levels of SSBs were higher in DU145 cells; 77% of the DU145 comet tails examined following Rucaparib treatment were class 3, compared to 10% and 38% class 3 comet tails in PNT1A and PC3 cells, respectively. Further investigation is required to elucidate why Rucaparib induces more SSBs in DU145 cells than PNT1A and PC3 cells despite equal cell death. A possible reason for this finding in DU145 cells is maspin deficiency, and consequently reduced DNA repair capacity and evasion of apoptosis. It has been documented that maspin inhibits tumour progression and induces apoptosis (Berardi et al., 2013). Studies have also demonstrated increased levels of apoptosis in DU145 cells transfected with maspin compared to

control cells (Li et al., 2007). The results indicate that DU145 cells are more prone to DNA damage, as would be expected in a cell line harbouring a *BRCAl* mutation (Yin et al., 2018). The data also postulates that less SSBs are needed to induce apoptosis in PNT1A and PC3 cells and this may be in part due to increased expression of maspin. Previous prostate cancer studies observed increased apoptosis in DU145 cells transfected with maspin; demonstrating a potential role for maspin in apoptosis (Li et al., 2007). A pro-apoptotic effect of maspin has also been reported in breast and squamous cell carcinoma cells (Liu et al., 2004, Zhu et al., 2017). Another contributing factor could be increased basal expression of IKK α in DU145 cells. Activation of NF- κ B by stimuli such as radiation and chemotherapy has been shown to protect tumour cells from apoptosis; highlighting the potential of NF- κ B inhibitors such as PARP inhibitors as adjuvant treatments to enhance the apoptotic response to traditional therapies (Baldwin, 2001).

Single strand DNA breaks were increased in response to TSA exposure in PNT1A, DU145 and PC3 cell lines. The effects were greatest in DU145 and PC3 cells; whereby 31% and 25% of comet tails indicative of strand breaks were class three, respectively. 3% of comet tails were class three in PNT1A cells exposed to TSA, highlighting the selective efficacy of TSA as an inhibitor of DNA SSB repair in tumour cells. Class three comet tails were 10% higher in DU145 cells than PC3 following treatment. Despite a statistical insignificance the data suggests that the effect of TSA treatment on DNA SSBs may be regulated by maspin expression status. It has been reported that histone hyperacetylation induced by inhibition of HDAC alters the structure of chromatin, which may expose DNA to DNA-damaging agents such as cytotoxic agents or reactive oxygen species (ROS) (Lee et al., 2010). Various studies have also demonstrated the selectivity of HDAC inhibitors as inducers of ROS, DNA damage and apoptosis in various types of cancer cells (Rosato et al., 2003, Shankar and Srivastava, 2008, Song et al., 2018). Inhibition of HDAC-1 has been shown to hinder DNA repair and enhance tumour cell sensitivity to DNA damaging agents (As reviewed by Li and Zhu (2014)).

Rucaparib and TSA co-treatment enhanced SSBs in DU145 and PC3 cells; 42% and 57% of comet tails were class 3 and 49% and 2% of comet tails were class four, respectively. Majority of comet tails were class 2 in PNT1A cells (77%). Co-treatment did not induce class 4 comet tails but 4%

of comets assessed were class 3. These results highlight the selectivity of co-treatment to tumours cells. SSBs were increased 24.5-fold (based on class 4 comet tails) in DU145 cells exposed to co-treatment compared to PC3 cells, demonstrating that DU145 cells are more prone to DNA damage and/or have a reduced DNA repair capacity. These results support the findings of others, who have shown that DU145 cells are defective in BRCA and are therefore more prone to DSBs due to ineffective DNA repair by HR (Yin et al., 2018). Maspin deficiency, and increased susceptibility to DNA damage and apoptosis, in DU145 cells, may also contribute to increased SSBs following co-treatment. Increased apoptosis and DNA damage has been reported in DU145 cells exposed to the PARPi Olaparib and HDACi SAHA combination (Chao and Goodman, 2014). These data demonstrate that PARP and HDAC inhibition is synthetically lethal in cells with mutated BRCA and reduced maspin expression.

6.4.2 The effects of Rucaparib and TSA on DSB formation

Results from γ H2AX immunofluorescence experiments presented in section 6.3.2 show an increase in γ H2AX foci following cell exposure to Rucaparib, at respective GI_{50} concentrations, compared to untreated controls. Rucaparib induced significantly more DSBs in PNT1A cells than DU145 and PC3 cells ($p \leq 0.05$ and $p \leq 0.01$, respectively). The results demonstrate that DNA DSBs accumulate in cells exposed to Rucaparib irrespective of their HR function and DNA repair capacity. Increased levels of DSBs in PNT1A cells exposed to Rucaparib, at respective GI_{50} concentration, highlight the increased ability of normal cells to survive in the presence of DSB's. Human fibroblast studies have also demonstrated an increased ability of normal cells to resolve drug induced DSBs compared to transformed cells (Chao and Goodman, 2014).

γ H2AX foci were increased in PNT1A cells exposed to TSA at GI_{50} , compared to control, highlighting the ability of normal cells to repair DNA breaks. TSA exposure did not significantly increase γ H2AX foci in the prostate cancer cell lines. Others have shown increased γ H2AX foci following HDACi in normal and transformed cells, suggesting that the accumulation of HDACi-induced DSBs is dependent on various genetic and cell specific mechanisms. The studies that have reported increased γ H2AX following HDACi have used different inhibitors and cell lines. For example, normal human foreskin epithelial cells and transformed LNCaP and A549 cells

exposed to the HDACi Vorinostat presented increased γ H2AX foci (Lee et al., 2010). Glioblastoma cells exposed to the HDACi SAHA also presented increased levels of γ H2AX foci (Rasmussen et al., 2016).

Rucaparib and TSA combination γ H2AX foci data presented in Figure 6.5- Figure 6.7 show that co-treatment significantly increases ($p < 0.01$) the accumulation of DSBs, compared to TSA treatment alone; but is less effective than Rucaparib as a single agent. Our findings are in contrast to the findings of others that have shown a significant increase in γ H2AX foci formation following SAHA and Olaparib, and SAHA and Veliparib co-treatment, at their respective GI_{50} concentrations, in Glioblastoma and prostate cell lines, respectively (Chao and Goodman, 2014, Rasmussen et al., 2016, Yin et al., 2018).

DU145 cells exposed to co-treatment were more susceptible to DNA DSBs than PNT1A and PC3 cells. γ H2AX foci levels were lowest in PC3 cells exposed to co-treatment. These findings may be in part due to the reduced expression of maspin and reduced repair capacity in DU145 cells. These results support the findings of others, who have shown that DU145 cells are defective in *BRCA* and are therefore more prone to DSBs due to ineffective DNA repair by HR (Yin et al., 2018). Maspin deficiency, and increased susceptibility to DNA damage and apoptosis, in DU145 cells, may also contribute to increased DNA damage following co-treatment. Increased apoptosis and DNA damage has been reported in DU145 cells exposed to the PARPi Olaparib and HDACi SAHA combination (Chao and Goodman, 2014). These data demonstrate that PARP and HDAC inhibition is synthetically lethal in cells with mutated *BRCA* and reduced maspin expression.

6.4.3 The effects of Rucaparib and TSA on the expression of RAD51

To further explore the effects of PARP and HDAC inhibition on DNA damage the expression of RAD51, a HR DNA repair protein, was investigated. RAD51 protein expression levels, presented in Figure 6.9, show basal expression of RAD51 in all prostate cell lines. Expression levels were highest in PC3 cells and lowest in DU145 cells. RAD51 is a biomarker of HR function and reduced expression levels in DU145 cells indicates a reduced ability to repair DBSs by HR. This supports the DNA damage data presented in Figure 6.8 where levels of DNA DSBs are higher in

DU145 cells exposed to Rucaparib and TSA co-treatment than PC3 and PNT1A cells. BRCA1 and BRCA2 mutations are associated with defective DNA repair by HR and have been reported in DU145 cells (Yin et al., 2018). To this end, RAD51 expression in these cells correlates with defective DNA repair by HR. Studies have demonstrated that reduced expression of RAD51 is associated with increased sensitivity to PARP inhibitors (McCabe et al., 2006, Liu et al., 2017, Cruz et al., 2018). These correspond to the data presented in 4.3.1 which show enhanced sensitivity to Rucaparib in *BRCA* mutant DU145 cells and decreased RAD51 expression in response to Rucaparib (Figure 6.9).

Reduced expression of NF- κ B p65 in DU145 cells (as shown in Figure 3.9) may contribute to defective DNA repair by HR, and consequently reduced RAD51 expression. Mouse embryonic fibroblasts (MEF) studies have reported increased genomic instability and compromised DNA repair in p65^{-/-} MEFs compared to p65^{+/+} MEF cells. Sub-lethal irradiation of p65^{-/-} cells and tissues was found to compromise DNA damage recovery. Similar results were also found in p65^{-/-} cells exposed to Doxorubicin, suggesting that inefficient DNA repair of cells deficient in p65 is not limited to irradiation (Wang et al., 2009a). NF- κ B p65 has also been shown to affect HR and the repair of DNA breaks arising spontaneously, or in response to genotoxic stress. K562 leukaemia cells exposed to the PARP inhibitor IQD were ~50% less responsive to treatment upon expression of p65 (Volcic et al., 2012). The studies support the protein expression data presented in Figure 3.9; whereby PARP and NF- κ B p65 protein expression levels are lowest in DU145 cells. The results imply that ineffective DNA repair by HR and reduced expression of RAD51 in DU145 cells may be in part due to reduced expression of PARP-1 and NF- κ B p65. It has also been reported that histone deacetylases regulate tumorigenesis by repressing the expression of tumour suppressor genes and DDR genes such as *BRCA1* (Li and Seto, 2016). Loss of maspin expression and therefore increased deacetylation of histones in DU145 cells may contribute to the differential expression of proteins identified in these cells.

An increase in RAD51 protein expression following Rucaparib exposure in PNT1A cells suggests functional DNA repair by HR, and this may contribute to the reduced sensitivity to Rucaparib in these cell lines. The RAD51 expression data in Figure 6.9 corresponds to the Rucaparib sensitivity

data presented in 4.3.1, whereby PNT1A cells were less sensitive to Rucaparib than DU145 and PC3 cells. HR function has been correlated to RAD51 focus formation and sensitivity to Rucaparib in primary ovarian cancer cultures and cell lines. Cells were classified into two groups, HR deficient or proficient, based on their ability to form RAD51 foci in response to DNA damage; irrespective of *BRCA* status. Increased RAD51 foci following exposure to Rucaparib was observed, demonstrating that RAD51 is a potential biomarker for HR function and sensitivity to Rucaparib in tumour cells (Mukhopadhyay et al., 2010).

DU145 cells exposed to Rucaparib presented reduced expression of RAD51, suggesting that PARP inhibitors are synthetically lethal to cells defective in HR. These findings are in support of other studies that demonstrate reduced expression of RAD51 and BRCA1 in nuclear and cytoplasmic DU145 cell extracts exposed to the PARP inhibitor Olaparib (Chao and Goodman, 2014). The results suggest that the differential effects of Rucaparib on DU145 cells and expression of RAD51 is in part due to dysfunctional HR rather than maspin deficiency. HDAC-1 inhibition has been shown to downregulate RAD51 and reduce DNA repair by HR in melanoma cell lines (Krumm et al., 2016). Maspin depleted DU145 cells express increased levels of HDAC-1 compared to PNT1A and PC3 cells and the expression levels of maspin remain the same following PARP inhibition (Figure 4.17). The expression of RAD51 was not affected by Rucaparib in PC3 cells, demonstrating the specificity of increased RAD51 in HR defective tumours exposed to DNA damage.

Exposure to the HDACi TSA did not affect the protein expression of RAD51 in PNT1A cells but expression was reduced in DU145 and PC3 cells. These findings are in line with other studies which have shown that HDAC inhibitors selectively hinder the expression of DNA DSB repair proteins in cancer cells but not in normal cells. The HDAC inhibitor PCI-24781 has been shown to hinder DNA DSB repair by HR; by reducing RAD51 expression levels and limiting function in colon cancer cell models. HCT116 colon-tumour-bearing mice exposed to oral doses of PCI-24781 also presented decreased tumour expression of RAD51 (Adimoolam et al., 2007). A similar effect has been observed in prostate and lung cancer cells exposed to the HDACi Vorinostat. Vorinostat induced DNA DSBs in normal and cancer cells, but suppression of the DNA DSB

repair proteins RAD50 and MRE11 occurred only in cancer cells. Normal cells were able to repair the DNA breaks despite continued culture with Vorinostat, highlighting the selectivity of Vorinostat as a cytotoxic agent in cancer cells (Lee et al., 2010). Downregulation of DNA repair genes by HDAC inhibition has been shown to increase the sensitivity of PC cells to DNA damaging agents and radio-sensitisation of HDACis has been linked to decreased expression of the HR proteins BRCA1 and RAD51. An inability of these proteins to bind to DNA DSBs has also been reported (Kachhap et al., 2010).

A further reduction in the expression of RAD51 in DU145 and PC3 cells exposed to Rucaparib and TSA in combination demonstrates that inhibition of PARP-1 and HDAC-1 is synthetically lethal to tumour cells and hinders HR DNA repair. These findings are consistent with other studies that have demonstrated reduced levels of RAD51 in cancer cells exposed to HDACi and PARPi co-treatment, and show that these effects are attributable to impaired DNA damage repair by HR and consequently enhanced DNA DSBs (Chao and Goodman, 2014, Rasmussen et al., 2016, Yin et al., 2018). Knockdown experiments also support the efficacy of combined PARP and HDAC inhibitor treatments in cancer cells; showing that loss of RAD51 enhances apoptosis in cells exposed to PARP and HDAC inhibitor co-treatment (Chao and Goodman, 2014). The results support a critical role of RAD51 in preventing DNA-damage induced cell death.

6.5 Summary

The *in vitro* studies presented in this chapter have shown that:

- Rucaparib induces SSBs in PNT1A, DU145 and PC3 cells at their respective GI_{50} concentrations. SSBs were increased in DU145 cells, followed by PC3 and PNT1A cells; showing that DU145 cells are more prone to DNA damage. This may be in part due to maspin deficiency as a result of increased expression of the NF-kB subunit $IKK\alpha$.
- TSA induces SSBs in PNT1A, DU145 and PC3 cells at their respective GI_{50} concentrations. SSBs were greatest in DU145 and PC3 cells highlighting a selective effect of TSA as an inhibitor of SSB repair in tumour cells.

- Rucaparib and TSA co-treatment selectively enhances SSBs in tumour cells; particularly DU145 cells. The results support that DU145 cells are more prone to DNA damage and have a reduced DNA repair capacity.
- Rucaparib induces significant levels of DSBs to PNT1A cells, at their respective GI_{50} concentration, demonstrating an increased ability for normal cells to survive in the presence of DSBs.
- Rucaparib, as a single agent, is more effective at inducing DNA DSBs than co-treatment. Co-treatment does induce more DNA DSBs in DU145 cells despite a 50% cell survival in all cell lines, but not more than Rucaparib alone. This differential affect may be in part due to maspin, $IKK\alpha$ and BRCA deficiency which hinders the ability of DU145 cells to repair DNA breaks by HR.
- Low expression of RAD51 in DU145 cells correlates with increased sensitivity to Rucaparib. Reduced RAD51 expression in DU145 cells exposed to Rucaparib demonstrates that Rucaparib is synthetically lethal to DU145 cells which are dysfunctional for DNA repair by HR.
- RAD51 expression is reduced in DU145 and PC3 cells exposed to TSA but not PNT1A cells. TSA selectively hinders DSB repair by HR in tumour cells.
- RAD51 expression is further reduced in DU145 and PC3 cells exposed to Rucaparib and TSA co-treatment, demonstrating that co-treatment inhibits DNA repair and is synthetically lethal to tumour cells.

6.6 Future work

The data presented supports the existing reports that the BRCA mutant, maspin depleted, DU145 cell line is more susceptible to DNA damage and has a reduced DNA repair capacity. Future work could include assessing the effects of Rucaparib and TSA on DNA damage and repair in a wide range of tumour cell lines deficient for maspin and proficient for $IKK\alpha$. Rucaparib and TSA induced DNA damage in isogenic paired prostate cancer cell lines that are either proficient or deficient for maspin, PARP-1 and $IKK\alpha$ could also be investigated. This would provide a significant amount of insight into the crosstalk between maspin and the NF- κ B pathways.

RAD51 expression data has provided fundamental insight into the effects of Rucaparib and TSA on DNA repair by HR. The studies carried out in this chapter investigated total RAD51 protein expression levels in cell samples but did not assess the accumulation of RAD51 nuclear foci in response to treatments. Assessment of RAD51 foci by immunofluorescence could be carried out in future studies to aid identification of HR functional status within cells. The effects of Rucaparib and TSA on DNA damage were investigated after 72-hour exposure to treatments. Future studies could also look at kinetics of DNA repair by following the effects of treatment over time and after removal of treatments. Reduced γ H2AX foci in response to drug removal would indicate an increased ability for cells to repair DNA DSBs in the absence of treatment.

Chapter Seven

Investigating the effects of Maspin and PARP-1 siRNA on prostate cell sensitivity to Rucaparib and TSA.

7.1 Introduction

This chapter investigates the effects of maspin and PARP-1 on prostate cell sensitivity to Rucaparib and TSA. Small interfering RNA (siRNA) were utilised to explore the roles of maspin and PARP-1 in cell survival following exposure to Rucaparib and TSA treatments.

7.1.1 Cell transfection

Transfection is the process of deliberately introducing genetic material into mammalian cells to enable the study of gene function (Thermo Fisher Scientific). Gene transfection can be achieved by various techniques such as viral, physical and chemical mediated gene delivery.

Viral transfection utilises the ability of a virus to introduce foreign DNA into mammalian cells. Commonly used viruses include retrovirus, lentivirus and adenovirus (Huang et al., 2011). The virus integrates into the host genome, is expressed and replicated within the host, passing the foreign DNA into subsequent generations of daughter cells. Viral transfection is highly efficient but can only deliver small pieces of DNA into cells, is labour intensive and may cause an inflammatory reaction or mutation due to random insertion into the host genome (Reviewed in Kim and Eberwine (2010) and Nayerossadat et al. (2012)).

Physical transfection methods include electroporation, sonoporation, microinjection and ultrasound. These methods are able to directly penetrate DNA into cells by electric impulse, fine needle puncture, or high-pressure gas, respectively. Physical transfection methods are effective for single or multiple targets at an intended location, however gene transportation to the nucleus is difficult due to restricted access in passing through the membrane and consequently low transfection efficiency (reviewed in Kaestner et al. (2015)). Physical methods are labour intensive, cause damage to the cell and require use of expensive equipment.

Chemical transfection methods are the most frequently used in mammalian cells and include cationic and neutral lipids such as Lipofectamine, FuGene 6 and HiPerFect. The principle of chemical transfection is similar to viral, whereby positively charged chemicals make complexes with negatively charged nucleic acids. These positively charged complexes are attracted to the negatively charged cell membrane and pass through it; to enable translocation to the cell nucleus (reviewed in Jin et al. (2014a)). Chemical transfection methods are advantageous to viral methods as they are less toxic, do not cause mutation and there is no size limitation on the DNA delivered to the cells. Efficiency of chemical transfection is dependent on cell membrane conditions and nucleic acid/chemical ratio (Ramamoorth and Narvekar, 2015).

7.1.1.1 siRNA

Small interfering RNA (siRNA) are double stranded RNA molecules which regulate gene expression. They exploit the RNA pathway by targeting complementary mRNA for degradation to induce gene silencing (Dana et al., 2017).

Delivery of siRNA into mammalian cells to induce gene silencing is achieved using the chemical transfection methods discussed in section 7.1.1. Successful silencing of a specific gene following siRNA transfection can be determined by assessment of protein expression levels, after a suitable incubation time. siRNA gene silencing is a commonly used technique to validate gene function and provides opportunity for the development of innovative therapies to treat diseases such as cancer. The potential of siRNA-based therapy has been increasingly recognised as an effective treatment for cancer, with the aim of blocking multiple disease-causing genes (reviewed in Mahmoodi Chalbatani et al. (2019)). Silencing of cancer-associated genes by siRNA has been shown to have antiproliferative and apoptotic effects in a range of cancer cells *in vitro*. For example, Melanoma cells subject to siRNA mediated knockdown of ribonucleotide reductase, a rate-limiting enzyme primarily expressed in proliferating cells such as cancer cells, presented reduced cell proliferation and increased cell cycle arrest (Zuckerman et al., 2011). Inhibition of cell proliferation and increased apoptosis has also been reported in colorectal and breast cancer cells subject to siRNA-mediated knockdown of STAT6; a transcription factor associated with cancer cell proliferation, increased malignancy and poor prognosis (Salguero-Aranda et al.,

2019). siRNAs have also shown promise in sensitising tumour cells to chemotherapy by silencing genes which are associated with drug resistance during chemotherapy (reviewed in Guo et al. (2013)). A barrier that must be overcome to ascertain effective widespread use of siRNA in the clinic is the potential for off target effects which may result in unpredictable cellular consequences and immune stimulation (reviewed in Singh et al. (2018)). To overcome this, drug delivery systems such as nanoparticles are being developed for the safe and effective delivery of siRNA therapies into tumour cells. Various siRNA therapies are currently undergoing clinical trials and one siRNA therapeutic, ONPATPRO™ (patisiran), has been FDA approved for commercial use (Hu et al., 2019). ONPATPRO™ is a lipid nanoparticle-based siRNA used to treat nerve damage caused by hereditary transthyretin amyloidosis (Akinc et al., 2019). The clinical approval of ONPATPRO paves the way for the development of universal siRNA therapeutics. There are still challenges to overcome due to the complexity of the microenvironment in the human body (Zhang et al., 2018).

The siRNA studies presented in this chapter were carried out to provide mechanism to the effects of Maspin and PARP-1 in cell survival following exposure to Rucaparib and TSA treatments. The siRNA sequences used to silence maspin and PARP-1 are presented in Chapter Two, Table 2.6. Throughout the studies presented in thesis, PNT1A, DU145 and PC3 cells have been used as prostate models and have shown some interesting patterns between NF- κ B, PARP-1 and maspin. However, ultimately, these cells are not isogenic and therefore patterns cannot be directly compared. Utilisation of siRNA in these cells to knock down PARP-1 and maspin proteins aims to provide a mechanism to the patterns previously observed in earlier chapters.

7.2 Chapter aims

The aims of this chapter are detailed below:

- Further investigate the expression of maspin and/or PARP-1 on the sensitivity to PARP-1 and HDAC-1 inhibitors. This was achieved through the selective knockdown of maspin or PARP-1

- Investigate the effects of Rucaparib and TSA, alone and in combination, in the presence of maspin siRNA on cell survival in PNT1A cells.
- Investigate the effects of Rucaparib and TSA, alone and in combination, in the presence of maspin siRNA on PARP-1 expression in PC3 cells.
- Investigate the effects of Rucaparib and TSA, alone and in combination, in the presence of PARP-1 siRNA on cell survival in DU145 and PC3 cells.

7.3 Results

7.3.1 Knockdown of maspin with siRNA in PNT1A and PC3 cells

Variation in siRNA sequences and a time course of target knockdown was investigated to determine optimal conditions for the silencing of maspin in PNT1A and PC3 cells. Cells were seeded and incubated overnight to enable cell adherence prior to lipid transfection (method described in Chapter Two, section 2.2.10) with 10nM of siRNA oligos targeting maspin or a non-specific control (-ve). Maspin expression levels were determined by Western blotting 24, 48 and 72-hours following siRNA transfection.

The data presented in Figure 7.1 and Figure 7.2 show knockdown of maspin using single siRNA sequences in PNT1A and PC3 cells, respectively. Percentage knockdown was determined against negative control siRNA as 100% at each timepoint. Maspin expression in negative control siRNA cell samples did not significantly differ to cells alone (data not shown).

Knockdown of maspin with maspin siRNA sequence #1 was not achieved in PNT1A cells at 24 and 48-hour timepoints (Figure 7.1). At 72 hours maspin expression was reduced by 62% in PNT1A cells transfected with maspin siRNA sequence #1. Maspin siRNA sequence #2 did not effectively knockdown maspin at any timepoint; at 72 hours maspin expression was reduced by 8% (Figure 7.1B).

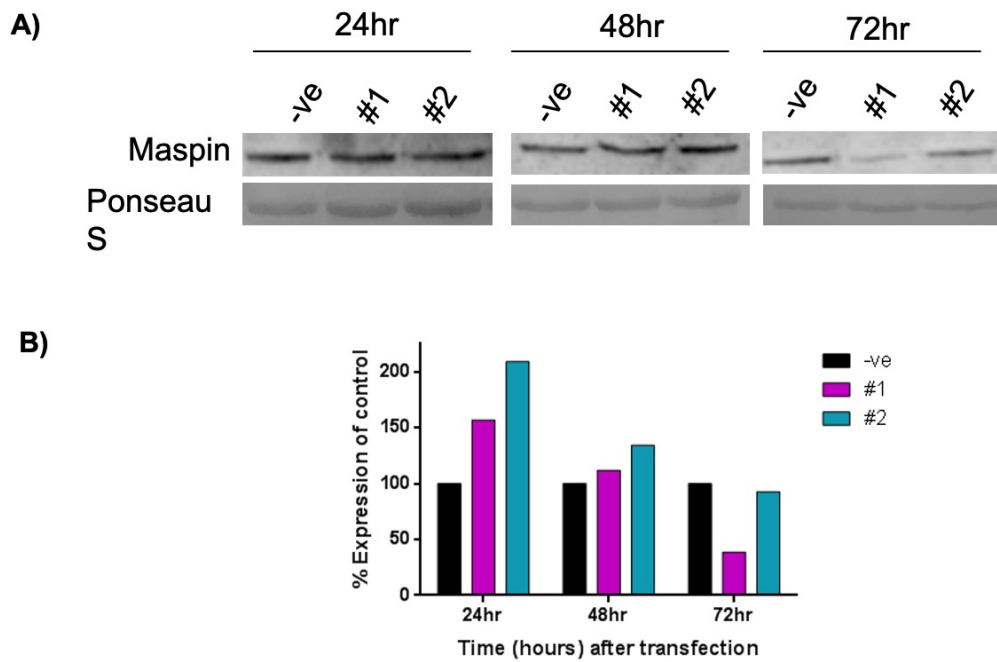


Figure 7.1: Time course of siRNA knockdown of Maspin in PNT1A cells.

(A) Western blot of whole cell extracts of PNT1A cells at 24, 48 and 72 hours after transfection with non-specific siRNA (-ve), or maspin single siRNA sequences (#1 and #2) at 10nM final concentrations. **(B)** Percentage knockdown of maspin in PNT1A cells vs -ve control.

Maspin expression was reduced in PC3 cells exposed to maspin siRNA sequences at 48 and 72 hours (Figure 7.2). At 48 hours, maspin expression was reduced by 93% and 91% in the presence of maspin siRNA #1 and #2, respectively. At 72 hours maspin expression was reduced by 69% and 90% in the presence of maspin siRNA #1 and #2, respectively.

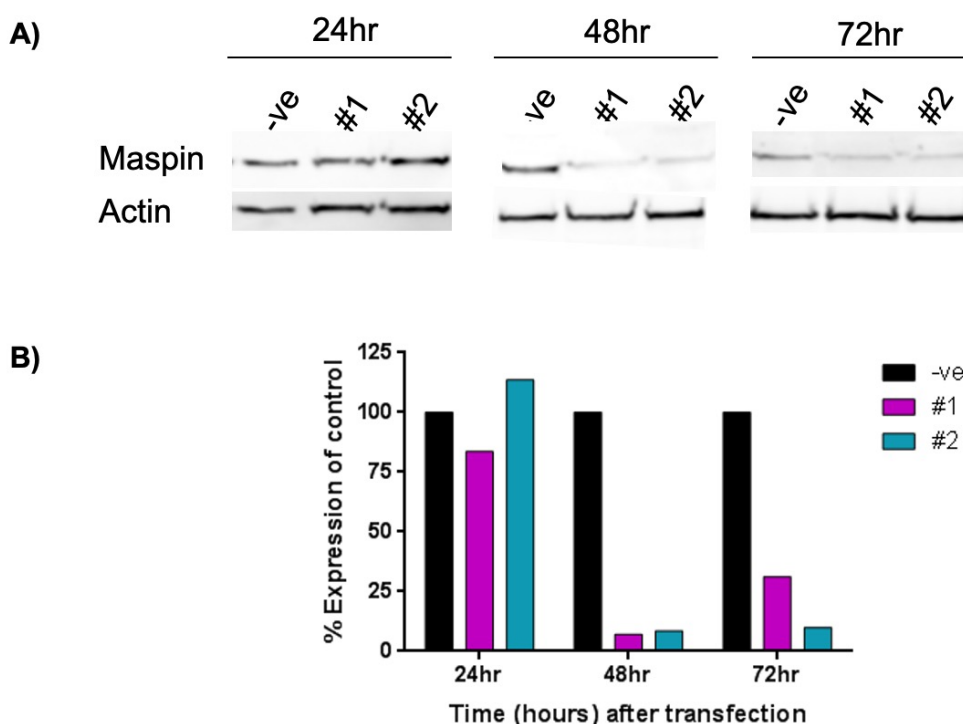


Figure 7.2: Time course of siRNA knockdown of Maspin in PC3 cells.

(A) Western blot of whole cell extracts of PC3 cells at 24, 48 and 72 hours after transfection with non-specific siRNA (-ve), or maspin single siRNA sequences (#1 and #2) at 10nM final concentrations. (B) Percentage knockdown of maspin in PC3 cells vs -ve control.

7.3.2 The effects of maspin on PNT1A cell sensitivity to Rucaparib and TSA.

Following identification of optimum maspin siRNA sequence and exposure timepoints for maspin knockdown, PNT1A cells transfected with maspin siRNA #1 were exposed to Rucaparib and/or TSA to investigate the effects of maspin knockdown on cell sensitivity to treatments, by SRB assay (Figure 7.3-Figure 7.5). Cancer cells harbour a number of genetic defects and therefore the PNT1A cell line (proficient for maspin, NF-kB and PARP-1) was selected to look at the effects of maspin knockdown in a non-cancerous cell line. Maspin protein expression levels were not investigated following exposure to drug treatments for 72 hours, therefore it cannot be confirmed whether maspin remains knocked down for the duration of the experiment.

Results presented in Figure 7.3 show a 21% reduction in PNT1A cell survival following maspin siRNA #1 transfection and Rucaparib treatment, compared to unsilenced cells exposed to

Rucaparib treatment alone at GI_{50} (27 μ M). Maspin siRNA #2 and Rucaparib treatment reduced cell survival by 10% compared to Rucaparib alone. Negative control siRNA increased cell survival by 10% compared to Rucaparib alone. Negative control siRNA increased cell survival by 17% in the presence of Rucaparib, compared to Rucaparib alone. There was no significant difference between maspin siRNA #1 combined with Rucaparib and Rucaparib alone; there was a significant difference ($p < 0.05$) in cell survival in cells exposed to maspin siRNA #1 combined with Rucaparib compared to negative control siRNA. Cells were exposed to siRNA sequences and Rucaparib for 72 hours and results were obtained by SRB assay.

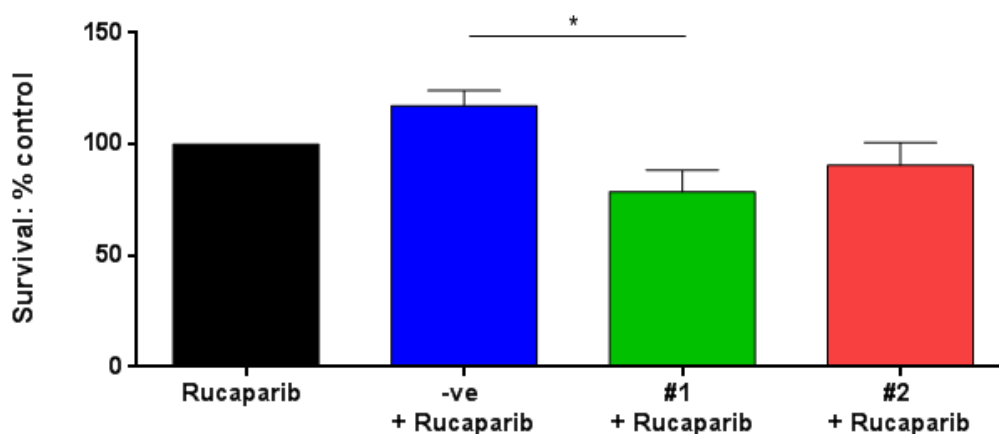


Figure 7.3: siRNA knockdown of maspin enhances PNT1A cell sensitivity to Rucaparib. Percentage survival of PNT1A cells relative to control following exposure to 10nM maspin siRNA and GI_{50} Rucaparib for 72 hours. Cell sensitivity was assessed using the SRB assay and differences between treatment conditions were statistically analysed in Graphpad PRISM (one-way ANOVA, * $p < 0.05$).

Results presented in Figure 7.4 show a 39% reduction in PNT1A cell survival following maspin siRNA #1 transfection and TSA treatment, compared to unsilenced cells exposed to TSA treatment alone at GI_{50} (188nM). Negative control siRNA increased cell survival by 11% in the presence of TSA, compared to TSA alone. Maspin siRNA #2 and TSA treatment reduced cell survival by 16% compared to TSA alone. There was no significant difference between maspin siRNA #1 combined with TSA and TSA alone; there was a significant difference ($p < 0.05$) in cell survival in cells exposed to maspin siRNA #1 combined with TSA compared to negative control siRNA.

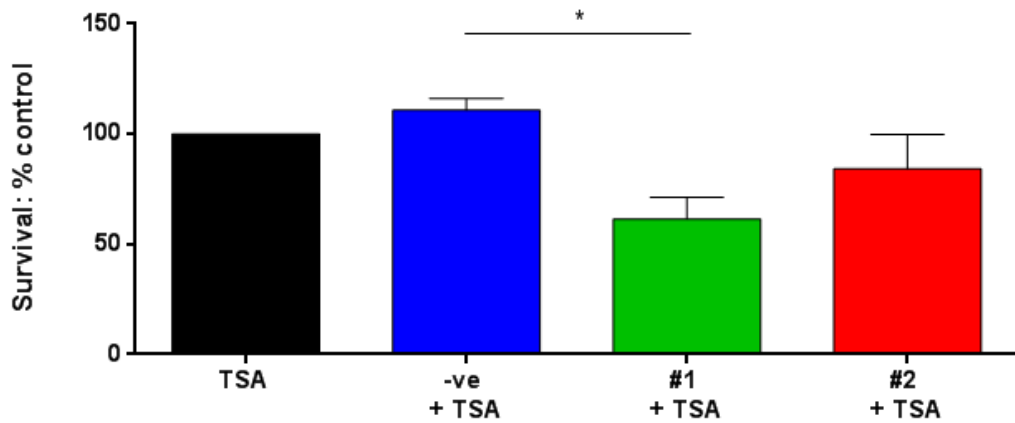


Figure 7.4: siRNA knockdown of maspin enhances PNT1A sensitivity to TSA.

Percentage survival of PNT1A cells relative to control following exposure to 10nM maspin siRNA and GI₅₀ TSA for 72 hours. Cell sensitivity was assessed using the SRB assay and differences between treatment conditions were statistically analysed in Graphpad PRISM (one-way ANOVA, *p<0.05).

Maspin knockdown enhanced PNT1A cell sensitivity to Rucaparib and TSA co-treatment, as shown in Figure 7.5. Cell survival was reduced by 39% and 19% in the presence of siRNA #1 and #2, respectively. Sensitivity to co-treatment was most significant in PNT1A cells transfected with maspin siRNA sequence #1 (p<0.05, one-way ANOVA). There was no significant difference between maspin siRNA #1 combined with co-treatment and co-treatment alone. There was a significant difference (p<0.05) in cell survival in cells exposed to maspin siRNA #1 combined with co-treatment compared to negative control siRNA.

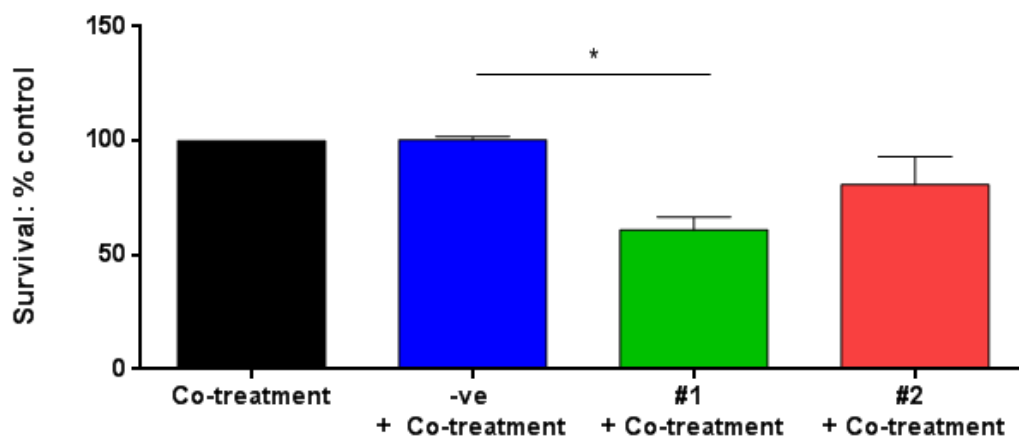


Figure 7.5: siRNA knockdown of maspin enhances PNT1A sensitivity to Rucaparib and TSA co-treatment.

Percentage survival of PNT1A cells relative to control following exposure to 10nM maspin siRNA and GI₅₀ Rucaparib and TSA co-treatment for 72 hours. Cell sensitivity was assessed using the SRB assay and differences between treatment conditions were statistically analysed in Graphpad PRISM (one-way ANOVA, p<0.05).

The data presented in Figure 7.3-Figure 7.5 show that PNT1A cell survival is reduced in the presence of maspin #1 siRNA and co-treatment, compared to maspin #1 siRNA and Rucaparib alone. However, cell survival in the presence of maspin siRNA #1 and co-treatment is no greater than maspin #1 siRNA and TSA alone. Co-treatment is not additive.

7.3.3 The effects of Maspin knockdown on PARP-1 protein expression following exposure to Rucaparib and TSA, alone and in combination.

Maspin expressing PC3 cells were selected for use to explore the effects of maspin on PARP-1 protein expression, following exposure to Rucaparib and TSA, alone and in combination. PC3 cells express the highest levels of PARP-1 (expression data presented in Chapter Three, Figure 3.8 and Figure 3.9) and are therefore a suitable model to investigate the effects of maspin on PARP-1 protein expression. DU145 cells express low levels of maspin and PARP-1 compared to PC3 cells. The expression of PARP-1 following maspin knockdown in PC3 cells will allow us to establish whether maspin deficiency in DU145 cells contributes to reduced expression of PARP-1.

PC3 cells were exposed to -ve or maspin siRNA sequences in the presence of Rucaparib and TSA, alone and in combination (Figure 7.6). PARP-1 protein levels were assessed by Western blotting using the method outlined in Chapter Two, 2.2.4. Briefly, PC3 cells were transfected with maspin siRNA for 48hours (as described in Chapter two, section 2.2.10) to achieve optimum knockdown and then dosed with Rucaparib and/or TSA at their respective GI₅₀ concentrations for 72-hours. Expression data presented in Figure 7.6 shows reduced expression of PARP-1 in PC3 cells transfected with maspin #1 siRNA, compared to negative control. PARP-1 expression was not reduced in PC3 cells transfected with maspin #2 siRNA. Earlier maspin siRNA studies have also shown reduced efficacy of this maspin siRNA sequence and the expression data is from a single experiment without loading control. PARP-1 expression levels in PC3 cells exposed to maspin #1 and #2 siRNA were reduced following exposure to Rucaparib and TSA, alone and in combination. These results are preliminary, repeat experiments and use of loading control are necessary to ensure reproducibility and validity of findings.

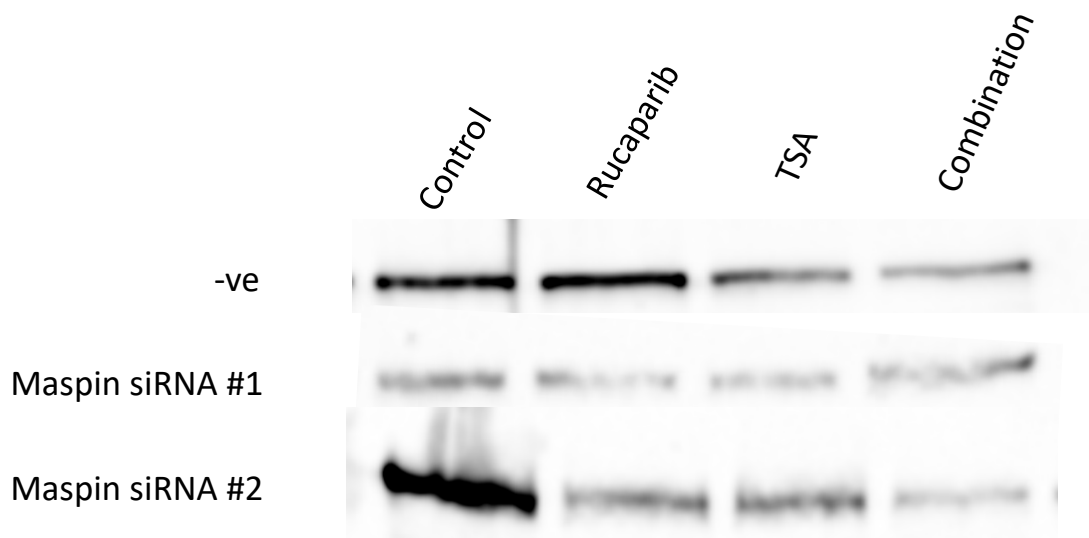


Figure 7.6: The effect of maspin on the protein expression of PARP-1 in PC3 cells exposed to Rucaparib and TSA, alone and in combination.

Western blot of whole PC3 cell extracts transfected with non-specific siRNA (-ve), or maspin single siRNA sequences (#1 and #2) at 10nM final concentration for 48 hours and then exposed to Rucaparib and TSA, alone and in combination, for a further 72-hours. Results are representative of a single experiment.

7.3.4 Knockdown of PARP-1 with siRNA in DU145 and PC3 cells

DU145 and PC3 cells were transfected with PARP-1 siRNA (method detailed in Chapter Two, 2.2.10) and protein expression levels were assessed by Western blotting (Chapter Two, 2.2.4) 24, 48 and 72-hours following transfection to determine the optimum timepoint required to achieve PARP-1 knockdown. Cells were seeded and incubated overnight to enable cell adherence prior to lipid transfection with 10nM of siRNA oligos targeting PARP-1 or non-specific control (-ve) (siRNA sequences presented in Table 2.6). Figure 7.7 shows successful knockdown of PARP-1 in DU145 and PC3 cells following PARP-1 siRNA transfection for 48 and 72 hours. PARP-1 knockdown is greatest 48 hours after siRNA transfection. Anti-actin loading control was not used.

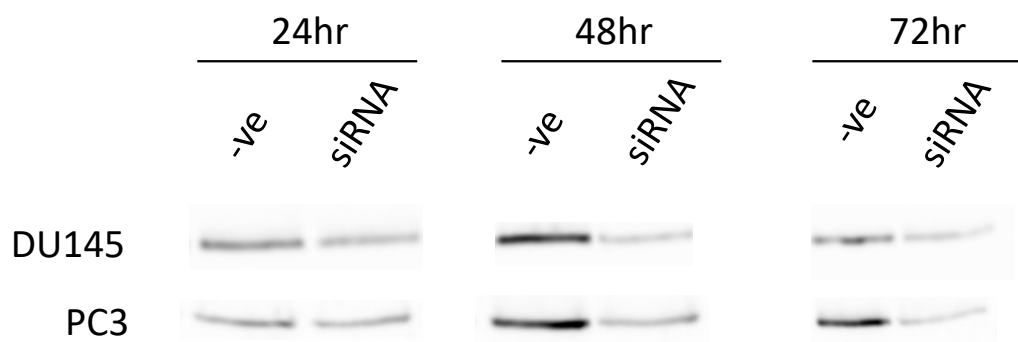


Figure 7.7: Time course of siRNA knockdown of PARP in DU145 and PC3 cells.

Western blot of whole cell extracts of DU145 and PC34 cells at 24, 48 and 72 hours after transfection with non-specific siRNA (-ve) or PARP-1 at 50nM final concentrations.

DU145 and PC3 cells were transfected with PARP-1 siRNA for 48 hours and exposed to Rucaparib and/or TSA for 72 hours to investigate the effects of PARP-1 on cell sensitivity to treatments (Figure 7.8-Figure 7.13).

DU145 cell sensitivity to Rucaparib was reduced 8% in the presence of PARP-1 siRNA, compared to cells exposed to Rucaparib alone. Survival was reduced by 6% in cells exposed to Rucaparib and -ve siRNA, compared to Rucaparib alone; as shown in Figure 7.8. Cell survival following Rucaparib exposure in the presence of siRNA was not significant.

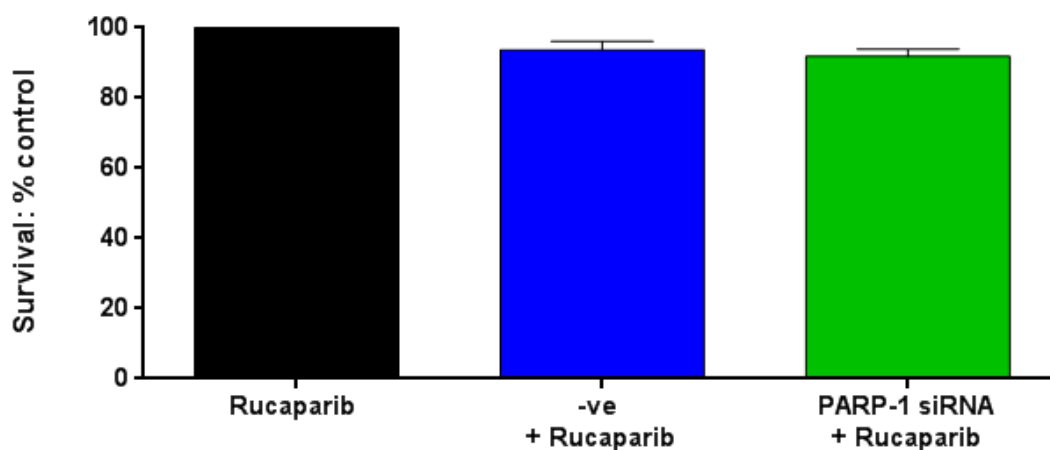


Figure 7.8: The effects of PARP-1 knockdown on DU145 cell sensitivity to Rucaparib. Percentage survival of DU145 cells relative to control following exposure to 50nM PARP-1 siRNA for 48 hours and 16 μ M Rucaparib for 72 hours. Cell sensitivity was assessed using the SRB assay and differences between treatment conditions were statistically analysed in GraphPad PRISM (one-way ANOVA).

The data presented in Figure 7.9 show a significant 12% reduction in cell survival in DU145 cells exposed to TSA treatment and PARP-1 siRNA, compared to cells exposed to TSA alone. Cells transfected with control siRNA were 8% more sensitive to TSA treatment than cells exposed to TSA alone, but less than cells subject to PARP-1 silencing. This was also significant.

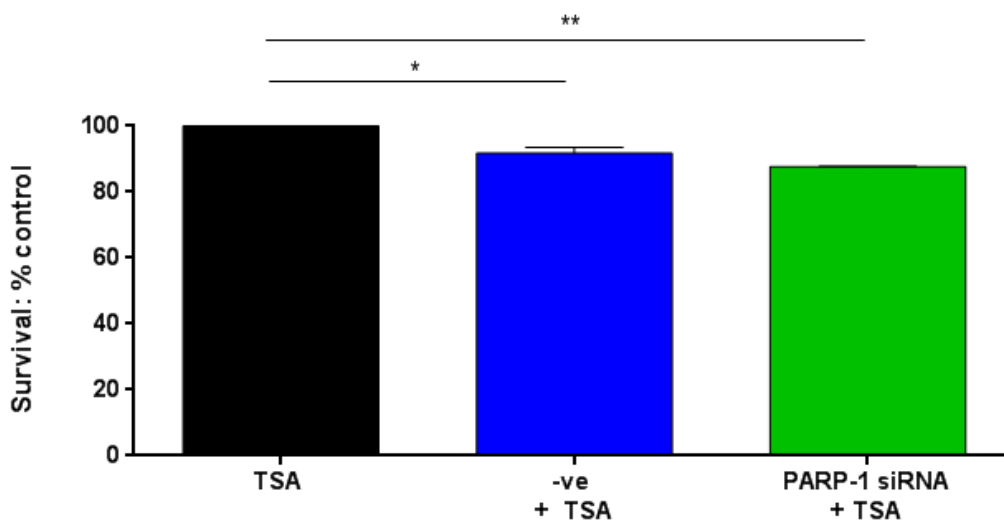


Figure 7.9: The effects of PARP-1 knockdown on DU145 cell sensitivity to TSA. Percentage survival of DU145 cells relative to control following exposure to 50nM PARP-1 siRNA for 48 hours and 45nM TSA for 72 hours. Cell sensitivity was assessed using the SRB assay and differences between treatment conditions were statistically analysed in GraphPad PRISM (one-way ANOVA, * $p < 0.05$, ** $p < 0.01$).

PARP-1 knockdown significantly enhanced DU145 cell sensitivity to Rucaparib and TSA co-treatment (Figure 7.10). Survival was reduced by 31% when cells were transfected with PARP-1

siRNA and exposed to co-treatment, compared to cells which were exposed to co-treatment alone. Cell survival of co-treated DU145 cells transfected with PARP-1 siRNA was 22% less than co-treated DU145 cells transfected with control siRNA. These results indicate that PARP-1 plays a role in cell sensitivity to Rucaparib and TSA co-treatment in DU145 cells.

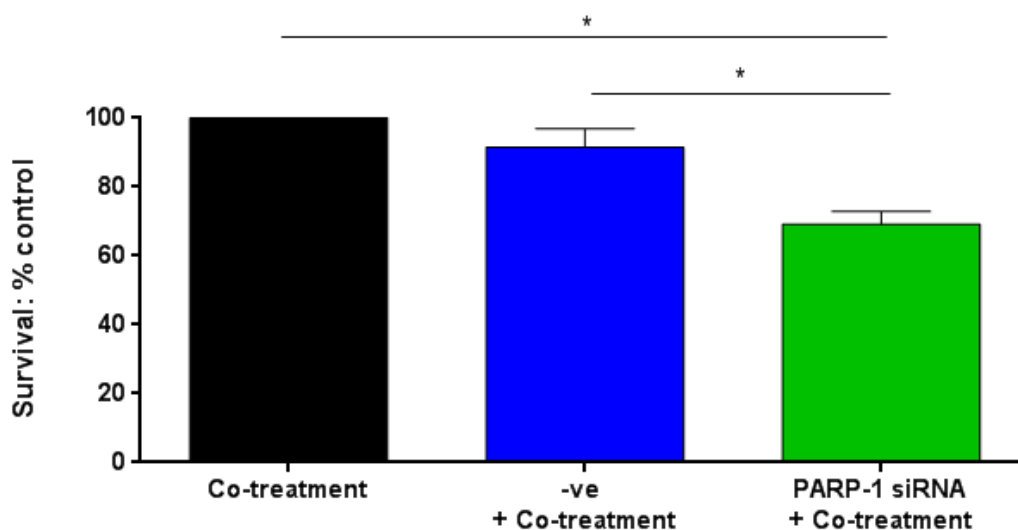


Figure 7.10: siRNA knockdown of PARP-1 enhances DU145 cell sensitivity to Rucaparib and TSA co-treatment.

Percentage survival of DU145 cells relative to control following exposure to 50nM PARP-1 siRNA for 48 hours and Rucaparib and TSA co-treatment for 72 hours. Cell sensitivity was assessed using the SRB assay and differences between treatment conditions were statistically analysed in GraphPad PRISM (one-way ANOVA, * $p < 0.05$).

PARP-1 siRNA and exposure to Rucaparib reduced PC3 cell survival by 16% compared to cells exposed to Rucaparib alone (Figure 7.11). Survival was reduced by 19% compared to control siRNA + Rucaparib. This result was not considered statistically significant.

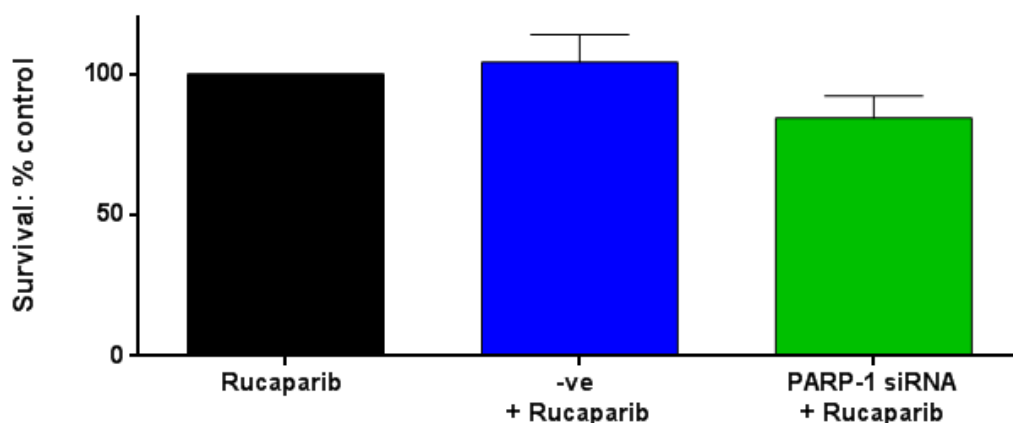


Figure 7.11: The effects of PARP-1 knockdown on PC3 cell sensitivity to Rucaparib.

Percentage survival of PC3 cells relative to control following exposure to 50nM PARP-1 siRNA for 48 hours and 16µM Rucaparib for 72 hours. Cell sensitivity was assessed using the SRB assay and differences between treatment conditions were statistically analysed in GraphPad PRISM (one-way ANOVA).

PARP-1 silencing significantly increased PC3 cell sensitivity to TSA treatment by 20%, compared to cells exposed to TSA, as shown in Figure 7.12. Control siRNA combined with TSA reduced PC3 cell survival by 3% compared to cells exposed to TSA alone. There was a 17% reduction in survival in PARP-1 silenced cells +TSA, compared to negative control.

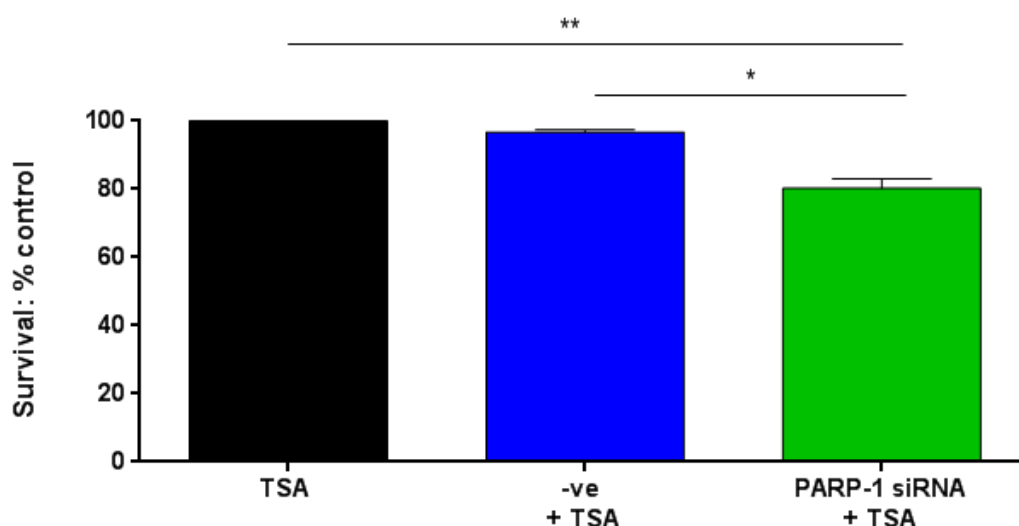


Figure 7.12: The effects of PARP-1 knockdown on PC3 sensitivity to TSA.

Percentage survival of PC3 cells relative to control following exposure to 50nM PARP-1 siRNA for 48 hours and 49nM TSA for 72 hours. Cell sensitivity was assessed using the SRB assay and differences between treatment conditions were statistically analysed in Graphpad PRISM (one-way ANOVA, *p<0.05, **p<0.01).

PARP-1 knockdown significantly enhanced PC3 cell sensitivity to Rucaparib and TSA co-treatment (Figure 7.13). Cell survival was 38% less when transfected with PARP-1 siRNA and exposed to co-treatment, compared to cells which were exposed to co-treatment alone. Cell survival in co-treated PC3 cells transfected with PARP-1 siRNA was significantly less ($p < 0.05$) than co-treated PC3 cells transfected with control siRNA (22% reduction).

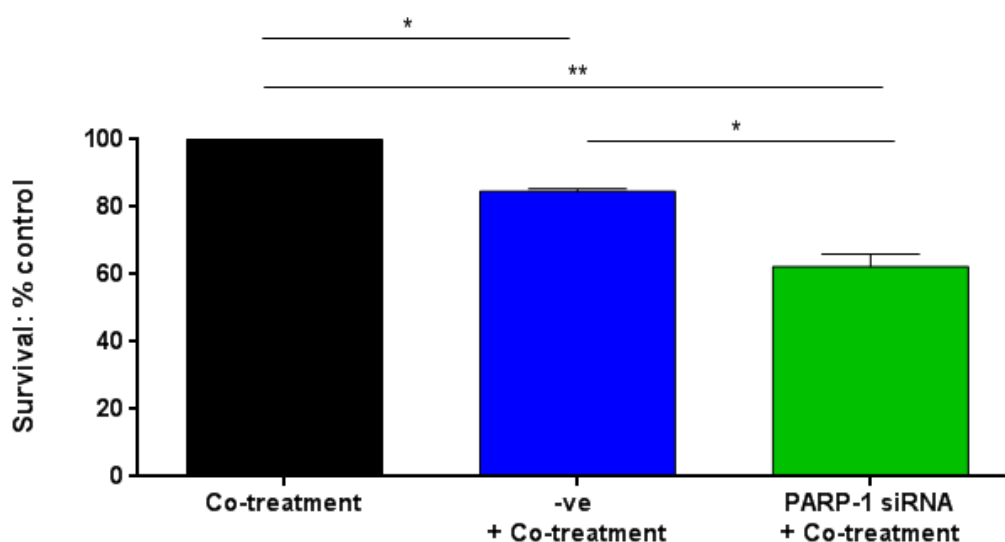


Figure 7.13: siRNA knockdown of PARP-1 enhances PC3 sensitivity to Rucaparib and TSA co-treatment.

Percentage survival of PC3 cells relative to control following exposure to 50nM PARP-1 siRNA for 48 hours and Rucaparib and TSA co-treatment for 72 hours. Cell sensitivity was assessed using the SRB assay and differences between treatment conditions were statistically analysed in Graphpad PRISM (one-way ANOVA, $*p < 0.05$, $**p < 0.01$).

The results presented in Figure 7.10 and Figure 7.13 demonstrate that PARP-1 silencing enhances cell sensitivity to Rucaparib and TSA co-treatment in DU145 and PC3 cells. Cell survival of DU145 and PC3 cells following PARP-1 silencing and exposure to co-treatment was compared and statistically analysed using an independent t-test. Data presented in Figure 7.14 shows no significant difference in cell survival between DU145 (69% survival) and PC3 (62% survival) cells subject to PARP-1 gene silencing and Rucaparib and TSA combined treatment.

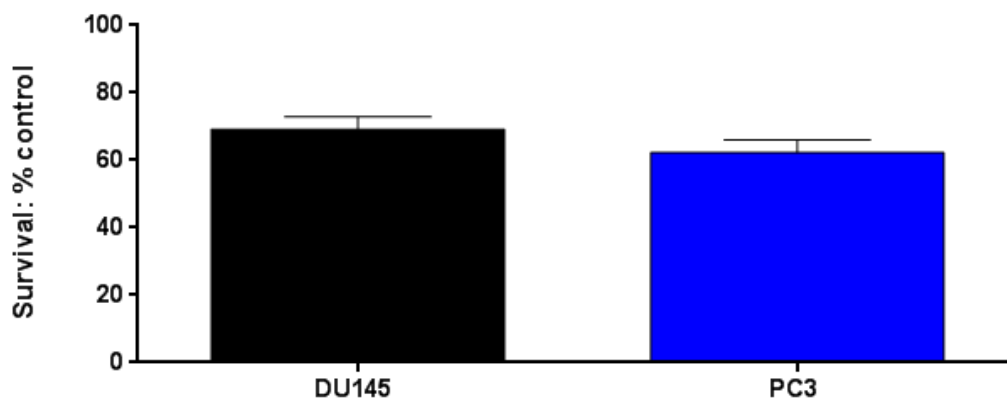


Figure 7.14: DU145 and PC3 cell survival following PARP-1 gene silencing and exposure to Rucaparib and TSA co-treatment. Basal PARP-1 status does not effect sensitivity to co-treatment.

7.4 Discussion

In this chapter, maspin and PARP-1 siRNA knockdown experiments were carried out to explore the role of maspin and PARP-1 expression on prostate cell behaviour and sensitivity to Rucaparib and TSA. PNT1A and PC3 cells were utilised to investigate the knock down of maspin and PARP-1 as these cells endogenously express these proteins. Based on previous optimisation studies, final concentrations of 10nM maspin (Louise Brown, unpublished results) and 50nM PARP-1 siRNA (Jill Hunter, unpublished results) were used.

7.4.1 The effects of maspin silencing on prostate cell sensitivity to Rucaparib and TSA.

The results presented in Figure 7.1 and Figure 7.2 show the optimum siRNA incubation times to achieve maspin knockdown in PNT1A and PC3 cells, respectively. A longer incubation time (72hours) was required to achieve successful maspin knockdown in PNT1A cells compared to PC3 cells (48hours). siRNA-induced gene knockdown efficiency and duration is dependent on a number of factors such as cell type, target mRNA turnover rate and cell location (Hong et al., 2014). These factors may explain the differences in knockdown between PNT1A and PC3 cells. There was no variance in proliferation rates between these cells (Table 3.4). PC3 cells express increased levels of maspin protein (Figure 3.9), therefore, maspin silencing is not likely due to the amount of basal maspin expression as the data shows silencing of maspin earlier (48hours) in PC3 cells, compared to PNT1A cells (72 hours). A potential reason for increased knockdown efficiency in PC3 cells may be maspin protein localisation in the cell. In mammalian cells intracellular proteins are targeted for proteasome degradation as part of cell regulation, such as

cell cycle and regulation of transcription factors (reviewed in Ciechanover (2005)). The data presented in Chapter Three, section 3.3.5, show that maspin is located in the cytoplasm and nucleus of PC3 cells but only the cytoplasm of PNT1A. Cytoplasmic localisation of maspin in PC3 cells may make maspin more readily targeted for degradation.

The PNT1A cell line model was utilised in the studies to provide mechanism on the effects of maspin on cell survival, in the presence of Rucaparib and TSA as single agents and in combination; to support patterns observed in earlier chapters where maspin depleted cell lines were shown to be more sensitive to Rucaparib. PNT1A cells are a “normal” wild type cell line proficient for maspin and could be considered the best prostate cell model to provide preliminary proof of principle data in our hands. siRNA-induced maspin silencing in PNT1A cells enhanced cell sensitivity to Rucaparib and TSA treatment, alone and in combination, demonstrating that maspin expression impacts cell sensitivity to PARP and HDAC inhibitors.

PNT1A cells were ~1.5-fold more sensitive to Rucaparib with maspin knockdown than maspin proficient cells exposed to cells exposed to control siRNA + Rucaparib. Maspin siRNA did not achieve 100% silencing and the effects on cell sensitivity would likely have been greater had it been achieved. The results are in line with our initial growth inhibition studies carried out in Chapter Four, section 4.3.1; whereby maspin depleted DU145 cells were 3.3 and 2-fold more sensitive to Rucaparib than PNT1A and PC3 cells, respectively. The results suggest that there is a selective sensitivity to Rucaparib in cells with less maspin; supporting a role for maspin as a predictor of sensitivity to PARP inhibitors. This may be in part due to enhanced expression of IKK α ; a driver of inflammation and carcinogenesis. Studies have demonstrated that active IKK α is coupled with metastatic potential through the attenuation of maspin. It has been shown that mutation preventing IKK α activation slows down PC growth and inhibits metastasis in human PC cells and a transgenic adenocarcinoma of the mouse prostate (TRAMP) model, and this was correlated to increased expression of maspin. Furthermore, siRNA-mediated knockdown of maspin increased the metastatic potential of IKK α ^{AA/AA} TRAMP cells (cells with an inactive allele of IKK α) to that of wild-type TRAMP cells (Luo et al., 2007). Immunohistological analysis of metastatic and non-metastatic cutaneous squamous cell carcinoma samples also reported an

inverse correlation between active IKK α and maspin. Samples negative for maspin were found exclusively in the metastatic group (Toll et al., 2015).

The protein expression data presented in Chapter Four, Figure 4.17, shows reduced expression of IKK α in maspin depleted DU145 cells exposed to Rucaparib; supporting a role for Rucaparib as an inhibitor of NF-kB in maspin deficient tumours. These results go hand in hand with data from previous studies which have demonstrated that potentiation of IR-induced cytotoxicity by PARP inhibition occurs only when NF-kB is present, suggesting that PARP-1 mediates its effects through NF-kB (Veuger et al., 2009, Hunter et al., 2012). The IKK α ^{-/-} MEF survival data in Chapter Four support the requirement for NF-kB to sensitise cells to PARP inhibitors; A GI₅₀ could not be achieved in IKK α ^{-/-} cells exposed to Rucaparib at increasing doses up to 50 μ M. These cells were shown to be proficient in the expression of maspin (Figure 3.13); supporting the prostate cell sensitivity data in Chapter Four where maspin proficient PNT1A and PC3 cells express reduced levels of IKK α . siRNA investigations have also demonstrated an inverse correlation between IKK α and maspin; reporting a significant upregulation of maspin in PC3 cells treated with IKK α siRNA for 48 hours (Mahato et al., 2011). PARP knockdown by PARP-1 siRNA has also evidenced reduced protein expression of IKK α in breast cancer models (Wielgos et al., 2018). These data support our findings and highlight the requirement of NF-kB for PARP signalling (Hassa et al., 2001).

HDAC-1 is highly expressed in some prostate cancers and its activity is considered a popular mechanism for the repression of various genes in cancer, such as tumour suppressor genes and genes which are implicated in cell cycle control and apoptosis (reviewed in Halkidou et al. (2004)). A link between increased HDAC-1 and a malignant phenotype has been reported, due to its role in modulating gene transcription and contribution to DNA damage signalling and repair on multiple levels (Weichert et al., 2008a, Weichert et al., 2008c). HDAC-1 targets various genes associated with the DNA damage response to mediate DNA repair, such as ATM, ATR, p53 and Ku70 (reviewed in Robert and Rassool (2012)). HDAC-1 prepares the chromatin surrounding DNA DSBs for activation of the DNA damage response pathway and assists in the sealing of

DSBs *via* NHEJ or HR (reviewed in Roos and Krumm (2016)). For example, HDAC1 proteins localise at the site of a DSB and promote binding of Ku70 for NHEJ. PARP-1 and Ku proteins compete for DNA repair (Wang et al., 2006). In the presence of reduced maspin and consequently increased HDAC-1, it could be postulated that there is a reduced ability for PARP-1 to access the DNA breaks and initiate repair.

It may be suggested that increased expression of HDAC-1 due to maspin silencing may contribute to increased PARP inhibitor sensitivity in cells which normally are HDAC-1 depleted and express increased levels of PARP-1. This effect may occur *via* the transcriptional repression of genes involved in DNA repair, such as PARP-1 and RAD51. Protein expression studies in this thesis have supported this theory, showing reduced expression of PARP-1 and RAD51 in maspin depleted DU145 cells, compared to maspin proficient cells (Figure 3.9 and Figure 6.9, respectively). Maspin silencing has also been shown to reduce the expression of PARP-1 in PC3 cells (Figure 7.6). HDAC-1 expression was not assessed but it is likely that it was upregulated in the absence of maspin. This is in line with protein expression data in Chapter Three and Chapter Four where DU145 cells, which express reduced levels of PARP-1, are most sensitive to Rucaparib. Maspin proficient PNT1A and PC3 cells, which express reduced levels of HDAC-1, exhibit reduced sensitivity to Rucaparib (data presented in Chapter Four). These cells also express increased levels of RAD51, indicating an ability to repair DSBs. To this end, we can postulate that silencing of maspin in PNT1A and PC3 cells will increase target for HDAC-1 inhibition which will in turn enhance cell sensitivity to TSA.

PNT1A cells were ~1.8-fold more sensitive to TSA following maspin knockdown with siRNA compared to those cells exposed to control siRNA + TSA; supporting that the loss of maspin is a tumorigenic event. Indeed, other studies have reported increased HDAC activity following maspin silencing by siRNA in PC3 cells (Li et al., 2006). More recently the same group suggested that down-regulation of maspin may increase pathological DNA methylation and epigenetic gene silencing in normal cells; contributing to a tumorigenic phenotype (Li et al., 2011). This may explain the increased sensitivity to TSA treatment in maspin silenced PNT1A cells. There was no significant difference in the cell sensitivity to TSA in maspin deficient and proficient DU145 and

PC3 cells in the studies presented in Chapter Four; indicating that the effect of TSA on cells is cell type dependant or independent to maspin expression status. Although the data suggests that the effects of TSA is independent to maspin expression status in these cells, given that the cells aren't isogenic and we don't know the complement of other complexes in which HDAC-1 may act, therefore, differences between these cell lines may not be as great as when using siRNA. The effects of TSA in the presence of maspin siRNA was not tested in DU145 and PC3 cell lines. The increased sensitivity to TSA in response to maspin knockdown in PNT1A cells may be due to increased HDAC activity, and therefore more target, and consequently changes to the acetylation state of transcription factors and other proteins in the cell, as previously discussed. PNT1A cells present increased DNA DSBs in the presence of chemical HDAC inhibition by TSA at GI_{50} (Table 4.3); demonstrating an ability for "normal" cells to withstand, and repair, DNA breaks induced by HDAC inhibition. This goes hand in hand with the RAD51 expression data presented in Chapter Six, Figure 6.9, where RAD51 expression, a marker for HR-mediated DNA repair, was not reduced in the presence of TSA, in PNT1A cells.

PNT1A cell sensitivity to Rucaparib and TSA co-treatment was enhanced ~1.6-fold in the presence of maspin siRNA compared to siRNA control cells exposed to co-treatment; demonstrating that maspin indeed affects cell sensitivity to treatments. Co-treatment was more effective than Rucaparib alone, but no more effective than TSA alone, in the presence of maspin siRNA, implying a rescue effect by Rucaparib. This does not fit with the sensitivity data in Chapter Four whereby co-treatment was additive in maspin depleted DU145 cells. However, there could be a range of things going on that may contribute to this finding such as the pleotropic effects of HDAC-1 inhibitors at the cellular level. Nevertheless, the data highlights that maspin affects cell response to treatments and provides a proof of principle for targeting tumours which are deficient for maspin.

7.4.2 The effects of maspin knockdown on PARP-1 protein expression in PC3 cells exposed to Rucaparib and TSA.

PC3 cells were utilised to investigate the effects of maspin knockdown on PARP-1 protein expression following PARP and HDAC inhibition. These cells express the highest levels of

PARP-1 and were selected for use to provide a proof of principle association between maspin and PARP-1 in a cancer model. The results presented in Figure 7.6 show reduced expression of PARP-1 in the presence of maspin siRNA; highlighting a correlation between maspin and PARP-1 protein expression. These findings are in line with the expression data presented in Chapter three section 3.3.5; whereby PARP-1 protein expression levels were low in maspin depleted DU145 cells and high in maspin proficient PC3 cells. Therefore, reduced expression of PARP-1 in response to maspin silencing in PC3 cells may be a potential mechanism to drive tumorigenesis via NFkB.

The expression of PARP-1 protein was further reduced in maspin silenced PC3 cells exposed to Rucaparib. These results demonstrate a correlation between maspin and PARP-1 expression levels. PARPi's, such as Rucaparib primarily inhibit PARP-1 enzyme activity rather than expression. A previous study explored the role of PARP-1 activity and expression in a range of human cancer cell lines; reporting no significant positive correlation between PARP-1 expression and PARP-1 activity (Zaremba et al., 2009). This is in line with the protein expression data for PARP-1 presented in Chapter Four, Figure 4.18 whereby the expression of PARP-1 protein was unchanged following inhibition of PARP activity by Rucaparib.

PARP-1 inhibition and increased histone deacetylase activity in response to maspin silencing may contribute to the reduction in PARP-1 protein expression shown in Figure 7.6. Histone modifications have been widely recognised in the control of gene expression and disease regulation (Chen et al., 2015). Increased HDAC activity influences biological processes that contribute to carcinogenesis such as cell proliferation and inflammation. HDAC activity has also been implicated in the modification of ADP ribosylation; a process implicated with PARP (Bassett and Barnett, 2014).

PARP-1 protein expression was reduced in maspin silenced PC3 cells treated with TSA, compared to maspin silenced PC3 cells without treatment. This result was unexpected as the data presented in Chapter Four, Figure 4.17, showed that PARP protein expression levels were not changed by exposure to TSA in maspin depleted DU145 cells. To this end, the findings suggest that the mechanism by which TSA inhibits HDAC-1 activity and epigenetically regulates PARP-

1 is independent to the inhibitory effects of HDAC-1 by maspin. It can be postulated that maspin, an endogenous inhibitor of HDAC-1, may regulate HDAC in a more specific and selective manner, dependent on cellular and molecular contents, compared to pharmacological HDAC inhibitors which can enhance the deacetylation of a large number of genes in an unspecific manner (reviewed in Kaplun et al. (2012)). This may explain why we see a reduction in the expression of PARP-1 following exposure to TSA in maspin silenced PC3 cells, compared to PC3 cells which expression maspin.

PARP-1 protein expression was reduced in maspin silenced PC3 cells exposed to Rucaparib and TSA co-treatment, but the effects were not greater than maspin silenced PC3 cells exposed to either Rucaparib or TSA as single agents. These data do not correlate to the DU145 data in Chapter Four, where DU145 cells (depleted in maspin) express reduced levels of PARP-1 protein in the presence of co-treatment, compared to either treatment alone (Figure 4.17). The varied effects of co-treatment on the expression of PARP-1 in maspin depleted/silenced cells could be due to the fact that these PC3 and DU145 are not isogenic and therefore differential off target effects of the drugs in combination may lead to changes in epigenetic regulation between cell lines. Furthermore, in PC3 cells, we have shown successful knockdown of maspin at 48 hours (Figure 7.2), although 100% knockdown was achieved and we can't confirm that maspin remains silenced for the duration of drug exposure (a further 72 hours from knockdown). This could also be attributable to the differential findings between maspin depleted DU145 cells and maspin silenced PC3 cells exposed to co-treatment. Nevertheless, the expression of PARP-1 protein is reduced in maspin silenced PC3 cells, compared to maspin expressing cells; with and without exposure to Rucaparib and TSA as single agents, and in combination.

7.4.3 The effects of PARP-1 silencing on prostate cell sensitivity to Rucaparib and TSA.

The results presented in Figure 7.7 show an optimum siRNA incubation time of 48 hours to achieve PARP-1 knockdown in DU145 and PC3 cells, respectively.

PARP-1 was silenced in DU145 and PC3 cells to investigate the theory of PARP-1 “trapping”. The theory proposed that PARP inhibition is more cytotoxic than PARP-1 loss/inactivation due

to the trapping of PARP-1 at DNA breaks (Murai et al., 2012). Our data aimed to elucidate whether PARP-1 silencing had a similar effect.

PARP-1 silencing had no significant effect on DU145 or PC3 cell sensitivity to Rucaparib (Figure 7.8 and Figure 7.11); suggesting that increased sensitivity to Rucaparib in DU145 cells (Chapter four) may not be an effect of low PARP-1 protein expression. A potential reason for a lack of significant alteration to Rucaparib sensitivity with PARP-1 silencing could be that 100% PARP-1 knockdown was not achieved and residual PARP activity may be present from PARP-1 and PARP-2; the closest paralog of PARP-1 (Luo and Kraus, 2012b). Another explanation for an insignificant sensitivity to Rucaparib is that we cannot be sure how long PARP-1 knockdown is lasting. Optimum knockdown was ascertained at 48 hours and was still occurring at 72 hours; but given that inhibitors were present for a further 72 hours following optimum knockdown, we cannot be sure that silencing is occurring for the duration of the experiment. As we were unable to achieve complete PARP-1 silencing or a loss of effect to Rucaparib we were unable to determine whether PARP-1 trapping occurs in the presence of PARP-1 silencing. The results conclude that the sensitivity to Rucaparib in DU145 cells (Chapter Four) is likely related to the differential expression of IKK α and maspin as opposed to PARP-1.

The data presented in Figure 7.9 show a 12% reduction in DU145 cell survival in the presence of TSA treatment and PARP-1 siRNA, compared to cells exposed to TSA alone. Cells transfected with control siRNA were 8% more sensitive to TSA treatment than cells exposed to TSA alone, but less sensitive than cells subject to PARP-1 silencing with TSA. Despite a 4% increase in sensitivity to TSA in DU145 cells exposed to PARP siRNA compared to control siRNA the effects were insignificant; highlighting that PARP-1 silencing had no effect on DU145 cell sensitivity to chemical HDAC inhibitors.

PC3 cells transfected with PARP-1 siRNA were significantly more sensitive to TSA than cells exposed to control siRNA + TSA. The mechanism responsible for enhanced PC3 cell sensitivity to TSA following PARP-1 silencing in these cells is unknown. It could be postulated that the effects are independent to PARP-1 and maspin expression. If these proteins were implicated, we would have expected TSA sensitivity to be variable in DU145 and PC3 cells, that express different

levels of PARP-1 and maspin proteins. Differential sensitivity to TSA was not found in these cells (growth inhibition data presented in Chapter Four, Table 4.3). We are unable to draw firm conclusions from the data as the cells lines that are not isogenic and express different proteins, thus additional complexities may be at play, however the siRNA data does add strength to the hypothesis that inhibition or knockdown of PARP-1 and HDAC-1 in combination has potential for cancer therapy.

Interestingly, PARP-1 silenced DU145 and PC3 cells were significantly more sensitive ($p < 0.05$, $p < 0.01$, respectively) to Rucaparib and TSA co-treatment than cells control siRNA cells + combination and cells which express PARP-1 exposed to combination alone. PARP-1 expression and regulation is a complex process involving various different mechanisms (Krishnakumar and Kraus, 2010). The effects of PARP-1 silencing and inhibition have been investigated in other studies that have used synchronised isogenic HeLa cells proficient or deficient for PARP-1. PARP-1 inhibition and silencing were shown to have differential effects on DNA SSB repair and radio sensitivity. SSB repair was reduced 10-fold in PARP-1 proficient cells compared to PARP-1 silenced cells exposed to PARP inhibition. PARP-1 silenced cells were 2.5-fold more sensitive to IR compared to PARP-1 proficient cells (Godon et al., 2008). PARP-1 siRNA prevents PARP-1 recognition and binding to DNA breaks to initiate NHEJ. This may allow other molecules to bind to the exposed DNA breaks, leading to the regulation and modification of other signalling pathways. Inhibition of residual PARP-1 enzymatic activity by Rucaparib limits PARP-1 enzymatic binding to the site of DNA breaks and binding of Rucaparib to DNA breaks prevents the binding of other molecules. This may explain why PARP-1 deficient cells are increasingly sensitive to Rucaparib and TSA co-treatment.

There was no significant difference in cell survival between DU145 and PC3 cells subject to PARP-1 silencing and co-treatment. These results are in line with the survival data in Chapter Four where there was no difference in cell sensitivity to co-treatment, at respective GI_{50} concentrations, between DU145 and PC3 cells. This reiterates that the effects of co-treatment in relation to PARP-1 expression may be independent to maspin status. The results in this chapter help to demonstrate the complex interplay between maspin, PARP-1 and drug actions and raises

questions about the role of NF- κ B in these responses. It can be postulated that PARP-1 inhibition and depletion limits DNA repair via NHEJ and consequently cells rely on HR for DNA repair. HDAC inhibitors limit HR, and therefore the drug combination is synthetically lethal to tumour cells.

7.5 Summary

The studies presented in this chapter have shown that:

- Maspin siRNA sensitises PNT1A cells to Rucaparib; demonstrating a selective sensitivity to PARP inhibitors in cell expressing reduced maspin. This may be in part mediated by increased levels of IKK α .
- TSA was not additive to cell sensitivity to Rucaparib in the presence of maspin siRNA.
- Maspin siRNA reduces the expression of PARP-1 in PC3 cells. A possible mechanism for this is increased levels of HDAC-1 due to maspin knockdown, and consequently deacetylation of PARP-1.
- Rucaparib and TSA treatments, alone and in combination, further reduce the expression of PARP-1 in the presence of maspin siRNA, but effects are greatest in cells exposed to Rucaparib and TSA as single agents.
- PARP siRNA does not affect sensitivity to Rucaparib in DU145 and PC3 cells, supporting that increased sensitivity to Rucaparib in DU145 cells is related to depleted levels of maspin rather than PARP-1.
- PARP siRNA does not enhance DU145 cell sensitivity to TSA but does PC3 cells. These effects may be due to interference with other molecular mechanisms within the cell lines.
- PARP siRNA significantly enhances DU145 and PC3 cell sensitivity to Rucaparib and TSA co-treatment. This may be due to synthetic lethality; whereby PARP-1 depletion and inhibition hinders DNA repair by NHEJ and inhibition of HDAC-1 by TSA limits repair via the HR backup pathway.

7.6 Future work

Future work could investigate the effects of maspin siRNA on PC3 cell sensitivity to treatments, to compare against the findings obtained in PNT1A cells. The effects of maspin siRNA on cell sensitivity to treatments could also be explored in isogenic cell lines proficient and deficient for IKK α to add strength to the known links between maspin and IKK α , and differential sensitivity to treatments. The effects of maspin siRNA on IKK α and HDAC-1 expression were not explored due to time constraints. Studies utilising IKK α siRNA to look at the expression of maspin and PARP-1 proteins would strengthen the existing data and confirm or refute a mechanism between maspin, IKK α and PARP-1. The effects of PARP-1 silencing on sensitivity to treatments, alone and in combination, could also be explored in isogenic cells proficient and deficient for PARP-1.

Chapter Eight

Summary and future directions

The increase in cancer incidence is evidenced by recent statistics suggesting that 1:2 people in the UK will develop the disease during their life. The most common forms of cancer in males and females are those of the prostate and mammary gland respectively, making research into these conditions of great importance. Of particular interest are new therapeutic targets and combinations potentially allowing specific focus on aggressive, metastatic cancers which are associated with a poor prognosis.

PARP inhibitors were originally developed for their ability to potentiate existing chemotherapeutics or radiotherapy. PARP inhibitors have been investigated and often found to be effective in a range of clinical settings, in combination with chemotherapies or as maintenance therapies in recurring tumours including those derived from the breast, ovaries, colon and prostate (reviewed in Mirza et al. (2018)). Studies have also investigated the efficacy of PARP inhibitors for the treatment of non-oncological diseases such as stroke, myocardial infarction, chronic heart failure and neurodegenerative diseases. Use of PARP inhibitors for myocardial infarction is the only non-oncological indication to result in clinical study (reviewed in Curtin and Szabo (2013)). In 2005 with the realisation that *BRCA* defective tumours are exquisitely sensitive to stand alone PARP inhibitor therapy, the landscape changed such that, in oncology, the focal point of research for the last 15 years has been cancers which are defective in *BRCA1/2* and DNA repair by homologous recombination (HR). More recently, and with the advent of a growing body of evidence and mechanisms of PARP inhibitor resistance (Noordermeer and van Attikum, 2019), PARP inhibitors in combination with other therapeutics has once again become a focus. Repurposing of PARP inhibitors is a vastly growing area and further research is needed to elucidate other novel ways of using these drugs (and other repair inhibitors) to provide personalised cancer therapy. Further successful clinical application of PARP inhibitors requires the identification of predictive markers for tumours likely to be susceptible. Described in this thesis are the stand-alone effects of the PARP inhibitor Rucaparib and then in combination with

the HDAC inhibitor TSA. This work did not investigate the potentiation of cancer therapeutics such as ionising radiation (IR).

Rucaparib was selected for use in the studies presented in this thesis. There are currently four PARP inhibitors approved by the FDA for anticancer therapy: Olaparib, Rucaparib, Niraparib and Talazoparib. Olaparib was the first PARPi to enter clinical practise for ovarian tumours and it has been extensively used in research studies. For example, in November 2018, 48% of ovarian cancer trials used Olaparib, compared to 7.3% of trials with Rucaparib (reviewed in Yi et al. (2019)). All approved PARPis have shown comparable inhibition of PARP-1, however, Rucaparib inhibits PARP-1, PARP-2 and PARP-3. PARP-3 has been reported to trigger the activity of PARP-1 in the absence of DNA. Additional inhibition of PARP-1 may potentiate Rucaparib's effects (reviewed in LaFargue et al. (2019)). Rucaparib is currently being researched in a range of advanced solid tumour types, independent of BRCA status, such as prostate and urethral cancers (Wilson et al., 2017, Garje et al., 2020).

It has recently been reported that the phenotypic and therapeutic relevance of *BRCA1/2* mutations is poorly defined in most cancer types (Jonsson et al., 2019). *BRCA1/2* mutation is not an agnostic marker for PARPi response and more biomarkers are required (reviewed in (Curtin et al., 2019)).

Maspin is required for epithelial specific gene expression. The expression level of Maspin in normal epithelial cells is much higher than that in malignant cells. It has pleiotropic effects; maspin has a large number of intracellular partners and has been shown to regulate cellular response to oxidative stress and increase tumour cell sensitivity to drug-induced apoptosis. Maspin also acts as a suppressor of metastasis in different types of cancer including prostate. In breast, colon, thyroid, lung, oral squamous, and prostate cancer, increased maspin expression predicts a better prognosis (reviewed in Berardi et al. (2013) and outlined in Table 1.4 and Table 1.5). Maspin interacts and endogenously inhibits HDAC-1 (Kaplun et al., 2012) and chemical inhibition of HDAC has been found to prevent activation of NF-kB (Place et al., 2005). Studies with PC cells and clinical specimens have demonstrated re-expression of maspin following inhibition of HDAC-1 (Abbas and Gupta, 2008). This antagonistic expression pattern may be in part due to reduced $IKK\alpha$.

The HDAC inhibitor TSA was selected for use in the studies presented in this thesis. It is commonly selected for use in laboratory investigations due to its high potency and toxicity. It is a cheap and effective HDAC inhibitor for use in preliminary experiments and was readily available within our laboratory. It exhibits the same biological effect as SAHA (Vorinostat), an analogue of TSA that has been approved for use in cutaneous T-cell lymphoma by the FDA (reviewed in Eckschlager et al. (2017)).

Previous work in our group has shown that PARP inhibitors mediate their effects via NF- κ B (Veuger et al., 2009, Hunter et al., 2012). An important paper in Nature suggested that a reason men get prostate cancer is because of the loss of maspin expression via a pathway downstream of NF- κ B (Luo et al., 2007).

The primary aim of the work presented in this thesis was to investigate the effects of PARP-1 and HDAC-1 inhibitors (alone and in combination) on cell behaviours in cell lines expressing varied levels of the tumour suppressor maspin. A relationship between maspin and NF- κ B was explored in relation to cell sensitivity to these treatments. To achieve this aim, at the outset of this work, a role for PARP-1 inhibitors in maspin deficient tumours was investigated.

The initial cell models intended for use in the studies carried out in this thesis were breast tumour MCF-7 cells. These cells are stably transfected with the pcDNA 3.2 vector containing maspin and mutant maspin to produce the stable cell lines MCF-7 empty vector (MCF-7 CTR), MCF-7 maspin (MCF-7 MTR) and MCF E224A (MCF-7 244) as described in (Ravenhill et al., 2010). During preliminary characterisation and optimisation studies, these cells presented inconsistent growth patterns and become frequently contaminated. Upon further investigation by Western blotting, the maspin transfected cell samples were found to lack expression of maspin; indicating that the plasmid had been lost. The transfected cells were obtained from an external source and it was not possible to generate new stably transfected cell lines. For this reason, these cell models were not suitable for use and were not taken forward in the experiments presented in this thesis.

The FDA has approved PARP inhibitors for treatment of metastatic breast, ovarian and related cancers. During this PhD project, in late 2018, the FDA granted “breakthrough therapy” status for the use of Rucaparib in *BRCA1/BRCA2*-mutated metastatic castrate-resistant prostate cancer (mCRPC); based on initial data from the TRITON-2 phase 2 clinical trial (Adashek et al., 2019). According to the drug manufacturer AstraZeneca, the FDA have also granted “breakthrough therapy” status for the use of Olaparib in patients with mCRPC (AstraZeneca, 2020). Thus, the data presented in this thesis utilised prostate cancer cell lines PC3 and DU145 proficient or depleted for Maspin, respectively. An immortalised prostate cell line, PNT1A was also used. Mouse embryonic fibroblasts (MEF) proficient and deficient for NFκB p65 and IKKα were also utilised to compare maspin protein expression levels and to investigate sensitivity to treatments. All cell lines were characterised in Chapter Three. Importantly, data presented in Chapter Three verified the characteristics of the cell models used throughout this thesis to ensure that cells were of the correct genotype and phenotype for subsequent studies. DU145 cells were selected for use as published data suggested that DU145 are entirely deficient of Maspin (Ravenhill et al., 2010). However, in our hands, DU145 cells express maspin albeit negligible levels at much lower levels than PC3 or PNT1A cells (maspin expression was 7.4 and 6-fold higher in PC3 and PNT1A cells compared to DU145 cells, respectively); therefore, these cells are referred to as maspin depleted cells throughout this thesis. Others have also reported increased expression of maspin in PC3 cells compared to DU145 cells (McKenzie et al., 2008). The effect of PARP and HDAC inhibitors on various biological endpoints such as cell survival, migration and DNA strand break formation were investigated in Chapters Four, Five and Six, respectively. In Chapter Seven mechanistic studies were carried out with use of siRNA to explore the roles of maspin and PARP-1 in cell survival following treatment with Rucaparib and TSA, alone and in combination.

A number of key conclusions were drawn from each section of this thesis, the most pertinent and novel being that;

- Maspin deficiency sensitises prostate tumours to the stand-alone effects of PARP inhibitors.

- PARP inhibitor stand-alone effects are at least in part mediated via down regulation of $IKK\alpha$
- Maspin expression may represent a novel predicative biomarker for PARP inhibitor sensitivity in prostate cancers.
- Combination of PARP-1 and HDAC inhibitors represents a promising therapeutic strategy for prostate cancer irrespective of *BRCA* status.

The key data underpinning these findings are summarised below. Two proposed models (Figure 8.1 shows both the stand-alone effects of Rucaparib in maspin depleted tumours (left side) and the many facets of PARP-1 action and potential effects of combination therapy (right side). Figure 8.2 shows a proposed mechanism of PARP trapping in response to combination therapy of Rucaparib and TSA) have been generated to summarise the findings and hypothesis generate by the work in this thesis.

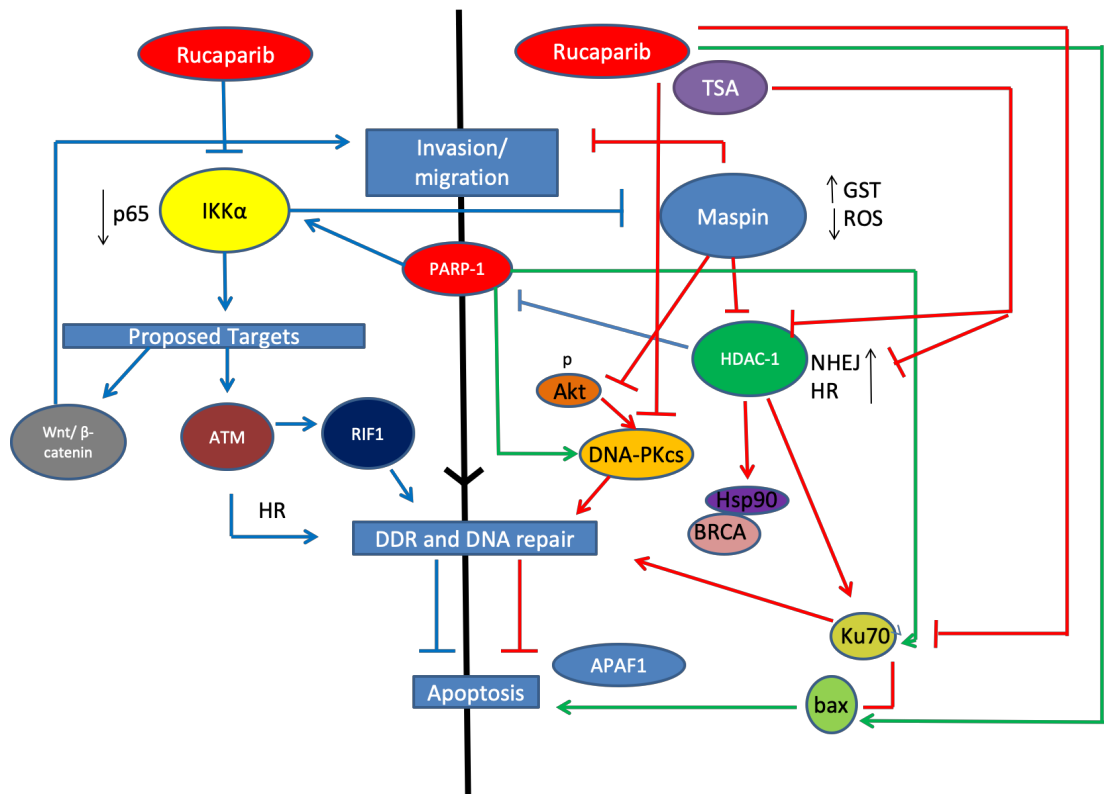


Figure 8.1: Hypothetical model for the stand-alone effects of Rucaparib and the many facets of PARP-1 action.

The left side of the model proposes the stand-alone effects of Rucaparib. In the presence of high IKK α , and consequently depleted maspin, Rucaparib targets IKK α and reduces it, independently of NF- κ B. IKK α inhibition by Rucaparib limits cell survival, migration and induces DNA breaks leading to apoptosis. These effects are mediated through the downregulation of proposed targets implicated in cell migration (β -catenin) and DNA damage and repair (ATM and RIF1); in response to inhibition of IKK α . Depleted maspin therefore acts as a biomarker for tumours high in IKK α which may be targeted by PARP inhibition for cancer therapy. Flat ends of lines represent inhibition and arrows represent excitatory effects. **The right side of the model** proposes that maspin inhibits HDAC-1 which limits stimulation of DNA-PKcs, deacetylation of Ku70 and sequestering of bax. Maspin also inhibits phosphorylation of Akt which reduces DNA-PKcs activity and DNA repair by NHEJ. Inhibition of HDAC-1 also causes hyperacetylation of HSP90, leading to its inhibition. Proteins that interact with HSP90 including BRCA cannot do so and are degraded. Rucaparib blocks/inhibits Ku70/DNA-PKcs and blocks NHEJ. It may also activate bax, leading to increased apoptosis. HDAC inhibition blocks DNA-PKcs and induces “BRCAness” and consequently a HR repair defect. Combined inhibition of Rucaparib and TSA inhibits DNA repair via both NHEJ and HR, resulting in synthetic lethality. Excess DNA damage resulting from combined treatment may also activate APAF1, a pro-apoptotic protein required for apoptosis. This proposed mechanism of action is depicted with red and green lines. Red lines with flat ends represent inhibition and red lines with arrows represent the downstream effects which are limited in the presence of maspin and therefore inhibition of HDAC-1. If maspin was depleted or inhibited these red arrows would be green. Green arrows show activation.

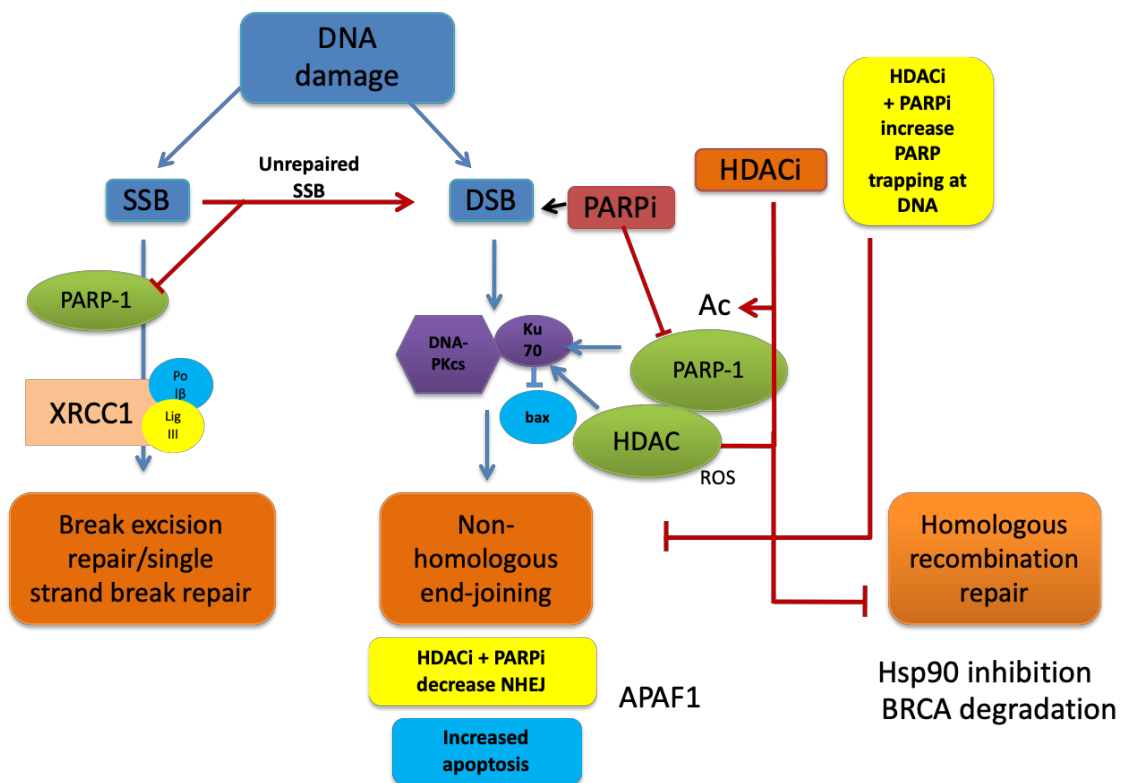


Figure 8.2: Hypothetical model for the combined effects of Rucaparib and TSA in the context of PARP trapping.

DSBs pose a major threat to genomic integrity. They arise as a result of exposure to DNA damaging agents such as IR and chemotherapy, ROS or when replication forks encounter DNA lesions. PARP inhibitors also limit the repair single strand DNA lesions and contribute to the accumulation of DSBs. In the presence of a HDACi, PARP-1 is acetylated and activated to activate and recruit DNA-PKcs for DNA repair by NHEJ. Inhibiting HDAC-1 causes acetylation of Ku70 leading to its inactivation and release of pro-apoptotic factor bax. The balance between DNA repair and cell death is dependent on the amount of DNA damage, damage tolerance or regulation of signalling pathways involved in DNA repair. Combined HDAC and PARP inhibition decreases NHEJ and increases apoptosis by trapping PARP-1 at the site of the DNA break which in turn, blocks access to DNA-PKcs. HDACi's also hinder DNA repair *via* HR and induce a “BRCAness phenotype”. Thus, in the presence of combined treatment, NHEJ is hindered, BRCA is degraded and cells are unable to rely on DNA repair *via* HR. Consequently, cells are subject to cell death.

The data presented in this thesis has contributed to a manuscript published in Molecular Cell Research in 2017 (Jenkinson et al., 2017). A further two manuscripts are under preparation;

- Repurposing of PARP inhibitors for maspin deficient tumours
- Co-targeting of HDAC and PARP for prostate cancer therapy

8.1 The stand-alone effects of the PARP inhibitor Rucaparib in prostate cells of varying maspin expression

Previous research has demonstrated that radio-resistance is mediated by NF- κ B activity since PARP inhibitors could only radio-sensitise NF- κ B proficient but not deficient tumour cell lines (Veuger et al., 2009, Hunter et al., 2012). Veuger et al, demonstrated that only p65^{+/+} MEFs and not p65^{-/-} MEFs were sensitised to IR by a very low non-toxic dose of 0.4 μ M PARP inhibitor. In the studies presented here, we explored the stand-alone effects of the PARP inhibitor Rucaparib at much higher doses of 0-50 μ M in the context of lowered or absent maspin with a view to provide insight into the potential interplay between PARP-1, maspin and NF- κ B.

NF- κ B plays a key role in the regulation of immune response and is activated by canonical and non-canonical pathways; both of which are tightly regulated by an IKK complex comprised of IKK α , IKK β and NEMO, as described in Chapter One.

Cell survival following exposure to Rucaparib, as measured by SRB assay and cell counting, correlated positively with maspin status, with the calculated GI₅₀ in PTN1A, PC3 and DU145 cells being 28 μ M, 16 μ M and 8 μ M, respectively. These survival data correlate with epifluorescence data in Chapter Four; indicating enhanced apoptosis in all cell lines exposed to Rucaparib with higher nuclear fragmentation and cell shrinkage in the DU145 cells. Maspin knockdown reduced levels of PARP-1 in PC3 cells (data presented in Figure 7.6) which is interesting as DU145 cells also have lower PARP expression than PC3 cells. One proposed mechanism is that reduced maspin will lead to elevated HDAC-1 levels, deacetylation of PARP-1 by HDAC-1 has been shown to affect PARP-1 at the transcriptional level through deacetylation of the promoter (Rajamohan et al., 2009). Therefore, it might be argued that it is this reduction in PARP-1 expression, and therefore activity, that leads to an increase in sensitivity to Rucaparib following maspin siRNA and thus may also account for the differential sensitivity to Rucaparib between DU145 and PC3 cells. PARP activity was not directly measured in the studies described here and this should certainly be carried out in future. However, data in Chapter Seven show that knockdown of PARP-1 in DU145 and PC3 cells did not significantly affect sensitivity to Rucaparib and it is therefore unlikely that enhanced sensitivity to Rucaparib is due to lower

PARP-1 levels. Many studies have attempted to correlate PARP-1 expression with sensitivity to PARP inhibitors and they give varied data and are context dependent. The vast majority conclude that higher PARP-1 activity correlates with increased sensitivity with many citing low PARP levels as a resistance mechanism. For example, a recent cervical cancer study reported a strong correlation between PARP activity and sensitivity to Olaparib (Bianchi et al., 2019). Moreover, addition of maspin siRNA #1 sensitised PTN1A cells to Rucaparib, enhancing sensitivity by ~1.5-fold, compared to control siRNA + Rucaparib. Interestingly, reduced cell survival following Rucaparib exposure was seen in p65^{-/-} MEFs while no GI₅₀ could be obtained in IKK α ^{-/-}MEFs. This led us to consider the possibility that stand-alone PARP inhibition can mediate effects via other subunits of NF-kB. It was hypothesised that IKK α activity could negatively regulate maspin expression particularly as p65^{-/-} MEFs express more IKK α than p65^{+/+} MEFs. In support of these findings; the IKK α knockout MEF cells expressed increased levels of maspin and DU145 cells depleted for maspin expressed the highest amount of IKK α . These findings are in line with other studies that have demonstrated downregulation of maspin by IKK α ; characterised by increased IKK α expression in the absence of maspin (Mahato et al., 2011, Alameda et al., 2011). The results from Chapter Three therefore confirmed an inverse correlation between maspin expression and IKK α . It has been shown that IKK α can interact with the promoter of the maspin gene which resulting in gene silencing. IKK α mediated inhibition of maspin expression has been proposed to commit prostate cancer to a metastatic fate (Luo et al., 2007). In line with this, our data using siRNA for maspin in PC3 cells (Chapter Five) showed increased cell migration as measured by xCELLigence, albeit this was a single experiment. Strikingly, knockdown of maspin (siRNA #1) enhanced PC3 cell migration by 23-fold at 48 hours. IKK α could therefore be targeted for prostate cancer therapy (reviewed in Gamble et al. (2012)), however, at the time of writing this thesis, IKK inhibitors are yet to be used therapeutically in the clinic. IKK α is an NF-kB activator and affects NF-kB in both of its two pathways (described in Chapter One) as well as having NF-kB independent roles. In the canonical pathway IKK α forms an IKK complex with IKK β and NEMO to mediate the phosphorylation of IKB α and in turn activate NF-kB. In the non-canonical pathway IKK α exerts its effects by liberating the RelB complex to enable NF-kB activation.

Several lines of evidence have indicated that IKK α functions as an oncogenic molecule and promoter of cancer progression and metastasis in a range of tumour types. Of specific relevance to the studies described here, the amount of nuclear IKK α in human prostate cell lines correlates with metastatic progression and studies have shown that a mutation preventing IKK α activation slows down prostate cancer growth and inhibits metastagenesis (Luo et al., 2007). Others have demonstrated that blocking IKK α expression in DU145 and PC3 cells using synthetic siRNAs inhibited prostate cancer cell invasiveness, migration, growth and attachment (Mahato et al., 2011). Interestingly, a nuclear function of IKK α has been implicated in tumour progression with nuclear IKK α promoting pancreatic cancer through inhibition of maspin expression (discussed in Alameda et al. (2011)). Cell localisation studies carried out in Chapter Three revealed that IKK α was both nuclear and cytoplasmic in all prostate cells, however, expression was predominantly cytoplasmic in the PTN1A and PC3 cells. Intriguingly, there was increased nuclear expression of IKK α , indicative of activation, in DU145 cells.

Maspin depleted DU145 cells expressed reduced levels of the NF-kB subunit p65 but increased levels of IKK α while PC3 cells expressed increased levels of NFkB p65 and reduced levels of IKK α . The results in Chapter Three therefore highlighted a correlation between maspin and NF-kB p65 and an inverse correlation between these proteins and IKK α . It may be that IKK α regulates the level of p65. For example, Lawrence et al. (2005) demonstrated accelerated removal of p65/p50 NF-kB subunits from proinflammatory gene promoters by IKK α which limited the activation of NF-kB. siRNA for PARP-1 has been shown by others to lower levels of IKK α (Wielgos et al., 2018). This was not investigated in the studies presented in this thesis. Although the effect of siRNA for PARP-1 on IKK α has been previously investigated, at the time of writing this thesis, no studies have been conducted on the effect of a PARP inhibitor on IKK α protein levels and correlated this with maspin status. Given there was a correlation between maspin levels and Rucaparib sensitivity, we investigated the effect of Rucaparib on IKK α protein expression levels. Protein expression data in Chapter Four demonstrated that Rucaparib was able to decrease the levels of IKK α in both PC3 and DU145 cells. Strikingly the level of IKK α was unchanged in the normal PTN1A cells that were least sensitive to Rucaparib. These results indicate that

activation of IKK α may be reduced in the presence of a PARP inhibitor, supporting the role of PARP-1 as a co-activator of NF- κ B. The expression of maspin and NF- κ B p65 in DU145 and PC3 cells exposed to Rucaparib for 72 hours was unchanged; indicating that sensitisation to Rucaparib may occur by altering the expression of IKK α and not p65. PARP inhibitor resistant cell lines have been shown to be re-sensitised by an IKK α inhibitor BAY 11-7082 (Nakagawa et al., 2015).

Others have also suggested that PARP inhibitors may mediate their effects *via* IKK α . Her2 overexpressed tumours are hypersensitive to PARP-1 inhibition independently of any defect in HR DNA repair (Wielgos et al., 2018). An earlier study by Merkhofer et al. (2010) reported that Her2 overexpression activates the canonical NF- κ B signalling pathway via the IKK α , catalytic subunit of the IKK complex, without the stimulation of an inflammatory stimuli such as TNF α . Thus, the sensitivity of Her2 overexpressing tumours to PARP inhibitors may in part be due to inhibition of IKK α activation of the canonical NF- κ B pathway. Although this is in line with our previous studies suggesting that potentiation of IR by a PARP inhibitor is mediated *via* NF- κ B p65, as described above (Veuger et al., 2009), expression data presented in this thesis suggest that the effect of stand-alone treatment with Rucaparib on IKK α is independent of the canonical pathway. The RelB protein expression data in Chapter Three suggests that the effects of Rucaparib on IKK α are also independent to the non-canonical NF- κ B signalling pathway. RelB protein expression levels were lowest in DU145 cells and highest in PC3 cells. Expression was confined to both the cytoplasm and nucleus of PNT1A and DU145 cells but confined only to the nucleus in PC3 cells. If the effects of Rucaparib were *via* the non-canonical NF- κ B signalling pathway, we would have expected PC3 cells, expressing high active levels of RelB, to be more sensitive to Rucaparib. In our hands, DU145 cells, expressing lower levels of RelB, were most sensitive.

Although IKK α is part of a signalosome complex with IKK β and NEMO, it is considered to have roles independent of NF- κ B activation. IKK α has been shown to exhibit pro-tumorigenic effects in its own right (Mahato et al., 2011, Colomer et al., 2018). Thus, our data suggest that the effects of Rucaparib on the survival and migration of prostate cancer cells are at least partly *via* the depletion of IKK α . These effects are likely to be mediated via substrates independent of its role

in NF- κ B signalling. Figure 8.1 outlines some of the proposed targets, although these were not investigated directly. Proposed IKK α targets include, maspin, Wnt/ β -catenin, ATM and RIF1. Although other targets are possible, and some may yet to be identified.

Knockdown of IKK α is known to inhibit migration in prostate cell lines and the xCELLigence data presented in Chapter Five show that Rucaparib reduces migration in both DU145 (42%) and PC3 cells (58%), in real-time, at 72-hours. However, the scratch assay data evidenced that Rucaparib did not limit DU145 migration, but reduced PC3 cell migration by ~32%, at 72-hours. DU145 cell migration data in response to Rucaparib is variable between the methods but it is clear that Rucaparib is most inhibitory to PC3 cell migration. It is possible that reduced IKK α following Rucaparib treatment is mediating an upregulation of maspin, leading to reduced cell migration. Indeed, others have shown that knockdown of IKK α sensitises cells to death and increases maspin expression (Mahato et al., 2011). However, as described above, the protein expression data from cell samples exposed to treatments (Figure 4.16-Figure 4.18) refutes the hypothesis that inhibition of IKK α by Rucaparib would enhance maspin expression as maspin expression was not affected by 72-hour exposure to Rucaparib. This is not unsurprising since our data shows that knockdown of maspin sensitises PTN1A cells to Rucaparib and therefore an alternative mechanism is more likely. For example, IKK α may be mediating its effects on migration via the Wnt/ β -catenin signalling pathway which is known to be involved in migration and invasion. Agarwal (2006) showed that reduction of Wnt-induced β -catenin-dependent activity *via* RNAi targeting IKK α led to significantly reduced migratory ability.

A recent study demonstrated that IKK α is important for the DNA damage response, specifically ATM activation and that this is independent of NF- κ B activation (Colomer et al., 2019). They showed that IKK α and ATM can interact, and abolishing IKK α attenuates ATM activation leading to a reduction in the phosphorylation of key DDR factors and consequently compromised DNA repair. There is a multitude of evidence for PARP-1 in ATM activation; reduced activation of ATM in the absence of PARP-1 and PARP-1 deficient cells exhibit ATM activity that is defective and reduced in HR repair. The effect of PARP inhibitors on ATM activation is proposed to demonstrate a “duality of response” in terms of ATM activation and this is context dependent

(Bryant and Helleday, 2006). Thus, reduced IKK α following Rucaparib exposure could be leading to reduced ATM activity and unrepaired DSBs. Rap1 interacting factor (RIF1) is also involved in DNA damage response signalling and maintaining genomic integrity (Kumar and Cheok, 2014). It acts downstream of ATM facilitating NHEJ. Its recruitment is compromised when IKK α is abolished.

Before considering the DNA strand break data from Chapter four, it is important to consider that the prostate cells used in this thesis were not isogenic and therefore increased sensitivity to Rucaparib in the DU145 cells may be in part due to other mechanisms such as dysfunctional *BRCA*. Human tumours defective in *BRCA* are unable to repair DNA DSBs via the error free HR repair pathway. Many studies have shown that PARP inhibitors are exquisitely toxic to these cells although the mechanistic basis remains to be fully elucidated. Evidence suggests that DU145 cells are *BRCA* defective (Yin et al., 2018). RAD51, a marker of HR function, was investigated in Chapter Six to confirm HR dysfunction in DU145 cells and to further explore the effects of inhibitors on HR repair. Protein expression data revealed lower basal RAD51 expression in DU145 cells and expression of RAD51 was further reduced in DU145 cells exposed to Rucaparib; confirming dysfunctional DNA repair *via* HR. These findings support previous reports that have evidenced the role of RAD51 as a biomarker for HR repair and sensitivity to PARP inhibitors (Cruz et al., 2018).

Heightened sensitivity to PARP inhibition has been observed in cells with other HR defects including *PTEN* deficiency. Like *BRCA* defects, *PTEN* deficiency is purported to be synthetically lethal with PARP inhibition (Mendes-Pereira et al., 2009). The PC3 cells are known to be null for *PTEN* although we did not independently test for this (Vlietstra et al., 1998, Byun et al., 2003). The impact of *PTEN* loss is controversial (reviewed in Michels et al. (2014)). Some studies have reported increased sensitivity to PARP inhibitors in the absence of *PTEN*, likely due to downregulation of RAD51 and consequently impaired HR; whereas others have failed to observe a correlation between *PTEN* status and RAD51 expression, PARP inhibitor sensitivity and the expression of genes associated with synthetic lethality. In our hands the latter was true; the data

in Figure 6.9 showed high basal expression of RAD51 in PC3 cells and expression was not reduced in the presence of Rucaparib.

As both PC3 and DU145 cells are both HR defective (due to *BRCA* mutation and *PTEN* deficiency, respectively) it is unlikely that this defect solely accounts for the enhanced sensitivity to Rucaparib seen in the DU145 cells. Also reduced expression of IKK α , in the presence of Rucaparib, occurred in both DU145 and PC3 cells; an event that is therefore independent of *BRCA* or *PTEN* status. The mechanism by which PARP inhibitors sensitise cells are likely to be overlapping rather than a single mechanism in a given cell at a given time. The data presented in this thesis suggests that the different sensitivities to Rucaparib between PC3 and DU145 cells is at least in part also a consequence of maspin expression. Whether it is maspin itself (for example *via* altered NHEJ) or maspin as a biomarker for high IKK α levels has yet to be determined.

The basal levels of DSBs were lowest in DU145 cells and highest in PTN1A cells which is contrary to what would be expected given the reported BRCA defect in DU145 cells which would be expected to contribute to a reduced DNA repair capacity. However, a BRCA defect would not account for the increased basal SSBs seen in the DU145 cells compared to the other cell lines. It can be postulated that the lower basal DSBs in the DU145 cells are a consequence of altered levels of maspin. Low maspin has been shown to lead to increased phosphorylation of AKT (Nam and Park, 2010) which in turn leads to increased activity of DNA-PKcs and an enhancement of NHEJ (reviewed in (Liu et al., 2014). PARP-1 also stimulates DNA-PKcs in the presence of NAD⁺ to facilitate DSB repair via NHEJ. Such reaction is blocked by PARP depletion or inhibition leading to a shift in repair, possibly by HR (Mitchell et al., 2009).

Thus, lower basal levels of DSBs in the background of HR defect is likely a consequence of NHEJ repair of these breaks which is not induced in maspin proficient PNT1A cells.

The high basal SSBs in DU145 cells are also likely to be a consequence of downregulated maspin. Endogenous maspin correlates with GST activity and therefore maspin depleted cells will exhibit elevated levels of ROS and DNA strand breaks as a consequence (Li et al., 2006). Indeed, knockdown of maspin in PC3 cells has been shown to increase intracellular ROS. ROS levels

were not measured in the work described in this thesis, but this should be factored into future work. These basal SSBs will activate PARP-1 and an inhibitor of PARP will prevent their repair through multiple mechanisms (as proposed in Figure 8.2); reduced IKK α , decreased BER and inhibition of DNA-PKcs and NHEJ. Therefore, to further elucidate the mechanisms underlying increased sensitivity to Rucaparib in maspin depleted cell lines, the effect of Rucaparib on the level of SSB and DSBs was investigated to enable comparison with cytotoxicity data in Chapter Four. Data presented in this thesis did not investigate break induction or measure the kinetics of repair but looked at levels of breaks following 72-hours and therefore their persistence. The studies described in Chapter Six demonstrated that PARP-1 inhibition by Rucaparib increased both SSB and DSBs in all prostate cell lines. More class 3 comets were seen in response to Rucaparib in DU145 cells compared to the other cell lines despite equal cell cytotoxicity (GI₅₀). The ability to recover and survive following DNA damage is postulated to correlate with repair capacity. Here, the data indicate that the number of breaks do not correlate directly with survival; indicating that in maspin depleted cells, a higher barrier of entry to cell death possibly exists. Indeed, maspin deficient cells are known to be resistant to apoptosis. To this end, a yeast 2-hybrid screen showed that maspin is an endogenous inhibitor of HDAC-1 (Li et al., 2006). Li et al. also confirmed a maspin/HDAC1 interaction in human prostate tissue and cell lines; siRNA of maspin in PC3 cells increased HDAC activity. This was not confirmed in the studies described here but should certainly be explored in future studies.

Low maspin and higher HDAC levels will increase deacetylation of Ku70 which in turn complexes with bax (Figure 8.1) This sequesters the complex and has been shown to be a mechanism by which ku can lead to radio-resistance (Lee et al., 2012). Rucaparib induced significant DSBs in PNT1A cells compared to DU145 and PC3 cells, despite 50% cell survival in all cells. These findings support the findings of others whereby normal cells have an increased ability to survive and resolve drug induced DSBs, compared to transformed cells. Taken together the data also highlights the need to exercise caution when attempting to correlate levels of breaks with survival. The outcomes seem to also be irrespective of p53 status. This is not unexpected

given the recent report of both p53 dependent and independent mechanisms of cell death caused by PARP inhibition (Nguyen et al., 2011)

Overall, the results summarised here show that Rucaparib can sensitise all prostate cells regardless of their HR status. Similarly, Luo et al. (2007) showed that reduction of PARP-1 by siRNA could reduce the growth and invasion capacity of prostate cancer cell lines regardless of the *BRCA1/2* mutation. Maspin correlates with response to stand alone treatment with Rucaparib. These results support the potential of maspin status as a biomarker of response for cancer therapy with PARP inhibitors in prostate cancer.

8.2 Sensitivity assay selection and the hormetic response

Cell viability and growth assays were carried out to identify a standardised method for measuring drug response. The data presented in Chapter Four identified the SRB assay as a primary screen for novel compounds against cell lines. This assay is inexpensive and was the only method where results correlated to data obtained from manual cell counts.

Discrepancies in drug sensitivity were found in WST-1 and Resazurin assays compared to manual cell counts. For example, the Rucaparib GI_{50} for DU145 cells was $37\mu\text{M}$ and $39\mu\text{M}$ in WST-1 and Resazurin assays, compared to $9\mu\text{M}$ in manual cell counts, respectively. A need for standardisation in pharmacological assays among researchers has been identified following the identification of inconsistencies between two large-scale studies on the sensitivity of hundreds of cell lines to various drugs (Haibe-Kains et al., 2013).

An interesting finding from the Rucaparib sensitivity studies in Chapter Four was a low dose hormetic response in DU145 and PC3 tumour cells, but not “normal” PNT1A cells. Increased cell proliferation in response to low dose Rucaparib ($3\mu\text{M}$) only occurred in Tetrazolium and Resazurin salt assays. These results are based on cell metabolism in culture, whereas SRB assay results are based on protein content that is directly proportional to cell mass. A hormetic response arises when homeostatic adaptations to low toxic doses of drug leads to increases cell proliferation as an adaptation to stress as a means to override the cytotoxic effects of the drug. This is overcome at higher doses of compound. This response is characterised in cancers (Calabrese, 2005) and

such defence mechanism is often a result of altered mitochondrial bioenergetics (reviewed in Porporato et al. (2018)). Further exploration into the effects of Rucaparib on mitochondrial bioenergetics were beyond the scope of this thesis but is warranted to confirm a “Warburg effect”; the metabolic switch from aerobic glycolysis to oxidative phosphorylation in tumour cells (Vander Heiden et al., 2009). PARP-1 has been implicated in the regulation of bioenergetic metabolism. PARP-1 activation has been shown to downregulate mitochondrial respiration and oxidative metabolism; leading to the onset of disease (reviewed in Bai and Canto (2012)). To this end, PARP inhibitors may serve as therapies, beyond BRCA mutations, to alter deregulated cellular bioenergetics; a hallmark of cancer and disease. This could be explored by measuring the specific activity of mitochondrial complexes using a Mitochondrial ToxGlo or Seahorse XF assay, to confirm a metabolic switch in response to treatment.

8.3 The stand-alone effects of the HDAC inhibitor TSA in prostate cells of varying maspin expression

Numerous studies have shown disordered expression of HDACs in human tumours. Higher expression of HDAC can predict poor patient prognosis independent of other variables such as tumour type. HDACs have pleiotropic effects on cellular processes which may explain their role in tumour development and resistance to therapy (discussed in Chapter One). The most widely studied effects of HDACs are angiogenesis, cell cycle, apoptosis and DNA repair (reviewed in Li and Zhu (2014)).

As eluded to in the preceding discussion, maspin is an endogenous HDAC-1 inhibitor and it is speculated that maspins effect on cell behaviour is in part conducted through HDAC1 inhibition. The class I HDACs contribute to DNA damage signalling on multiple levels; HDAC1 and 2 have a central role in preparing the chromatin surrounding the DSB for the activation of the DDR and sealing of the DSB by NHEJ or HR (reviewed in Roos and Krumm (2016)). Results in Chapter Six showed reduced expression of RAD51 in tumour cells exposed to TSA, providing evidence that HDAC inhibitors such as TSA hinder DSB repair by HR in tumour cells. Others have also reported a reduction in RAD51 expression following treatment with the HDACi Valproic acid (Kachhap et al., 2010). High HDAC1 levels in maspin depleted cells will also promote the DNA

damage response through selective stimulation of NHEJ via deacetylation of Ku70, for example. Ku70 then serves as a scaffold for other factors involved in repair. Conversely, inhibition of HDAC *via* maspin might be expected to specifically upregulate genes that promote cell cycle arrest and down regulate genes involved tumour survival including those involved in the DNA damage response (Figure 8.1). Our data briefly discussed above and further below, support this.

The work described in this thesis looked at the level of HDAC-1 in the prostate cell lines and correlated this with maspin expression and sensitivity to the HDAC inhibitor TSA; a potent and specific inhibitor of class 1 and 2 HDACs. In Chapter three, the data showed that PC3 cells have lower HDAC-1 protein expression than maspin depleted DU145 cells, providing further evidence that maspin suppresses HDAC1 expression. Previous studies have shown that the pan HDAC inhibitor SAHA, an analog of TSA, can selectively sensitise prostate cancer cells as measured by survival. Moreover, they demonstrate differences in sensitivity amongst DU145 and PC3 cells (Chao and Goodman, 2014). In line with this, studies in Chapter Four highlighted increased sensitivity to TSA in DU145 and PC3 cells versus PTN1A cells, demonstrating a tumour specific effect. The selective effect in tumour versus normal cells is proposed to be a consequence of HDAC overexpression in tumours which we propose could result –in part- from reduced maspin. To this end, the data in Chapter Seven showed that Maspin knockdown in PTN1A cells increased sensitivity to TSA 1.8-fold. Thus, we would expect to see greater sensitivity to an HDAC inhibitor in maspin deficient tumours with high HDAC expression. Our finding is limited as HDAC-1 levels were not measured following maspin knockdown and we cannot conclude definitively that this increased sensitivity is mediated via increased HDAC-1 expression. Moreover, the finding that there was no significant difference between DU145 and PC3 cell sensitivity (measured by SRB and counting) following exposure to TSA for 72 hours suggests that there may be an alternative mechanism driving sensitivity to HDAC inhibitors or that we cannot simply correlate maspin or HDAC-1 levels with sensitivity. To this end, the literature presents opposing findings to maspin expression and sensitivity to HDAC inhibitors. Li et al. (2006) demonstrate that the HDAC inhibitor M344 was more effective in maspin low cell lines. This was not the case in our studies.

To add further uncertainty, the effect of HDAC inhibitors on the expression of maspin is also variable. The majority of data in the literature suggests that maspin is increased in response to HDAC inhibition (Abbas and Gupta, 2008, Liao et al., 2014) while others show no effect (Horswill et al., 2008) and perhaps unexpectedly -in our hands- TSA treatment reduced maspin expression in PNT1A and DU145 cells but not PC3 cells. The effects of HDAC inhibition may be inhibitor and cell-type specific.

Increased maspin would be expected to reduce cell migration and despite our data suggesting that TSA reduces maspin expression, cell migration data presented in Chapter Five demonstrated reduced cell migration in DU145 and PC3 cells but not PTN1A cells exposed to a GI_{50} of TSA. This data is in line with the growth inhibition studies presented in Chapter Four although the effect of treatment with TSA on cell migration was greater in PC3 cells. The latter finding may be a consequence of higher HDAC activity in these cells. These data demonstrate a tumour specific affect and that, at least in our hands, the mechanism of reduced migration may be independent of maspin in DU145 cells.

Sensitivity to HDAC inhibitors may depend on other mechanisms that differ between normal and cells. Normal cells have a greater capacity to repair and survive DNA damage. They exhibit greater genomic stability and have a greater complement of functioning repair pathways. The selectivity of HDACi in tumour cells could be a result of HDACi causing DNA damage that only normal cells are able repair. The γ H2AX foci data in Chapter Six supports this, showing that TSA, at GI_{50} concentration, induces more DSBs in PNT1A cells compared to DU145 and PC3 cells, despite the survival in all cell lines. As described above, both DU145 and PC3 cells are likely HR defective due to *BRCA* mutation and loss of *PTEN*, respectively. Thus, sensitivity to HDAC inhibitors in our cell lines and the lack of difference between DU145 and PC3 cells may relate to HR deficiency. Without HR repair capacity, NHEJ will be relied upon which TSA is likely to block based on the mechanism previously described (Figure 8.1). In line with this, Wiegman et al. (2015) showed that BRCA competent cell lines displayed reduced sensitivity to all HDACi tested compared to BRCA mutant cell lines. Several HDAC inhibitors repress expression of HR proteins including Rad51. HDAC inhibitors have also been shown to increase the proapoptotic

protein Bax, leading to a reduced threshold for the induction of apoptosis (Singh et al., 2005). In support of this, epifluorescence data in Chapter Four showed that HDAC inhibition by TSA, at GI_{50} , increased nuclear condensation and fragmentation in all cell lines, compared to untreated cells. Nuclear condensation was increased 2.4, 1.3 and 3.2-fold and nuclear fragmentation 5.2, 3.4 and 1.8-fold in PNT1A, DU145 and PC3 cells, respectively. These data indicate that TSA was apoptotic in all cell lines at GI_{50} .

Data in Chapter five demonstrated that TSA increased SSBs in all cells especially DU145 and PC3 cells but the level of DSBs was not altered which was unexpected. HDAC inhibitors are known to increase the levels of intracellular ROS which will mediate induction of DNA strand breaks; although ROS were not specifically measured in the studies described here. Moreover, inhibition of repair pathways by TSA will lead to reduced/slowed repair of breaks. The alkaline comet assay does not necessarily only measure single strand breaks but can also measure incomplete excision repair sites and double strand breaks (Pu et al., 2015). The time point investigated of 72 hours looks only at persistent breaks and so does not give a full picture of strand break induction and resolution in our models. However, as outlined above, DSBs were not significantly increased in DU145 and PC3 cells exposed to TSA but were increased in PNT1A cells. If we take the right side of model 1 presented in Figure 8.1, it could be that ku70 is acetylated, rescuing DNA repair and limiting apoptosis in response to HDAC inhibition in tumour cells. However, PARP-1 is activated which will in turn recruit and upregulate DNA-PKcs and consequently DNA repair *via* NHEJ. Therefore, at 72 hours, no more DNA breaks are identified as they have been resolved prior to this timepoint.

Overall, the work presented in this thesis and published literature agree that there is a selective toxicity for HDAC inhibitors towards tumour cells over normal cells. HDAC inhibitors are able to induce cell death in tumour cells and in our hands – prostate cancer cell lines. However, it is clear that there is no consistent marker by which sensitivity can be predicted in tumour cells. Evidence presented in this thesis is contradictory and together with the literature, shows that sensitivity depends very much on the HDAC inhibitor employed, the methods of end point assessment and the cell line or model used. Toxicity amongst tumour cells is unlikely to result

from the same mechanism in each case and is instead cell line and context dependent. Moreover, HDAC inhibitors have a global impact on the acetylation status of many genes and overlapping mechanisms are more likely than an exclusive mode of action. This makes employing HDAC inhibitors as a targeted therapy for cancer difficult to implement. Indeed, the use of an HDAC inhibitor as stand-alone therapy has been disappointing in clinical trials with little clinical benefit for solid tumours including prostate cancer (reviewed in Kaushik et al. (2015)). Instead, combinations of HDAC inhibitors with other small molecules may enable a specific mechanism of action to be harnessed and potentiated (Thurn et al., 2011). Indeed, this is a growing area of research and one such area is the combination with PARP inhibitors.

The enhanced sensitivity of maspin depleted tumours to Rucaparib and endogenous inhibition of HDAC-1 by maspin, led to the novel idea of combining Rucaparib with the HDAC-1 inhibitor, TSA, with a view to further enhance cell sensitivity to either treatment alone; particularly cells deficient for maspin that express increased levels of HDAC-1. At the outset of the work described here, only a handful of studies had investigated combination of PARP and HDAC inhibitors for cancer therapy (Zhang et al., 2012, Jasek et al., 2014, Chao and Goodman, 2014, Min et al., 2015). At the time of writing this, numerous studies have sought to investigate the combination of HDACi and PARPi for cancer therapy (Rasmussen et al., 2016, Marijon et al., 2018, Yin et al., 2018). Nevertheless, not all studies are consistent with one another and there are many contentions that are not openly acknowledged by each of the papers.

The studies described in this thesis extend these studies and confirm the work of others who show that HDAC-1 and PARP-1 inhibitors in combination decrease cell survival compared to treatments alone. Nevertheless, the pleiotropic effects of maspin and HDAC-1 mean that cell line models are not elegant enough to decipher exact mechanisms of these molecules and therefore specific gene knockdown studies are required. In some instances, the effects of HDAC-1 and PARP-1 inhibitor combined treatments differ from others and overall show that the effects will be cell and drug type dependent.

8.4 The combined effects of the PARP inhibitor Rucaparib and the HDAC inhibitor TSA in prostate cells of varying maspin expression

Combinations of PARP inhibitors with other molecules has been based on 3 key biological interactions:

1) Increasing levels of DNA damage to ultimately tip the cell over the threshold level for survival across to death via apoptosis.

2) Increased “PARP trapping”. PARP inhibitors increase cell kill via two mechanisms; inhibition of PARylation which increases the binding of PARP to DNA by prevention of automodification and release and by reducing base excision repair. “Trapped” PARP-DNA complexes are more cytotoxic than unrepaired single-strand breaks since they simultaneously prevent access to the break by other repair factors. Such ‘tethering’ was originally proposed by (Veuger et al., 2003, Veuger et al., 2004) and has since been demonstrated by others (Murai et al., 2012, Robert et al., 2016, Hopkins et al., 2019). HDACs have been shown to differentially acetylate not just ku70/80 but also PARP-1 leading to PARP trapping (Robert et al., 2016); a theory initially proposed by (Veuger et al., 2003).

3) Simulating an HR defect in proficient tumours. The efficacy of PARP inhibitors in tumours deficient in HR repair such as those with *BRCA* mutations has led to the development of strategies to pharmacologically mimic HR deficiency in tumours for sensitisation to PARP-1 inhibitors. HDAC inhibitors have emerged as a class of therapeutic agents which mimic HR deficiency and sensitise cells to DNA repair inhibitors by impairing the repair of DNA DSBs, leading to cell death (Chao and Goodman, 2014).

HDAC inhibitors have been shown to induce a “*BRCAness*” phenotype in tumour cells (Ha et al., 2014) and are therefore an attractive treatment to synergise with PARP inhibitors and induce synthetic lethality. HSP90 stabilises many tumour suppressors. Hyperacetylation of HSP90 leads to its inhibition and proteins that interact with HSP90 including BRCA cannot do so thus leading to their degradation (Kim et al., 2017). The loss of HR capacity thus requires a reliance on NHEJ

pathway which as demonstrated here (Figure 8.2) is upregulated by PARP and therefore susceptible to inhibition by a PARP inhibitor.

It is clear that there are multiple mechanisms by which we might see enhanced effects on survival endpoints in cancer cells exposed to a combination of a PARP inhibitor and an HDAC inhibitor. These mechanisms are unlikely to be mutually exclusive.

Studies have supported the rationale to combine HDAC inhibitors with PARP inhibitors, irrespective of BRCA expression, for cancer therapeutics. They have not explored the effects of co-treatment in the context maspin. HDAC-inhibitor mediated depletion of HR has been shown to sensitise breast cancer cells to the PARP inhibitor Veliparib irrespective of BRCA status (Ha et al., 2014), highlighting the potential of PARP-1 and HDAC-1 inhibitor co-treatment in tumours. Briefly, the data in Chapter Four demonstrated a 1.5-fold increase in sensitivity to Rucaparib, at GI_{50} , in both DU145 and PC3 cells co-treated with TSA at GI_{50} , compared to PNT1A cells. Survival was reduced by 64%, 49% and 42% in PNT1A cells exposed to Rucaparib, TSA and combination, respectively. Survival was reduced by 39%, 20% and 70% in DU145 cells, and 51%, 28% and 74% in PC3 cells exposed to Rucaparib, TSA and combination, respectively. The epifluorescence data in Chapter Four highlighted an increased effect of co-treatment on the nuclear morphology of all cells, particularly DU145 and PC3 cells which presented increased nuclear fragmentation, membrane blebbing and apoptotic bodies compared to cells exposed to Rucaparib and TSA as single agents. Co-treatment did not have an increased effect on the nuclear morphology of PNT1A cells exposed to co-treatment, compared to Rucaparib and TSA as single agents. These data support an important tumour specific sensitivity to co-treatment and this is in line with other studies (Chao and Goodman, 2014, Yin et al., 2018). At their GI_{50} concentrations, survival following co-treatment was not significantly different between DU145 and PC3 cells, indicating that sensitivity to co-treatment may be independent of maspin status. Although, GI_{50} concentration for Rucaparib was 2-fold higher in PC3 cells. Maspin siRNA and combination treatment were no more effective than maspin siRNA and TSA and Rucaparib alone, in PNT1A cells. This finding was not comparable to the survival data in Chapter Four whereby maspin depleted DU145 cells were most sensitive to combined treatment, compared to treatments alone.

However, the data do demonstrate increased sensitivity to combined treatment in the presence of maspin siRNA, suggesting that maspin may play a role in sensitivity to co-treatment.

Combined Rucaparib and TSA treatment selectively enhanced SSBs in tumour cells; particularly DU145 cells. Reduced expression of maspin in DU145 cells exposed to co-treatment (Chapter Four) also supports a potential role of maspin in cell death susceptibility. Overall the SSB studies in Chapter Six have shown that DU145 cells are more prone to SSB DNA damage and these findings are in line with the growth inhibition data presented in Chapter Four. Moreover, when the inhibitors were used in combination at GI_{50} concentrations, DU145 cells were more susceptible to DSBs than PNT1A and PC3 cells. DSB levels were lowest in PC3 cells. Others have shown a significant increase in DSBs in DU145 cells exposed to the PARPi Olaparib and HDACi SAHA in combination, at 48-hours, compared to Olaparib and SAHA alone. This effect was not observed in RWPE-1 epithelial cells, demonstrating that the effects of combined treatment on DSBs was selective to tumour cells and not epithelial cells (Chao and Goodman, 2014). This finding has also been reported in a more recent prostate study that utilised the PARPi Veliparib in combination with HDACi SAHA (Yin et al., 2018). In previous studies, Veuger et al. (2004) looked at whether a PARPi increases breaks or is directly inhibiting NHEJ via a decrease in DNA-PK activity and were able to show that it is the latter.

The proposed model presented in Figure 8.2 shows that in the presence of an HDAC inhibitor, PARP will be acetylated and activated which in turn will lead to reciprocal activation of DNA-PKcs and recruitment to promote NHEJ. Conversely, an HDAC inhibitor will also acetylate Ku70 leading to its inactivation and release of bax. Thus, there is a simultaneous stimulation of repair and apoptosis and the cell may be tipped towards one or the other depending on the amount of damage or regulation of each signalling pathway. Moreover, inhibiting IKK α by Rucaparib will lead to breaks that require HDAC mediated up regulation of repair which will be simultaneously inhibited by TSA. That being said, there is no significant difference between DU145 and PC3 cell survival in the presence of combined Rucaparib and TSA at GI_{50} concentrations, despite variances in DSBs. Levels of DSBs do not correlate to cell survival and it is postulated that different

mechanisms are happening in each cell line and the drugs may be inducing various off target effects which are cell type specific.

Individual enzyme activity and specific forms of repair were not measured in this study, however, previous studies within the group (Veuger et al. (2004)) have shown that in the presence of adequate substrate (the absence of inhibitors), PARP1 and DNA-PK co-operate at the sites of DNA damage and regulate the activity of one another. In the presence of an inhibitor, the activation of one by the other will be prevented and the inhibited enzyme will 'block' the access of the other. PARP was also shown to have preferential binding to blunt ended breaks and will therefore bind first at the site of a break. 'Trapping' of PARP at the site of a break will impede NHEJ. The combined use of a PARP inhibitor and an HDAC inhibitor will lead to increased apoptosis as NHEJ will be blocked via PARP trapping and acetylation of ku70 with concomitant release of Bax. Indeed, Robert et al. (2016) show that TSA can decrease NHEJ by acetylation and by PARP trapping. Excess damage resulting from the combined action of the inhibitors may also activate APAF1, a pro-apoptotic protein required for apoptosis that is part of the apoptosome complex. APAF1 is upregulated in a Ku dependent manner (reviewed in De Zio et al. (2013)). The balance of breaks and complement of active repair pathways will thus decide the cell fate. Thus, we hypothesised that inhibited PARP will be more deleterious than loss of PARP and therefore lead to excessive DNA damage such that the balance will be tilted in favour of apoptosis (Figure 8.2).

To demonstrate this, an elegant set of data described in this thesis enabled us to compare PARP-1 siRNA + TSA to Rucaparib + TSA on cell survival. In all prostate cancer cell lines, Rucaparib +TSA was more deleterious than PARP1 siRNA and TSA (29% versus 88% and 27% versus 80% survival in DU145 and PC3 cells, respectively). Taken together, these data point towards PARP trapping as a predominant mechanism of cell death. However, we must acknowledge the caveat that PARP-1 siRNA did not induce a complete knockdown of PARP-1 and it was not confirmed that knockdown lasted as far out as the timepoints of the studies. Thus, there may be some upregulation of NHEJ as a consequence of residual/return of PARP activity. This study should therefore be repeated in PARP^{+/+} and PARP^{-/-} MEFs.

Some of the studies investigating PARP-1 and HDAC inhibitors have demonstrated synergy between the compounds (Chao and Goodman, 2014, Rasmussen et al., 2016, Yin et al., 2018, Marijon et al., 2018). We do not see synergy with Rucaparib and TSA. The combination of TSA and Rucaparib can be equated to the use of DNA-PK and PARP inhibitors in combination since our models suggest that both a PARP inhibitor and an HDAC inhibitor will act in a large part via reduction of NHEJ. DNA-PK and PARP inhibitors have at least additive effects (Veuger et al 2003). TSA combined with Rucaparib was more effective at preventing the clearance of DSBs than Rucaparib alone in DU145 cells but not more effective in PNT1A and PC3 cells; this may be due to overlap in pathways.

A characteristic feature of malignancies, including prostate cancer, is the ability of cancer cells to invade surrounding tissues and migrate into distant tissues. The data presented here built on those of others by also looking at the effects of the inhibitors in combination on migration. xCELLigence cell migration data presented in Chapter Five showed reduced cell migration PC3 cells exposed to Rucaparib and TSA in combination, compared to DU145 cells. Scratch assay data showed no significant reduction in cell migration in PNT1A, DU145 and PC3 cells exposed to combination treatment, compared to Rucaparib and TSA as single agents. Despite variation in results between methods the data indicates that the effects of co-treatment on cell migration are cell type specific. PC3 cells are less migratory throughout treatment conditions and this correlates with the role of maspin. However, PC3 cells subject to co-treatment were found to express reduced levels of maspin (Figure 4.18). Maspin plays a role in limiting cell migration, therefore, increased cell migration would have been expected in response to a reduction in maspin. Reduced maspin expression and migration in PC3 cells exposed to co-treatment highlights maspin's pleiotropic effects. It also suggests that the effects of co-treatment on cell migration may be independent to maspin expression.

Reports have demonstrated that HDAC enzymes are important for HR mediated DNA repair and assembly of RAD51 foci, showing decreased RAD51 and HR-mediated DNA repair in the presence of HDAC inhibitors (Adimoolam et al., 2007). To this end, combination of a HDAC inhibitor with a PARP inhibitor was predicted to be selectively toxic; particularly in *BRCA* mutant

DU145 cells which are deficient for HR DNA repair. A further reduction of RAD51 in tumour cells exposed to combined treatment, as shown in Figure 6.9, demonstrates the selectivity of these agents to inhibit DNA repair and induce synthetic lethality.

In summary, TSA sensitises tumour cells to Rucaparib irrespective of maspin expression status. This sensitisation is in line with other studies that have demonstrated reduced cell viability in prostate tumours exposed to PARP-1 and HDAC-1 inhibitors combined, compared to agents alone (Chao and Goodman, 2014, Yin et al., 2018). Maspin expression did not correlate with sensitivity to combined treatments at GI_{50} , albeit the concentration of Rucaparib required to achieve GI_{50} in PC3 cells was 2-fold greater than that required for DU145 cells. Maspin siRNA + combined treatment increased PNT1A cell sensitivity, compared to cells exposed to combined treatment alone. Although the PNT1A cells are “normal” prostate cells, this preliminary finding indicates that maspin can affect cell response to combined treatment and provides a proof of principle for targeting tumours which are deficient for maspin. Nevertheless, our data shows increased sensitivity to co-treatment in tumour cells of varied maspin expression and this is likely a result of PARP trapping and a reduced capacity for DNA repair by NHEJ and HR, and consequently synthetic lethality.

8.5 General conclusions

At the outset of this body of work, the aim was to investigate a possible link between maspin, PARP1 and NF- κ B with a view to repurposing PARP inhibitors in a subset of tumours or identifying a biomarker of predicted sensitivity.

As work progressed, the realisation that maspin is an endogenous HDAC1 inhibitor driving varied levels of HDAC1 in tumour cells coupled with the concept that HDACs are often overexpressed in tumours and are a poor predictor of prognosis meant the work was expanded to include the HDAC1/2 inhibitor, TSA. Whilst Rucaparib and TSA used alone were able to sensitise all cell lines tested, only Rucaparib sensitivity correlated with maspin expression. No differential effects of TSA between tumour cells of varied maspin expression were observed in the studies presented in this thesis. Ultimately, amongst a growing background of similar studies, we tested the

combination of a PARP inhibitor (Rucaparib) and an HDAC inhibitor (TSA). Two working models (Figure 8.1 and Figure 8.2) have been proposed and which warrant further investigation. The models proposed fit our findings and extends those already in the literature.

Although there are many studies in the literature aimed at investigating individual aspects of the model(s) put forward here and most support the key findings described in this thesis -none have attempted to piece the interrelated roles of PARP, NF- κ B and maspin together as we have here. The results add to the controversy surrounding maspins differential tumour suppressive effects in tumours. The data in this thesis also highlighted a potential mechanism between NF- κ B, maspin and HDAC-1; a mechanism for potential for therapeutic exploitation (Figure 8.1). An inverse correlation was demonstrated between maspin and IKK α as well as p65. However, tumour metastasis is a complex and progressive process, so it is unlikely that the inverse correlation between these proteins are the sole regulators of tumourigenesis.

We have provided several lines of evidence that a PARP inhibitor stand-alone effects can be via IKK α particularly in maspin deficient tumour cells.

The pleiotropic actions (eg HDACs are transcription factors, repair factors signal transducing molecules) of each of these proteins along with their differing and altering expression levels in each cell line in response to drug exposure has meant that drawing up an effective model that encompasses all events/pathways/mechanism is not possible. Moreover, the literature presents no consensus on the relationship between HDAC1 or PARP expression levels and sensitivity to the compounds. It is therefore unlikely that the events/pathways/mechanisms are the same for every scenario but rather will be dependent on tissue and cell type. This was further confounded by the fact that DU145 cells are *BRCA* defective and PC3 cells are *PTEN* null

In summary our intriguing and novel results point to a broader utility of PARP inhibitors in the treatment of prostate cancer beyond hereditary BRCA1-and BRCA2-deficient tumours. The series of investigations presented in this thesis add some insight into the interaction of maspin and NF- κ B proteins and how this can affect sensitivity to PARP-1 and HDAC-1 inhibitors, however, they have not elucidated a specific mechanism between these molecules. The use of siRNA

strengthened the findings by demonstrating increased sensitivity to Rucaparib in the absence of maspin. PARP silencing had no effect on cell sensitivity to Rucaparib in tumour cells, further supporting that sensitivity to PARP inhibition may be mediated by maspin. Our data shows increased sensitivity to co-treatment in tumour cells of varied maspin expression and this is likely a result of PARP trapping and a reduced capacity for DNA repair by NHEJ and HR, and consequently synthetic lethality.

There is scope for these molecules to be utilised as biomarkers to predict therapeutic response and our evidence proposes that maspin depletion which indicates high IKK α may be one such marker for PARP-1 inhibition.

Our results also demonstrate the efficacy of combined Rucaparib and TSA treatment in tumours, irrespective of maspin expression status. The data points to a proposed mechanism whereby combined Rucaparib and TSA increase PARP-1 trapping at DNA breaks, leading to the downregulation of key DNA repair pathways and consequently synthetic lethality.

The studies highlight the importance of utilising different cell models to eliminate cell-type specific effects and to limit generalisations that are not applicable to a broader context. The studies have also highlighted the importance of utilising proficient and deficient cell lines and siRNA to explore mechanistic interactions between molecules in cell models, and to provide a proof of principle for future scoping.

8.6 Future work

This has been a huge endeavour and many questions remain. However, all the work taken together in this thesis demonstrate one very important point – cell line models are not sufficient to enable conclusive models to be designed even with the addition of siRNA.

Future work relevant to specific areas of study have been described in each chapter, however, summarising the investigations as a whole has highlighted other potential avenues for future investigation.

Western blots for protein expression in response to treatments are a snapshot in time and are not kinetic. Assessment of protein expression at multiple time points throughout treatment exposure will extend and consolidate this work. Western blotting should also be carried out to look at the expression levels of HDAC-1 and IKK α in response to maspin siRNA. Isogenic cell lines proficient and deficient for maspin could also be utilised and phosphorylated IKK α for activation relative to maspin could be measured. These studies would strengthen our findings and confirm the link between IKK α and maspin.

It is important to assess the specific DNA repair pathways in each of the cell lines and measure the changes in those repair pathways following treatment with each of the inhibitors. Both induction and kinetics of repair need to be carried out. This will help to elucidate the mechanisms underlying HDAC and PARP inhibition and the role of these inhibitors in altering the response to DNA damage.

With regards to drug treatments, GI₅₀ doses were used in the studies presented throughout this thesis. It would be useful to calculate a combination index (CI). CI is a model that accounts for the entire shape of the growth inhibition curve and determines whether drug combination is synergistic. The effects of PARP inhibition in combination with an ATM inhibitor could also be assessed. We propose that IKK α targets ATM for DNA repair. It would be interesting to see whether PARP-1 inhibitors synergise with ATM inhibitors to limit IKK α and compromise DNA repair for cancer therapy.

The extent to which acetylation of PARP-1 induced by TSA contributes to PARP trapping and decreased NHEJ activity could be investigated using HDAC inhibitors and cell lines stably knocked down for PARP-1 or overexpressed PARP-1 mutants of 3 key lysine residues of acetylation.

Appendix

Appendix One

DU145 and PC3 cell allele reports

Reports were obtained from NorthGene, Newcastle UK.

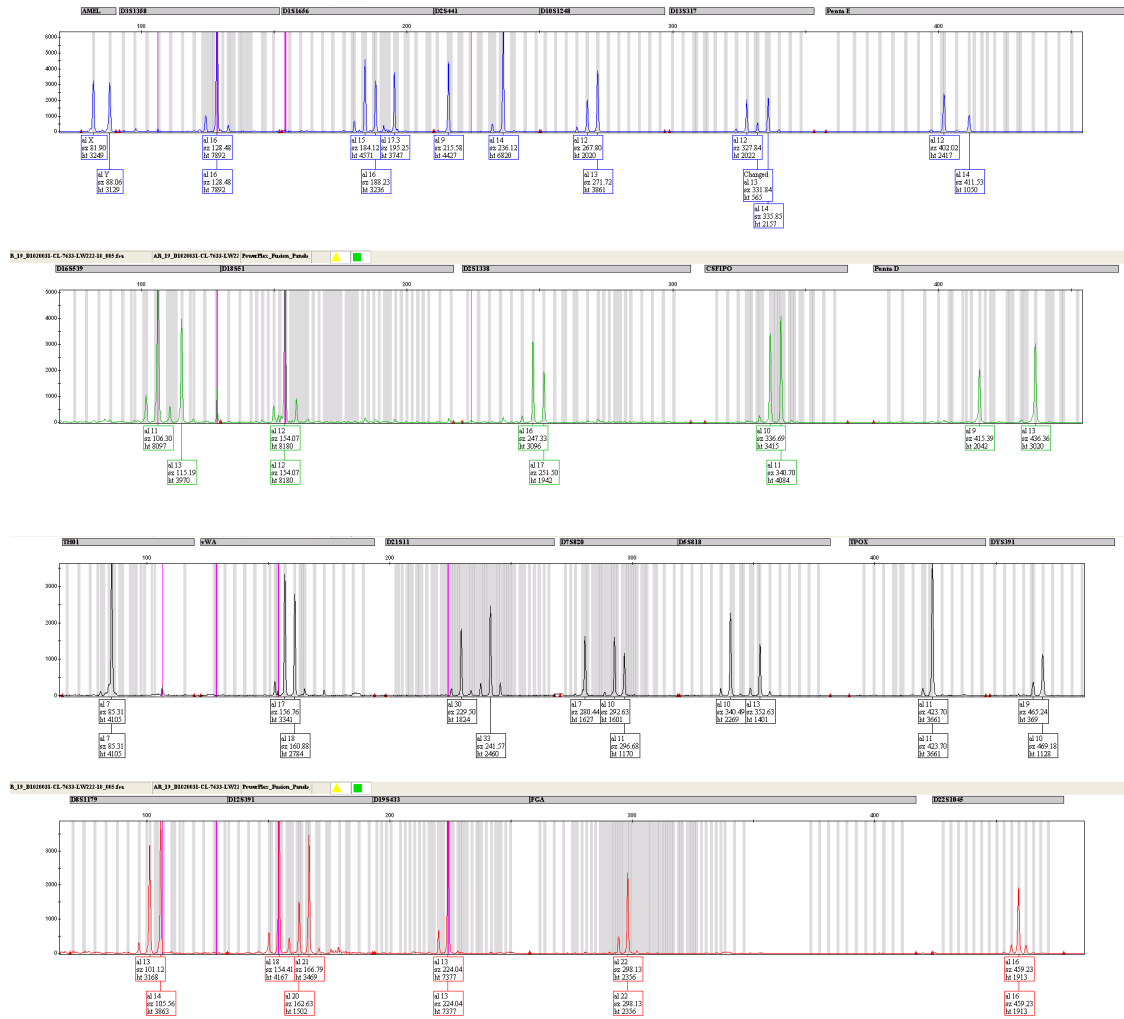


Figure A 1: DU145 allele report from Northgene.

Appendix Two

Maspin transfection reduces MCF-7 cell sensitivity to Rucaparib

The sensitivity of breast cancer (MCF-7) cells to Rucaparib was assessed by SRB assay at 72 hours. Cells transfected with maspin (MTR) or mutated maspin (244) were less sensitive to Rucaparib than MCF-7 control (CTR) cells (Figure A3). Rucaparib concentrations of 26 μ M, 24 μ M and 9 μ M were required to achieve GI₅₀ in MCF MTR, 244 and CTR cells, respectively. These results support the survival data presented in Chapter Four of this thesis whereby maspin depleted prostate cancer (DU145) cells were most sensitive to Rucaparib.

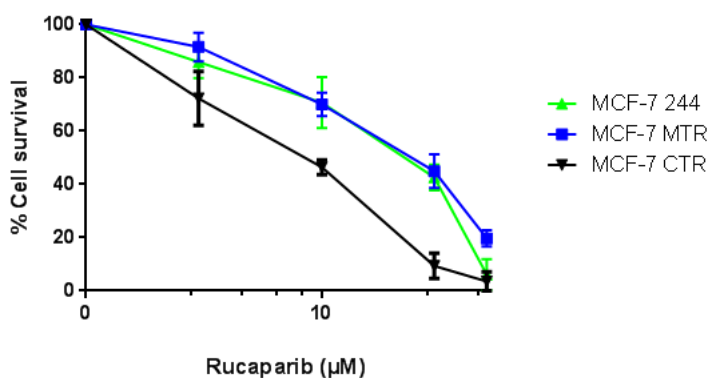


Figure A 3: Breast cancer cell growth inhibition by Rucaparib.

MCF-7 cells previously transfected with empty vector pcDNA3.2 (MCF-7 CTR), pcDNA3.2 maspin (MCF-7 MTR) and pcDNA3.2 mutant maspin (MCF-7 244) were treated with Rucaparib at various concentrations for 72 hours to investigate the effects of maspin on cell sensitivity to Rucaparib. Results were obtained by SRB assay and data shown is representative of three independent experiments and presented as mean \pm SEM.

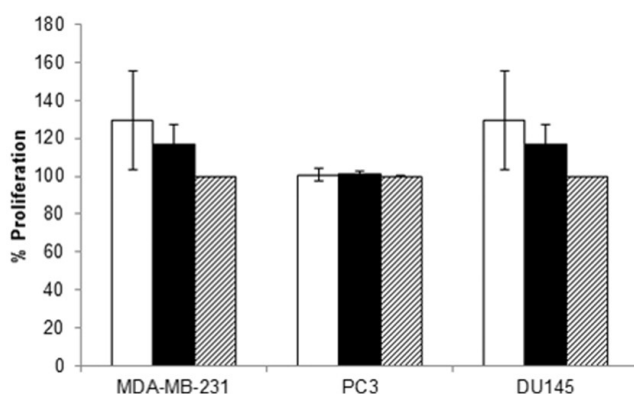
Appendix Three

Named publication

Jenkinson, S.E., Brown, L.J., Ombor, J., Milburn, J.A., Smulders-Srinivasan, T., Veuger, S., Edwards, D.R. and Bass, R., 2017. Identification of novel peptide motifs in the serpin maspin that affect vascular smooth muscle cell function. *Biochimica et Biophysica Acta (BBA)-Molecular Cell Research*, 1864(2), pp.336-344.

Contribution to publication

To investigate the effect of the novel maspin peptides S4B and S5B on breast and prostate cancer cell proliferation by WST-1 assay (method outlined in Chapter Two, section 2.2.3.1). The peptides were designed from the structural moieties of maspin; S4B and S5B were derived from strand 4 and 5 of maspin beta sheet B, respectively. The peptides did not affect tumour cell proliferation, supporting that the effects of S4B and S5B on cell proliferation are specific to vascular smooth muscle cells.



Supplementary Figure: S4B and S5B do not affect the proliferation of breast or prostate cancer cell lines. The effect of peptides on cancer cell lines MDA-MB-231 (breast), PC3 (prostate) and DU145 (prostate) was determined by WST-1 assay after 48-hour incubations in 10 μ M of S4B (open bars), S5B (closed bars) or S4/5B control (hatched bars). No significant changes were observed in proliferation compared to the control peptide. All data are combined from three separate experiments. Data presented as mean \pm SEM.

References

- ABBAS, A. & GUPTA, S. 2008. The role of histone deacetylases in prostate cancer. *Epigenetics*, 3, 300-9.
- ABRAHAM, S., ZHANG, W., GREENBERG, N. & ZHANG, M. 2003. Maspin functions as tumor suppressor by increasing cell adhesion to extracellular matrix in prostate tumor cells. *J Urol*, 169, 1157-61.
- ADASHEK, J. J., JAIN, R. K. & ZHANG, J. 2019. Clinical Development of PARP Inhibitors in Treating Metastatic Castration-Resistant Prostate Cancer. *Cells*, 8.
- ADIMOOLAM, S., SIRISAWAD, M., CHEN, J., THIEMANN, P., FORD, J. M. & BUGGY, J. J. 2007. HDAC inhibitor PCI-24781 decreases RAD51 expression and inhibits homologous recombination. *Proc Natl Acad Sci U S A*, 104, 19482-7.
- AGARWAL, A. F., RYUICHI, LERNER, NATALIA, KELLEHER, CLARE AND SIZEMORE, NYWANA . 2006. The IKK/NFkB & B-catenin pathway is critical for migration, invasion and metastasis in colorectal cancer. *American Association for Cancer Research*, 66.
- AKINC, A., MAIER, M. A., MANOHARAN, M., FITZGERALD, K., JAYARAMAN, M., BARROS, S., ANSELL, S., DU, X., HOPE, M. J., MADDEN, T. D., MUI, B. L., SEMPLE, S. C., TAM, Y. K., CIUFOLINI, M., WITZIGMANN, D., KULKARNI, J. A., VAN DER MEEL, R. & CULLIS, P. R. 2019. The Onpattro story and the clinical translation of nanomedicines containing nucleic acid-based drugs. *Nat Nanotechnol*, 14, 1084-1087.
- ALAMEDA, J. P., MORENO-MALDONADO, R., FERNANDEZ-ACENERO, M. J., NAVARRO, M., PAGE, A., JORCANO, J. L., BRAVO, A., RAMIREZ, A. & CASANOVA, M. L. 2011. Increased IKKalpha expression in the basal layer of the epidermis of transgenic mice enhances the malignant potential of skin tumors. *PLoS One*, 6, e21984.
- ALLGAYER, J., KITSER, N., VON DER LIPPEN, C., EPE, B. & KHOBTA, A. 2013. Modulation of base excision repair of 8-oxoguanine by the nucleotide sequence. *Nucleic Acids Res*, 41, 8559-71.
- ALMEIDA, G. S., BAWN, C. M., GALLER, M., WILSON, I., THOMAS, H. D., KYLE, S., CURTIN, N. J., NEWELL, D. R. & MAXWELL, R. J. 2017. PARP inhibitor rucaparib induces changes in NAD levels in cells and liver tissues as assessed by MRS. *NMR Biomed*, 30.
- ALMEIDA, J. L., COLE, K. D. & PLANT, A. L. 2016. Standards for Cell Line Authentication and Beyond. *PLoS Biol*, 14, e1002476.
- ALVAREZ SECORD, A., DARCY, K. M., HUTSON, A., HUANG, Z., LEE, P. S., JEWELL, E. L., HAVRILESKY, L. J., MARKMAN, M., MUGGIA, F. & MURPHY, S. K. 2011. The regulation of MASPIN expression in epithelial ovarian cancer: association with p53 status, and MASPIN promoter methylation: a gynecologic oncology group study. *Gynecol Oncol*, 123, 314-9.
- ANNUNZIATA, C. M., STAVNES, H. T., KLEINBERG, L., BERNER, A., HERNANDEZ, L. F., BIRNER, M. J., STEINBERG, S. M., DAVIDSON, B. & KOHN, E. C. 2010. Nuclear factor kappaB transcription factors are coexpressed and convey a poor outcome in ovarian cancer. *Cancer*, 116, 3276-84.
- ASHBURNER, B. P., WESTERHEIDE, S. D. & BALDWIN, A. S., JR. 2001. The p65 (RelA) subunit of NF-kappaB interacts with the histone deacetylase (HDAC) corepressors HDAC1 and HDAC2 to negatively regulate gene expression. *Mol Cell Biol*, 21, 7065-77.
- ASTRAZENECA. 2020. *Lynparza regulatory submission granted Priority Review in the US for HRR-mutated metastatic castration-resistant prostate cancer* [Online]. AstraZeneca. Available: <https://www.astrazeneca.com/media-centre/press-releases/2020/lynparza-regulatory-submission-granted-priority-review-in-the-us-for-hrr-mutated-metastatic-castration-resistant-prostate-cancer-20012020.html> [Accessed 2020].
- BAI, P. & CANTO, C. 2012. The role of PARP-1 and PARP-2 enzymes in metabolic regulation and disease. *Cell Metab*, 16, 290-5.

- BALDWIN, A. S. 2001. Control of oncogenesis and cancer therapy resistance by the transcription factor NF-kappaB. *J Clin Invest*, 107, 241-6.
- BANERJEE, S., KAYE, S. B. & ASHWORTH, A. 2010. Making the best of PARP inhibitors in ovarian cancer. *Nat Rev Clin Oncol*, 7, 508-19.
- BASS, R., FERNÁNDEZ, A.-M. A. M. & ELLIS, V. 2002. Maspin inhibits cell migration in the absence of protease inhibitory activity. *Journal of Biological Chemistry*, 277, 46845-46848.
- BASS, R., WAGSTAFF, L., RAVENHILL, L. & ELLIS, V. 2009. Binding of extracellular maspin to beta1 integrins inhibits vascular smooth muscle cell migration. *J Biol Chem*, 284, 27712-20.
- BASSETT, S. A. & BARNETT, M. P. 2014. The role of dietary histone deacetylases (HDACs) inhibitors in health and disease. *Nutrients*, 6, 4273-301.
- BEGG, A. C., STEWART, F. A. & VENS, C. 2011. Strategies to improve radiotherapy with targeted drugs. *Nature Reviews Cancer*, 11, 239-253.
- BEN-PORATH, I. & WEINBERG, R. A. 2004. When cells get stressed: an integrative view of cellular senescence. *J Clin Invest*, 113, 8-13.
- BENJAMIN, R. C. & GILL, D. M. 1980. ADP-ribosylation in mammalian cell ghosts. Dependence of poly (ADP-ribose) synthesis on strand breakage in DNA. *Journal of Biological Chemistry*, 255, 10493-10501.
- BERARDI, R., MORGESE, F., ONOFRI, A., MAZZANTI, P., PISTELLI, M., BALLATORE, Z., SAVINI, A., DE LISA, M., CARAMANTI, M., RINALDI, S., PAGLIARETTA, S., SANTONI, M., PIERANTONI, C. & CASCINU, S. 2013. Role of maspin in cancer. *Clinical and Translational Medicine*, 2, 8-8.
- BERNARDO, M. M., MENG, Y., LOCKETT, J., DYSON, G., DOMBKOWSKI, A., KAPLUN, A., LI, X., YIN, S., DZINIC, S., OLIVE, M., DEAN, I., KRASS, D., MOIN, K., BONFIL, R. D., CHER, M., SAKR, W. & SHENG, S. 2011. Maspin reprograms the gene expression profile of prostate carcinoma cells for differentiation. *Genes Cancer*, 2, 1009-22.
- BERTHON, P., CUSSENOT, O., HOPWOOD, L., LEDUC, A. & MAITLAND, N. 1995. Functional expression of sv40 in normal human prostatic epithelial and fibroblastic cells - differentiation pattern of nontumorigenic cell-lines. *Int J Oncol*, 6, 333-43.
- BETTSTETTER, M., WOENCKHAUS, M., WILD, P. J., RUMMELE, P., BLASZYK, H., HARTMANN, A., HOFSTADTER, F. & DIETMAIER, W. 2005. Elevated nuclear maspin expression is associated with microsatellite instability and high tumour grade in colorectal cancer. *J Pathol*, 205, 606-14.
- BHAKTA-GUHA, D. & EFFERTH, T. 2015. Hormesis: Decoding Two Sides of the Same Coin. *Pharmaceuticals (Basel)*, 8, 865-83.
- BHUTE, V. J. & PALECEK, S. P. 2015. Metabolic responses induced by DNA damage and poly (ADP-ribose) polymerase (PARP) inhibition in MCF-7 cells. *Metabolomics*, 11, 1779-1791.
- BI, Y., VERGINADIS, II, DEY, S., LIN, L., GUO, L., ZHENG, Y. & KOUMENIS, C. 2018. Radiosensitization by the PARP inhibitor olaparib in BRCA1-proficient and deficient high-grade serous ovarian carcinomas. *Gynecol Oncol*, 150, 534-544.
- BIANCHI, A., LOPEZ, S., ALTWERGER, G., BELLONE, S., BONAZZOLI, E., ZAMMATARO, L., MANZANO, A., MANARA, P., PERRONE, E., ZEYBEK, B., HAN, C., MENDERES, G., RATNER, E., SILASI, D. A., HUANG, G. S., AZODI, M., NEWBERG, J. Y., PAVLICK, D. C., ELVIN, J., FRAMPTON, G. M., SCHWARTZ, P. E. & SANTIN, A. D. 2019. PARP-1 activity (PAR) determines the sensitivity of cervical cancer to olaparib. *Gynecol Oncol*, 155, 144-150.
- BIJNSDORP, I. V., GIOVANNETTI, E. & PETERS, G. J. 2011. Analysis of drug interactions. *Methods Mol Biol*, 731, 421-34.
- BILANI, N., BAHMAD, H. & ABOU-KHEIR, W. 2017. Prostate Cancer and Aspirin Use: Synopsis of the Proposed Molecular Mechanisms. *Front Pharmacol*, 8, 145.
- BISWAS, D. K., SHI, Q., BAILY, S., STRICKLAND, I., GHOSH, S., PARDEE, A. B. & IGLEHART, J. D. 2004. NF-kappa B activation in human breast cancer specimens and its role in cell proliferation and apoptosis. *Proc Natl Acad Sci U S A*, 101, 10137-42.
- BODENSTINE, T. M., SEFTOR, R. E., KHALKHALI-ELLIS, Z., SEFTOR, E. A., PEMBERTON, P. A. & HENDRIX, M. J. 2012. Maspin: molecular mechanisms and therapeutic implications. *Cancer and Metastasis Reviews*, 31, 529-551.

- BOLTZE, C., SCHNEIDER-STOCK, R., QUEDNOW, C., HINZE, R., MAWRIN, C., HRIBASCHEK, A., ROESSNER, A. & HOANG-VU, C. 2003. Silencing of the maspin gene by promoter hypermethylation in thyroid cancer. *Int J Mol Med*, 12, 479-84.
- BORREGO-SOTO, G., ORTIZ-LOPEZ, R. & ROJAS-MARTINEZ, A. 2015. Ionizing radiation-induced DNA injury and damage detection in patients with breast cancer. *Genet Mol Biol*, 38, 420-32.
- BRANTLEY, D. M., CHEN, C. L., MURAOKA, R. S., BUSHDID, P. B., BRADBERRY, J. L., KITTRELL, F., MEDINA, D., MATRISIAN, L. M., KERR, L. D. & YULL, F. E. 2001. Nuclear factor-kappaB (NF-kappaB) regulates proliferation and branching in mouse mammary epithelium. *Mol Biol Cell*, 12, 1445-55.
- BRYANT, H. E. & HELLEDAY, T. 2006. Inhibition of poly (ADP-ribose) polymerase activates ATM which is required for subsequent homologous recombination repair. *Nucleic Acids Res*, 34, 1685-91.
- BRYANT, H. E., PETERMANN, E., SCHULTZ, N., JEMTH, A. S., LOSEVA, O., ISSAEVA, N., JOHANSSON, F., FERNANDEZ, S., MCGLYNN, P. & HELLEDAY, T. 2009. PARP is activated at stalled forks to mediate Mre11 - dependent replication restart and recombination. *The EMBO journal*, 28, 2601-2615.
- BRYANT, H. E., SCHULTZ, N., THOMAS, H. D., PARKER, K. M., FLOWER, D., LOPEZ, E., KYLE, S., MEUTH, M., CURTIN, N. J. & HELLEDAY, T. 2005. Specific killing of BRCA2-deficient tumours with inhibitors of poly(ADP-ribose) polymerase. *Nature*, 434, 913-7.
- BUURMAN, R., GURLEVIK, E., SCHAFFER, V., EILERS, M., SANDBOTHE, M., KREIPE, H., WILKENS, L., SCHLEGELBERGER, B., KUHNEL, F. & SKAWRAN, B. 2012. Histone deacetylases activate hepatocyte growth factor signaling by repressing microRNA-449 in hepatocellular carcinoma cells. *Gastroenterology*, 143, 811-820 e15.
- BYUN, D. S., CHO, K., RYU, B. K., LEE, M. G., PARK, J. I., CHAE, K. S., KIM, H. J. & CHI, S. G. 2003. Frequent monoallelic deletion of PTEN and its reciprocal association with PIK3CA amplification in gastric carcinoma. *Int J Cancer*, 104, 318-27.
- CALABRESE, C. R., ALMASSY, R., BARTON, S., BATEY, M. A., CALVERT, A. H., CANAN-KOCH, S., DURKACZ, B. W., HOSTOMSKY, Z., KUMPF, R. A., KYLE, S., LI, J., MAEGLEY, K., NEWELL, D. R., NOTARIANNI, E., STRATFORD, I. J., SKALITZKY, D., THOMAS, H. D., WANG, L. Z., WEBBER, S. E., WILLIAMS, K. J. & CURTIN, N. J. 2004. Anticancer chemosensitization and radiosensitization by the novel poly(ADP-ribose) polymerase-1 inhibitor AG14361. *J Natl Cancer Inst*, 96, 56-67.
- CALABRESE, E. J. 2005. Cancer biology and hormesis: human tumor cell lines commonly display hormetic (biphasic) dose responses. *Crit Rev Toxicol*, 35, 463-582.
- CANCER RESEARCH, U. *A study of rucaparib in advanced prostate cancer (TRITON3)* [Online]. Cancer Research UK. Available: <https://www.cancerresearchuk.org/about-cancer/find-a-clinical-trial/a-study-of-rucaparib-in-advanced-prostate-cancer-triton3> [Accessed].
- CANCER RESEARCH UK. Available: <http://www.cancerresearchuk.org/about-cancer/cancers-in-general/treatment/chemotherapy/chemotherapy-side-effects> [Accessed 07/04/2016].
- CANCER RESEARCH UK. Available: <http://www.cancerresearchuk.org/health-professional/cancer-statistics/incidence/common-cancers-compared#heading-Zero> [Accessed 12/10/2015].
- CANCER RESEARCH UK. Available: <http://www.cancerresearchuk.org/about-cancer/what-is-cancer/how-cancer-starts/types-of-cancer> [Accessed 04/10/2017].
- CANCER RESEARCH UK. Available: <http://about-cancer.cancerresearchuk.org/about-cancer/prostate-cancer/about> [Accessed].
- CANCER RESEARCH UK. Available: <http://www.cancerresearchuk.org/about-cancer/type/breast-cancer/about/risks/definite-breast-cancer-risks> [Accessed 11/12/2015].
- CANNAN, W. J. & PEDERSON, D. S. 2016. Mechanisms and Consequences of Double-Strand DNA Break Formation in Chromatin. *J Cell Physiol*, 231, 3-14.

- CAO, D., WILENTZ, R. E., ABBRUZZESE, J. L., HO, L. & MAITRA, A. 2005. Aberrant expression of maspin in idiopathic inflammatory bowel disease is associated with disease activity and neoplastic transformation. *Int J Gastrointest Cancer*, 36, 39-46.
- CAO, L. L., SONG, X., PEI, L., LIU, L., WANG, H. & JIA, M. 2017. Histone deacetylase HDAC1 expression correlates with the progression and prognosis of lung cancer: A meta-analysis. *Medicine (Baltimore)*, 96, e7663.
- CAPES-DAVIS, A., THEODOSOPOULOS, G., ATKIN, I., DREXLER, H. G., KOHARA, A., MACLEOD, R. A., MASTERS, J. R., NAKAMURA, Y., REID, Y. A., REDDEL, R. R. & FRESHNEY, R. I. 2010. Check your cultures! A list of cross-contaminated or misidentified cell lines. *Int J Cancer*, 127, 1-8.
- CELLA, N., CONTRERAS, A., LATHA, K., ROSEN, J. M. & ZHANG, M. 2006. Maspin is physically associated with β 1 integrin regulating cell adhesion in mammary epithelial cells. *The FASEB journal*, 20, 1510-1512.
- CHABNER, B. A. & ROBERTS, T. G. 2005. Chemotherapy and the war on cancer. *Nature Reviews Cancer*, 5, 65-72.
- CHAMBON, P., WEILL, J., DOLY, J., STROSSER, M. & MANDEL, P. 1966. On the formation of a novel adenylic compound by enzymatic extracts of liver nuclei. *Biochemical and biophysical research communications*, 25, 638-643.
- CHAMBON, P., WEILL, J. & MANDEL, P. 1963. Nicotinamide mononucleotide activation of a new DNA-dependent polyadenylic acid synthesizing nuclear enzyme. *Biochemical and biophysical research communications*, 11, 39-43.
- CHANG, J., VARGHESE, D. S., GILLAM, M. C., PEYTON, M., MODI, B., SCHILTZ, R. L., GIRARD, L. & MARTINEZ, E. D. 2012. Differential response of cancer cells to HDAC inhibitors trichostatin A and depsipeptide. *Br J Cancer*, 106, 116-25.
- CHAO, O. S. & GOODMAN, O. B., JR. 2014. Synergistic loss of prostate cancer cell viability by coinhibition of HDAC and PARP. *Mol Cancer Res*, 12, 1755-66.
- CHAPPELL, W. H., LEHMANN, B. D., TERRIAN, D. M., ABRAMS, S. L., STEELMAN, L. S. & MCCUBREY, J. A. 2012. p53 expression controls prostate cancer sensitivity to chemotherapy and the MDM2 inhibitor Nutlin-3. *Cell Cycle*, 11, 4579-88.
- CHEN, H. P., ZHAO, Y. T. & ZHAO, T. C. 2015. Histone deacetylases and mechanisms of regulation of gene expression. *Crit Rev Oncog*, 20, 35-47.
- CHEN, W., LI, Z., BAI, L. & LIN, Y. 2011. NF-kappaB in lung cancer, a carcinogenesis mediator and a prevention and therapy target. *Front Biosci (Landmark Ed)*, 16, 1172-85.
- CHEN, Y. & DU, H. 2018. The promising PARP inhibitors in ovarian cancer therapy: From Olaparib to others. *Biomed Pharmacother*, 99, 552-560.
- CHEN, Z., FAN, Z., MCNEAL, J. E., NOLLEY, R., CALDWELL, M. C., MAHADEVAPPA, M., ZHANG, Z., WARRINGTON, J. A. & STAMEY, T. A. 2003. Hepsin and maspin are inversely expressed in laser capture microdissected prostate cancer. *J Urol*, 169, 1316-9.
- CHENG, Z. X., SUN, B., WANG, S. J., GAO, Y., ZHANG, Y. M., ZHOU, H. X., JIA, G., WANG, Y. W., KONG, R., PAN, S. H., XUE, D. B., JIANG, H. C. & BAI, X. W. 2011. Nuclear factor-kappaB-dependent epithelial to mesenchymal transition induced by HIF-1alpha activation in pancreatic cancer cells under hypoxic conditions. *PLoS One*, 6, e23752.
- CHER, M. L., BILIRAN, H. R., JR., BHAGAT, S., MENG, Y., CHE, M., LOCKETT, J., ABRAMS, J., FRIDMAN, R., ZACHAREAS, M. & SHENG, S. 2003. Maspin expression inhibits osteolysis, tumor growth, and angiogenesis in a model of prostate cancer bone metastasis. *Proc Natl Acad Sci U S A*, 100, 7847-52.
- CHIAL, H. 2008. Tumor suppressor (TS) genes and the two-hit hypothesis. *Nature Education*, 1, 177.
- CHOI, E. S., HAN, G., PARK, S. K., LEE, K., KIM, H. J., CHO, S. D. & KIM, H. M. 2013. A248, a novel synthetic HDAC inhibitor, induces apoptosis through the inhibition of specificity protein 1 and its downstream proteins in human prostate cancer cells. *Mol Med Rep*, 8, 195-200.
- CHRISTMANN, M., TOMICIC, M. T., ROOS, W. P. & KAINA, B. 2003. Mechanisms of human DNA repair: an update. *Toxicology*, 193, 3-34.

- CHUA, R., SETZER, S., GOVINDARAJAN, B., SEXTON, D., COHEN, C. & ARBISER, J. L. 2009. Maspin expression, angiogenesis, prognostic parameters, and outcome in malignant melanoma. *J Am Acad Dermatol*, 60, 758-66.
- CIECHANOVER, A. 2005. Intracellular protein degradation: from a vague idea, through the lysosome and the ubiquitin-proteasome system, and onto human diseases and drug targeting (Nobel lecture). *Angew Chem Int Ed Engl*, 44, 5944-67.
- CITARELLI, M., TEOTIA, S. & LAMB, R. S. 2010. Evolutionary history of the poly (ADP-ribose) polymerase gene family in eukaryotes. *BMC evolutionary biology*, 10, 308.
- CLANCY, S. 2008. DNA damage & repair: mechanisms for maintaining DNA integrity. *Nature Education*, 1, 103.
- CLEMENT-SCHATLO, V., MARINO, D., BURKHARDT, K., TETA, P., LEYVRAZ, F., SCHATLO, B., FRANK, S., SCHALLER, K., CASTELLA, V. & RADOVANOVIC, I. 2012. Quantification, self-renewal, and genetic tracing of FL1(+) tumor-initiating cells in a large cohort of human gliomas. *Neuro Oncol*, 14, 720-35.
- COLLINS, A. R., AI-GUO, M. & DUTHIE, S. J. 1995. The kinetics of repair of oxidative DNA damage (strand breaks and oxidised pyrimidines) in human cells. *Mutation Research/DNA Repair*, 336, 69-77.
- COLOMER, C., MARGALEF, P., GONZALEZ, J., VERT, A., BIGAS, A. & ESPINOSA, L. 2018. IKKalpha is required in the intestinal epithelial cells for tumour stemness. *Br J Cancer*, 118, 839-846.
- COLOMER, C., MARGALEF, P., VILLANUEVA, A., VERT, A., PECHARROMAN, I., SOLE, L., GONZALEZ-FARRE, M., ALONSO, J., MONTAGUT, C., MARTINEZ-INIESTA, M., BERTRAN, J., BORRAS, E., IGLESIAS, M., SABIDO, E., BIGAS, A., BOULTON, S. J. & ESPINOSA, L. 2019. IKKalpha Kinase Regulates the DNA Damage Response and Drives Chemo-resistance in Cancer. *Mol Cell*, 75, 669-682 e5.
- CORMIER, N., YEO, A., FIORENTINO, E. & PAXSON, J. 2015. Optimization of the Wound Scratch Assay to Detect Changes in Murine Mesenchymal Stromal Cell Migration After Damage by Soluble Cigarette Smoke Extract. *J Vis Exp*, e53414.
- COUSSENS, L. M. & WERB, Z. 2002. Inflammation and cancer. *Nature*, 420, 860-867.
- CROCE, C. M. 2008. Oncogenes and Cancer. *New England Journal of Medicine*, 358, 502-511.
- CRUZ, C., CASTROVIEJO-BERMEJO, M., GUTIERREZ-ENRIQUEZ, S., LLOP-GUEVARA, A., IBRAHIM, Y. H., GRIS-OLIVER, A., BONACHE, S., MORANCHO, B., BRUNA, A., RUEDA, O. M., LAI, Z., POLANSKA, U. M., JONES, G. N., KRISTEL, P., DE BUSTOS, L., GUZMAN, M., RODRIGUEZ, O., GRUESO, J., MONTALBAN, G., CARATU, G., MANCUSO, F., FASANI, R., JIMENEZ, J., HOWAT, W. J., DOUGHERTY, B., VIVANCOS, A., NUCIFORO, P., SERRES-CREIXAMS, X., RUBIO, I. T., OAKNIN, A., CADOGAN, E., BARRETT, J. C., CALDAS, C., BASELGA, J., SAURA, C., CORTES, J., ARRIBAS, J., JONKERS, J., DIEZ, O., O'CONNOR, M. J., BALMANA, J. & SERRA, V. 2018. RAD51 foci as a functional biomarker of homologous recombination repair and PARP inhibitor resistance in germline BRCA-mutated breast cancer. *Ann Oncol*, 29, 1203-1210.
- CURTIN, N. J. 2012. DNA repair dysregulation from cancer driver to therapeutic target. *Nature Reviews Cancer*, 12, 801.
- CURTIN, N. J. 2013. Inhibiting the DNA damage response as a therapeutic manoeuvre in cancer. *Br J Pharmacol*, 169, 1745-65.
- CURTIN, N. J., DREW, Y. & SHARMA-SAHA, S. 2019. Why BRCA mutations are not tumour-agnostic biomarkers for PARP inhibitor therapy. *Nat Rev Clin Oncol*, 16, 725-726.
- CURTIN, N. J. & SZABO, C. 2013. Therapeutic applications of PARP inhibitors: anticancer therapy and beyond. *Mol Aspects Med*, 34, 1217-56.
- CURTIN, N. J., WANG, L. Z., YIAKOUVAKI, A., KYLE, S., ARRIS, C. A., CANAN-KOCH, S., WEBBER, S. E., DURKACZ, B. W., CALVERT, H. A., HOSTOMSKY, Z. & NEWELL, D. R. 2004. Novel poly(ADP-ribose) polymerase-1 inhibitor, AG14361, restores sensitivity to temozolomide in mismatch repair-deficient cells. *Clin Cancer Res*, 10, 881-9.
- DAI, Y., RAHMANI, M., DENT, P. & GRANT, S. 2005. Blockade of histone deacetylase inhibitor-induced RelA/p65 acetylation and NF-kappaB activation potentiates apoptosis in

- leukemia cells through a process mediated by oxidative damage, XIAP downregulation, and c-Jun N-terminal kinase 1 activation. *Mol Cell Biol*, 25, 5429-44.
- DANA, H., CHALBATANI, G. M., MAHMOODZADEH, H., KARIMLOO, R., REZAEIAN, O., MORADZADEH, A., MEHMANDOOST, N., MOAZZEN, F., MAZRAEH, A., MARMARI, V., EBRAHIMI, M., RASHNO, M. M., ABADI, S. J. & GHARAGOUZLO, E. 2017. Molecular Mechanisms and Biological Functions of siRNA. *Int J Biomed Sci*, 13, 48-57.
- DANIEL, R. A., ROZANSKA, A. L., THOMAS, H. D., MULLIGAN, E. A., DREW, Y., CASTELBUONO, D. J., HOSTOMSKY, Z., PLUMMER, E. R., BODDY, A. V., TWEDDLE, D. A., CURTIN, N. J. & CLIFFORD, S. C. 2009. Inhibition of poly(ADP-ribose) polymerase-1 enhances temozolomide and topotecan activity against childhood neuroblastoma. *Clin Cancer Res*, 15, 1241-9.
- DANIYAL, M., SIDDIQUI, Z. A., AKRAM, M., ASIF, H., SULTANA, S. & KHAN, A. 2014. Epidemiology, etiology, diagnosis and treatment of prostate cancer. *Asian Pac J Cancer Prev*, 15, 9575-8.
- DAVIS, A. J. & CHEN, D. J. 2013. DNA double strand break repair via non-homologous end-joining. *Translational cancer research*, 2, 130.
- DE MURCIA, G. & DE MURCIA, J. M. 1994. Poly (ADP-ribose) polymerase: a molecular nick-sensor. *Trends in biochemical sciences*, 19, 172-176.
- DE MURCIA, G., SCHREIBER, V., MOLINETE, M., SAULIER, B., POCH, O., MASSON, M., NIEDERGANG, C. & DE MURCIA, J. M. 1994. Structure and function of poly (ADP-ribose) polymerase. *Molecular and cellular biochemistry*, 138, 15-24.
- DE MURCIA, J. M., NIEDERGANG, C., TRUCCO, C., RICOUL, M., DUTRILLAUX, B., MARK, M., OLIVER, F. J., MASSON, M., DIERICH, A. & LEMEURE, M. 1997. Requirement of poly (ADP-ribose) polymerase in recovery from DNA damage in mice and in cells. *Proceedings of the National Academy of Sciences*, 94, 7303-7307.
- DE RUIJTER, A. J., VAN GENNIP, A. H., CARON, H. N., KEMP, S. & VAN KUILENBURG, A. B. 2003. Histone deacetylases (HDACs): characterization of the classical HDAC family. *Biochem J*, 370, 737-49.
- DE VOS, M., SCHREIBER, V. & DANTZER, F. 2012. The diverse roles and clinical relevance of PARPs in DNA damage repair: current state of the art. *Biochemical pharmacology*, 84, 137-146.
- DE ZIO, D., CIANFANELLI, V. & CECCONI, F. 2013. New insights into the link between DNA damage and apoptosis. *Antioxid Redox Signal*, 19, 559-71.
- DEEKS, E. D. 2015. Olaparib: first global approval. *Drugs*, 75, 231-40.
- DELANEY, C. A., WANG, L. Z., KYLE, S., WHITE, A. W., CALVERT, A. H., CURTIN, N. J., DURKACZ, B. W., HOSTOMSKY, Z. & NEWELL, D. R. 2000. Potentiation of temozolomide and topotecan growth inhibition and cytotoxicity by novel poly(adenosine diphosphoribose) polymerase inhibitors in a panel of human tumor cell lines. *Clin Cancer Res*, 6, 2860-7.
- DOMANN, F. E., RICE, J. C., HENDRIX, M. J. & FUTSCHER, B. W. 2000. Epigenetic silencing of maspin gene expression in human breast cancers. *Int J Cancer*, 85, 805-10.
- DREW, Y., LEDERMANN, J., HALL, G., REA, D., GLASSPOOL, R., HIGHLEY, M., JAYSON, G., SLUDDEN, J., MURRAY, J., JAMIESON, D., HALFORD, S., ACTON, G., BACKHOLER, Z., MANGANO, R., BODDY, A., CURTIN, N. & PLUMMER, R. 2016. Phase 2 multicentre trial investigating intermittent and continuous dosing schedules of the poly(ADP-ribose) polymerase inhibitor rucaparib in germline BRCA mutation carriers with advanced ovarian and breast cancer. *Br J Cancer*, 114, 723-30.
- DREW, Y. & PLUMMER, R. 2009. PARP inhibitors in cancer therapy: two modes of attack on the cancer cell widening the clinical applications. *Drug Resist Updat*, 12, 153-6.
- DREXLER, H. G. & UPHOFF, C. C. 2002. Mycoplasma contamination of cell cultures: Incidence, sources, effects, detection, elimination, prevention. *Cytotechnology*, 39, 75-90.
- DUNGEY, F. A., LOSER, D. A. & CHALMERS, A. J. 2008. Replication-dependent radiosensitization of human glioma cells by inhibition of poly(ADP-Ribose) polymerase: mechanisms and therapeutic potential. *Int J Radiat Oncol Biol Phys*, 72, 1188-97.
- DURKACZ, B. W., OMIDIJI, O., GRAY, D. A. & SHALL, S. 1980. (ADP-ribose)_n participates in DNA excision repair. *Nature*, 283, 593-6.

- DZIAMAN, T., LUDWICZAK, H., CIESLA, J. M., BANASZKIEWICZ, Z., WINCZURA, A., CHMIELARCZYK, M., WISNIEWSKA, E., MARSZALEK, A., TUDEK, B. & OLINSKI, R. 2014. PARP-1 expression is increased in colon adenoma and carcinoma and correlates with OGG1. *PLoS One*, 9, e115558.
- DZINIC, S. H., CHEN, K., THAKUR, A., KAPLUN, A., BONFIL, R. D., LI, X., LIU, J., BERNARDO, M. M., SALIGANAN, A., BACK, J. B., YANO, H., SCHALK, D. L., TOMASZEWSKI, E. N., BEYDOUN, A. S., DYSON, G., MUJAGIC, A., KRASS, D., DEAN, I., MI, Q. S., HEATH, E., SAKR, W., LUM, L. G. & SHENG, S. 2014. Maspin expression in prostate tumor elicits host anti-tumor immunity. *Oncotarget*, 5, 11225-36.
- ECKSCHLAGER, T., PLCH, J., STIBOROVA, M. & HRABETA, J. 2017. Histone Deacetylase Inhibitors as Anticancer Drugs. *Int J Mol Sci*, 18.
- FARMER, H., MCCABE, N., LORD, C. J., TUTT, A. N., JOHNSON, D. A., RICHARDSON, T. B., SANTAROSA, M., DILLON, K. J., HICKSON, I., KNIGHTS, C., MARTIN, N. M., JACKSON, S. P., SMITH, G. C. & ASHWORTH, A. 2005. Targeting the DNA repair defect in BRCA mutant cells as a therapeutic strategy. *Nature*, 434, 917-21.
- FIGUEROA-GONZALEZ, G. & PEREZ-PLASENCIA, C. 2017. Strategies for the evaluation of DNA damage and repair mechanisms in cancer. *Oncol Lett*, 13, 3982-3988.
- FISHER, A. E., HOCHEGGER, H., TAKEDA, S. & CALDECOTT, K. W. 2007. Poly (ADP-ribose) polymerase 1 accelerates single-strand break repair in concert with poly (ADP-ribose) glycohydrolase. *Molecular and cellular biology*, 27, 5597-5605.
- FITZGERALD, M., OSHIRO, M., HOLTAN, N., KRAGER, K., CULLEN, J. J., FUTSCHER, B. W. & DOMANN, F. E. 2003. Human pancreatic carcinoma cells activate maspin expression through loss of epigenetic control. *Neoplasia*, 5, 427-36.
- FRANCO, R., SCHONEVELD, O., GEORGAKILAS, A. G. & PANAYIOTIDIS, M. I. 2008. Oxidative stress, DNA methylation and carcinogenesis. *Cancer Letters*, 266, 6-11.
- FRELIN, C., IMBERT, V., GRIESSINGER, E., PEYRON, A. C., ROCHET, N., PHILIP, P., DAGEVILLE, C., SIRVENT, A., HUMMELBERGER, M., BERARD, E., DREANO, M., SIRVENT, N. & PEYRON, J. F. 2005. Targeting NF-kappaB activation via pharmacologic inhibition of IKK2-induced apoptosis of human acute myeloid leukemia cells. *Blood*, 105, 804-11.
- FUTSCHER, B. W., O'MEARA, M. M., KIM, C. J., RENNELS, M. A., LU, D., GRUMAN, L. M., SEFTOR, R. E., HENDRIX, M. J. & DOMANN, F. E. 2004. Aberrant methylation of the maspin promoter is an early event in human breast cancer. *Neoplasia*, 6, 380-9.
- GAMBLE, C., MCINTOSH, K., SCOTT, R., HO, K. H., PLEVIN, R. & PAUL, A. 2012. Inhibitory kappa B Kinases as targets for pharmacological regulation. *Br J Pharmacol*, 165, 802-19.
- GAO, F., SHI, H. Y., DAUGHTY, C., CELLA, N. & ZHANG, M. 2004. Maspin plays an essential role in early embryonic development. *Development*, 131, 1479-89.
- GARJE, R., VADDEPALLY, R. K. & ZAKHARIA, Y. 2020. PARP Inhibitors in Prostate and Urothelial Cancers. *Front Oncol*, 10, 114.
- GARNETT, M. J., EDELMAN, E. J., HEIDORN, S. J., GREENMAN, C. D., DASTUR, A., LAU, K. W., GRENINGER, P., THOMPSON, I. R., LUO, X., SOARES, J., LIU, Q., IORIO, F., SURDEZ, D., CHEN, L., MILANO, R. J., BIGNELL, G. R., TAM, A. T., DAVIES, H., STEVENSON, J. A., BARTHORPE, S., LUTZ, S. R., KOGERA, F., LAWRENCE, K., MCLAREN-DOUGLAS, A., MITROPOULOS, X., MIRONENKO, T., THI, H., RICHARDSON, L., ZHOU, W., JEWITT, F., ZHANG, T., O'BRIEN, P., BOISVERT, J. L., PRICE, S., HUR, W., YANG, W., DENG, X., BUTLER, A., CHOI, H. G., CHANG, J. W., BASELGA, J., STAMENKOVIC, I., ENGELMAN, J. A., SHARMA, S. V., DELATTRE, O., SAEZ-RODRIGUEZ, J., GRAY, N. S., SETTLEMAN, J., FUTREAL, P. A., HABER, D. A., STRATTON, M. R., RAMASWAMY, S., MCDERMOTT, U. & BENES, C. H. 2012. Systematic identification of genomic markers of drug sensitivity in cancer cells. *Nature*, 483, 570-5.
- GARTLER, S. M. 1967. Genetic markers as tracers in cell culture. *Natl Cancer Inst Monogr*, 26, 167-95.
- GEISLER, J. 2015. *Choosing the best detection method: Absorbance vs. Fluorescence*. [Online]. Biocompare. Available: <https://www.biocompare.com/Bench-Tips/173963-Choosing-the-Best-Detection-Method-Absorbance-vs-Fluorescence/> [Accessed].

- GIANSANTI, V., DONA, F., TILLHON, M. & SCOVASSI, A. I. 2010. PARP inhibitors: new tools to protect from inflammation. *Biochem Pharmacol*, 80, 1869-77.
- GIBSON, B. A. & KRAUS, W. L. 2012. New insights into the molecular and cellular functions of poly (ADP-ribose) and PARPs. *Nature reviews Molecular cell biology*, 13, 411-424.
- GILMORE, T. D. 2006. Introduction to NF- κ B: players, pathways, perspectives. *Oncogene*, 25, 6680-6684.
- GIOPANO, I., LILIS, I., PAPADAKI, H., PAPADAS, T. & STATHOPOULOS, G. T. 2017. A link between RelB expression and tumor progression in laryngeal cancer. *Oncotarget*, 8, 114019-114030.
- GLOBAL BURDEN OF DISEASE CANCER, C. 2015. The global burden of cancer 2013. *JAMA Oncology*, 1, 505-527.
- GLOZAK, M. A. & SETO, E. 2007. Histone deacetylases and cancer. *Oncogene*, 26, 5420-32.
- GODON, C., CORDELIÈRES, F. P., BIARD, D., GIOCANTI, N., MEGNIN-CHANET, F., HALL, J. & FAVAUDON, V. 2008. PARP inhibition versus PARP-1 silencing: different outcomes in terms of single-strand break repair and radiation susceptibility. *Nucleic Acids Res*, 36, 4454-64.
- GOKTUNA, S. I., CANLI, O., BOLLRATH, J., FINGERLE, A. A., HORST, D., DIAMANTI, M. A., PALLANGYO, C., BENNECKE, M., NEBELSIEK, T., MANKAN, A. K., LANG, R., ARTIS, D., HU, Y., PATZELT, T., RULAND, J., KIRCHNER, T., TAKETO, M. M., CHARIOT, A., ARKAN, M. C. & GRETEN, F. R. 2014. IKK α promotes intestinal tumorigenesis by limiting recruitment of M1-like polarized myeloid cells. *Cell Rep*, 7, 1914-25.
- GOULET, B., KENNETTE, W., ABLACK, A., POSTENKA, C. O., HAGUE, M. N., MYMRYK, J. S., TUCK, A. B., GIGUERE, V., CHAMBERS, A. F. & LEWIS, J. D. 2011. Nuclear localization of maspin is essential for its inhibition of tumor growth and metastasis. *Lab Invest*, 91, 1181-7.
- GRADA, A., OTERO-VINAS, M., PRIETO-CASTRILLO, F., OBAGI, Z. & FALANGA, V. 2017. Research Techniques Made Simple: Analysis of Collective Cell Migration Using the Wound Healing Assay. *J Invest Dermatol*, 137, e11-e16.
- GROSELJ, B., SHARMA, N. L., HAMDY, F. C., KERR, M. & KILTIE, A. E. 2013. Histone deacetylase inhibitors as radiosensitisers: effects on DNA damage signalling and repair. *Br J Cancer*, 108, 748-54.
- GU, L., WANG, Z., ZUO, J., LI, H. & ZHA, L. 2018. Prognostic significance of NF- κ B expression in non-small cell lung cancer: A meta-analysis. *PLoS One*, 13, e0198223.
- GUO, R. X., QIAO, Y. H., ZHOU, Y., LI, L. X., SHI, H. R. & CHEN, K. S. 2008. Increased staining for phosphorylated AKT and nuclear factor- κ B p65 and their relationship with prognosis in epithelial ovarian cancer. *Pathol Int*, 58, 749-56.
- GUO, W., CHEN, W., YU, W., HUANG, W. & DENG, W. 2013. Small interfering RNA-based molecular therapy of cancers. *Chin J Cancer*, 32, 488-93.
- GURZU, S., KADAR, Z., SUGIMURA, H., ORLOWSKA, J., BARA, T., BARA, T., JR., SZEDERJESI, J. & JUNG, I. 2016. Maspin-related Orchestration of Aggressiveness of Gastric Cancer. *Appl Immunohistochem Mol Morphol*, 24, 326-36.
- HA, K., FISKUS, W., CHOI, D. S., BHASKARA, S., CERCHIETTI, L., DEVARAJ, S. G., SHAH, B., SHARMA, S., CHANG, J. C., MELNICK, A. M., HIEBERT, S. & BHALLA, K. N. 2014. Histone deacetylase inhibitor treatment induces 'BRCAness' and synergistic lethality with PARP inhibitor and cisplatin against human triple negative breast cancer cells. *Oncotarget*, 5, 5637-50.
- HAIBE-KAINS, B., EL-HACHEM, N., BIRKBAK, N. J., JIN, A. C., BECK, A. H., AERTS, H. J. & QUACKENBUSH, J. 2013. Inconsistency in large pharmacogenomic studies. *Nature*, 504, 389-93.
- HAINCE, J.-F., MCDONALD, D., RODRIGUE, A., DÉRY, U., MASSON, J.-Y., HENDZEL, M. J. & POIRIER, G. G. 2008. PARP1-dependent kinetics of recruitment of MRE11 and NBS1 proteins to multiple DNA damage sites. *Journal of Biological Chemistry*, 283, 1197-1208.
- HALKIDOU, K., GAUGHAN, L., COOK, S., LEUNG, H. Y., NEAL, D. E. & ROBSON, C. N. 2004. Upregulation and nuclear recruitment of HDAC1 in hormone refractory prostate cancer. *Prostate*, 59, 177-89.

- HANAHAHAN, D. & WEINBERG, ROBERT A. 2011. Hallmarks of Cancer: The Next Generation. *Cell*, 144, 646-674.
- HASSA, P. & HOTTIGER, M. 2002. The functional role of poly (ADP-ribose) polymerase 1 as novel coactivator of NF- κ B in inflammatory disorders. *Cellular and Molecular Life Sciences*, 59, 1534-1553.
- HASSA, P. O., COVIC, M., HASAN, S., IMHOF, R. & HOTTIGER, M. O. 2001. The enzymatic and DNA binding activity of PARP-1 are not required for NF-kappa B coactivator function. *J Biol Chem*, 276, 45588-97.
- HASSA, P. O., HAENNI, S. S., BUERKI, C., MEIER, N. I., LANE, W. S., OWEN, H., GERSBACH, M., IMHOF, R. & HOTTIGER, M. O. 2005. Acetylation of poly(ADP-ribose) polymerase-1 by p300/CREB-binding protein regulates coactivation of NF-kappaB-dependent transcription. *J Biol Chem*, 280, 40450-64.
- HAYDEN, M. S. & GHOSH, S. 2008. Shared principles in NF-kappaB signaling. *Cell*, 132.
- HAYDEN, M. S. & GHOSH, S. 2012. NF-kappaB, the first quarter-century: remarkable progress and outstanding questions. *Genes Dev*, 26, 203-34.
- HE, Y., CHEN, F., CAI, Y. & CHEN, S. 2015. Knockdown of tumor protein D52-like 2 induces cell growth inhibition and apoptosis in oral squamous cell carcinoma. *Cell Biol Int*, 39, 264-71.
- HÉBERLÉ, E., AMÉ, J.-C., ILLUZZI, G., DANTZER, F. & SCHREIBER, V. 2015. Discovery of the PARP superfamily and focus on the lesser exhibited but not lesser talented members. *PARP Inhibitors for Cancer Therapy*. Springer.
- HELLEDAY, T., LO, J., VAN GENT, D. C. & ENGELWARD, B. P. 2007. DNA double-strand break repair: from mechanistic understanding to cancer treatment. *DNA repair*, 6, 923-935.
- HIGGINS, L. H., WITHERS, H. G., GARBENS, A., LOVE, H. D., MAGNONI, L., HAYWARD, S. W. & MOYES, C. D. 2009. Hypoxia and the metabolic phenotype of prostate cancer cells. *Biochim Biophys Acta*, 1787, 1433-43.
- HOEIJMAKERS, J. H. 2001. Genome maintenance mechanisms for preventing cancer. *nature*, 411, 366.
- HOESEL, B. & SCHMID, J. A. 2013. The complexity of NF- κ B signaling in inflammation and cancer. *Mol Cancer*, 12, 1-15.
- HONG, S. W., JIANG, Y., KIM, S., LI, C. J. & LEE, D. K. 2014. Target gene abundance contributes to the efficiency of siRNA-mediated gene silencing. *Nucleic Acid Ther*, 24, 192-8.
- HOPKINS, T. A., AINSWORTH, W. B., ELLIS, P. A., DONAWHO, C. K., DIGIAMMARINO, E. L., PANCHAL, S. C., ABRAHAM, V. C., ALGIRE, M. A., SHI, Y., OLSON, A. M., JOHNSON, E. F., WILSBACHER, J. L. & MAAG, D. 2019. PARP1 Trapping by PARP Inhibitors Drives Cytotoxicity in Both Cancer Cells and Healthy Bone Marrow. *Mol Cancer Res*, 17, 409-419.
- HORSWILL, M. A., NARAYAN, M., WAREJCKA, D. J., CIRILLO, L. A. & TWINING, S. S. 2008. Epigenetic silencing of maspin expression occurs early in the conversion of keratocytes to fibroblasts. *Exp Eye Res*, 86, 586-600.
- HOU, A. H. 2009. The role of LHRH antagonists in the treatment of prostate cancer. *Oncology*, 23, 626.
- HU, B., WENG, Y., XIA, X. H., LIANG, X. J. & HUANG, Y. 2019. Clinical advances of siRNA therapeutics. *J Gene Med*, 21, e3097.
- HUANG, S., PETTAWAY, C. A., UEHARA, H., BUCANA, C. D. & FIDLER, I. J. 2001. Blockade of NF-kappaB activity in human prostate cancer cells is associated with suppression of angiogenesis, invasion, and metastasis. *Oncogene*, 20, 4188-97.
- HUANG, W.-C. & HUNG, M.-C. 2013. Beyond NF- κ B activation: nuclear functions of I κ B kinase α . *J Biomed Sci*, 20, 28.
- HUANG, Y., LIU, X., DONG, L., LIU, Z., HE, X. & LIU, W. 2011. Development of viral vectors for gene therapy for chronic pain. *Pain Res Treat*, 2011, 968218.
- HUBER, M. A., AZOITEI, N., BAUMANN, B., GRÜNERT, S., SOMMER, A., PEHAMBERGER, H., KRAUT, N., BEUG, H. & WIRTH, T. 2004. NF- κ B is essential for epithelial-mesenchymal transition and metastasis in a model of breast cancer progression. *J Clin Invest*, 114.

- HUMPHREY, P. A. 2004. Gleason grading and prognostic factors in carcinoma of the prostate. *Modern pathology*, 17, 292-306.
- HUNG, M. C. & LINK, W. 2011. Protein localization in disease and therapy. *J Cell Sci*, 124, 3381-92.
- HUNTER, J. E., WILLMORE, E., IRVING, J. A. E., HOSTOMSKY, Z., VEUGER, S. J. & DURKACZ, B. W. 2012. NF- κ B mediates radio-sensitization by the PARP-1 inhibitor, AG-014699. *Oncogene*, 31, 251-264.
- ILINA, O. & FRIEDL, P. 2009. Mechanisms of collective cell migration at a glance. *J Cell Sci*, 122, 3203-8.
- ISRAEL, A. 2010. The IKK complex, a central regulator of NF-kappaB activation. *Cold Spring Harb Perspect Biol*, 2, a000158.
- IVASHKEVICH, A., REDON, C. E., NAKAMURA, A. J., MARTIN, R. F. & MARTIN, O. A. 2012. Use of the gamma-H2AX assay to monitor DNA damage and repair in translational cancer research. *Cancer Lett*, 327, 123-33.
- JACKSON, S. P. 2002. Sensing and repairing DNA double-strand breaks. *Carcinogenesis*, 23, 687-696.
- JAMALADDIN, S., KELLY, R. D., O'REGAN, L., DOVEY, O. M., HODSON, G. E., MILLARD, C. J., PORTOLANO, N., FRY, A. M., SCHWABE, J. W. & COWLEY, S. M. 2014. Histone deacetylase (HDAC) 1 and 2 are essential for accurate cell division and the pluripotency of embryonic stem cells. *Proc Natl Acad Sci U S A*, 111, 9840-5.
- JANSSENS, S. & TSCHOPP, J. 2006. Signals from within: the DNA-damage-induced NF-kappaB response. *Cell Death Differ*, 13, 773-84.
- JASEK, E., GAJDA, M., LIS, G. J., JASINSKA, M. & LITWIN, J. A. 2014. Combinatorial effects of PARP inhibitor PJ34 and histone deacetylase inhibitor vorinostat on leukemia cell lines. *Anticancer Res*, 34, 1849-56.
- JAVLE, M. & CURTIN, N. 2011. The role of PARP in DNA repair and its therapeutic exploitation. *British journal of cancer*, 105, 1114.
- JENKINSON, S. E., BROWN, L. J., OMBOR, J., MILBURN, J. A., SMULDERS-SRINIVASAN, T., VEUGER, S., EDWARDS, D. R. & BASS, R. 2017. Identification of novel peptide motifs in the serpin maspin that affect vascular smooth muscle cell function. *Biochim Biophys Acta Mol Cell Res*, 1864, 336-344.
- JIANG, N., MENG, Y., ZHANG, S., MENSAH-OSMAN, E. & SHENG, S. 2002. Maspin sensitizes breast carcinoma cells to induced apoptosis. *Oncogene*, 21, 4089-98.
- JIANG, R., XIA, Y., LI, J., DENG, L., ZHAO, L., SHI, J., WANG, X. & SUN, B. 2010. High expression levels of IKKalpha and IKKbeta are necessary for the malignant properties of liver cancer. *Int J Cancer*, 126, 1263-74.
- JIANG, X., LI, W., LI, X., BAI, H. & ZHANG, Z. 2019. Current status and future prospects of PARP inhibitor clinical trials in ovarian cancer. *Cancer Manag Res*, 11, 4371-4390.
- JIN, L., ZENG, X., LIU, M., DENG, Y. & HE, N. 2014a. Current progress in gene delivery technology based on chemical methods and nano-carriers. *Theranostics*, 4, 240-55.
- JIN, R., YI, Y., YULL, F. E., BLACKWELL, T. S., CLARK, P. E., KOYAMA, T., SMITH, J. A. & MATUSIK, R. J. 2014b. NF- κ B gene signature predicts prostate cancer progression. *Cancer research*, 74, 2763-2772.
- JIN, R. J., LHO, Y., CONNELLY, L., WANG, Y., YU, X., SAINT JEAN, L., CASE, T. C., ELLWOOD-YEN, K., SAWYERS, C. L., BHOWMICK, N. A., BLACKWELL, T. S., YULL, F. E. & MATUSIK, R. J. 2008a. The nuclear factor-kappaB pathway controls the progression of prostate cancer to androgen-independent growth. *Cancer Res*, 68, 6762-9.
- JIN, X., WANG, Z., QIU, L., ZHANG, D., GUO, Z., GAO, Z., DENG, C., WANG, F., WANG, S. & GUO, C. 2008b. Potential biomarkers involving IKK/RelA signal in early stage non-small cell lung cancer. *Cancer Sci*, 99, 582-9.
- JONSSON, P., BANDLAMUDI, C., CHENG, M. L., SRINIVASAN, P., CHAVAN, S. S., FRIEDMAN, N. D., ROSEN, E. Y., RICHARDS, A. L., BOUVIER, N., SELCUKLU, S. D., BIELSKI, C. M., ABIDA, W., MANDELKER, D., BIRSOY, O., ZHANG, L., ZEHIR, A., DONOGHUE, M. T. A., BASELGA, J., OFFIT, K., SCHER, H. I., O'REILLY, E. M., STADLER, Z. K., SCHULTZ, N., SOCCI, N. D., VIALE,

- A., LADANYI, M., ROBSON, M. E., HYMAN, D. M., BERGER, M. F., SOLIT, D. B. & TAYLOR, B. S. 2019. Tumour lineage shapes BRCA-mediated phenotypes. *Nature*, 571, 576-579.
- KACHHAP, S. K., ROSMUS, N., COLLIS, S. J., KORTENHORST, M. S., WISSING, M. D., HEDAYATI, M., SHABBEER, S., MENDONCA, J., DEANGELIS, J., MARCHIONNI, L., LIN, J., HOTI, N., NORTIER, J. W., DEWEESE, T. L., HAMMERS, H. & CARDUCCI, M. A. 2010. Downregulation of homologous recombination DNA repair genes by HDAC inhibition in prostate cancer is mediated through the E2F1 transcription factor. *PLoS One*, 5, e11208.
- KAESTNER, L., SCHOLZ, A. & LIPP, P. 2015. Conceptual and technical aspects of transfection and gene delivery. *Bioorg Med Chem Lett*, 25, 1171-6.
- KAIGHN, M. E., NARAYAN, K. S., OHNUKI, Y., LECHNER, J. F. & JONES, L. W. 1979. Establishment and characterization of a human prostatic carcinoma cell line (PC-3). *Invest Urol*, 17, 16-23.
- KALTSCHMIDT, B., KALTSCHMIDT, C., HEHNER, S. P., DROGE, W. & SCHMITZ, M. L. 1999. Repression of NF-kappaB impairs HeLa cell proliferation by functional interference with cell cycle checkpoint regulators. *Oncogene*, 18, 3213-25.
- KAPLUN, A., DZINIC, S., BERNARDO, M. & SHENG, S. 2012. Tumor suppressor maspin as a rheostat in HDAC regulation to achieve the fine-tuning of epithelial homeostasis. *Crit Rev Eukaryot Gene Expr*, 22, 249-58.
- KARIN, M. 2009. NF- κ B as a critical link between inflammation and cancer. *Cold Spring Harbor perspectives in biology*, 1, a000141.
- KARIN, M., CAO, Y., GRETEN, F. R. & LI, Z.-W. 2002. NF- κ B in cancer: from innocent bystander to major culprit. *Nature reviews cancer*, 2, 301-310.
- KAUR, G. & DUFOUR, J. M. 2012. Cell lines: Valuable tools or useless artifacts. *Spermatogenesis*, 2, 1-5.
- KAUSHIK, D., VASHISTHA, V., ISHARWAL, S., SEDIQE, S. A. & LIN, M. F. 2015. Histone deacetylase inhibitors in castration-resistant prostate cancer: molecular mechanism of action and recent clinical trials. *Ther Adv Urol*, 7, 388-95.
- KENT, E. C. & HUSSAIN, M. H. 2003. Neoadjuvant therapy for prostate cancer: an Oncologist's perspective. *Reviews in urology*, 5, S28.
- KHALKHALI-ELLIS, Z. 2006. Maspin: the new frontier. *Clin Cancer Res*, 12, 7279-83.
- KHANAREE, C., CHAIRATVIT, K., ROYTRAKUL, S. & WONGNOPPAVICH, A. 2013. Reactive center loop moiety is essential for the maspin activity on cellular invasion and ubiquitin-proteasome level. *Oncol Res*, 20, 427-35.
- KIM, H. J. & BAE, S. C. 2011. Histone deacetylase inhibitors: molecular mechanisms of action and clinical trials as anti-cancer drugs. *Am J Transl Res*, 3, 166-79.
- KIM, H. R., KIM, E. J., YANG, S. H., JEONG, E. T., PARK, C., LEE, J. H., YOUN, M. J., SO, H. S. & PARK, R. 2006a. Trichostatin A induces apoptosis in lung cancer cells via simultaneous activation of the death receptor-mediated and mitochondrial pathway? *Exp Mol Med*, 38, 616-24.
- KIM, J., JANG, K. T., KIM, K. H., PARK, J. W., CHANG, B. J., LEE, K. H., LEE, J. K., HEO, J. S., CHOI, S. H., CHOI, D. W., RHEE, J. C. & LEE, K. T. 2010a. Aberrant maspin expression is involved in early carcinogenesis of gallbladder cancer. *Tumour Biol*, 31, 471-6.
- KIM, J. Y., SHEN, S., DIETZ, K., HE, Y., HOWELL, O., REYNOLDS, R. & CASACCIA, P. 2010b. HDAC1 nuclear export induced by pathological conditions is essential for the onset of axonal damage. *Nat Neurosci*, 13, 180-9.
- KIM, M. S., BLAKE, M., BAEK, J. H., KOHLHAGEN, G., POMMIER, Y. & CARRIER, F. 2003. Inhibition of histone deacetylase increases cytotoxicity to anticancer drugs targeting DNA. *Cancer Res*, 63, 7291-300.
- KIM, M. Y., ZHANG, T. & KRAUS, W. L. 2005. Poly (ADP-ribose) ation by PARP-1:PAR-laying'NAD+ into a nuclear signal. *Genes & development*, 19, 1951-1967.
- KIM, N. H., KIM, S. N. & KIM, Y. K. 2011. Involvement of HDAC1 in E-cadherin expression in prostate cancer cells; its implication for cell motility and invasion. *Biochem Biophys Res Commun*, 404, 915-21.

- KIM, T. K. & EBERWINE, J. H. 2010. Mammalian cell transfection: the present and the future. *Anal Bioanal Chem*, 397, 3173-8.
- KIM, Y., KIM, A., SHARIP, A., SHARIP, A., JIANG, J., YANG, Q. & XIE, Y. 2017. Reverse the Resistance to PARP Inhibitors. *Int J Biol Sci*, 13, 198-208.
- KIM, Y. K., LEE, E. K., KANG, J. K., KIM, J. A., YOU, J. S., PARK, J. H., SEO, D. W., HWANG, J. W., KIM, S. N., LEE, H. Y., LEE, H. W. & HAN, J. W. 2006b. Activation of NF-kappaB by HDAC inhibitor apicidin through Sp1-dependent de novo protein synthesis: its implication for resistance to apoptosis. *Cell Death Differ*, 13, 2033-41.
- KLOTZ, L. & EMBERTON, M. 2014. Management of low risk prostate cancer [mdash] active surveillance and focal therapy. *Nature reviews Clinical oncology*, 11, 324-334.
- KLOTZ, L., ZHANG, L., LAM, A., NAM, R., MAMEDOV, A. & LOBLAW, A. 2009. Clinical results of long-term follow-up of a large, active surveillance cohort with localized prostate cancer. *Journal of Clinical Oncology*, 28, 126-131.
- KOMMU, S., EDWARDS, S. & EELES, R. 2004. The Clinical Genetics of Prostate Cancer. *Hereditary Cancer in Clinical Practice*, 2, 111.
- KORDES, U., KRAPPMANN, D., HEISSMEYER, V., LUDWIG, W. D. & SCHEIDEREIT, C. 2000. Transcription factor NF-kappaB is constitutively activated in acute lymphoblastic leukemia cells. *Leukemia*, 14, 399-402.
- KOWALCZYKOWSKI, S. C. 2015. An overview of the molecular mechanisms of recombinational DNA repair. *Cold Spring Harbor perspectives in biology*, 7, a016410.
- KRISHNAKUMAR, R. & KRAUS, W. L. 2010. The PARP side of the nucleus: molecular actions, physiological outcomes, and clinical targets. *Mol Cell*, 39, 8-24.
- KROKAN, H. E. & BJØRÅS, M. 2013. Base excision repair. *Cold Spring Harbor perspectives in biology*, 5, a012583.
- KRUMM, A., BARCKHAUSEN, C., KUCUK, P., TOMASZOWSKI, K. H., LOQUAI, C., FAHRER, J., KRAMER, O. H., KAINA, B. & ROOS, W. P. 2016. Enhanced Histone Deacetylase Activity in Malignant Melanoma Provokes RAD51 and FANCD2-Triggered Drug Resistance. *Cancer Res*, 76, 3067-77.
- KUFE, D. W., POLLOCK, R. E., WEICHELBAUM, R. R., BAST, R. C., GANSLER, T. S., HOLLAND, J. F. & FREI, E. 2003. Holland-Frei cancer medicine.
- KUMAR, R. & CHEOK, C. F. 2014. RIF1: a novel regulatory factor for DNA replication and DNA damage response signaling. *DNA Repair (Amst)*, 15, 54-9.
- LAFARGUE, C. J., DAL MOLIN, G. Z., SOOD, A. K. & COLEMAN, R. L. 2019. Exploring and comparing adverse events between PARP inhibitors. *Lancet Oncol*, 20, e15-e28.
- LAGGER, G., O'CARROLL, D., REMBOLD, M., KHIER, H., TISCHLER, J., WEITZER, G., SCHUETTENGRUBER, B., HAUSER, C., BRUNMEIR, R., JENUWEIN, T. & SEISER, C. 2002. Essential function of histone deacetylase 1 in proliferation control and CDK inhibitor repression. *EMBO J*, 21, 2672-81.
- LANGELIER, M.-F., PLANCK, J. L., ROY, S. & PASCAL, J. M. 2011. Crystal structures of poly (ADP-ribose) polymerase-1 (PARP-1) zinc fingers bound to DNA structural and functional insights into DNA-dependent PARP-1 activity. *Journal of biological chemistry*, 286, 10690-10701.
- LANGELIER, M.-F., SERVENT, K. M., ROGERS, E. E. & PASCAL, J. M. 2008. A third zinc-binding domain of human poly (ADP-ribose) polymerase-1 coordinates DNA-dependent enzyme activation. *Journal of biological chemistry*, 283, 4105-4114.
- LATHA, K., ZHANG, W., CELLA, N., SHI, H. Y. & ZHANG, M. 2005. Maspin mediates increased tumor cell apoptosis upon induction of the mitochondrial permeability transition. *Mol Cell Biol*, 25, 1737-48.
- LAW, R. H., IRVING, J. A., BUCKLE, A. M., RUZYLA, K., BUZZA, M., BASHTANNYK-PUHALOVICH, T. A., BEDDOE, T. C., NGUYEN, K., WORRALL, D. M. & BOTTOMLEY, S. P. 2005. The high resolution crystal structure of the human tumor suppressor maspin reveals a novel conformational switch in the G-helix. *Journal of Biological Chemistry*, 280, 22356-22364.

- LAW, R. H., ZHANG, Q., MCGOWAN, S., BUCKLE, A. M., SILVERMAN, G. A., WONG, W., ROSADO, C. J., LANGENDORF, C. G., PIKE, R. N., BIRD, P. I. & WHISSTOCK, J. C. 2006. An overview of the serpin superfamily. *Genome Biol*, 7, 216.
- LAWRENCE, T., BEBIEN, M., LIU, G. Y., NIZET, V. & KARIN, M. 2005. IKK α limits macrophage NF-kappaB activation and contributes to the resolution of inflammation. *Nature*, 434.
- LEE, D. Y., PARK, C. S., KIM, H. S., KIM, J. Y., KIM, Y. C. & LEE, S. 2008. Maspin and p53 protein expression in gastric adenocarcinoma and its clinical applications. *Appl Immunohistochem Mol Morphol*, 16, 13-8.
- LEE, J. H., CHOY, M. L., NGO, L., FOSTER, S. S. & MARKS, P. A. 2010. Histone deacetylase inhibitor induces DNA damage, which normal but not transformed cells can repair. *Proc Natl Acad Sci U S A*, 107, 14639-44.
- LEE, S. J., JANG, H. & PARK, C. 2012. Maspin increases Ku70 acetylation and Bax-mediated cell death in cancer cells. *Int J Mol Med*, 29, 225-30.
- LEOPIZZI, M., COCCHIOLA, R., MILANETTI, E., RAIMONDO, D., POLITI, L., GIORDANO, C., SCANDURRA, R. & SCOTTO D'ABUSCO, A. 2017. IKK α inhibition by a glucosamine derivative enhances Maspin expression in osteosarcoma cell line. *Chem Biol Interact*, 262, 19-28.
- LESSARD, L., MES-MASSON, A. M., LAMARRE, L., WALL, L., LATTOUF, J. B. & SAAD, F. 2003. NF-kappa B nuclear localization and its prognostic significance in prostate cancer. *BJU Int*, 91, 417-20.
- LEWIS, R. & HORNBERGER, B. 2016. The current state of prostate-specific antigen testing. *Journal of the American Academy of PAs*, 29, 51-53.
- LI, X., CHEN, D., YIN, S., MENG, Y., YANG, H., LANDIS-PIWOWAR, K. R., LI, Y., SARKAR, F. H., REDDY, G. P., DOU, Q. P. & SHENG, S. 2007. Maspin augments proteasome inhibitor-induced apoptosis in prostate cancer cells. *J Cell Physiol*, 212, 298-306.
- LI, X., KAPLUN, A., LONARDO, F., HEATH, E., SARKAR, F. H., IRISH, J., SAKR, W. & SHENG, S. 2011. HDAC1 inhibition by maspin abrogates epigenetic silencing of glutathione S-transferase pi in prostate carcinoma cells. *Mol Cancer Res*, 9, 733-45.
- LI, X., YIN, S., MENG, Y., SAKR, W. & SHENG, S. 2006. Endogenous inhibition of histone deacetylase 1 by tumor-suppressive maspin. *Cancer Res*, 66, 9323-9.
- LI, Y. & SETO, E. 2016. HDACs and HDAC Inhibitors in Cancer Development and Therapy. *Cold Spring Harb Perspect Med*, 6.
- LI, Z., SHI, H. Y. & ZHANG, M. 2005. Targeted expression of maspin in tumor vasculatures induces endothelial cell apoptosis. *Oncogene*, 24, 2008-19.
- LI, Z. & ZHU, W. G. 2014. Targeting histone deacetylases for cancer therapy: from molecular mechanisms to clinical implications. *Int J Biol Sci*, 10, 757-70.
- LIANG, C. C., PARK, A. Y. & GUAN, J. L. 2007. In vitro scratch assay: a convenient and inexpensive method for analysis of cell migration in vitro. *Nat Protoc*, 2, 329-33.
- LIAO, X. H., LI, Y. Q., WANG, N., ZHENG, L., XING, W. J., ZHAO, D. W., YAN, T. B., WANG, Y., LIU, L. Y., SUN, X. G., HU, P., ZHOU, H. & ZHANG, T. C. 2014. Re-expression and epigenetic modification of maspin induced apoptosis in MCF-7 cells mediated by myocardin. *Cell Signal*, 26, 1335-46.
- LIM, D. & NGEOW, J. 2016. Evaluation of the methods to identify patients who may benefit from PARP inhibitor use. *Endocr Relat Cancer*, 23, R267-85.
- LIN, K. T., WANG, Y. W., CHEN, C. T., HO, C. M., SU, W. H. & JOU, Y. S. 2012. HDAC inhibitors augmented cell migration and metastasis through induction of PKCs leading to identification of low toxicity modalities for combination cancer therapy. *Clin Cancer Res*, 18, 4691-701.
- LINDHOLM, P. F., BUB, J., KAUL, S., SHIDHAM, V. B. & KAJDACSZY-BALLA, A. 2000. The role of constitutive NF-kappaB activity in PC-3 human prostate cancer cell invasive behavior. *Clin Exp Metastasis*, 18, 471-9.
- LIU, H., SHI, J., ANANDAN, V., WANG, H. L., DIEHL, D., BLANSFIELD, J., GERHARD, G. & LIN, F. 2012. Reevaluation and identification of the best immunohistochemical panel (pVHL,

- Maspin, S100P, IMP-3) for ductal adenocarcinoma of the pancreas. *Arch Pathol Lab Med*, 136, 601-9.
- LIU, J., YIN, S., REDDY, N., SPENCER, C. & SHENG, S. 2004. Bax mediates the apoptosis-sensitizing effect of maspin. *Cancer Res*, 64, 1703-11.
- LIU, Q., TURNER, K. M., ALFRED YUNG, W. K., CHEN, K. & ZHANG, W. 2014. Role of AKT signaling in DNA repair and clinical response to cancer therapy. *Neuro Oncol*, 16, 1313-23.
- LIU, W. & SHOU, C. 2011. Mycoplasma hyorhinis and Mycoplasma fermentans induce cell apoptosis and changes in gene expression profiles of 32D cells. *Biol Res*, 44, 383-91.
- LIU, X., YU, Y., ZHANG, J., LU, C., WANG, L., LIU, P. & SONG, H. 2018. HDAC1 Silencing in Ovarian Cancer Enhances the Chemotherapy Response. *Cell Physiol Biochem*, 48, 1505-1518.
- LIU, Y., BURNES, M. L., MARTIN-TREVINO, R., GUY, J., BAI, S., HAROUAKA, R., BROOKS, M. D., SHANG, L., FOX, A., LUTHER, T. K., DAVIS, A., BAKER, T. L., COLACINO, J., CLOUTHIER, S. G., SHAO, Z. M., WICHA, M. S. & LIU, S. 2017. RAD51 Mediates Resistance of Cancer Stem Cells to PARP Inhibition in Triple-Negative Breast Cancer. *Clin Cancer Res*, 23, 514-522.
- LLOYD, F. P., JR., SLIVOVA, V., VALACHOVICOVA, T. & SLIVA, D. 2003. Aspirin inhibits highly invasive prostate cancer cells. *Int J Oncol*, 23, 1277-83.
- LLOYD, T., HOUNSOME, L., MEHAY, A., MEE, S., VERNE, J. & COOPER, A. 2015. Lifetime risk of being diagnosed with, or dying from, prostate cancer by major ethnic group in England 2008–2010. *BMC Medicine*, 13, 171.
- LUNDHOLT, B. K., SCUDDER, K. M. & PAGLIARO, L. 2003. A simple technique for reducing edge effect in cell-based assays. *Journal of biomolecular screening*, 8, 566-570.
- LUO, J.-L., TAN, W., RICONO, J. M., KORCHYNSKYI, O., ZHANG, M., GONIAS, S. L., CHERESH, D. A. & KARIN, M. 2007. Nuclear cytokine-activated IKK[agr] controls prostate cancer metastasis by repressing Maspin. *Nature*, 446, 690-694.
- LUO, X. & KRAUS, W. L. 2012a. On PAR with PARP: cellular stress signaling through poly (ADP-ribose) and PARP-1. *Genes & development*, 26, 417-432.
- LUO, X. & KRAUS, W. L. 2012b. On PAR with PARP: cellular stress signaling through poly(ADP-ribose) and PARP-1. *Genes Dev*, 26, 417-32.
- MA, L., SHEN, Y., ZHOU, P., ZHOU, J. & GUO, F. 2012. [NF-κB subunits regulate maspin expression in prostate cancer cells in vitro]. *Zhonghua zhong liu za zhi [Chinese journal of oncology]*, 34, 165-168.
- MAASS, N., HOJO, T., RÖSEL, F., IKEDA, T., JONAT, W. & NAGASAKI, K. 2001. Down regulation of the tumor suppressor gene maspin in breast carcinoma is associated with a higher risk of distant metastasis. *Clinical Biochemistry*, 34, 303-307.
- MACHTENS, S., SERTH, J., BOKEMEYER, C., BATHKE, W., MINSSEN, A., KOLLMANNBERGER, C., HARTMANN, J., KNUCHEL, R., KONDO, M., JONAS, U. & KUCZYK, M. 2001. Expression of the p53 and Maspin protein in primary prostate cancer: correlation with clinical features. *Int J Cancer*, 95, 337-42.
- MACKLEY, J. R., ANDO, J., HERZYK, P. & WINDER, S. J. 2006. Phenotypic responses to mechanical stress in fibroblasts from tendon, cornea and skin. *Biochem J*, 396, 307-16.
- MAEHARA, Y., ANAI, H., TAMADA, R. & SUGIMACHI, K. 1987. The ATP assay is more sensitive than the succinate dehydrogenase inhibition test for predicting cell viability. *Eur J Cancer Clin Oncol*, 23, 273-6.
- MAESAWA, C., OGASAWARA, S., YASHIMA-ABO, A., KIMURA, T., KOTANI, K., MASUDA, S., NAGATA, Y., IWAYA, T., SUZUKI, K., OYAKE, T., AKIYAMA, Y., KAWAMURA, H. & MASUDA, T. 2006. Aberrant maspin expression in gallbladder epithelium is associated with intestinal metaplasia in patients with cholelithiasis. *J Clin Pathol*, 59, 328-30.
- MAHATO, R., QIN, B. & CHENG, K. 2011. Blocking IKKalpha expression inhibits prostate cancer invasiveness. *Pharm Res*, 28, 1357-69.
- MAHMOODI CHALBATANI, G., DANA, H., GHARAGOUZLOO, E., GRIJALVO, S., ERITJA, R., LOGSDON, C. D., MEMARI, F., MIRI, S. R., RAD, M. R. & MARMARI, V. 2019. Small interfering RNAs (siRNAs) in cancer therapy: a nano-based approach. *Int J Nanomedicine*, 14, 3111-3128.

- MANN, M., KUMAR, S., SHARMA, A., CHAUHAN, S. S., BHATLA, N., KUMAR, S., BAKHSI, S., GUPTA, R. & KUMAR, L. 2019. PARP-1 inhibitor modulate beta-catenin signaling to enhance cisplatin sensitivity in cancer cervix. *Oncotarget*, 10, 4262-4275.
- MAO, Z., BOZZELLA, M., SELUANOV, A. & GORBUNOVA, V. 2008. DNA repair by nonhomologous end joining and homologous recombination during cell cycle in human cells. *Cell cycle*, 7, 2902-2906.
- MARIJON, H., LEE, D. H., DING, L., SUN, H., GERY, S., DE GRAMONT, A. & KOEFFLER, H. P. 2018. Co-targeting poly(ADP-ribose) polymerase (PARP) and histone deacetylase (HDAC) in triple-negative breast cancer: Higher synergism in BRCA mutated cells. *Biomed Pharmacother*, 99, 543-551.
- MARKS, P. A. 2010. The clinical development of histone deacetylase inhibitors as targeted anticancer drugs. *Expert Opin Investig Drugs*, 19, 1049-66.
- MARTÍN-OLIVA, D., O'VALLE, F., MUNOZ-GAMEZ, J. A., VALENZUELA, M. T., NUNEZ, M. I., AGUILAR, M., DE ALMODOVAR, J. R., DEL MORAL, R. G. & OLIVER, F. J. 2004. Crosstalk between PARP-1 and NF-[kappa] B modulates the promotion of skin neoplasia. *Oncogene*, 23, 5275.
- MARTIN-OLIVA, D., O'VALLE, F., MUNOZ-GAMEZ, J. A., VALENZUELA, M. T., NUNEZ, M. I., AGUILAR, M., RUIZ DE ALMODOVAR, J. M., GARCIA DEL MORAL, R. & OLIVER, F. J. 2004. Crosstalk between PARP-1 and NF-kappaB modulates the promotion of skin neoplasia. *Oncogene*, 23, 5275-83.
- MARX, V. 2014. Cell-line authentication demystified. *Nat Methods*, 11, 483-8.
- MASTERS, J. R. 2002. HeLa cells 50 years on: the good, the bad and the ugly. *Nat Rev Cancer*, 2, 315-9.
- MATEO, J., CARREIRA, S., SANDHU, S., MIRANDA, S., MOSSOP, H., PEREZ-LOPEZ, R., NAVA RODRIGUES, D., ROBINSON, D., OMLIN, A., TUNARIU, N., BOYSEN, G., PORTA, N., FLOHR, P., GILLMAN, A., FIGUEIREDO, I., PAULDING, C., SEED, G., JAIN, S., RALPH, C., PROTHEROE, A., HUSSAIN, S., JONES, R., ELLIOTT, T., MCGOVERN, U., BIANCHINI, D., GOODALL, J., ZAFEIRIOU, Z., WILLIAMSON, C. T., FERRALDESCHI, R., RIISNAES, R., EBBS, B., FOWLER, G., RODA, D., YUAN, W., WU, Y. M., CAO, X., BROUGH, R., PEMBERTON, H., A'HERN, R., SWAIN, A., KUNJU, L. P., EELES, R., ATTARD, G., LORD, C. J., ASHWORTH, A., RUBIN, M. A., KNUDSEN, K. E., FENG, F. Y., CHINNAIYAN, A. M., HALL, E. & DE BONO, J. S. 2015. DNA-Repair Defects and Olaparib in Metastatic Prostate Cancer. *N Engl J Med*, 373, 1697-708.
- MAYO, M. W., DENLINGER, C. E., BROAD, R. M., YEUNG, F., REILLY, E. T., SHI, Y. & JONES, D. R. 2003. Ineffectiveness of histone deacetylase inhibitors to induce apoptosis involves the transcriptional activation of NF-kappa B through the Akt pathway. *J Biol Chem*, 278, 18980-9.
- MCCABE, N., TURNER, N. C., LORD, C. J., KLUZEK, K., BIALKOWSKA, A., SWIFT, S., GIAVARA, S., O'CONNOR, M. J., TUTT, A. N., ZDZIENICKA, M. Z., SMITH, G. C. & ASHWORTH, A. 2006. Deficiency in the repair of DNA damage by homologous recombination and sensitivity to poly(ADP-ribose) polymerase inhibition. *Cancer Res*, 66, 8109-15.
- MCCANN, K. E. & HURVITZ, S. A. 2018. Advances in the use of PARP inhibitor therapy for breast cancer. *Drugs Context*, 7, 212540.
- MCKENZIE, S., SAKAMOTO, S. & KYPRIANOU, N. 2008. Maspin modulates prostate cancer cell apoptotic and angiogenic response to hypoxia via targeting AKT. *Oncogene*, 27, 7171-9.
- MCNULTY, S. E., DEL ROSARIO, R., CEN, D., MEYSKENS, F. L., JR. & YANG, S. 2004. Comparative expression of NFkappaB proteins in melanocytes of normal skin vs. benign intradermal naevus and human metastatic melanoma biopsies. *Pigment Cell Res*, 17, 173-80.
- MENDES-PEREIRA, A. M., MARTIN, S. A., BROUGH, R., MCCARTHY, A., TAYLOR, J. R., KIM, J. S., WALDMAN, T., LORD, C. J. & ASHWORTH, A. 2009. Synthetic lethal targeting of PTEN mutant cells with PARP inhibitors. *EMBO Mol Med*, 1, 315-22.
- MERKHOFER, E. C., COGSWELL, P. & BALDWIN, A. S. 2010. Her2 activates NF-kappaB and induces invasion through the canonical pathway involving IKKalpha. *Oncogene*, 29, 1238-48.

- MEYSKENS, F. L., JR., BUCKMEIER, J. A., MCNULTY, S. E. & TOHIDIAN, N. B. 1999. Activation of nuclear factor-kappa B in human metastatic melanomacells and the effect of oxidative stress. *Clin Cancer Res*, 5, 1197-202.
- MICHELS, J., VITALE, I., SAPARBAEV, M., CASTEDO, M. & KROEMER, G. 2014. Predictive biomarkers for cancer therapy with PARP inhibitors. *Oncogene*, 33, 3894-907.
- MILLER, C. J., KASSEM, H. S., PEPPER, S. D., HEY, Y., WARD, T. H. & MARGISON, G. P. 2003. Mycoplasma infection significantly alters microarray gene expression profiles. *Biotechniques*, 35, 812-4.
- MIN, A., IM, S. A., KIM, D. K., SONG, S. H., KIM, H. J., LEE, K. H., KIM, T. Y., HAN, S. W., OH, D. Y., KIM, T. Y., O'CONNOR, M. J. & BANG, Y. J. 2015. Histone deacetylase inhibitor, suberoylanilide hydroxamic acid (SAHA), enhances anti-tumor effects of the poly (ADP-ribose) polymerase (PARP) inhibitor olaparib in triple-negative breast cancer cells. *Breast Cancer Res*, 17, 33.
- MINAMIYA, Y., ONO, T., SAITO, H., TAKAHASHI, N., ITO, M., MITSUI, M., MOTOYAMA, S. & OGAWA, J. 2011. Expression of histone deacetylase 1 correlates with a poor prognosis in patients with adenocarcinoma of the lung. *Lung Cancer*, 74, 300-4.
- MIRZA, M. R., PIGNATA, S. & LEDERMANN, J. A. 2018. Latest clinical evidence and further development of PARP inhibitors in ovarian cancer. *Ann Oncol*, 29, 1366-1376.
- MIRZAYANS, R., ANDRAIS, B., SCOTT, A., TESSIER, A. & MURRAY, D. 2007. A sensitive assay for the evaluation of cytotoxicity and its pharmacologic modulation in human solid tumor-derived cell lines exposed to cancer-therapeutic agents. *J Pharm Pharm Sci*, 10, 298s-311s.
- MITCHELL, J., SMITH, G. C. & CURTIN, N. J. 2009. Poly(ADP-Ribose) polymerase-1 and DNA-dependent protein kinase have equivalent roles in double strand break repair following ionizing radiation. *Int J Radiat Oncol Biol Phys*, 75, 1520-7.
- MOHSIN, S. K., ZHANG, M., CLARK, G. M. & CRAIG ALLRED, D. 2003. Maspin expression in invasive breast cancer: association with other prognostic factors. *J Pathol*, 199, 432-5.
- MOORE, K., COLOMBO, N., SCAMBIA, G., KIM, B. G., OAKNIN, A., FRIEDLANDER, M., LISYANSKAYA, A., FLOQUET, A., LEARY, A., SONKE, G. S., GOURLEY, C., BANERJEE, S., OZA, A., GONZALEZ-MARTIN, A., AGHAJANIAN, C., BRADLEY, W., MATHEWS, C., LIU, J., LOWE, E. S., BLOOMFIELD, R. & DISILVESTRO, P. 2018. Maintenance Olaparib in Patients with Newly Diagnosed Advanced Ovarian Cancer. *N Engl J Med*, 379, 2495-2505.
- MORTEN, B. C., SCOTT, R. J. & AVERY-KIEJDA, K. A. 2016. Comparison of Three Different Methods for Determining Cell Proliferation in Breast Cancer Cell Lines. *J Vis Exp*.
- MUKHOPADHYAY, A., ELATTAR, A., CERBINSKAITE, A., WILKINSON, S. J., DREW, Y., KYLE, S., LOS, G., HOSTOMSKY, Z., EDMONDSON, R. J. & CURTIN, N. J. 2010. Development of a functional assay for homologous recombination status in primary cultures of epithelial ovarian tumor and correlation with sensitivity to poly(ADP-ribose) polymerase inhibitors. *Clin Cancer Res*, 16, 2344-51.
- MUNSHI, A., KURLAND, J. F., NISHIKAWA, T., TANAKA, T., HOBBS, M. L., TUCKER, S. L., ISMAIL, S., STEVENS, C. & MEYN, R. E. 2005. Histone deacetylase inhibitors radiosensitize human melanoma cells by suppressing DNA repair activity. *Clin Cancer Res*, 11, 4912-22.
- MURAI, J., HUANG, S. Y., DAS, B. B., RENAUD, A., ZHANG, Y., DOROSHOW, J. H., JI, J., TAKEDA, S. & POMMIER, Y. 2012. Trapping of PARP1 and PARP2 by Clinical PARP Inhibitors. *Cancer Res*, 72, 5588-99.
- MURAI, J., HUANG, S. Y., RENAUD, A., ZHANG, Y., JI, J., TAKEDA, S., MORRIS, J., TEICHER, B., DOROSHOW, J. H. & POMMIER, Y. 2014. Stereospecific PARP trapping by BMN 673 and comparison with olaparib and rucaparib. *Mol Cancer Ther*, 13, 433-43.
- MURAKAMI, J., ASAUMI, J., MAKI, Y., TSUJIGIWA, H., KURODA, M., NAGAI, N., YANAGI, Y., INOUE, T., KAWASAKI, S., TANAKA, N., MATSUBARA, N. & KISHI, K. 2004. Effects of demethylating agent 5-aza-2(')-deoxycytidine and histone deacetylase inhibitor FR901228 on maspin gene expression in oral cancer cell lines. *Oral Oncol*, 40, 597-603.

- MURNYAK, B., KOUHSARI, M. C., HERSHKOVITCH, R., KALMAN, B., MARKO-VARGA, G., KLEKNER, A. & HORTOBAGYI, T. 2017. PARP1 expression and its correlation with survival is tumour molecular subtype dependent in glioblastoma. *Oncotarget*, 8, 46348-46362.
- NAKAGAWA, Y., SEDUKHINA, A. S., OKAMOTO, N., NAGASAWA, S., SUZUKI, N., OHTA, T., HATTORI, H., ROCHE-MOLINA, M., NARVAEZ, A. J., JEYASEKHARAN, A. D., BERNAL, J. A. & SATO, K. 2015. NF-kappaB signaling mediates acquired resistance after PARP inhibition. *Oncotarget*, 6, 3825-39.
- NAKSHATRI, H., BHAT-NAKSHATRI, P., MARTIN, D. A., GOULET, R. J., JR. & SLEDGE, G. W., JR. 1997. Constitutive activation of NF-kappaB during progression of breast cancer to hormone-independent growth. *Mol Cell Biol*, 17, 3629-39.
- NAM, E. & PARK, C. 2010. Maspin suppresses survival of lung cancer cells through modulation of Akt pathway. *Cancer Res Treat*, 42, 42-7.
- NAYEROSSADAT, N., MAEDEH, T. & ALI, P. A. 2012. Viral and nonviral delivery systems for gene delivery. *Adv Biomed Res*, 1, 27.
- NEWBOLD, A., FALKENBERG, K. J., PRINCE, H. M. & JOHNSTONE, R. W. 2016. How do tumor cells respond to HDAC inhibition? *FEBS J*, 283, 4032-4046.
- NGAMKITIDECHAKUL, C., WAREJCKA, D. J., BURKE, J. M., O'BRIEN, W. J. & TWINING, S. S. 2003. Sufficiency of the reactive site loop of maspin for induction of cell-matrix adhesion and inhibition of cell invasion. Conversion of ovalbumin to a maspin-like molecule. *J Biol Chem*, 278, 31796-806.
- NGUYEN, D., ZAJAC-KAYE, M., RUBINSTEIN, L., VOELLER, D., TOMASZEWSKI, J. E., KUMMAR, S., CHEN, A. P., POMMIER, Y., DOROSHOW, J. H. & YANG, S. X. 2011. Poly(ADP-ribose) polymerase inhibition enhances p53-dependent and -independent DNA damage responses induced by DNA damaging agent. *Cell Cycle*, 10, 4074-82.
- NICE. 2019. *Another treatment option for ovarian cancer approved for the Cancer Drugs Fund* [Online]. NICE. Available: <https://www.nice.org.uk/news/article/another-treatment-option-for-ovarian-cancer-approved-for-the-cancer-drugs-fund> [Accessed 2019].
- NICKOLOFF, J. A., JONES, D., LEE, S. H., WILLIAMSON, E. A. & HROMAS, R. 2017. Drugging the Cancers Addicted to DNA Repair. *J Natl Cancer Inst*, 109.
- NIJMAN, S. M. 2011. Synthetic lethality: general principles, utility and detection using genetic screens in human cells. *FEBS Lett*, 585, 1-6.
- NIKFARJAM, L. & FARZANEH, P. 2012a. Prevention and detection of Mycoplasma contamination in cell culture. *Cell J*, 13, 203-12.
- NIKFARJAM, L. & FARZANEH, P. 2012b. Prevention and Detection of Mycoplasma Contamination in Cell Culture. *Cell Journal (Yakhteh)*, 13, 203-212.
- NIMS, R. W., SYKES, G., COTTRILL, K., IKONOMI, P. & ELMORE, E. 2010. Short tandem repeat profiling: part of an overall strategy for reducing the frequency of cell misidentification. *In Vitro Cell Dev Biol Anim*, 46, 811-9.
- NISHIDA, N., YANO, H., NISHIDA, T., KAMURA, T. & KOJIRO, M. 2006. Angiogenesis in cancer. *Vasc Health Risk Manag*, 2, 213-9.
- NISHIZUKA, Y., UEDA, K., NAKAZAWA, K. & HAYAISHI, O. 1967. Studies on the Polymer of Adenosine Diphosphate Ribose I. ENZYMIC FORMATION FROM NICOTINAMIDE ADENINE DINUCLEOTIDE IN MAMMALIAN NUCLEI. *Journal of Biological Chemistry*, 242, 3164-3171.
- NOMURA, F., YAGUCHI, M., TOGAWA, A., MIYAZAKI, M., ISOBE, K., MIYAKE, M., NODA, M. & NAKAI, T. 2000. Enhancement of poly-adenosine diphosphate-ribosylation in human hepatocellular carcinoma. *J Gastroenterol Hepatol*, 15, 529-35.
- NOORDERMEER, S. M. & VAN ATTIKUM, H. 2019. PARP Inhibitor Resistance: A Tug-of-War in BRCA-Mutated Cells. *Trends Cell Biol*, 29, 820-834.
- O'DONOVAN, M. 2012. A critique of methods to measure cytotoxicity in mammalian cell genotoxicity assays. *Mutagenesis*, 27, 615-21.
- OECKINGHAUS, A. & GHOSH, S. 2009. The NF- B family of transcription factors and its regulation. *Cold Spring Harb Perspect Biol*, 1.

- OLIVER, F. J., MÉNISSIER - DE MURCIA, J., NACCI, C., DECKER, P., ANDRIANTSITOHAINA, R., MULLER, S., DE LA RUBIA, G., STOCLET, J. C. & DE MURCIA, G. 1999. Resistance to endotoxic shock as a consequence of defective NF - κ B activation in poly (ADP - ribose) polymerase - 1 deficient mice. *The EMBO journal*, 18, 4446-4454.
- ORELLANA, E. A. & KASINSKI, A. L. 2016. Sulforhodamine B (SRB) Assay in Cell Culture to Investigate Cell Proliferation. *Bio Protoc*, 6.
- OSGUTHORPE, D. & HAGLER, A. 2011. Mechanism of androgen receptor antagonism by bicalutamide in the treatment of prostate cancer. *Biochemistry*, 50, 4105-4113.
- OSSOVSKAYA, V., KOO, I. C., KALDJIAN, E. P., ALVARES, C. & SHERMAN, B. M. 2010. Upregulation of Poly (ADP-Ribose) Polymerase-1 (PARP1) in Triple-Negative Breast Cancer and Other Primary Human Tumor Types. *Genes Cancer*, 1, 812-21.
- OSTLING, O. & JOHANSON, K. J. 1984. Microelectrophoretic study of radiation-induced DNA damages in individual mammalian cells. *Biochem Biophys Res Commun*, 123, 291-8.
- PALLA, V. V., KARAOLANIS, G., KATAFIGIOTIS, I., ANASTASIOU, I., PATAPIS, P., DIMITROULIS, D. & PERREA, D. 2017. gamma-H2AX: Can it be established as a classical cancer prognostic factor? *Tumour Biol*, 39, 1010428317695931.
- PALMER, T. D., ASHBY, W. J., LEWIS, J. D. & ZIJLSTRA, A. 2011. Targeting tumor cell motility to prevent metastasis. *Adv Drug Deliv Rev*, 63, 568-81.
- PARBIN, S., KAR, S., SHILPI, A., SENGUPTA, D., DEB, M., RATH, S. K. & PATRA, S. K. 2014. Histone deacetylases: a saga of perturbed acetylation homeostasis in cancer. *J Histochem Cytochem*, 62, 11-33.
- PARK, M. H. & HONG, J. T. 2016. Roles of NF-kappaB in Cancer and Inflammatory Diseases and Their Therapeutic Approaches. *Cells*, 5.
- PEMBERTON, P. A., TIPTON, A. R., PAVLOFF, N., SMITH, J., ERICKSON, J. R., MOUCHABECK, Z. M. & KIEFER, M. C. 1997. Maspin is an intracellular serpin that partitions into secretory vesicles and is present at the cell surface. *J Histochem Cytochem*, 45, 1697-706.
- PERKINS, N. D. 2012. The diverse and complex roles of NF-kB subunits in cancer. *Nat Rev Cancer*, 12.
- PETRIE, R. J., DOYLE, A. D. & YAMADA, K. M. 2009. Random versus directionally persistent cell migration. *Nat Rev Mol Cell Biol*, 10, 538-49.
- PFEIFFER, P., GOEDECKE, W. & OBE, G. 2000. Mechanisms of DNA double-strand break repair and their potential to induce chromosomal aberrations. *Mutagenesis*, 15, 289-302.
- PIRES, B. R., MENCALHA, A. L., FERREIRA, G. M., DE SOUZA, W. F., MORGADO-DIAZ, J. A., MAIA, A. M., CORREA, S. & ABDELHAY, E. S. 2017. NF-kappaB Is Involved in the Regulation of EMT Genes in Breast Cancer Cells. *PLoS One*, 12, e0169622.
- PIRES, B. R. B., SILVA, R., FERREIRA, G. M. & ABDELHAY, E. 2018. NF-kappaB: Two Sides of the Same Coin. *Genes (Basel)*, 9.
- PITOT, H. C. 1993. The molecular biology of carcinogenesis. *Cancer*, 72, 962-970.
- PITTIUS, C. W., SANKARAN, L., TOPPER, Y. J. & HENNIGHAUSEN, L. 1988. Comparison of the regulation of the whey acidic protein gene with that of a hybrid gene containing the whey acidic protein gene promoter in transgenic mice. *Mol Endocrinol*, 2, 1027-32.
- PLACE, R. F., NOONAN, E. J. & GIARDINA, C. 2005. HDAC inhibition prevents NF-kappa B activation by suppressing proteasome activity: down-regulation of proteasome subunit expression stabilizes I kappa B alpha. *Biochem Pharmacol*, 70, 394-406.
- PLUMMER, R., JONES, C., MIDDLETON, M., WILSON, R., EVANS, J., OLSEN, A., CURTIN, N., BODDY, A., MCHUGH, P., NEWELL, D., HARRIS, A., JOHNSON, P., STEINFELDT, H., DEWJI, R., WANG, D., ROBSON, L. & CALVERT, H. 2008. Phase I study of the poly(ADP-ribose) polymerase inhibitor, AG014699, in combination with temozolomide in patients with advanced solid tumors. *Clin Cancer Res*, 14, 7917-23.
- PLUMMER, R., LORIGAN, P., STEVEN, N., SCOTT, L., MIDDLETON, M. R., WILSON, R. H., MULLIGAN, E., CURTIN, N., WANG, D., DEWJI, R., ABBATTISTA, A., GALLO, J. & CALVERT, H. 2013. A phase II study of the potent PARP inhibitor, Rucaparib (PF-01367338, AG014699), with temozolomide in patients with metastatic melanoma demonstrating evidence of chemopotential. *Cancer Chemother Pharmacol*, 71, 1191-9.

- PODHORECKA, M., SKLADANOWSKI, A. & BOZKO, P. 2010. H2AX Phosphorylation: Its Role in DNA Damage Response and Cancer Therapy. *J Nucleic Acids*, 2010.
- PONTEN, F., GRY, M., FAGERBERG, L., LUNDBERG, E., ASPLUND, A., BERGLUND, L., OKSVOLD, P., BJORLING, E., HOBER, S., KAMPF, C., NAVANI, S., NILSSON, P., OTTOSSON, J., PERSSON, A., WERNERUS, H., WESTER, K. & UHLEN, M. 2009. A global view of protein expression in human cells, tissues, and organs. *Mol Syst Biol*, 5, 337.
- PORPORATO, P. E., FILIGHEDDU, N., PEDRO, J. M. B., KROEMER, G. & GALLUZZI, L. 2018. Mitochondrial metabolism and cancer. *Cell Res*, 28, 265-280.
- PRITCHARD, C. C., MATEO, J., WALSH, M. F., DE SARKAR, N., ABIDA, W., BELTRAN, H., GAROFALO, A., GULATI, R., CARREIRA, S., EELES, R., ELEMENTO, O., RUBIN, M. A., ROBINSON, D., LONIGRO, R., HUSSAIN, M., CHINNAIYAN, A., VINSON, J., FILIPENKO, J., GARRAWAY, L., TAPLIN, M. E., ALDUBAYAN, S., HAN, G. C., BEIGHTOL, M., MORRISSEY, C., NGHIEM, B., CHENG, H. H., MONTGOMERY, B., WALSH, T., CASADEI, S., BERGER, M., ZHANG, L., ZEHIR, A., VIJAI, J., SCHER, H. I., SAWYERS, C., SCHULTZ, N., KANTOFF, P. W., SOLIT, D., ROBSON, M., VAN ALLEN, E. M., OFFIT, K., DE BONO, J. & NELSON, P. S. 2016. Inherited DNA-Repair Gene Mutations in Men with Metastatic Prostate Cancer. *N Engl J Med*, 375, 443-53.
- PROSTATE CANCER UK. Available: <https://prostatecanceruk.org/prostate-information/about-prostate-cancer> [Accessed 07/11/2017].
- PROSTATE CANCER UK. Available: <https://prostatecanceruk.org/prostate-information/prostate-tests> [Accessed 05/12/2017].
- PROSTATE CANCER UK.
- PU, X., WANG, Z. & KLAUNIG, J. E. 2015. Alkaline Comet Assay for Assessing DNA Damage in Individual Cells. *Curr Protoc Toxicol*, 65, 3 12 1-3 12 11.
- RAJAMOCHAN, S. B., PILLAI, V. B., GUPTA, M., SUNDARESAN, N. R., BIRUKOV, K. G., SAMANT, S., HOTTIGER, M. O. & GUPTA, M. P. 2009. SIRT1 promotes cell survival under stress by deacetylation-dependent deactivation of poly(ADP-ribose) polymerase 1. *Mol Cell Biol*, 29, 4116-29.
- RAMAKRISHNAN GEETHAKUMARI, P., SCHIEWER, M. J., KNUDSEN, K. E. & KELLY, W. K. 2017. PARP Inhibitors in Prostate Cancer. *Curr Treat Options Oncol*, 18, 37.
- RAMAMOORTHY, M. & NARVEKAR, A. 2015. Non viral vectors in gene therapy- an overview. *J Clin Diagn Res*, 9, GE01-6.
- RASMUSSEN, R. D., GAJJAR, M. K., JENSEN, K. E. & HAMERLIK, P. 2016. Enhanced efficacy of combined HDAC and PARP targeting in glioblastoma. *Mol Oncol*, 10, 751-63.
- RATUSHNYI, A., LOBANOVA, M. AND ZHIDKOVA, O 2017. Functional state and morphology of mesenchymal stem cells after oxidative stress. *Free Radical Biology and Medicine*, 108, S81.
- RAVENHILL, L., WAGSTAFF, L., EDWARDS, D. R., ELLIS, V. & BASS, R. 2010. G-helix of Maspin Mediates Effects on Cell Migration and Adhesion. *The Journal of Biological Chemistry*, 285, 36285-36292.
- RAVENNA, L., PRINCIPESSA, L., VERDINA, A., SALVATORI, L., RUSSO, M. A. & PETRANGELI, E. 2014. Distinct phenotypes of human prostate cancer cells associate with different adaptation to hypoxia and pro-inflammatory gene expression. *PLoS One*, 9, e96250.
- REISSMANN, T., SCHALLY, A., BOUCHARD, P., RIETHMÜLLER, H. & ENGEL, J. 2000. The LHRH antagonist cetrorelix: a review. *Human Reproduction Update*, 6, 322-331.
- RIDDICK, A. C., SHUKLA, C. J., PENNINGTON, C. J., BASS, R., NUTTALL, R. K., HOGAN, A., SETHIA, K. K., ELLIS, V., COLLINS, A. T., MAITLAND, N. J., BALL, R. Y. & EDWARDS, D. R. 2005. Identification of degradome components associated with prostate cancer progression by expression analysis of human prostatic tissues. *Br J Cancer*, 92, 2171-80.
- RIGGS, M. G., WHITTAKER, R. G., NEUMANN, J. R. & INGRAM, V. M. 1977. n-Butyrate causes histone modification in HeLa and Friend erythroleukaemia cells. *Nature*, 268, 462-4.
- RISS, T. L., MORAVEC, R. A., NILES, A. L., DUELLMAN, S., BENINK, H. A., WORZELLA, T. J. & MINOR, L. 2004. Cell Viability Assays. In: SITTAMPALAM, G. S., COUSSENS, N. P., BRIMACOMBE, K., GROSSMAN, A., ARKIN, M., AULD, D., AUSTIN, C., BAELL, J., BEJCEK, B., CAAVEIRO, J.

- M. M., CHUNG, T. D. Y., DAHLIN, J. L., DEVANARYAN, V., FOLEY, T. L., GLICKSMAN, M., HALL, M. D., HAAS, J. V., INGLESE, J., IVERSEN, P. W., KAHL, S. D., KALES, S. C., LAL-NAG, M., LI, Z., MCGEE, J., MCMANUS, O., RISS, T., TRASK, O. J., JR., WEIDNER, J. R., WILDEY, M. J., XIA, M. & XU, X. (eds.) *Assay Guidance Manual*. Bethesda (MD).
- RIVLIN, N., BROSH, R., OREN, M. & ROTTER, V. 2011. Mutations in the p53 tumor suppressor gene important milestones at the various steps of tumorigenesis. *Genes & cancer*, 2, 466-474.
- ROBERT, C., NAGARIA, P. K., PAWAR, N., ADEWUYI, A., GOJO, I., MEYERS, D. J., COLE, P. A. & RASSOOL, F. V. 2016. Histone deacetylase inhibitors decrease NHEJ both by acetylation of repair factors and trapping of PARP1 at DNA double-strand breaks in chromatin. *Leuk Res*, 45, 14-23.
- ROBERT, C. & RASSOOL, F. V. 2012. HDAC inhibitors: roles of DNA damage and repair. *Adv Cancer Res*, 116, 87-129.
- RODRIGUEZ, M. I., PERALTA-LEAL, A., O'VALLE, F., RODRIGUEZ-VARGAS, J. M., GONZALEZ-FLORES, A., MAJUELOS-MELGUIZO, J., LOPEZ, L., SERRANO, S., DE HERREROS, A. G., RODRIGUEZ-MANZANEQUE, J. C., FERNANDEZ, R., DEL MORAL, R. G., DE ALMODOVAR, J. M. & OLIVER, F. J. 2013. PARP-1 regulates metastatic melanoma through modulation of vimentin-induced malignant transformation. *PLoS Genet*, 9, e1003531.
- ROH, M. S., KIM, C. W., PARK, B. S., KIM, G. C., JEONG, J. H., KWON, H. C., SUH, D. J., CHO, K. H., YEE, S. B. & YOO, Y. H. 2004. Mechanism of histone deacetylase inhibitor Trichostatin A induced apoptosis in human osteosarcoma cells. *Apoptosis*, 9, 583-9.
- ROMAR, G. A., KUPPER, T. S. & DIVITO, S. J. 2016. Research Techniques Made Simple: Techniques to Assess Cell Proliferation. *J Invest Dermatol*, 136, e1-7.
- ROOS, W. P. & KRUMM, A. 2016. The multifaceted influence of histone deacetylases on DNA damage signalling and DNA repair. *Nucleic Acids Res*, 44, 10017-10030.
- ROPERO, S. & ESTELLER, M. 2007. The role of histone deacetylases (HDACs) in human cancer. *Mol Oncol*, 1, 19-25.
- ROSATO, R. R., ALMENARA, J. A. & GRANT, S. 2003. The histone deacetylase inhibitor MS-275 promotes differentiation or apoptosis in human leukemia cells through a process regulated by generation of reactive oxygen species and induction of p21CIP1/WAF1 1. *Cancer Res*, 63, 3637-45.
- ROULEAU, M., PATEL, A., HENDZEL, M. J., KAUFMANN, S. H. & POIRIER, G. G. 2010. PARP inhibition: PARP1 and beyond. *Nat Rev Cancer*, 10, 293-301.
- RUSCETTI, T., LEHNERT, B. E., HALBROOK, J., LE TRONG, H., HOEKSTRA, M. F., CHEN, D. J. & PETERSON, S. R. 1998. Stimulation of the DNA-dependent protein kinase by poly (ADP-ribose) polymerase. *Journal of Biological Chemistry*, 273, 14461-14467.
- SAGER, R. 1997. Expression genetics in cancer: shifting the focus from DNA to RNA. *Proc Natl Acad Sci U S A*, 94, 952-5.
- SALEMI, M., GALIA, A., FRAGGETTA, F., LA CORTE, C., PEPE, P., LA VIGNERA, S., IMPROTA, G., BOSCO, P. & CALOGERO, A. E. 2013. Poly (ADP-ribose) polymerase 1 protein expression in normal and neoplastic prostatic tissue. *Eur J Histochem*, 57, e13.
- SALGUERO-ARANDA, C., SANCHO-MENSAT, D., CANALS-LORENTE, B., SULTAN, S., REGINALD, A. & CHAPMAN, L. 2019. STAT6 knockdown using multiple siRNA sequences inhibits proliferation and induces apoptosis of human colorectal and breast cancer cell lines. *PLoS One*, 14, e0207558.
- SAMPSON, N., NEUWIRT, H., PUHR, M., KLOCKER, H. & EDER, I. E. 2013. In vitro model systems to study androgen receptor signaling in prostate cancer. *Endocr Relat Cancer*, 20, R49-64.
- SARKAR, S., ABUJAMRA, A. L., LOEW, J. E., FORMAN, L. W., PERRINE, S. P. & FALLER, D. V. 2011. Histone deacetylase inhibitors reverse CpG methylation by regulating DNMT1 through ERK signaling. *Anticancer Res*, 31, 2723-32.
- SCHIEWER, M. J., GOODWIN, J. F., HAN, S., BRENNER, J. C., AUGELLO, M. A., DEAN, J. L., LIU, F., PLANCK, J. L., RAVINDRANATHAN, P., CHINNAIYAN, A. M., MCCUE, P., GOMELLA, L. G., RAJ, G. V., DICKER, A. P., BRODY, J. R., PASCAL, J. M., CENTENERA, M. M., BUTLER, L. M.,

- TILLEY, W. D., FENG, F. Y. & KNUDSEN, K. E. 2012. Dual roles of PARP-1 promote cancer growth and progression. *Cancer Discov*, 2, 1134-49.
- SCHIEWER, M. J. & KNUDSEN, K. E. 2014. Transcriptional roles of PARP1 in cancer. *Mol Cancer Res*, 12, 1069-80.
- SENESE, S., ZARAGOZA, K., MINARDI, S., MURADORE, I., RONZONI, S., PASSAFARO, A., BERNARD, L., DRAETTA, G. F., ALCALAY, M., SEISER, C. & CHIOCCA, S. 2007. Role for histone deacetylase 1 in human tumor cell proliferation. *Mol Cell Biol*, 27, 4784-95.
- SETO, E. & YOSHIDA, M. 2014. Erasers of histone acetylation: the histone deacetylase enzymes. *Cold Spring Harb Perspect Biol*, 6, a018713.
- SEYFRIED, T. N. & HUYSENTRUYT, L. C. 2013. On the origin of cancer metastasis. *Crit Rev Oncog*, 18, 43-73.
- SHANKAR, S. & SRIVASTAVA, R. K. 2008. Histone deacetylase inhibitors: mechanisms and clinical significance in cancer: HDAC inhibitor-induced apoptosis. *Adv Exp Med Biol*, 615, 261-98.
- SHAO, L. J., SHI, H. Y., AYALA, G., ROWLEY, D. & ZHANG, M. 2008. Haploinsufficiency of the maspin tumor suppressor gene leads to hyperplastic lesions in prostate. *Cancer Res*, 68, 5143-51.
- SHARMA, A., SINGH, K. & ALMASAN, A. 2012. Histone H2AX phosphorylation: a marker for DNA damage. *Methods Mol Biol*, 920, 613-26.
- SHEN, Y., AOYAGI-SCHARBER, M. & WANG, B. 2015. Trapping Poly(ADP-Ribose) Polymerase. *J Pharmacol Exp Ther*, 353, 446-57.
- SHENG, S., CAREY, J., SEFTOR, E. A., DIAS, L., HENDRIX, M. J. & SAGER, R. 1996. Maspin acts at the cell membrane to inhibit invasion and motility of mammary and prostatic cancer cells. *Proc Natl Acad Sci U S A*, 93, 11669-74.
- SHI, H. Y., LIANG, R., TEMPLETON, N. S. & ZHANG, M. 2002. Inhibition of breast tumor progression by systemic delivery of the maspin gene in a syngeneic tumor model. *Mol Ther*, 5, 755-61.
- SHI, H. Y., ZHANG, W., LIANG, R., ABRAHAM, S., KITTRELL, F. S., MEDINA, D. & ZHANG, M. 2001. Blocking tumor growth, invasion, and metastasis by maspin in a syngeneic breast cancer model. *Cancer Res*, 61, 6945-51.
- SHI, Y., ZHOU, F., JIANG, F., LU, H., WANG, J. & CHENG, C. 2014. PARP inhibitor reduces proliferation and increases apoptosis in breast cancer cells. *Chin J Cancer Res*, 26, 142-7.
- SHUKLA, S., ABBAS, A. AND GUPTA, S 2015. Apigenin increases maspin expression and suppresses invasiveness in prostate cancer cells. *106th Annual meeting of the American Association for Cancer Research*. Philadelphia, USA: Cancer Research
- SHUKLA, S., MACLENNAN, G. T., FU, P., PATEL, J., MARENGO, S. R., RESNICK, M. I. & GUPTA, S. 2004. Nuclear factor-kappaB/p65 (Rel A) is constitutively activated in human prostate adenocarcinoma and correlates with disease progression. *Neoplasia*, 6, 390-400.
- SHUKLA, S., MACLENNON, G., FU, P. AND GUPTA, S 2008. Apigenin blocks tumor growth, invasion and metastasis by upregulation of maspin in TRAMP model
- . *Cancer Research American Association for Cancer Research*.
- SIEBENLIST, U., FRANZOSO, G. & BROWN, K. 1994. Structure, regulation and function of NF-kappa B. *Annu Rev Cell Biol*, 10, 405-55.
- SIGMA ALDRICH, U. Available: https://www.sigmaaldrich.com/catalog/product/sigma/cb_95012614?lang=en®ion=GB [Accessed 13/06/2018].
- SILVA, M. T. 2010. Secondary necrosis: the natural outcome of the complete apoptotic program. *FEBS Lett*, 584, 4491-9.
- SINGH, A., TRIVEDI, P. & JAIN, N. K. 2018. Advances in siRNA delivery in cancer therapy. *Artif Cells Nanomed Biotechnol*, 46, 274-283.

- SINGH, T. R., SHANKAR, S. & SRIVASTAVA, R. K. 2005. HDAC inhibitors enhance the apoptosis-inducing potential of TRAIL in breast carcinoma. *Oncogene*, 24, 4609-23.
- SMITH, L. M., WILLMORE, E., AUSTIN, C. A. & CURTIN, N. J. 2005. The novel poly(ADP-Ribose) polymerase inhibitor, AG14361, sensitizes cells to topoisomerase I poisons by increasing the persistence of DNA strand breaks. *Clin Cancer Res*, 11, 8449-57.
- SMITH, S. 2001. The world according to PARP. *Trends in biochemical sciences*, 26, 174-179.
- SOLOMON, L. A., MUNKARAH, A. R., SCHIMP, V. L., ARABI, M. H., MORRIS, R. T., NASSAR, H. & ALI-FEHMI, R. 2006. Maspin expression and localization impact on angiogenesis and prognosis in ovarian cancer. *Gynecol Oncol*, 101, 385-9.
- SONG, M. S., SALMENA, L. & PANDOLFI, P. P. 2012. The functions and regulation of the PTEN tumour suppressor. *Nat Rev Mol Cell Biol*, 13, 283-96.
- SONG, S. Y., LEE, S. K., KIM, D. H., SON, H. J., KIM, H. J., LIM, Y. J., LEE, W. Y., CHUN, H. K. & RHEE, J. C. 2002. Expression of maspin in colon cancers: its relationship with p53 expression and microvessel density. *Dig Dis Sci*, 47, 1831-5.
- SONG, X., WU, J. Q., YU, X. F., YANG, X. S. & YANG, Y. 2018. Trichostatin A inhibits proliferation of triple negative breast cancer cells by inducing cell cycle arrest and apoptosis. *Neoplasma*, 65, 898-906.
- SPANO, D., HECK, C., DE ANTONELLIS, P., CHRISTOFORI, G. & ZOLLO, M. Molecular networks that regulate cancer metastasis. *Seminars in cancer biology*, 2012. Elsevier, 234-249.
- SPEIT, G. & HARTMANN, A. 2006. The comet assay: a sensitive genotoxicity test for the detection of DNA damage and repair. *Methods Mol Biol*, 314, 275-86.
- STONE, K. R., MICKEY, D. D., WUNDERLI, H., MICKEY, G. H. & PAULSON, D. F. 1978a. Isolation of a human prostate carcinoma cell line (DU 145). *Int J Cancer*, 21, 274-81.
- STONE, K. R., MICKEY, D. D., WUNDERLI, H., MICKEY, G. H. & PAULSON, D. F. 1978b. Isolation of a human prostate carcinoma cell line (DU 145). *International journal of cancer*, 21, 274-281.
- STYPULA-CYRUS, Y., DAMANIA, D., KUNTE, D. P., CRUZ, M. D., SUBRAMANIAN, H., ROY, H. K. & BACKMAN, V. 2013. HDAC up-regulation in early colon field carcinogenesis is involved in cell tumorigenicity through regulation of chromatin structure. *PLoS One*, 8, e64600.
- SUN, S. C. & LEY, S. C. 2008. New insights into NF-kappaB regulation and function. *Trends Immunol*, 29, 469-78.
- SUNADA, S., NAKANISHI, A. & MIKI, Y. 2018. Crosstalk of DNA double-strand break repair pathways in poly(ADP-ribose) polymerase inhibitor treatment of breast cancer susceptibility gene 1/2-mutated cancer. *Cancer Sci*, 109, 893-899.
- SWINDALL, A. F., STANLEY, J. A. & YANG, E. S. 2013. PARP-1: friend or foe of DNA damage and repair in tumorigenesis? *Cancers*, 5, 943-958.
- SZKLARCZYK, D., MORRIS, J. H., COOK, H., KUHN, M., WYDER, S., SIMONOVIC, M., SANTOS, A., DONCHEVA, N. T., ROTH, A., BORK, P., JENSEN, L. J. & VON MERING, C. 2017. The STRING database in 2017: quality-controlled protein-protein association networks, made broadly accessible. *Nucleic Acids Res*, 45, D362-D368.
- TAI, D. I., TSAI, S. L., CHANG, Y. H., HUANG, S. N., CHEN, T. C., CHANG, K. S. & LIAW, Y. F. 2000. Constitutive activation of nuclear factor kappaB in hepatocellular carcinoma. *Cancer*, 89, 2274-81.
- TAI, S., SUN, Y., SQUIRES, J. M., ZHANG, H., OH, W. K., LIANG, C. Z. & HUANG, J. 2011. PC3 is a cell line characteristic of prostatic small cell carcinoma. *The Prostate*, 71, 1668-1679.
- TAK, P. P. & FIRESTEIN, G. S. 2001. NF-kappaB: a key role in inflammatory diseases. *J Clin Invest*, 107, 7-11.
- TAKANAMI, I., ABIKO, T. & KOIZUMI, S. 2008. Expression of maspin in non-small-cell lung cancer: correlation with clinical features. *Clin Lung Cancer*, 9, 361-6.
- TAKI, M., ABIKO, K., BABA, T., HAMANISHI, J., YAMAGUCHI, K., MURAKAMI, R., YAMANOI, K., HORIKAWA, N., HOSOE, Y., NAKAMURA, E., SUGIYAMA, A., MANDAI, M., KONISHI, I. & MATSUMURA, N. 2018. Snail promotes ovarian cancer progression by recruiting myeloid-derived suppressor cells via CXCR2 ligand upregulation. *Nat Commun*, 9, 1685.

- TANG, Z., DING, S., HUANG, H., LUO, P., QING, B., ZHANG, S. & TANG, R. 2017. HDAC1 triggers the proliferation and migration of breast cancer cells via upregulation of interleukin-8. *Biol Chem*, 398, 1347-1356.
- TAPLICK, J., KURTEV, V., KROBOTH, K., POSCH, M., LECHNER, T. & SEISER, C. 2001. Homooligomerisation and nuclear localisation of mouse histone deacetylase 1. *J Mol Biol*, 308, 27-38.
- TAUNTON, J., HASSIG, C. A. & SCHREIBER, S. L. 1996. A mammalian histone deacetylase related to the yeast transcriptional regulator Rpd3p. *Science*, 272, 408-11.
- TENTORI, L., LEONETTI, C., SCARSELLA, M., MUZI, A., MAZZON, E., VERGATI, M., FORINI, O., LAPIDUS, R., XU, W., DORIO, A. S., ZHANG, J., CUZZOCREA, S. & GRAZIANI, G. 2006. Inhibition of poly(ADP-ribose) polymerase prevents irinotecan-induced intestinal damage and enhances irinotecan/temozolomide efficacy against colon carcinoma. *FASEB J*, 20, 1709-11.
- THERMO FISHER SCIENTIFIC, U. *Introduction to transfection* [Online]. USA: Thermo Fisher Scientific. Available: <https://www.thermofisher.com/uk/en/home/references/gibco-cell-culture-basics/transfection-basics/introduction-to-transfection.html> [Accessed 2020].
- THOMAS, H. D., CALABRESE, C. R., BATEY, M. A., CANAN, S., HOSTOMSKY, Z., KYLE, S., MAEGLEY, K. A., NEWELL, D. R., SKALITZKY, D., WANG, L. Z., WEBBER, S. E. & CURTIN, N. J. 2007. Preclinical selection of a novel poly(ADP-ribose) polymerase inhibitor for clinical trial. *Mol Cancer Ther*, 6, 945-56.
- THURN, K. T., THOMAS, S., MOORE, A. & MUNSTER, P. N. 2011. Rational therapeutic combinations with histone deacetylase inhibitors for the treatment of cancer. *Future Oncol*, 7, 263-83.
- TILBORGHES, S., CORTHOUTS, J., VERHOEVEN, Y., ARIAS, D., ROLFO, C., TRINH, X. B. & VAN DAM, P. A. 2017. The role of Nuclear Factor-kappa B signaling in human cervical cancer. *Crit Rev Oncol Hematol*, 120, 141-150.
- TOLL, A., MARGALEF, P., MASFERRER, E., FERRANDIZ-PULIDO, C., GIMENO, J., PUJOL, R. M., BIGAS, A. & ESPINOSA, L. 2015. Active nuclear IKK correlates with metastatic risk in cutaneous squamous cell carcinoma. *Arch Dermatol Res*, 307, 721-9.
- TORGOVNICK, A. & SCHUMACHER, B. 2015. DNA repair mechanisms in cancer development and therapy. *Frontiers in genetics*, 6, 157.
- TORJESEN, I. 2015. Half of the UK population can expect a diagnosis of cancer. *BMJ*, 350.
- TOSOIAN, J. J., MAMAWALA, M., EPSTEIN, J. I., LANDIS, P., WOLF, S., TROCK, B. J. & CARTER, H. B. 2015. Intermediate and longer-term outcomes from a prospective active-surveillance program for favorable-risk prostate cancer. *Journal of Clinical Oncology*, 33, 3379-3385.
- TREPAT, X., CHEN, Z. & JACOBSON, K. 2012. Cell migration. *Compr Physiol*, 2, 2369-92.
- TSUJI, N., KOBAYASHI, M., NAGASHIMA, K., WAKISAKA, Y. & KOIZUMI, K. 1976. A new antifungal antibiotic, trichostatin. *J Antibiot (Tokyo)*, 29, 1-6.
- UMEKITA, Y., SOUDA, M. & YOSHIDA, H. 2006. Expression of maspin in colorectal cancer. *In Vivo*, 20, 797-800.
- VANDER HEIDEN, M. G., CANTLEY, L. C. & THOMPSON, C. B. 2009. Understanding the Warburg effect: the metabolic requirements of cell proliferation. *Science*, 324, 1029-33.
- VAUGHAN, L., GLANZEL, W., KORCH, C. & CAPES-DAVIS, A. 2017. Widespread Use of Misidentified Cell Line KB (HeLa): Incorrect Attribution and Its Impact Revealed through Mining the Scientific Literature. *Cancer Res*, 77, 2784-2788.
- VEUGER, S. J., CURTIN, N. J., RICHARDSON, C. J., SMITH, G. C. & DURKACZ, B. W. 2003. Radiosensitization and DNA repair inhibition by the combined use of novel inhibitors of DNA-dependent protein kinase and poly(ADP-ribose) polymerase-1. *Cancer Res*, 63, 6008-15.
- VEUGER, S. J., CURTIN, N. J., SMITH, G. C. & DURKACZ, B. W. 2004. Effects of novel inhibitors of poly (ADP-ribose) polymerase-1 and the DNA-dependent protein kinase on enzyme activities and DNA repair. *Oncogene*, 23, 7322.

- VEUGER, S. J., HUNTER, J. E. & DURKACZ, B. W. 2009. Ionizing radiation-induced NF-kappaB activation requires PARP-1 function to confer radioresistance. *Oncogene*, 28, 832-42.
- VIGUSHIN, D. M., ALI, S., PACE, P. E., MIRSAIDI, N., ITO, K., ADCOCK, I. & COOMBES, R. C. 2001. Trichostatin A is a histone deacetylase inhibitor with potent antitumor activity against breast cancer in vivo. *Clin Cancer Res*, 7, 971-6.
- VLIETSTRA, R. J., VAN ALEWIJK, D. C., HERMANS, K. G., VAN STEENBRUGGE, G. J. & TRAPMAN, J. 1998. Frequent inactivation of PTEN in prostate cancer cell lines and xenografts. *Cancer Res*, 58, 2720-3.
- VOLCIC, M., KARL, S., BAUMANN, B., SALLES, D., DANIEL, P., FULDA, S. & WIESMULLER, L. 2012. NF-kappaB regulates DNA double-strand break repair in conjunction with BRCA1-CtIP complexes. *Nucleic Acids Res*, 40, 181-95.
- WADA, K., MAESAWA, C., AKASAKA, T. & MASUDA, T. 2004. Aberrant expression of the maspin gene associated with epigenetic modification in melanoma cells. *J Invest Dermatol*, 122, 805-11.
- WALKINSHAW, D. R. & YANG, X. J. 2008. Histone deacetylase inhibitors as novel anticancer therapeutics. *Curr Oncol*, 15, 237-43.
- WALTON, T. J., LI, G., SETH, R., MCARDLE, S. E., BISHOP, M. C. & REES, R. C. 2008. DNA demethylation and histone deacetylation inhibition co-operate to re-express estrogen receptor beta and induce apoptosis in prostate cancer cell-lines. *Prostate*, 68, 210-22.
- WAN, F. & LENARDO, M. J. 2010. The nuclear signaling of NF-kappaB: current knowledge, new insights, and future perspectives. *Cell Res*, 20, 24-33.
- WANG, J., JACOB, N. K., LADNER, K. J., BEG, A., PERKO, J. D., TANNER, S. M., LIYANARACHCHI, S., FISHEL, R. & GUTTRIDGE, D. C. 2009a. RelA/p53 functions to maintain cellular senescence by regulating genomic stability and DNA repair. *EMBO Rep*, 10, 1272-8.
- WANG, J., YI, S., ZHOU, J., ZHANG, Y. & GUO, F. 2016. The NF-kappaB subunit RelB regulates the migration and invasion abilities and the radio-sensitivity of prostate cancer cells. *Int J Oncol*, 49, 381-92.
- WANG, L., LIANG, C., LI, F., GUAN, D., WU, X., FU, X., LU, A. & ZHANG, G. 2017. PARP1 in Carcinomas and PARP1 Inhibitors as Antineoplastic Drugs. *Int J Mol Sci*, 18.
- WANG, L., ZOU, X., BERGER, A. D., TWISS, C., PENG, Y., LI, Y., CHIU, J., GUO, H., SATAGOPAN, J., WILTON, A., GERALD, W., BASCH, R., WANG, Z., OSMAN, I. & LEE, P. 2009b. Increased expression of histone deacetylases (HDACs) and inhibition of prostate cancer growth and invasion by HDAC inhibitor SAHA. *Am J Transl Res*, 1, 62-71.
- WANG, M., WU, W., WU, W., ROSIDI, B., ZHANG, L., WANG, H. & ILIAKIS, G. 2006. PARP-1 and Ku compete for repair of DNA double strand breaks by distinct NHEJ pathways. *Nucleic acids research*, 34, 6170-6182.
- WANG, M. C., YANG, Y. M., LI, X. H., DONG, F. & LI, Y. 2004. Maspin expression and its clinicopathological significance in tumorigenesis and progression of gastric cancer. *World J Gastroenterol*, 10, 634-7.
- WANG, W., NAG, S. A. & ZHANG, R. 2015a. Targeting the NFkappaB signaling pathways for breast cancer prevention and therapy. *Curr Med Chem*, 22, 264-89.
- WANG, X., XU, J., WANG, H., WU, L., YUAN, W., DU, J. & CAI, S. 2015b. Trichostatin A, a histone deacetylase inhibitor, reverses epithelial-mesenchymal transition in colorectal cancer SW480 and prostate cancer PC3 cells. *Biochem Biophys Res Commun*, 456, 320-6.
- WANG, Z., LI, Y., LV, S. & TIAN, Y. 2013. Inhibition of proliferation and invasiveness of ovarian cancer C13* cells by a poly(ADP-ribose) polymerase inhibitor and the role of nuclear factor-kappaB. *J Int Med Res*, 41, 1577-85.
- WEICHERT, W., BOEHM, M., GEKELER, V., BAHRA, M., LANGREHR, J., NEUHAUS, P., DENKERT, C., IMRE, G., WELLER, C., HOFMANN, H. P., NIESPOREK, S., JACOB, J., DIETEL, M., SCHEIDEREIT, C. & KRISTIANSEN, G. 2007. High expression of RelA/p53 is associated with activation of nuclear factor-kappaB-dependent signaling in pancreatic cancer and marks a patient population with poor prognosis. *Br J Cancer*, 97, 523-30.
- WEICHERT, W., DENKERT, C., NOSKE, A., DARB-ESFAHANI, S., DIETEL, M., KALLOGER, S. E., HUNTSMAN, D. G. & KOBEL, M. 2008a. Expression of class I histone deacetylases

- indicates poor prognosis in endometrioid subtypes of ovarian and endometrial carcinomas. *Neoplasia*, 10, 1021-7.
- WEICHERT, W., ROSKE, A., GEKELER, V., BECKERS, T., STEPHAN, C., JUNG, K., FRITZSCHE, F. R., NIESPOREK, S., DENKERT, C., DIETEL, M. & KRISTIANSEN, G. 2008b. Histone deacetylases 1, 2 and 3 are highly expressed in prostate cancer and HDAC2 expression is associated with shorter PSA relapse time after radical prostatectomy. *Br J Cancer*, 98, 604-10.
- WEICHERT, W., ROSKE, A., NIESPOREK, S., NOSKE, A., BUCKENDAHL, A. C., DIETEL, M., GEKELER, V., BOEHM, M., BECKERS, T. & DENKERT, C. 2008c. Class I histone deacetylase expression has independent prognostic impact in human colorectal cancer: specific role of class I histone deacetylases in vitro and in vivo. *Clin Cancer Res*, 14, 1669-77.
- WEINSTEIN, J. N. & LORENZI, P. L. 2013. Cancer: Discrepancies in drug sensitivity. *Nature*, 504, 381-3.
- WELTY, C. J., COWAN, J. E., NGUYEN, H., SHINOHARA, K., PEREZ, N., GREENE, K. L., CHAN, J. M., MENG, M. V., SIMKO, J. P. & COOPERBERG, M. R. 2015. Extended followup and risk factors for disease reclassification in a large active surveillance cohort for localized prostate cancer. *The Journal of urology*, 193, 807-811.
- WHITE, A. W., CURTIN, N. J., EASTMAN, B. W., GOLDING, B. T., HOSTOMSKY, Z., KYLE, S., LI, J., MAEGLEY, K. A., SKALITZKY, D. J., WEBBER, S. E., YU, X. H. & GRIFFIN, R. J. 2004. Potentiation of cytotoxic drug activity in human tumour cell lines, by amine-substituted 2-arylbenzimidazole-4-carboxamide PARP-1 inhibitors. *Bioorg Med Chem Lett*, 14, 2433-7.
- WIEGMANS, A. P., YAP, P. Y., WARD, A., LIM, Y. C. & KHANNA, K. K. 2015. Differences in Expression of Key DNA Damage Repair Genes after Epigenetic-Induced BRCAness Dictate Synthetic Lethality with PARP1 Inhibition. *Mol Cancer Ther*, 14, 2321-31.
- WIELGOS, M. E., ZHANG, Z., RAJBHANDARI, R., COOPER, T. S., ZENG, L., FORERO, A., ESTEVA, F. J., OSBORNE, C. K., SCHIFF, R., LOBUGLIO, A. F., NOZELL, S. E. & YANG, E. S. 2018. Trastuzumab-Resistant HER2(+) Breast Cancer Cells Retain Sensitivity to Poly (ADP-Ribose) Polymerase (PARP) Inhibition. *Mol Cancer Ther*, 17, 921-930.
- WILSON, R. H., EVANS, T. J., MIDDLETON, M. R., MOLIFE, L. R., SPICER, J., DIERAS, V., ROXBURGH, P., GIORDANO, H., JAW-TSAI, S., GOBLE, S. & PLUMMER, R. 2017. A phase I study of intravenous and oral rucaparib in combination with chemotherapy in patients with advanced solid tumours. *Br J Cancer*, 116, 884-892.
- WIRTH, M. P., HAKENBERG, O. W., FROEHLER, M., BALK, S. P., BUBLEY, G. J. & TAPLIN, M.-E. 2007. Antiandrogens in the treatment of prostate cancer. *European urology*, 51, 306-314.
- WU, S., YU, L., CHENG, Z., SONG, W., ZHOU, L. & TAO, Y. 2012. Expression of maspin in non-small cell lung cancer and its relationship to vasculogenic mimicry. *J Huazhong Univ Sci Technolog Med Sci*, 32, 346-352.
- WU, Y., ALVAREZ, M., SLAMON, D. J., KOEFFLER, P. & VADGAMA, J. V. 2010. Caspase 8 and maspin are downregulated in breast cancer cells due to CpG site promoter methylation. *BMC Cancer*, 10, 32.
- XIA, Y., SHEN, S. & VERMA, I. M. 2014. NF-kappaB, an active player in human cancers. *Cancer Immunol Res*, 2, 823-30.
- XIAO, G. & FU, J. 2011. NF-kB and cancer: a paradigm of Yin-Yang. *American Journal of Cancer Research*, 1, 192-221.
- XIE, H. J., NOH, J. H., KIM, J. K., JUNG, K. H., EUN, J. W., BAE, H. J., KIM, M. G., CHANG, Y. G., LEE, J. Y., PARK, H. & NAM, S. W. 2012. HDAC1 inactivation induces mitotic defect and caspase-independent autophagic cell death in liver cancer. *PLoS One*, 7, e34265.
- XU, W., NGO, L., PEREZ, G., DOKMANOVIC, M. & MARKS, P. A. 2006. Intrinsic apoptotic and thioredoxin pathways in human prostate cancer cell response to histone deacetylase inhibitor. *Proc Natl Acad Sci U S A*, 103, 15540-5.
- XU, Y., JOSSON, S., FANG, F., OBERLEY, T. D., ST CLAIR, D. K., WAN, X. S., SUN, Y., BAKTHAVATCHALU, V., MUTHUSWAMY, A. & ST CLAIR, W. H. 2009. RelB enhances

- prostate cancer growth: implications for the role of the nuclear factor-kappaB alternative pathway in tumorigenicity. *Cancer Res*, 69, 3267-71.
- YAMAGUCHI, N., ITO, T., AZUMA, S., ITO, E., HONMA, R., YANAGISAWA, Y., NISHIKAWA, A., KAWAMURA, M., IMAI, J., WATANABE, S., SEMBA, K. & INOUE, J. 2009. Constitutive activation of nuclear factor-kappaB is preferentially involved in the proliferation of basal-like subtype breast cancer cell lines. *Cancer Sci*, 100, 1668-74.
- YAMAGUCHI, T., CUBIZOLLES, F., ZHANG, Y., REICHERT, N., KOHLER, H., SEISER, C. & MATTHIAS, P. 2010. Histone deacetylases 1 and 2 act in concert to promote the G1-to-S progression. *Genes Dev*, 24, 455-69.
- YANG, C. M., JI, S., LI, Y., FU, L. Y., JIANG, T. & MENG, F. D. 2017. beta-Catenin promotes cell proliferation, migration, and invasion but induces apoptosis in renal cell carcinoma. *Onco Targets Ther*, 10, 711-724.
- YI, M., DONG, B., QIN, S., CHU, Q., WU, K. & LUO, S. 2019. Advances and perspectives of PARP inhibitors. *Exp Hematol Oncol*, 8, 29.
- YILMAZ, M. & CHRISTOFORI, G. 2010. Mechanisms of motility in metastasizing cells. *Mol Cancer Res*, 8, 629-42.
- YIN, H. & GLASS, J. 2006. In prostate cancer cells the interaction of C/EBPalpha with Ku70, Ku80, and poly(ADP-ribose) polymerase-1 increases sensitivity to DNA damage. *J Biol Chem*, 281, 11496-505.
- YIN, L., LIU, Y., PENG, Y., PENG, Y., YU, X., GAO, Y., YUAN, B., ZHU, Q., CAO, T., HE, L., GONG, Z., SUN, L., FAN, X. & LI, X. 2018. PARP inhibitor veliparib and HDAC inhibitor SAHA synergistically co-target the UHRF1/BRCA1 DNA damage repair complex in prostate cancer cells. *J Exp Clin Cancer Res*, 37, 153.
- YOSHIDA, M., KIJIMA, M., AKITA, M. & BEPPU, T. 1990. Potent and specific inhibition of mammalian histone deacetylase both in vivo and in vitro by trichostatin A. *J Biol Chem*, 265, 17174-9.
- ZAREMBA, T. & CURTIN, N. J. 2007. PARP inhibitor development for systemic cancer targeting. *Anticancer Agents Med Chem*, 7, 515-23.
- ZAREMBA, T., KETZER, P., COLE, M., COULTHARD, S., PLUMMER, E. R. & CURTIN, N. J. 2009. Poly(ADP-ribose) polymerase-1 polymorphisms, expression and activity in selected human tumour cell lines. *Br J Cancer*, 101, 256-62.
- ZHA, R. H., SUR, S., BOEKHOVEN, J., SHI, H. Y., ZHANG, M. & STUPP, S. I. 2015. Supramolecular assembly of multifunctional maspin-mimetic nanostructures as a potent peptide-based angiogenesis inhibitor. *Acta biomaterialia*, 12, 1-10.
- ZHANG, J. X., LI, D. Q., HE, A. R., MOTWANI, M., VASILIOU, V., ESWARAN, J., MISHRA, L. & KUMAR, R. 2012. Synergistic inhibition of hepatocellular carcinoma growth by cotargeting chromatin modifying enzymes and poly (ADP-ribose) polymerases. *Hepatology*, 55, 1840-51.
- ZHANG, M. 2004. Multiple functions of maspin in tumor progression and mouse development. *Front Biosci*, 9, 2218-26.
- ZHANG, M., MAASS, N., MAGIT, D. & SAGER, R. 1997a. Transactivation through Ets and Ap1 transcription sites determines the expression of the tumor-suppressing gene maspin. *Cell Growth Differ*, 8, 179-86.
- ZHANG, M., MAGIT, D., BOTTERI, F., SHI, H. Y., HE, K., LI, M., FURTH, P. & SAGER, R. 1999. Maspin plays an important role in mammary gland development. *Dev Biol*, 215, 278-87.
- ZHANG, M., MAGIT, D. & SAGER, R. 1997b. Expression of maspin in prostate cells is regulated by a positive Ets element and a negative hormonal responsive element site recognized by androgen receptor. *Proceedings of the National Academy of Sciences of the United States of America*, 94, 5673-5678.
- ZHANG, M., VOLPERT, O., SHI, Y. H. & BOUCK, N. 2000a. Maspin is an angiogenesis inhibitor. *Nat Med*, 6, 196-9.
- ZHANG, P., AN, K., DUAN, X., XU, H., LI, F. & XU, F. 2018. Recent advances in siRNA delivery for cancer therapy using smart nanocarriers. *Drug Discov Today*, 23, 900-911.

- ZHANG, P., YANG, Y., ZWEIDLER-MCKAY, P. & HUGHES, D. P. 2013. Retraction: Critical role of notch signaling in osteosarcoma invasion and metastasis. *Clin Cancer Res*, 19, 5256-7.
- ZHANG, Q., HELFAND, B. T., JANG, T. L., ZHU, L. J., CHEN, L., YANG, X. J., KOZLOWSKI, J., SMITH, N., KUNDU, S. D., YANG, G., RAJI, A. A., JAVONOVIC, B., PINS, M., LINDHOLM, P., GUO, Y., CATALONA, W. J. & LEE, C. 2009. Nuclear factor-kappaB-mediated transforming growth factor-beta-induced expression of vimentin is an independent predictor of biochemical recurrence after radical prostatectomy. *Clin Cancer Res*, 15, 3557-67.
- ZHANG, S., WEAR, D. J. & LO, S. 2000b. Mycoplasmal infections alter gene expression in cultured human prostatic and cervical epithelial cells. *FEMS Immunol Med Microbiol*, 27, 43-50.
- ZHANG, W. & ZHANG, M. 2002. Tissue microarray analysis of maspin expression and its reverse correlation with mutant p53 in various tumors. *Int J Oncol*, 20, 1145-50.
- ZHANG, Y., CARR, T., DIMTCHEV, A., ZAER, N., DRITSCHILO, A. & JUNG, M. 2007. Attenuated DNA damage repair by trichostatin A through BRCA1 suppression. *Radiat Res*, 168, 115-24.
- ZHANG, Y., XU, Q., LIU, G., HUANG, H., LIN, W., HUANG, Y., CHI, Z., CHEN, S., LAN, K., LIN, J. & ZHANG, Y. 2015. Effect of histone deacetylase on prostate carcinoma. *Int J Clin Exp Pathol*, 8, 15030-4.
- ZHANG, Z., MA, J., LI, N., SUN, N. & WANG, C. 2006. Expression of nuclear factor-kappaB and its clinical significance in nonsmall-cell lung cancer. *Ann Thorac Surg*, 82, 243-8.
- ZHENG, H. C. & GONG, B. C. 2017. The roles of maspin expression in gastric cancer: a meta- and bioinformatics analysis. *Oncotarget*, 8, 66476-66490.
- ZHU, H., MAO, Q., LIU, W., YANG, Z., JIAN, X., QU, L. & HE, C. 2017. Maspin suppresses growth, proliferation and invasion in cutaneous squamous cell carcinoma cells. *Oncol Rep*, 37, 2875-2882.
- ZOU, Z., ANISOWICZ, A., HENDRIX, M., THOR, A., NEVEU, M., SHENG, S., RAFIDI, K., SEFTOR, E. & SAGER, R. 1994. Maspin, a serpin with tumor-suppressing activity in human mammary epithelial cells. *Science*, 263, 526-529.
- ZOU, Z., GAO, C., NAGAICH, A. K., CONNELL, T., SAITO, S., MOUL, J. W., SETH, P., APPELLA, E. & SRIVASTAVA, S. 2000. p53 regulates the expression of the tumor suppressor gene maspin. *J Biol Chem*, 275, 6051-4.
- ZOU, Z., ZHANG, W., YOUNG, D., GLEAVE, M. G., RENNIE, P., CONNELL, T., CONNELLY, R., MOUL, J., SRIVASTAVA, S. & SESTERHENN, I. 2002. Maspin expression profile in human prostate cancer (CaP) and in vitro induction of Maspin expression by androgen ablation. *Clin Cancer Res*, 8, 1172-7.
- ZUCKERMAN, J. E., HSUEH, T., KOYA, R. C., DAVIS, M. E. & RIBAS, A. 2011. siRNA knockdown of ribonucleotide reductase inhibits melanoma cell line proliferation alone or synergistically with temozolomide. *J Invest Dermatol*, 131, 453-60.

